

1983

Structural and electronic influences on phosphite basicity and its application to heterogeneous and homogeneous catalysis

David Evan Schiff
Iowa State University

Follow this and additional works at: <https://lib.dr.iastate.edu/rtd>

 Part of the [Inorganic Chemistry Commons](#)

Recommended Citation

Schiff, David Evan, "Structural and electronic influences on phosphite basicity and its application to heterogeneous and homogeneous catalysis " (1983). *Retrospective Theses and Dissertations*. 8960.
<https://lib.dr.iastate.edu/rtd/8960>

This Dissertation is brought to you for free and open access by the Iowa State University Capstones, Theses and Dissertations at Iowa State University Digital Repository. It has been accepted for inclusion in Retrospective Theses and Dissertations by an authorized administrator of Iowa State University Digital Repository. For more information, please contact digirep@iastate.edu.

INFORMATION TO USERS

This reproduction was made from a copy of a document sent to us for microfilming. While the most advanced technology has been used to photograph and reproduce this document, the quality of the reproduction is heavily dependent upon the quality of the material submitted.

The following explanation of techniques is provided to help clarify markings or notations which may appear on this reproduction.

1. The sign or "target" for pages apparently lacking from the document photographed is "Missing Page(s)". If it was possible to obtain the missing page(s) or section, they are spliced into the film along with adjacent pages. This may have necessitated cutting through an image and duplicating adjacent pages to assure complete continuity.
2. When an image on the film is obliterated with a round black mark, it is an indication of either blurred copy because of movement during exposure, duplicate copy, or copyrighted materials that should not have been filmed. For blurred pages, a good image of the page can be found in the adjacent frame. If copyrighted materials were deleted, a target note will appear listing the pages in the adjacent frame.
3. When a map, drawing or chart, etc., is part of the material being photographed, a definite method of "sectioning" the material has been followed. It is customary to begin filming at the upper left hand corner of a large sheet and to continue from left to right in equal sections with small overlaps. If necessary, sectioning is continued again—beginning below the first row and continuing on until complete.
4. For illustrations that cannot be satisfactorily reproduced by xerographic means, photographic prints can be purchased at additional cost and inserted into your xerographic copy. These prints are available upon request from the Dissertations Customer Services Department.
5. Some pages in any document may have indistinct print. In all cases the best available copy has been filmed.

**University
Microfilms
International**

300 N. Zeeb Road
Ann Arbor, MI 48106

8407124

Schiff, David Evan

STRUCTURAL AND ELECTRONIC INFLUENCES ON PHOSPHITE BASICITY
AND ITS APPLICATION TO HETEROGENEOUS AND HOMOGENEOUS
CATALYSIS

Iowa State University

Ph.D. 1983

University
Microfilms
International 300 N. Zeeb Road, Ann Arbor, MI 48106

PLEASE NOTE:

In all cases this material has been filmed in the best possible way from the available copy. Problems encountered with this document have been identified here with a check mark .

1. Glossy photographs or pages _____
2. Colored illustrations, paper or print _____
3. Photographs with dark background _____
4. Illustrations are poor copy
5. Pages with black marks, not original copy
6. Print shows through as there is text on both sides of page _____
7. Indistinct, broken or small print on several pages
8. Print exceeds margin requirements _____
9. Tightly bound copy with print lost in spine _____
10. Computer printout pages with indistinct print
11. Page(s) _____ lacking when material received, and not available from school or author.
12. Page(s) _____ seem to be missing in numbering only as text follows.
13. Two pages numbered _____. Text follows.
14. Curling and wrinkled pages _____
15. Other _____

University
Microfilms
International

Structural and electronic influences on phosphite
basicity and its application to heterogeneous and
homogeneous catalysis

by

David Evan Schiff

A Dissertation Submitted to the
Graduate Faculty in Partial Fulfillment of the
Requirements for the Degree of
DOCTOR OF PHILOSOPHY

Department: Chemistry
Major: Inorganic Chemistry

Approved:

Signature was redacted for privacy.

In Charge of Major Work

Signature was redacted for privacy.

For the Major Department

Signature was redacted for privacy.

For the Graduate College

Iowa State University
Ames, Iowa

1983

TABLE OF CONTENTS

	Page
PREFACE	1
PART 1. THE CATALYTIC PROPERTIES OF HOMOGENEOUS AND HETEROGENEOUS NiL_4 (L = PHOSPHITE) COMPLEXES	12
INTRODUCTION	13
Hydrocyanation of olefins	38
Unanswered questions in Gultneh's work	42
Heterogenized homogeneous catalysts	47
EXPERIMENTAL PROCEDURES	56
Preparations	60
Results and discussion	78
Use of Lewis acid cocatalysts in the isomerization of 3-butenitrile	91
Crystal and molecular structure of $Ni(6)_4$	102
Effect of substitution of oxygens in the phosphorinane ring by carbon	112
Asymmetric isomerization of $(CH_3CH_2)(CH_3)C=CHCH_2CN$	135
Hydrocyanation of 1,3-butadiene to adiponitrile	136
Heterogenized NiL_4 catalysts	141
PART II. STEREOELECTRONIC EFFECTS OF CYCLIZATION IN AMINO- PHOSPHINE SYSTEMS: A STRUCTURAL, PES, AND NMR STUDY OF $Me_2NP(OCH_2)_2CMe_2$ AND $CH_2(CH_2CH_2)_2NP(OCH_2)_2CMe_2$	153
INTRODUCTION	154
Experimental procedures	157
Preparations	159
Experimental details for X-ray data collection for compounds <u>20</u> and <u>21</u>	162
Results and discussion	164

PART III. THE USE OF PHOSPHORUS CONTAINING DERIVATIZING REAGENTS FOR THE ANALYSIS OF ALCOHOLS	188
INTRODUCTION	189
EXPERIMENTAL PROCEDURES	194
Results and discussion	196
CONCLUSIONS	203
REFERENCES	205
ACKNOWLEDGMENTS	215
APPENDIX 1. STRUCTURE FACTORS FOR $\text{Ni}(\underline{6})_4$	216
APPENDIX 2. STRUCTURE FACTORS FOR <u>30</u>	222
APPENDIX 3. STRUCTURE FACTORS FOR <u>20</u>	227
APPENDIX 4. STRUCTURE FACTORS FOR <u>21</u>	232

LIST OF TABLES

Table 1.	2
Compounds described in this thesis	
Table 2.	20
Various ligand cone angles for some selected phosphorus ligands	
Table 3.	29
Rates of catalytic isomerization of 3-butenitrile by NiL_4/acid (1/10) systems in benzene at 25°C as a function of the size of the exocyclic phosphorus substituent	
Table 4.	46
Rates of isomerization of 3-butenitrile by $\text{NiL}_4/\text{F}_3\text{CCOOH}$ systems in benzene at 25°C	
Table 5.	48
Relative advantages and disadvantages of different types of catalysts	
Table 6.	61
Ranges of chemical shift (rel. to H_3PO_4) for compounds discussed in this thesis	
Table 7.	80
^{31}P NMR chemical shifts and $J_{\text{P-H}}$ values of some selected monocyclic phosphite ligands upon protonation with FSO_3H at -50°C	
Table 8.	83
^{31}P - ^{77}Se spin-spin couplings and ^{31}P NMR chemical shifts (rel. to H_3PO_4) of some selected selenophosphoryl compounds.	
Table 9.	92
Comparison of activity of Lewis acids to H^+ as a cocatalyst in the isomerization of 3-butenitrile.	

Table 10.	97
^{27}Al NMR data for various AlCl_3 , ligand, and NiL_4 complex mixtures.	
Table 11.	100
^{27}Al NMR data for various AlCl_2Et , ligand, and NiL_4 complex mixtures	
Table 12.	104
The final positional parameters for atoms contained in $\text{Ni}(\underline{6})_4$ with their estimated standard deviations (in parentheses)	
Table 13.	105
Bond distances (\AA) and their estimated standard deviations (in parentheses) for $\text{Ni}(\underline{6})_4$.	
Table 14.	106
Bond angles ($^\circ$) and their estimated standard deviations (in parentheses) for $\text{Ni}(\underline{6})_4$	
Table 15.	107
Thermal parameters and their estimated standard deviations (in parentheses) for $\text{Ni}(\underline{6})_4$	
Table 16.	123
Final positional parameters and their estimated standard deviations (in parentheses) for <u>meso</u> - $(\text{C}_6\text{H}_5)_3\text{C}(\text{O})\text{P}[\text{CH}_2\text{C}(\text{CH}_3)_2\text{H}]_2\text{CH}_2$ (30)	
Table 17.	125
Bond distances (\AA) and their estimated standard deviations (in parentheses) for <u>meso</u> - $(\text{C}_6\text{H}_5)_3\text{C}(\text{O})\text{P}[\text{CH}_2\text{C}(\text{CH}_3)\text{H}]_2\text{CH}_2$	
Table 18.	126
Bond angles ($^\circ$) and their estimated standard deviations (in parentheses) for <u>meso</u> - $(\text{C}_6\text{H}_5)_3\text{C}(\text{O})\text{P}[\text{CH}_2\text{C}(\text{CH}_3)\text{H}]_2\text{CH}_2$ (30)	

Table 19.	127
Thermal parameters and their estimated standard deviations (in parentheses) for <u>meso</u> -(C ₆ H ₅) ₃ C(O)P[CH ₂ C(CH ₃)H] ₂ CH ₂ (30)	
Table 20.	133
³¹ P NMR chemical shifts for selected phosphorinane compounds	
Table 21.	140
The preparation of adiponitrile from butadiene and HCN using various catalyst systems at 120° in xylene	
Table 22.	146
The number of turnovers per unit time produced by various [Ni(23)(L) ₂] _n polymers versus their homogeneous NiL ₄ complexes for the isomerization of 3-butenitrile	
Table 23.	151
Amount of H ⁺ /nickel found in NiL ₄ /XN-1010 resin catalysts	
Table 24.	152
Number of turnovers/unit time of supported NiL ₄ complexes versus their homogeneous analogue for the isomerization of 3-butenitrile	
Table 25.	165
Bond distances (Å), angles (°), and their standard deviations for Me ₂ NP(OCH ₂) ₂ CMe ₂ (20)	
Table 26.	166
Bond distances (Å), angle (°), and their standard deviations for CH ₂ (CH ₂ CH ₂)NP(OCH ₂)CMe ₂ (21)	
Table 27.	167
Final positional parameters and their standard deviations for Me ₂ NP(OCH ₂) ₂ CMe ₂ (20)	
Table 28.	168
Final positional parameters and their standard deviations for CH ₂ (CH ₂ CH ₂) ₂ NP(OCH ₂) ₂ CMe ₂ (21)	

Table 29.	169
Final thermal parameters and their standard deviations (in parentheses) for $\text{Me}_2\text{NP}(\text{OCH}_2)_2\text{CMe}_2$ (20)	
Table 30.	170
Final thermal parameters and their standard deviations (in parentheses) for $\text{CH}_2(\text{CH}_2\text{CH}_2)_2\text{NP}(\text{OCH}_2)_2\text{CMe}_2$ (21)	
Table 31.	180
Ionization energies	
Table 32.	184
^{31}P NMR chemical shifts (ppm) and $J_{^{31}\text{P}-^{77}\text{Se}}$ coupling constants (Hz)	
Table 33.	193
Phosphorus chemical shifts of model compound derivatives	
Table 34.	197
Phosphorus chemical shifts of 1,3,2-dioxaphospholanyl derivatives of various alcohols ($\text{OCH}_2\text{CH}_2\text{OP-OR}$)	
Table 35.	198
Comparison of ratios of peak areas of 1,3,2-dioxaphospholanyl derivatives ($\text{OCH}_2\text{CH}_2\text{OPOR}$) to PPh_3 under conditions of broad band decoupling.	
Table 36.	199
Comparison of ratios peak areas of 1,3,2-dioxaphospholanyl derivatives ($\text{OCH}_2\text{CH}_2\text{OPOR}$) to PPh_3 under conditions of gated decoupling.	
Table 37.	200
Results of ^{31}P NMR analysis of alcohol mixtures using 14 as a derivatizing reagent, PPh_3 as an internal standard, and broad band decoupling	

Table 38.

201

Results of ^{31}P NMR analysis of alcohol mixtures using 14 as a derivatizing reagent, PPh_3 as an internal standard, and gated decoupling techniques.

LIST OF FIGURES

	Page
Figure 1.	14
Bonding in transition metal carbonyl complexes	
Figure 2.	19
Ligand cone angle as defined by Tolman	
Figure 3.	36
Geometric arrangement of the P, O, and C atoms and the ester oxygen P orbitals in a bicyclic phosphorus ester (X = lone pair or oxygen) if sp^2 hybridization is assumed	
Figure 4.	84
Resonance structures for a phenoxy group	
Figure 5.	87
^{31}P NMR spectrum of a C_6D_6 solution of $\text{Ni}(\underline{6})_4$ acidified with 5 equivalents of F_3CCOOH at room temperature	
Figure 6.	88
^{31}P NMR spectrum of a C_6D_6 solution of $\text{Ni}(\underline{20})_4$ acidified with 1 equivalent of F_3CCOOH at 200 K	
Figure 7.	89
^{31}P NMR spectrum of a C_6D_6 solution of $\text{Ni}(\underline{20})_4$ acidified with 2 equivalents of F_3CCOOH at 200 K	
Figure 8.	90
^{31}P NMR spectrum of a C_6D_6 solution of $\text{Ni}(\underline{20})_4$ acidified with 10 equivalents of F_3CCOOH at 200 K	
Figure 9.	109
ORTEP diagram of $\text{Ni}(\underline{6})_4$	
Figure 10.	121
Mass spectrum of <u>29</u>	

Figure 11.	122
Mass spectrum of <u>30</u>	
Figure 12.	129
ORTEP diagram of <u>30</u>	
Figure 13.	130
Unit cell diagram of <u>30</u>	
Figure 14.	142
Proposed structure of metal complex polymer	
Figure 15.	156
Orientation of electron pairs in each of the two possible conformations of 2-dimethylamino-1,3,2-dioxaphosphorinane	
Figure 16.	171
ORTEP diagram of <u>20</u>	
Figure 17.	172
ORTEP diagram of <u>21</u>	
Figure 18.	173
Unit cell diagram of <u>20</u>	
Figure 19.	174
Unit cell diagram of <u>21</u>	
Figure 20.	178
UV photoelectron spectrum of <u>20</u>	
Figure 21.	179
UV photoelectron spectrum of <u>21</u>	
Figure 22.	182
MO diagram for nitrogen and phosphorus lone pairs in $P(NMe_2)_3$	

- Figure 23. 186
Conformation of $\text{Me}_2\text{NP}(\text{OMe})_2$ as calculated by semiempirical MNDO methods
- Figure 24. 186
Proposed conformation of 16

LIST OF SCHEMES

	Page
Scheme 1.	25
The mechanism of isomerization of η^2 and η^4 -3-methylene-4-vinyldihydrofuran-2(3H)-one complexes of Fe(0). Note: R groups on compounds succeeding <u>A</u> left off for clarity.	
Scheme 2.	26
The mechanism for the isomerization of 1-butene using acidified $\text{Ni}(\text{P}(\text{OEt})_3)_4$	
Scheme 3.	39
Decomposition of σ -bound metal alkyl cyanide species to form alkyl nitriles	
Scheme 4.	54
Attachment of metal carbonyl compounds to derivatized silica gel.	
Scheme 5.	68
The synthesis of <u>meso</u> -2,4-dimethyl-1,5-dibromopentane	
Scheme 6.	92
Proposed mechanism of Gultneh for the interaction of a NiL_4 complex and AlCl_3	

PREFACE

The steric and electronic properties of phosphorus ligands are known to vary widely. This dissertation discusses work done during the study of the properties of different monocyclic and bicyclic phosphite esters and how these properties influence the catalytic activity of the NiL_4 complexes which they form.

X-ray, PES, and NMR studies of some selected aminophosphite compounds were carried out in order to understand how their unique structural and electronic properties could influence the catalytic properties of their NiL_4 complexes.

We were also successful in producing two new types of heterogenized NiL_4 complexes which we hoped would have properties similar to that of a homogeneous NiL_4 catalyst, yet would also have the desirable characteristics of a heterogeneous catalyst.

In addition, this dissertation will describe the development of an analytical procedure for quantifying alcohols contained within a mixture, by means of a phosphorus derivatizing reagent. The actual analysis entailed the quantitative measurement of the phosphorus-containing alcohol derivative using ^{31}P NMR techniques.

A list of compounds discussed in this dissertation is included in Table 1.

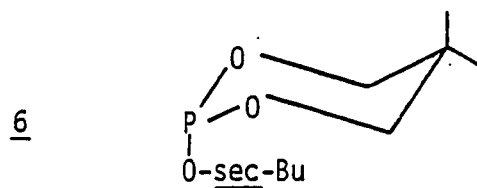
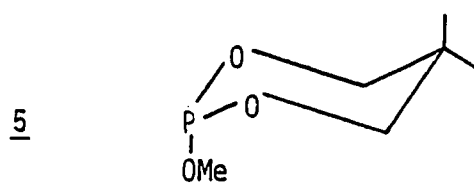
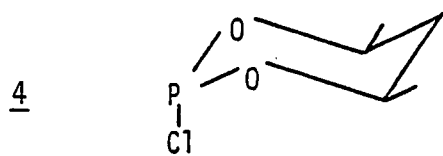
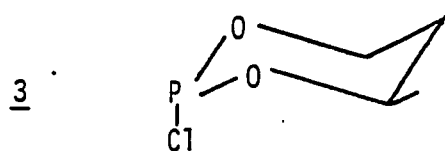
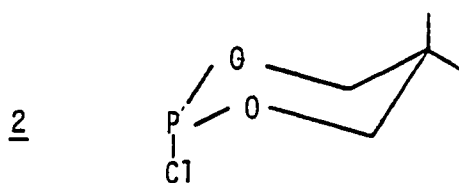
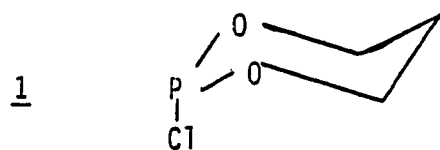
Table 1. Compounds described in this thesis

Table 1. (Continued)

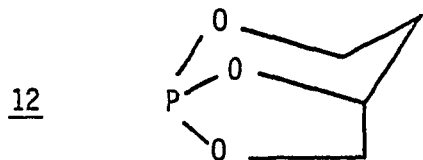
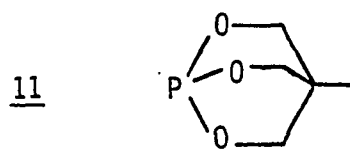
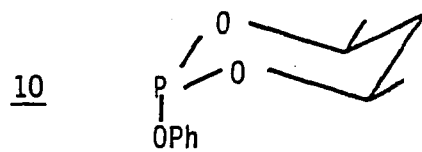
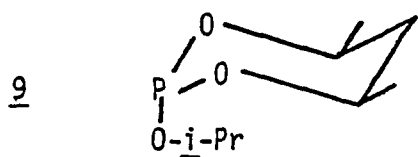
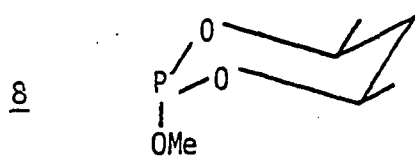
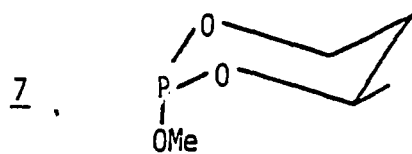


Table 1. (Continued)

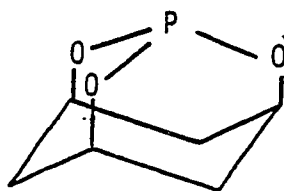
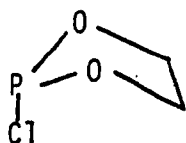
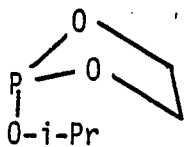
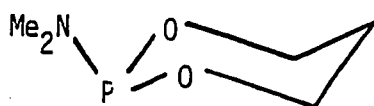
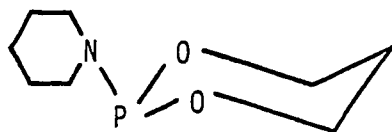
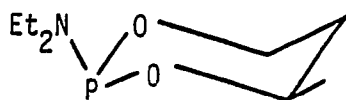
131415161718

Table 1. (Continued)

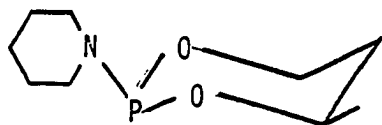
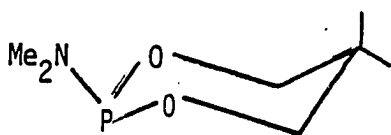
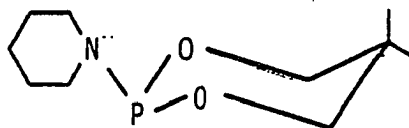
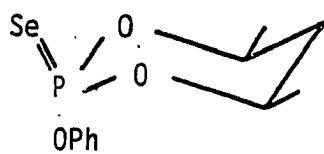
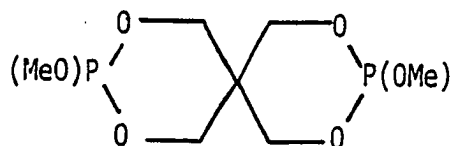
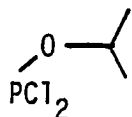
192021222324

Table 1. (Continued)

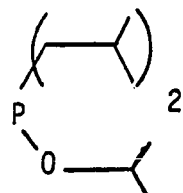
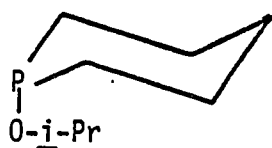
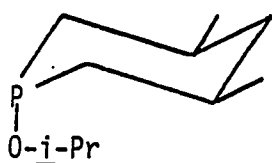
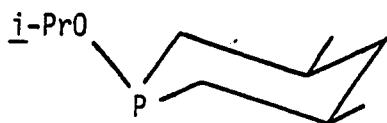
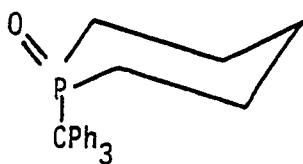
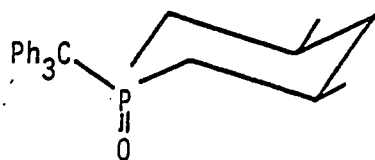
252627282930

Table 1. (Continued)

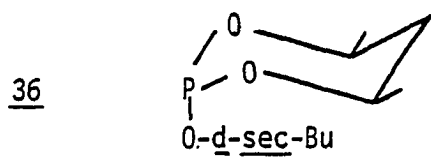
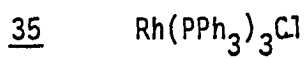
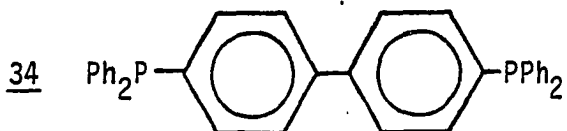
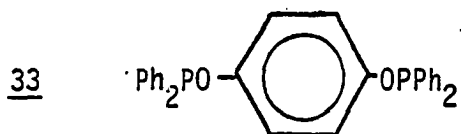
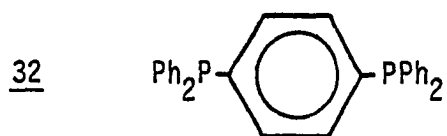
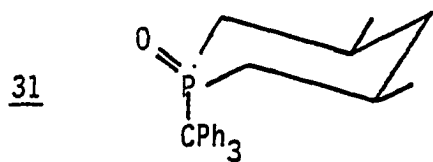


Table 1. (Continued)

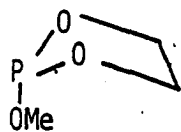
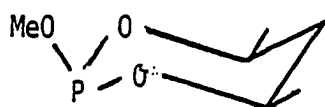
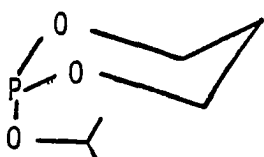
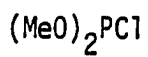
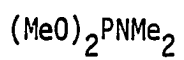
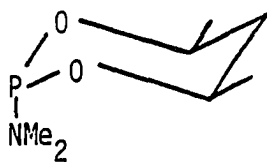
373839404142

Table 1. (Continued)

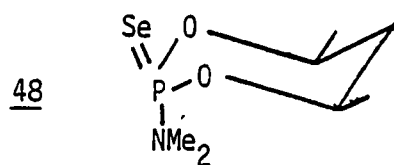
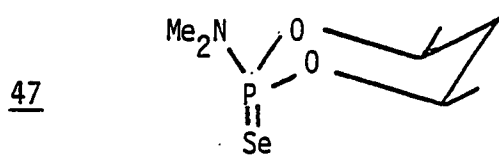
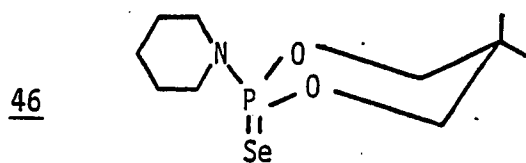
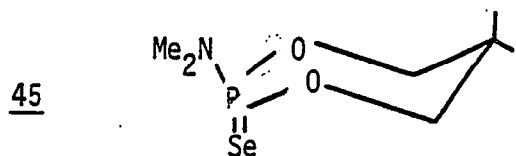
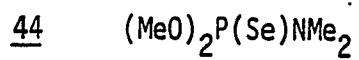
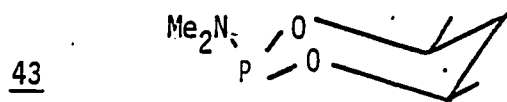


Table 1. (Continued)

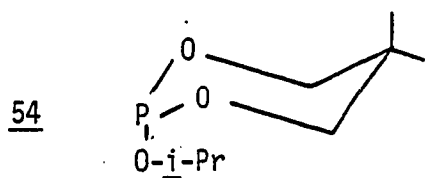
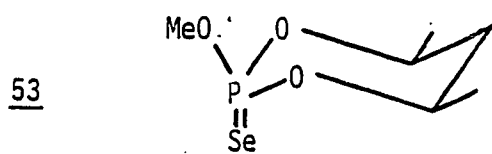
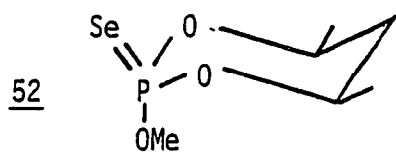
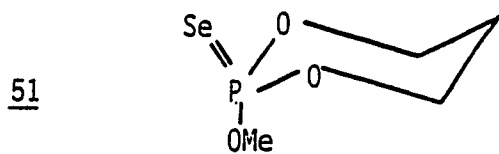
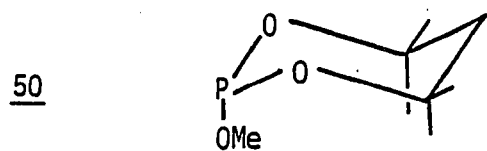
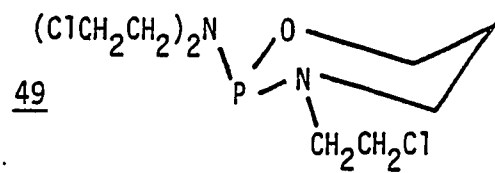
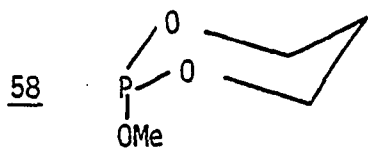
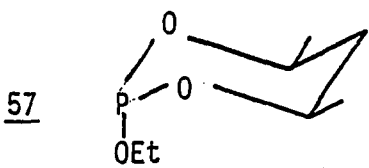
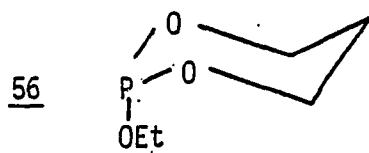
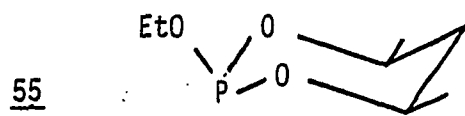


Table 1. (continued)



PART 1:

THE CATALYTIC PROPERTIES OF HOMOGENEOUS AND HETEROGENEOUS

NiL_4 (L = PHOSPHITE) COMPLEXES

INTRODUCTION

One of the most novel features of transition metals is their ability to adopt many different oxidation states. This is perhaps one of the most important factors in their capacity to act as catalysts in a variety of organic reactions (1,2). The ability of a transition metal to adopt lower oxidation states is facilitated by the coordination of electron soft ligands such as PR_3 , P(OR)_3 , SR_2 , CO , C_6H_6 , etc.

In most cases, transition metals bind ligands in a manner which provides 18 electrons in their valence shell. These complexes are then said to be coordinatively saturated. In order for these complexes to act as catalytically active species, they must first dissociate one of their ligands to form electron deficient complexes. In most cases, these are 16 electron intermediates which are then able to bind small molecules such as olefins, hydrogen, nitrogen, alkyl halides, etc. Upon coordination, these small molecules undergo changes in their electronic structure which facilitate their further reaction while coordinated to the metal atom. This feature is best illustrated by the pioneering work of Dewar, and Chatt and Duncanson (3,4) on the bonding of olefins to metal atoms. In their model, the electron density contained in the double bond is donated to the metal atom via a σ bond while at the same time electron density is returned to the olefin through its anti-bonding orbitals. This redistribution of electron density is suggested by the observation of an increase in the C-C distance of the coordinated olefin compared to that found in the uncoordinated olefin (4,5). X-ray crystal-

lographic studies of olefin complexes such as $\text{Ni}(\text{CH}_2=\text{CH}_2)(\text{P}(\text{O}-\text{O}-\text{C}_6\text{H}_4\text{CH}_3)_3)_2$ and $\text{Ni}(\text{CH}_2=\text{CH}_2)(\text{PPh}_3)_2$ (5) have shown that the olefin loses its planarity upon coordination. This is indicative of extensive rehybridization of the olefinic carbon atoms from sp^2 to sp^3 . It is the weakening of the olefin's double bond, which activates it toward reactions with other atoms and smaller molecules, such as H and CO, which are also bound to the metal atom.

The ability of a transition metal to act as a catalyst depends very strongly upon the steric and electronic interactions between the ligands contained in the coordination sphere of the metal atom. The electronic interaction between a ligand such as CO and a metal atom can also be described by the Dewar-Chatt-Duncanson model (Fig. 1) (4). In this model, a pair of electrons is donated to the metal atom from the CO

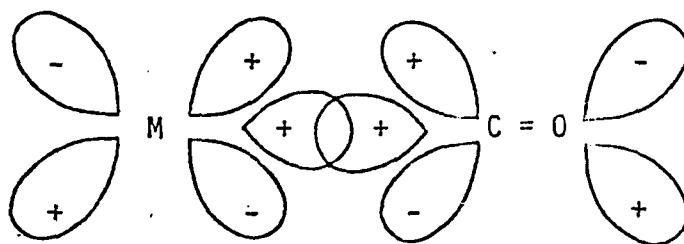


Fig. 1. Bonding in transition metal carbonyl complexes

ligand via a σ bond. At the same time, electron density is returned to the CO ligand via a π bond formed by the antibonding orbitals of the CO and the d orbitals on the metal, which causes a weakening of the C-O bond. Support for this theory has been well-documented by the decrease

in the $\nu(\text{C}=\text{O})$ stretching frequency of CO upon coordination to metals such as Fe, Co, etc. (6).

Back donation of electron density has also been postulated to occur in other ligands which contain atoms having low-lying unoccupied d orbitals, such as phosphorus, sulfur, arsenic and selenium. In the case of phosphorus, it has been known for many years that the donor-acceptor properties of the ligands are highly dependent upon the groups bonded to phosphorus (7).

Tolman (8) has been able to quantify the contributions of these substituents from the donor-acceptor properties of phosphorus. The contribution of the substituent to the A_1 CO stretching frequency of various $\text{Ni}(\text{CO})_3\text{L}$ complexes, where $\text{L} = \text{PX}_1\text{X}_2\text{X}_3$, has been quantified by the substituent additivity coefficient (χ_1) of X. The effect of this contribution on the A_1 stretching frequency is given by equation 1.

$$\nu(\text{CO})_{A_1} = 2056 + \sum_{i=1}^3 \chi_i \text{cm}^{-1} \quad (1)$$

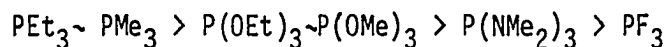
The values of χ_1 range from 0.0 for a t-butyl group to 19.6 for a trifluoromethyl group. Clearly, the more electron withdrawing a group, the higher its χ_i value. It has also been observed that ligands which are good π -acceptors also cause the A_1 CO stretching frequency of these complexes to be higher. Of course, it is impossible to quantify the relative donor-acceptor properties of a phosphorus ligand solely on the basis of a single CO stretching frequency. In fact, it has been argued

that the phosphorus-metal σ bond is the major factor in determining the $\nu(\text{CO})$ frequency for the CO ligands contained within the complex (9,10).

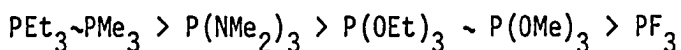
Over the past several years many methods have been developed to quantify the donor properties (or basicity) of phosphorus. Protonation of phosphorus ligands with strong acids such as $\text{F}_3\text{CCO}_2\text{H}$, followed by subsequent ^{31}P NMR analysis have shown that $J_{\text{P-H}}$ is related to the basicity of the phosphorus ligand (10). It has been argued (11,12) that the less basic the phosphorus ligand is, the higher the positive charge at the phosphorus nucleus. This increase in positive charge then causes an increase in the value of $J_{\text{P-H}}$ upon protonation.

Other workers have been successful in correlating phosphorus ligand basicity to the $31\text{p}_{-77}\text{Se}$ values of their corresponding selenides (13), the $\nu_{\text{B-H}}$ values of their borane adducts (14) and the $J_{183\text{W}-31\text{P}}$ values found in $\text{W}(\text{CO})_5\text{L}$ complexes (15,16). Recent work by Yarbrough and Hall (17) has shown that photoelectron spectroscopy can furnish information which distinguishes π -acceptor and σ -donor properties of a phosphorus ligand. The photoelectron spectra of $\text{LM}(\text{CO})_5$ where $\text{M} = \text{Cr}, \text{Mo}$ and W and $\text{L} = \text{PEt}_3, \text{PMe}_3, \text{P}(\text{NMe}_2)_3, \text{P}(\text{OEt})_3, \text{P}(\text{OMe})_3$ or PF_3 were reported. The authors compared the spectra of these complexes to that of the free ligands. Information on the σ donor ability of the ligands was obtained by comparing the difference in the ionization potentials of M-P bond to that of the lone pair in the free ligand. It was assumed that the greater the donor ability of ligand, the smaller the difference in ionization potential of the M-P bond to that of the lone pair in the free ligand. This allowed them to rank the donor ability of these ligands

while complexed to the metal atom in the following order:

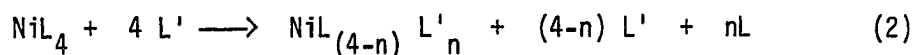


It should be noted that the relative order of P(OMe)_3 and $\text{P(NMe}_2)_3$ is opposite to what Cowley and co-workers (18) have found for the uncoordinated ligand. The π -acceptor abilities of these ligands were determined by the amount that the t_{2g} orbitals of the metal atom were split into e and b_2 groups by the ligands. The amount of splitting of these orbitals by the ligands fell into the following order:



This order is opposite to the order of increasing π -acidity based on electronegativity considerations. The switch in the order of $\text{P(NMe}_2)_3$ and the phosphites in going from σ basicity to π -acidity is attributed to the interaction between occupied and unoccupied orbitals on both phosphorus and its substituents.

The steric properties of a phosphorus ligand have also been shown to be important in describing the overall properties of the ligand. Tolman and co-workers (19,20) has shown that the steric properties of the phosphorus ligand play a dominate role in influencing the position of the following equilibrium (Eq. 2).



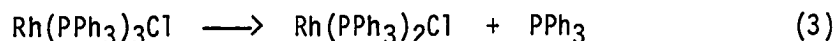
He has shown that the smaller the size of the ligand, the more stable the resulting complex is toward ligand replacement. In order to quantify

steric properties of a ligand, Tolman defines the ligand cone angle as the apex angle of a cylindrical cone, centered at 2.28Å from the center of the phosphorus atom (Fig. 2). (This distance exemplifies the average distance found between a metal atom and a phosphorus ligand.) The cone is constructed so that it just touches the van der Waals radii of the outermost atoms. The value of the ligand cone angle, which can be determined by using space-filling models, ranges from 101° for the rather nonsterically demanding P(OCH₂)₃CCH₃ to 212° for the bulky P(mesityl)₃ ligand (Table 2).

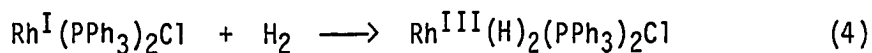
Having the ability to determine the electronic and steric properties of a ligand, one should be able to relate these properties to the reactivity of a metal complex containing these ligands, toward small molecules such as olefins, hydrogen, or CO, etc. With this knowledge one should be able to custom design a metal complex for use as a catalyst.

A good example of how a ligand can influence a transition metal complex's catalytic behavior is perhaps best demonstrated by Wilkinson's catalyst. Wilkinson catalyst, Rh(PPh₃)₃Cl, (21,22) is one of the best known homogeneous hydrogenation catalysts. The proposed mechanism of its role in the hydrogenation of an olefin is :

Ligand dissociation



Oxidative addition



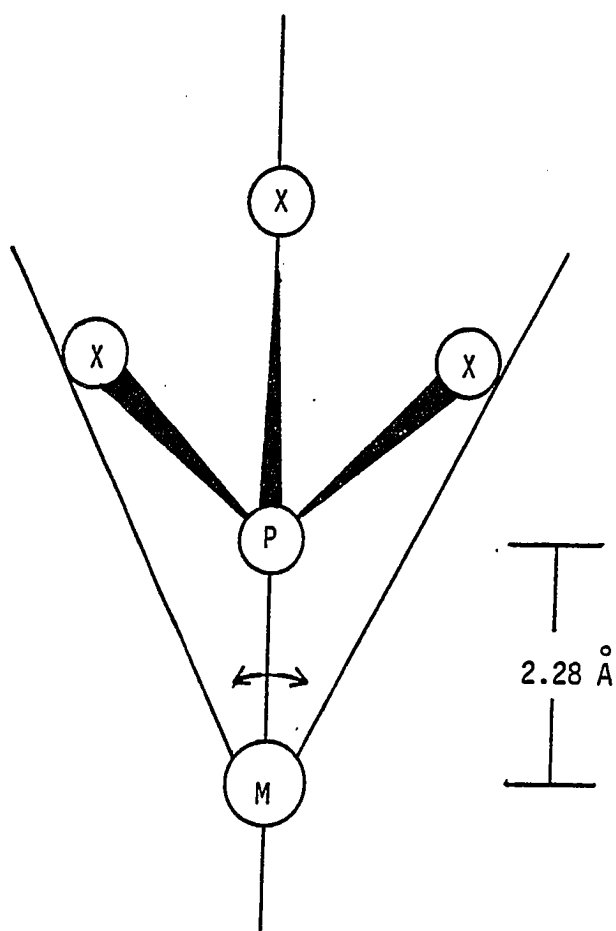
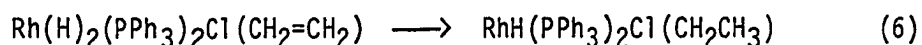
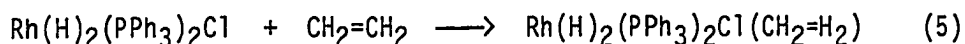
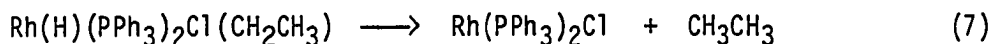


Figure 2. Ligand cone angle as defined by Tolman (19)

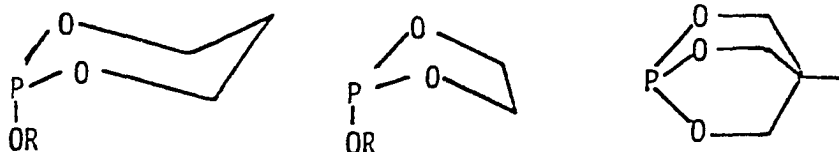
Table 2. Various ligand cone angles for some selected phosphorus ligands (19,20)

Ligand	Cone Angle (°)
$P(OCH_2)_3CCH_3$	101
PF_3	104
$P(OMe)_3$	107
$P(OEt)_3$	109
PCl_3	124
$P(O-\underline{i}\text{-Pr})_3$	130
$P(O-\underline{o}\text{-tol})_3$	141
$P(NMe_2)_3$	157
$P(\text{mesityl})_3$	212

Olefin addition and insertionReductive elimination

In each of these steps, the properties of the phosphine ligand has a great effect upon this reaction since the analogous phosphite complex $\text{Rh}(\text{P}(\text{OPh})_3)_2\text{Cl}$ has been shown to be completely inactive as a hydrogenation catalyst (21). At first, this difference was attributed to the greater π -acidity of the phosphite over the phosphine, which was believed to lower the amount of electron density on the metal, thus changing the metal's electronic properties. However, this difference in activity has more recently been attributed to the failure of a $\text{P}(\text{OPh})_3$ ligand to dissociate and provide an open site for coordination of hydrogen or an olefin (22). This failure to dissociate is a consequence of the reduced steric bulk of $\text{P}(\text{OPh})_3$ compared to that of PPh_3 . This is borne out by the differences in the ligand cone angle of 128° to 145° for $\text{P}(\text{OPh})_3$ and PPh_3 , respectively (Table 2) (19).

Over the last two decades, our group has focused interest on the chemistry of various monocyclic, and bicyclic ligands exemplified by structures of the types below (12,23,24). A great deal of work has also been done to understand both the steric and electronic properties of these ligands (24,25,26,27). Based on our present knowledge of these

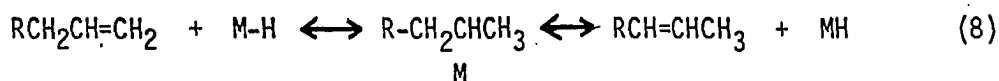


R = alkyl or aryl

ligands it seemed reasonable to attempt to correlate these properties to the catalytic activities of some selected transition metal complexes which they form.

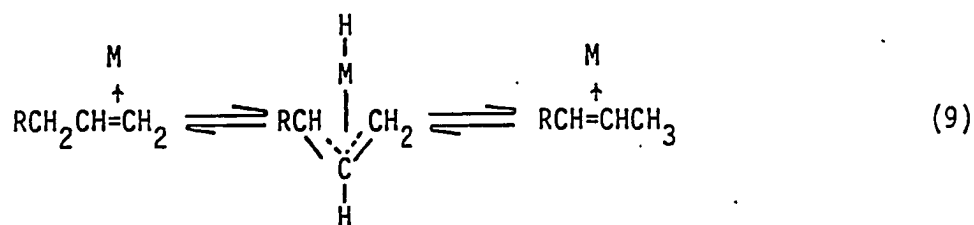
The homogeneous catalytic isomerization of an olefin provides an excellent system to probe the effects of the properties of the ligand on the rate of catalysis by a given complex. This is due in part to the overall relative simplicity of the mechanism involved.

The catalytic isomerization of olefins has been shown to proceed by two different mechanisms (1). The first involves a σ -bonded alkyl intermediate which is formed by olefin insertion into a metal hydride bond. This is then followed by β -hydrogen elimination to give the isomerized product (Eq. 8).



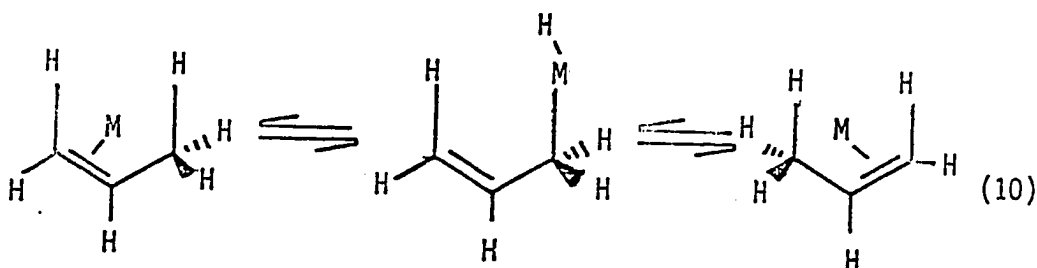
This mechanism requires the formation of a metal hydrogen bond followed by a 1,2-hydrogen shift. In most cases, the hydride is supplied by either a protic acid or molecular hydrogen. Examples of catalytic systems which proceed via such a mechanism are $\text{HCo}(\text{CO})_4$ (28), $((\text{C}_2\text{H}_4)_2\text{RhCl})_2/\text{HCl}$ (29), $\text{HNi}(\text{P}(\text{OEt})_3)_4^+$ (30) and $\text{PtCl}_2(\text{PPh}_3)_2 \text{SnCl}_4/\text{H}_2$ (31).

The second mechanism requires the formation of a π or σ allyl-metal intermediates. The π -allyl metal hydride mechanism proceeds via reaction (9).



This mechanism was shown to be operative in the isomerization of allyl alcohol to propionaldehyde by $\text{Fe}(\text{CO})_5$ (32). Further, deuterium labeling experiments by Hendrix and co-workers (33) confirmed the existence of a 1,3-hydrogen shift, required by the π -allylic mechanism.

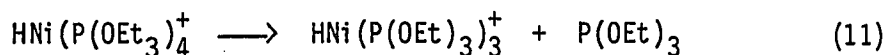
Green and Hughes (34,35) proposed a modification of this mechanism which involves the formation of a σ -bonded allyl intermediate (Eq. 10).



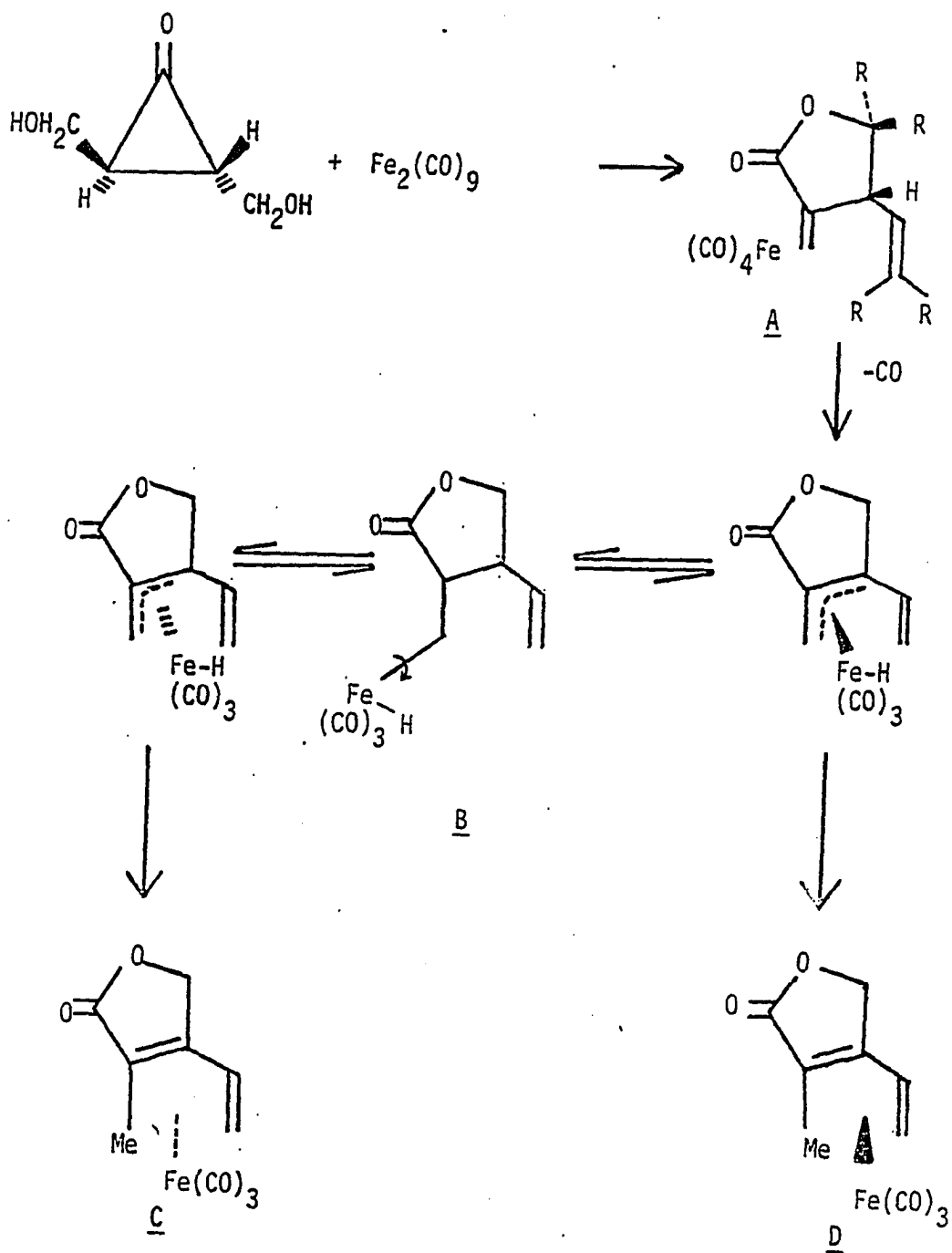
This mechanism requires the metal atom to insert into C-H bond followed by elimination of the metal to reform a new C-H bond with concurrent isomerization of the double bond. This mechanism has been substantiated by the thermal rearrangement of η^2 and η^4 -3-methylene-4-vinyldihydro-

furan-2(3H)-one complexes of iron(0) (Scheme 1) (34). Optically active A in Scheme 1 rearranges regiospecifically, but with extensive racemization in the formation of C and D. Green and Hughes (35) contend that this racemization can only occur by means of a terminal σ bonded allylic intermediate B.

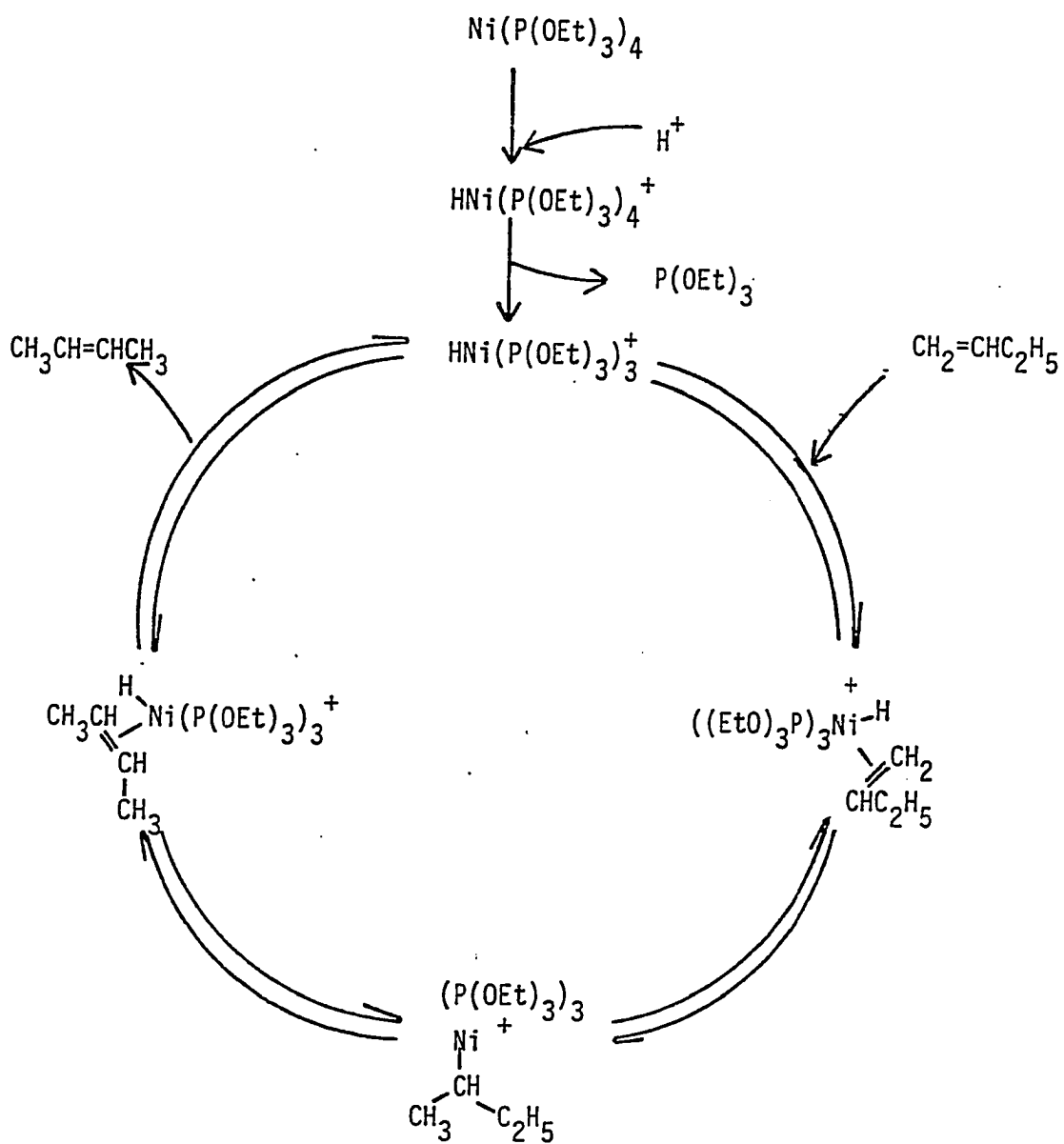
In 1970 C. A. Tolman reported that under strongly acid conditions $\text{Ni}(\text{P}(\text{OEt})_3)_4$ could be protonated (36). It was found that protonation of the complex labilized a triethyl phosphite ligand. It was shown by spectrophotometric methods that the rate constant increased from $4.9 \times 10^{-6} \text{ sec}^{-1}$ to $1.5 \times 10^{-2} \text{ sec}^{-1}$ for the dissociation (Eq. 11) of $\text{Ni}(\text{P}(\text{OEt})_3)_4$ upon addition of acid. Further work has shown that the



protonated nickel complex can efficiently isomerize 1-butene via the mechanism proposed in Scheme 2 (36,37). Both spectrophotometric and ^{31}P NMR (30) analysis indicate that the protonation of $\text{Ni}(\text{P}(\text{OEt})_3)_4$ is extremely facile. However, the rate-determining step was found to be the dissociation of a $\text{P}(\text{OEt})_3$ ligand to form the coordinatively unsaturated species, $\text{HNi}(\text{P}(\text{OEt})_3)_3^+$. Dissociation of a $\text{P}(\text{OEt})_3$ ligand is probably facilitated by weakening of the nickel-phosphorus bond. This is due in part to the decrease in π back donation to the phosphite ligand from the metal, caused by the coordination of the proton to the nickel. This was borne out by the work of Gultneh (38) which showed that complexes such as $\text{Ni}(\underline{11})_4$ were protonated to a small extent in solution. It is thought



Scheme 1. The mechanism of isomerization of η^2 and η^4 -3-methylene-4-vinyl dihydrofuran-2(3H)-one complexes of $\text{Fe}(0)$. Note, R groups on compounds succeeding **A** left off for clarity



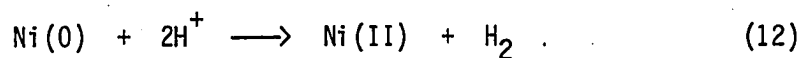
Scheme 2. The mechanism for the isomerization of 1-butene using acidified $\text{Ni}(\text{P}(\text{OEt})_3)_4$ (19)

that the high π -acceptor capacity of 11 sufficiently lowers the basicity of nickel, thus causing it not to be protonated.

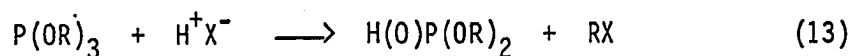
The role of the acid in this catalysis mechanism is that of an initiator. Tolman has shown (36) that in D_2SO_4/CH_3OD solutions, $DNiL_4^+$ forms rapidly. However, the deuterium is found in only 1 out of 120 isomerized butene molecules. This indicates that the nickel atom exchanges the deuterium atom for a proton in the isomerizing olefin. Subsequent coordination of a nondeuterated 1-butene which results in the formation of nondeuterated 2-butene. The protonated nickel atom can only redeuterate after it has recaptured a free phosphite ligand to form $HNiL_4^+$ which is then able to exchange with the solvent.

As much as the acid is the key to starting up the catalytic mechanism, it is also the key to ending it. Deactivation of the complex toward catalysis is known to occur via two pathways.

1. Oxidation of the zero-valent nickel atom to Ni(II). Calculation of the E_0 potential for (Eq. 12) yields 0.25 volts.



2. Acid-catalyzed solvolysis of dissociated ligands. Examples of acid catalyzed solvolysis of alkyl phosphites have been known for many years (Eq. 13) (39).



This reaction should be important in the catalysis mechanism since the dissociation of a $P(OEt)_3$ ligand takes place in a highly acidic medium. One might expect that this reaction would favor an increase in the catalysis rate because it shifts the dissociation equilibrium toward $HNiL_3^+$ species. However, in actuality it is presumed that further dissociation takes place leading to the formation of $HNiL_2^+$ and $HNiL^+$ species which are more readily oxidized to Ni(II) in the highly acidic media.

Armed with this basic information, Gultneh and Verkade began a study of the catalytic properties of various NiL_4 complexes where L is a monocyclic or bicyclic phosphite ligand. One of the most important findings of this study was that small changes in the structure of the phosphite leads to a large increase in the rate of catalytic isomerization of 3-butenitrile (Table 3). As can be seen in Table 3, the amount of catalysis is maximized for ligands which have methyl groups in the 4,6 equatorial positions. The increased rate of catalysis by the ligand in the NiL_4 complex was found to follow the trend:

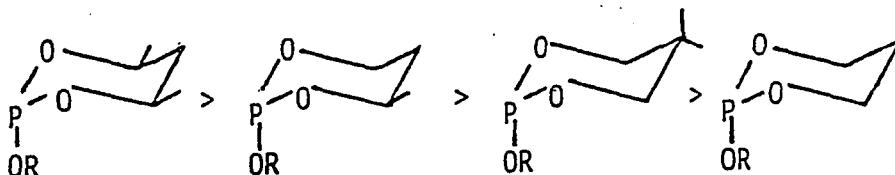
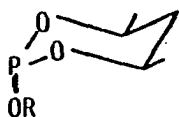
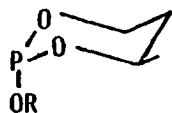


Table 3. Rates of catalytic isomerization of 3-butenitrile by NiL_4/acid (1/10) systems in benzene at 25°C as a function of the size of the exocyclic phosphorus substituent ^a(38)

L	$\text{NiL}_4/\text{F}_3\text{CCOOH}$			$\text{NiL}_4/\text{Cl}_3\text{CCOOH}$		
	cycles over initial 30 min (± 3)	$t_{1/2}$ (min) (± 0.2 min)	cis/trans (2-butene-nitrile) (± 0.2)	cycles over initial 30 min (± 3)	$t_{1/2}$ (± 0.2 min)	cis/trans (2-butene-nitrile) (± 0.2)



R = Me	(5.0 min) ^{bc}	<1.0	1.5	107	8.0	1.7
R = <u>n</u> -Pr	(4.0 min)	<1.0	1.6	110	7.5	1.6
R = <u>i</u> -Pr	(3.0 min) ^b	<1.0	1.5	115	7.0	1.6
R = <u>t</u> -Bu	(5.0 min) ^c	<1.0	1.5	104	8.0	1.5
R = <u>sec</u> -Bu	(5.0 min) ^d	<1.0	1.7	104	8.0	1.7
R = <u>1</u> -bornyl	20	>8 hrs	1.6	10	12 hrs	1.5
R = <u>1</u> -menthyl	20	>8 hrs	1.4	10	12 hrs	1.6
R = α -(methoxy-carbonyl)benzyl	0	--	--	--	--	--



R = Me	92	12.0	1.4	62	30.0	1.7
R = <u>i</u> -Pr	108	8.0	1.6	68	29.0	1.5
R = <u>t</u> -Bu	96	9.0	1.5	64	29.0	1.5
R = <u>1</u> -bornyl	0	--	--	0	--	--
R = <u>1</u> -menthyl	0	--	--	0	--	--
R = α -(methoxy-carbonyl)benzene	0	--	--	0	--	--
<hr/>						
P(OMe) ₃	74	15.0	1.3	52	40.0	1.7
P(OEt) ₃	52	38	1.4	28	115	1.6
P(O- <u>i</u> -Pr) ₃	35	7 hrs	1.3	25	8 hrs	1.4

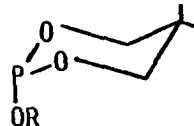
^a[acid]:[NiL₄]:[olefin] = 10:1:124

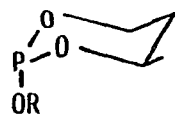
^bOn increasing the substrate to complex ratio to 992, a rate of 640 cycles in 30 min was obtained.

^cUnder the conditions in footnote b, a rate of 740 cycles in 30 min was obtained.

^dUnder the conditions in footnote b, a rate of 680 cycles in 30 min was obtained.

Table 3 (Continued)

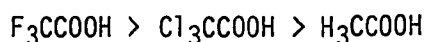
L	NiL ₄ /F ₃ CCOOH			NiL ₄ /Cl ₃ CCOOH		
	cycles over initial 30 min (±3)	t _{1/2} (min) (±0.2 min)	cis/trans (2-butene- nitrile) (±0.2)	cycles over initial 30 min (±3)	t _{1/2} (min) (±0.2 min)	cis/trans (2-butene- nitrile) (±0.2)
						
R = Me	60	35.0	1.4	30	110	1.6
R = Et	0	--	--	0	--	--
R = <u>i</u> -Pr	0	--	--	0	--	--
R = <u>t</u> -Bu	0	--	--	0	--	--
R = <u>1</u> -bornyl	0	--	--	0	--	--
R = <u>1</u> -menthyl	0	--	--	0	--	--
R = α-(methoxy- carbonyl)benzene	0	--	--	0	--	--



R = -Me	92	12.0	1.4	62	30.0	1.7
R = <u>i</u> -Pr	108	8.0	1.6	68	29.0	1.5
R = <u>t</u> -Bu	96	9.0	1.5	64	29.0	1.5
R = <u>1</u> -bornyl	0	--	--	0	--	--
R = <u>1</u> -menthyl	0	--	--	0	--	--
R = α -(methoxy-carbonyl)benzene	0	--	--	0	--	--
<hr/>						
P(OMe) ₃	74	15.0	1.3	52	40.0	1.7
P(OEt) ₃	52	38	1.4	28	115	1.6
P(O- <u>i</u> -Pr) ₃	35	7 hrs	1.3	25	8 hrs	1.4

For complexes containing 4-methyl or 4,6-dimethyl groups, the catalysis rate was found to be maximized when an isopropoxy group was in the exocyclic position. Complexes with ligands which contained either 5,5-dimethyl groups or no substitution at all were found to be active only when a methoxy group was in the exocyclic position. These differences were explained on the basis of increased steric interactions which favored dissociation in complexes with ligands containing 4,6-dimethyl groups.

Studies also revealed that the amount and type of acid used had a great effect on the overall catalysis rate. Maximum rates of isomerization were observed when a ratio of 10 H⁺ to 1 Ni was used. At higher ratios there was a marked decrease in the rates of catalysis, probably due to an increase in the amount of solvolysis of the dissociated ligand. The effect of solvolysis of the ligand is that more dissociated nickel species, such as NiL₂ and NiL are produced in solution. These complexes are more easily oxidized than the NiL₄ complexes by the acid to catalytically inactive Ni(II) species. It was also found that for a given complex the amount of catalysis increased with the type of acid used, according to the trend:



This is reasonable since protonation of the complex is expected to increase with increasing acid strength. Protonation of these NiL₄ complexes can be observed by ³¹P NMR. All of these complexes show single peaks in the ³¹P NMR spectrum in the narrow region of 155 to 150 ppm

relative to H_3PO_4 . Upon addition of acid to the solution containing the NiL_4 complex, a characteristic yellow color develops, indicative of protonation. Subsequent low temperature ^{31}P NMR analysis shows the formation of a doublet in the range from 134 to 128 ppm with a $J_{\text{P-H}}$ of 29-39 Hz. This range of coupling constants has been observed in other compounds that have hydrogen coupling to phosphorus through a metal atom (40).

In all cases, the effect of adding excess ligand retards the rate and extent of catalysis. This is most pronounced for the least catalytically active system, $\text{Ni}(\underline{11})_4/\text{F}_3\text{CCOOH}$. This agrees with the belief that the most catalytically active systems are those which have the most extensive ligand dissociation. Excess ligand would decrease the amount of dissociation to a greater extent in a less easily dissociated system.

Throughout the initial study it was shown that ligand basicity was very important in determining whether a particular complex acted as an efficient catalyst. Complexes of ligands such as 11 and 15 were shown to protonate to only a small extent (~5%) with $\text{F}_3\text{CCO}_2\text{H}$ (in benzene or methylene chloride). This small extent of protonation was shown by the failure of solutions containing these compounds to turn yellow in color upon addition of acid and the appearance of a doublet of relatively small intensity for the protonated species compared to the large singlet which is observed for the unprotonated NiL_4 complex. This lack of protonation is due in large part to the reduced phosphorus basicity of the ligand and the subsequent decrease in the overall nucleophilicity of the complex. The decrease in basicity of these ligands has been evidenced by their

higher J_{P-H} values when protonated, the higher $J_{31P-77Se}$ values for their corresponding selenides, and the higher ν_{CO} values found in their $Ni(CO)_3L$ complexes (38), compared to the corresponding values for the more basic ligands, 8 and 9, which are known to form NiL_4 complexes that fully protonate in solution (38).

The decreased basicity of 11 has been explained via the concept of increased molecular constraint (12). As can be seen in Fig. 3, the oxygen p orbitals in the bicyclic phosphorus ester are orthogonal to the phosphorus lone-pair, resulting in minimal interaction between the lone-pairs. This in turn causes a decrease in the energy of the phosphorus lone-pairs thus making the lone pair less polarizable by electron acceptors such as H^+ and BH_3 . At the same time, geometrical constraint of the P-O-C linkage causes the oxygen lone pairs to rehybridize from sp^2 to sp^3 resulting in a reduction of phosphorus-oxygen $d_{\pi}-p_{\pi}$ overlap (41). This reduction in overlap results in a decrease in the amount of electron density that is returned to phosphorus, thus causing an increase in the amount of positive charge on phosphorus. It is the combination of the orthogonality of the lone-pairs and the effects of molecular constraint which results in the decrease in basicity of 11 (12,42).

A significant result of these studies (38) was that Lewis acids such as $AlCl_3$, $ZnCl_2$ and $TiCl_3$ were found to act as efficient cocatalysts in place of protic acids, such as F_3CCO_2H . $AlCl_3$ was found to act as efficiently as H^+ in terms of the amount of isomerization catalysis observed over the course of thirty minutes.

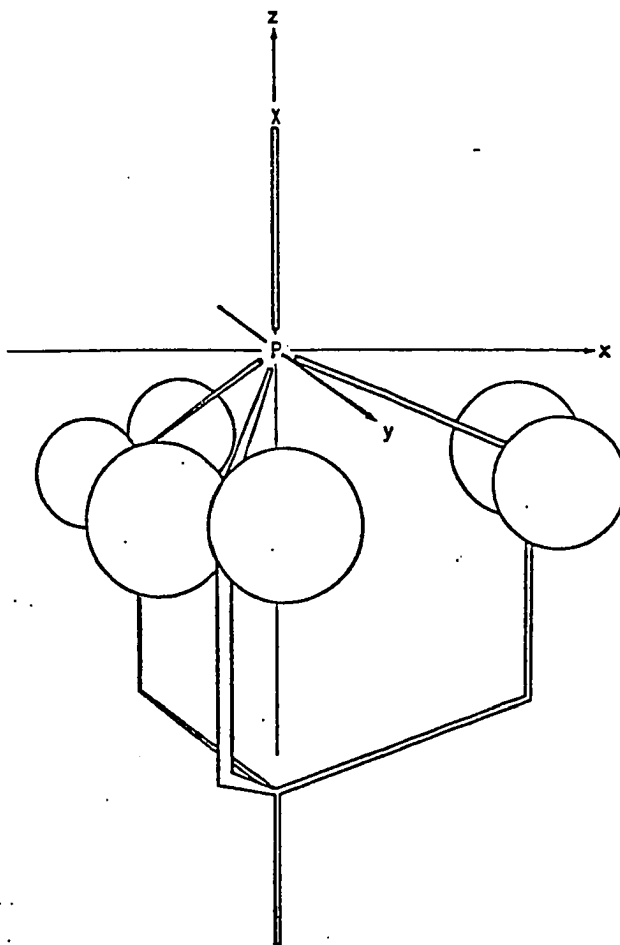
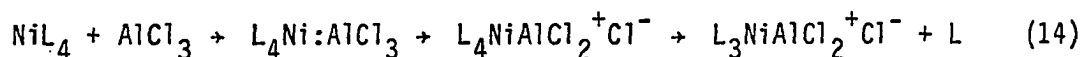
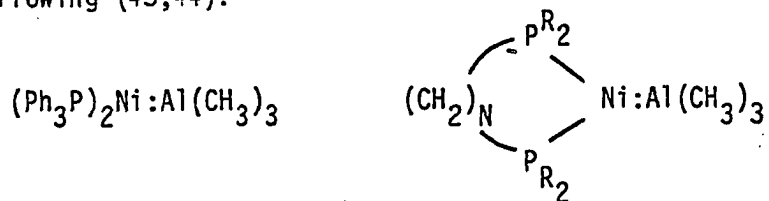


Figure 3. Geometric arrangement of the P, O, and C atoms and the ester oxygen p orbitals in a bicyclic phosphorus ester (X = lone pair or oxygen) if sp^2 hybridization is assumed (12)

Gultneh reports that for AlCl_3 , the catalytically active species is formed from a $\text{NiL}_4:\text{AlCl}_3$ adduct. Evidence for this adduct is based upon the appearance of a band in the visible spectrum of a $\text{NiL}_4/\text{AlCl}_3$ mixture in CH_2Cl_2 (λ_{max} 335 nm) which is similar to that observed for the HNiL_4^+ species. Gultneh postulates (38) that ligand dissociation to form a catalytically active species occurs upon formation of a positively charged nickel-aluminum intermediate (Eq. 14). The only evidence given



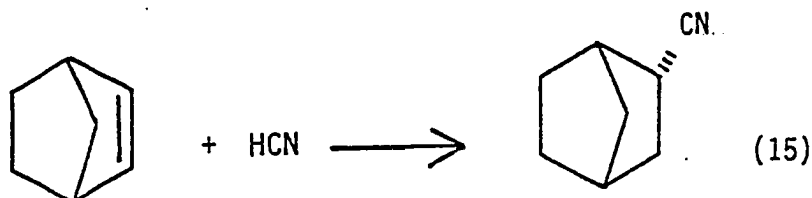
for the existence of such an intermediate is the extremely low molar conductance of $15.4 \text{ ohm}^{-1} \text{ cm}^2 \text{ mole}^{-2}$, which was observed for complex $\text{Ni}(\underline{8})_4$ and AlCl_3 in CH_3CN . However, this result still does not rule out the possible formation of a $\text{NiL}_4:\text{AlCl}_3$ adduct which is somehow involved in the catalytic mechanism, since examples of nickel complexes that form adducts with Lewis acids are known. Examples of these types of complexes are the following (43,44):



However, an alternate explanation of the role of a Lewis acid in isomerization catalysis will be described in this thesis.

Hydrocyanation of olefins

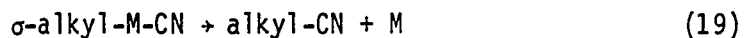
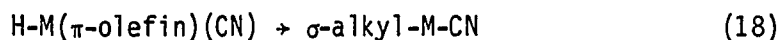
The catalytic hydrocyanation of olefins has been an area of interest to industrial chemists for many years. This interest has grown primarily because of the economic value in producing compounds such as acrylonitrile and adiponitrile from the hydrocyanation of ethylene and 1,3-butadiene, respectively. As a result, much of the data on this reaction are found in the patent literature (45,46). A recent review by Brown (47) lists many examples of transition metal complexes that are capable of catalyzing the addition of HCN to olefins. For example, $\text{Ru}(\text{PPh}_3)_3\text{Cl}_2$ (48) and $\text{Co}_2(\text{CO})_8$ (49) are both known to catalyze the hydrocyanation of $\text{CH}_3\text{CH}=\text{CHCH}_2\text{CN}$ to $\text{NC}(\text{CH}_2)_4\text{CN}$ and $\text{CH}_3\text{CH}(\text{CN})(\text{CH}_2)_2\text{CN}$. $\text{Co}_2(\text{CO})_6\text{L}_2$ (48) (where $\text{L} = \text{PPh}_3$ or $\text{P}(\text{OPh})_3$), is known to catalyze the hydrocyanation of norbornene (Eq. 15).



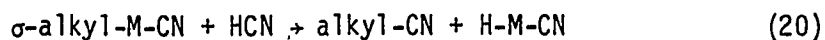
There are even more examples of hydrocyanation catalysts which contain phosphite ligands. In particular, complexes such as $\text{CoH}(\text{P}(\text{OPh})_3)_4$ (50), $\text{Ni}(\text{P}(\text{OR})_3)_4$ (51), $\text{Pd}(\text{P}(\text{OR})_3)_4$ (52) and $\text{Mo}(\text{P}(\text{OPh})_3)_3(\text{CO})_3/\text{TiCl}_3$ (53) have been shown to be effective hydrocyanation catalysts.

The mechanism of hydrocyanation has yet to be totally elucidated but the results of experiments seem to imply the following mechanism (47):

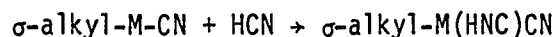




The last step in the mechanism has been a source of dispute. Kwiatek and co-workers (54,55) have proposed, based upon work with the formation of alkyl nitriles from alkylpentacyanocobaltate(III), that equation 19 should be rewritten:



This step is believed to occur via protonation of the coordinated cyanide ligand to form a coordinated hydrogen isocyanide. The isocyanide group then inserts into the metal alkyl bond and then decomposes to form an alkyl nitrile and a protonated metal species (Scheme 3).

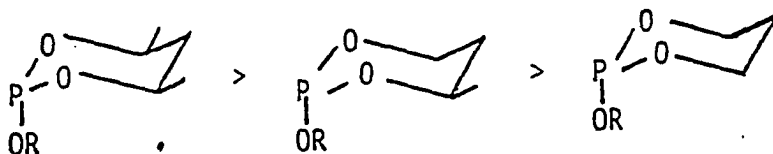


Scheme 3. Decomposition of σ -bound metal alkyl cyanide species to form alkyl nitriles (47,53)

The reason for the use of phosphite ligands rather than phosphines in these catalysts may be due in part to the increased π -acidity of the phosphite which causes the phosphite to impair the extent to which CN^- complexes to the metal atom. Other studies have shown that these metal

complexes are eventually inactivated as catalysts due to formation of metal cyanide compounds such as $\text{Ni}(\text{CN})_2$ (47) and $\text{Co}(\text{CN})_6^{-3}$ (49). The decomposition is also inhibited by adding excess ligand which again impedes the formation of these compounds. It has also been reported (56,57) that Lewis acids such as ZnCl_2 act as efficient cocatalysts in hydrocyanation. Though the mechanism of its activity is not known, it is believed that the ZnCl_2 in the presence of HCN promotes formation of the catalytically active species $[\text{HNiL}_n]^+[\text{ZnCl}_2\text{CN}]^-$.

Gultneh (38) has carried out a study of the use of the previously mentioned NiL_4 complexes as hydrocyanation catalysts. The trend observed for increased amounts of hydrocyanation of olefins such as allylbenzene, norbornene, norbornadiene, cyclopentene and cyclooctene with various monocyclic ligands was :



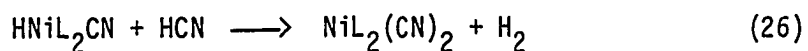
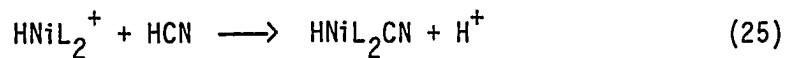
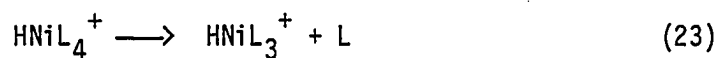
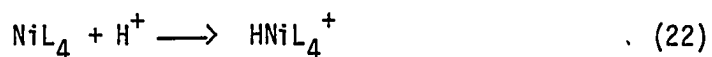
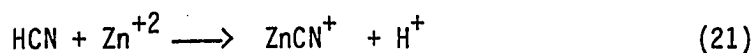
In the case of the 4-methyl and 4,6-dimethyl-1,3,2-dioxaphosphorinanes it was observed that by increasing the size of the exocyclic group from methyl to isopropyl, there was an increase in catalytic activities of the NiL_4 complexes. The extent of catalysis was found to decrease when larger groups such as menthyl or bornyl were placed in the exocyclic positions on the phosphorinane ring. However, the rates of catalysis still proceeded moderately. This was not the case in isomerization of 3-butenitrile wherein such large groups completely

deactivated the complex. Attempts to form catalytically active complexes for the hydrocyanation of olefins with bicyclic and 5-membered ring cyclic phosphite ligands proved to be unsuccessful. This is probably due in part to the reduced overall basicity of these ligands which in turn reduced the basicity of the NiL_4 complexes. Since HCN is itself such a weak acid, the degree to which the nickel atom is protonated is further reduced. The combination of these effects probably led to the inactivity of these complexes.

Previous work has shown that the more active catalyst systems for the hydrocyanation of olefins are those which contain Lewis acids (48). Gultneh (38) found ZnCl_2 to be the most active cocatalyst. Attempts to use AlCl_3 as a cocatalyst in the hydrocyanation of norbornene showed that the $\text{AlCl}_3/\text{NiL}_4$ catalyst mixture produced half the number of catalytic cycles as did the $\text{ZnCl}_2/\text{NiL}_4$ mixture. In attempts to hydrocyanate allylbenzene, the $\text{AlCl}_3/\text{NiL}_4$ mixture proved to be completely inactive, while the $\text{ZnCl}_2/\text{NiL}_4$ showed some activity. The failure to hydrocyanate any of the allylbenzene by $\text{NiL}_4/\text{AlCl}_3$ was in part due to the complete and facile isomerization of the allyl benzene to the more stable conjugated product, 1-phenylpropene. This isomerization occurred before any appreciable amount of hydrocyanation could take place.

As stated previously, the degree of isomerization of 3-butenitrile was reduced upon adding excess ligand to the catalyst mixture. During the hydrocyanation of olefins, it was found that in many cases the rate of catalysis increased when excess ligand was added. However, it was also observed that the optimum amount of excess ligand added depended

entirely on the ligand used. The optimum ratio of L/NiL₄ varied from 3 for Ni(P(OEt)₃)₄ to 18 for Ni(8)₄. The reason for adding excess ligand is to prevent complexation of more than one molecule of HCN to the nickel atom as suggested by the mechanism (Eqs. 21-26) of Gultneh (38) for the deactivation of the NiL₄ catalyst.



Formation of complexes such as NiL₂(CN)₂ would force the catalysis to stop due to the irreversible oxidation of the NiL₄ complexes to these Ni(II) species.

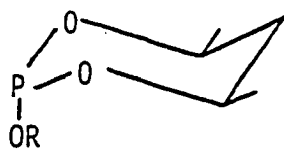
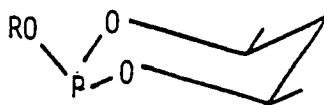
Unanswered questions in Gultneh's work

Though quite extensive, Yilma Gultneh's work left some unanswered questions:

1. Tolman had been very explicit in proving that steric factors were extremely important in determining the extent of dissociation in NiL_4 complexes. However, it would seem reasonable that electronic effects should have some role in the catalytic properties of a given NiL_4 complex. The question was raised if it would be possible to isolate this electronic effect by selectively comparing the catalytic activity of some NiL_4 complexes containing ligands that were heretofore untried. Until now only complexes which contained ligands that had alkoxy exocyclic groups had been tried. We were interested in how the replacement of an alkoxy group by an amine group in the exocyclic position of the ligand would change the activity of the resulting complex. This was of special interest since the electronic properties of these types of ligands have been found to be markedly different from those with alkoxy exocyclic groups (58).

2. In explaining the catalytic properties of the NiL_4 (ZnCl_2 or AlCl_3) system for the isomerization of olefins, Gultneh (38) proposed that the catalytically active intermediate was a dissociated $[\text{NiL}_4\text{ZnCl}^+]\text{Cl}^-$ complex or an $\text{NiL}_4:\text{AlCl}_3$ adduct. However, the evidence for the existence of these intermediates was tenuous at best. It was necessary to prove concretely the existence of these intermediates or else develop an alternative mechanism which could better explain the results that had been obtained.

3. Mosbo (58) had shown that 1,3,2-dioxaphosphorinanes existed as two different conformational isomers, A and B.

AB

It was shown that when the exocyclic group was an alkoxy group, conformation A was the more thermodynamically stable isomer. Isomer B was considered to be the thermodynamically more unstable isomer since the lone-pair on phosphorus was repelled by two lone-pair p orbitals on each of the two cyclic oxygens. A consequence of this isomerism is that the basicity of these isomers are different. Previous work has shown that isomer B is more basic than isomer A (59). This increase in basicity has been ascribed to lone pair interactions which raises the energy of the phosphorus lone pair thus making it more polarizable. Gultneh (38) contends that large exocyclic groups on these 1,3,2-dioxaphosphorinanes are forced to adopt an equatorial position, with respect to the ring, due to steric interactions with the other ligands contained in the complex. This would then change the basicity of the ligand which could then influence the catalytic activity of the complex. In order to prove or disprove this contention, we deemed it worthwhile to attempt an x-ray structural analysis of a NiL_4 complex which contained a ligand with a large exocyclic group. This was done in order to determine if the ligand was forced to adopt the more basic conformation due to steric interactions.

An x-ray structural analysis of one of these complexes would also be helpful in determining if there are indeed steric interactions between

the 4,6 methyl groups on adjacent ligands, which would promote ligand dissociation.

4. Gultneh has shown that there is a 20 fold increase in the catalytic activity of $\text{Ni}(\underline{9})_4$ versus its acyclic analogue, $\text{Ni}(\text{P}(\text{O}-\underline{i}\text{-Pr})_3)_4$. In order to investigate the effect of geometrical constraint on the P-O-C angles in the cyclic 4,6-dimethyl phosphorinanes and how that effect influences the catalytic properties of a NiL_4 complex, it was thought useful to prepare the phosphinite analogues 27 and 28. As can be seen in Table 4, there is a marked decrease in the difference in catalytic activity of the NiL_4 complexes of the phosphinite ligands versus the phosphite ligands. It was suggested (38) that there is only a small difference in the steric requirements of 9 and $\text{P}(\text{O}-\underline{i}\text{-Pr})_3$. Therefore, it was thought that the differences in the catalytic activities of the complexes could be attributed to small differences in the electronic properties of the ligands in going from $\text{P}(\text{O}-\underline{i}\text{-Pr})_3$ to 9.

In describing the properties of 27, Gultneh (38) gives no information about the distribution of conformational isomers. It is known (60) that analogous phosphorinanes do show a conformational equilibrium between conformers (Eq. 27).

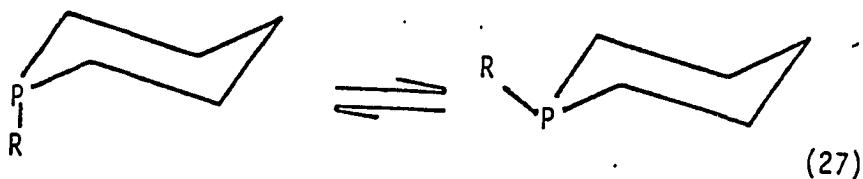


Table 4. Rates of isomerization of 3-butenitrile by $\text{NiL}_4/\text{F}_3\text{CCOOH}$ systems in benzene at 25^oa (38)

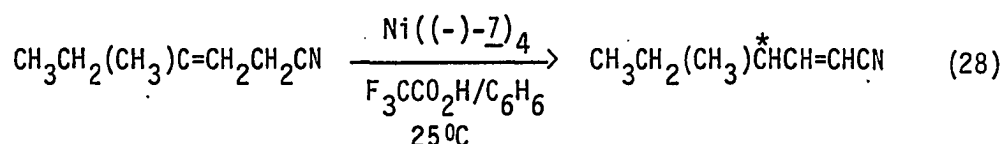
L	Cycles over 30 min (± 2)	cis/trans (2-butenitriles) (± 0.1)
<u>25</u>	32	1.0
<u>28</u>	36	1.1
$\text{P}(\text{O-}i\text{-Pr})_3$	35	1.3
<u>9</u>	740	1.6

^a $\text{Ni}/\text{H}^+/\text{3-butenitrile} = 1/10/124$

The equilibrium position is determined in part by the steric bulk of the exocyclic R group. Quin and Featherman (60) have shown that when R = CH_3 , the equatorial conformation is preferred by only a small margin ($k_e/a = 2.03$). Therefore, in the case of 27 and 28 it should be reasonable to assume that a similar isomeric distribution between equatorial and axial isopropoxy groups should exist. Since the literature provided no information on the conformational distribution of these cyclic phosphinites, it was thought to be important to determine this first and then attempt to separate 27 from 28. Once this separation was completed, it would be possible to prepare NiL_4 complexes of both isomers and investigate any differences in their catalytic activities. In fact, by using a mixture of isomers it would be possible to prepare up to five different complexes of the type $\text{Ni}(\text{27})_{4-n}(\text{28})_n$ where $n = 0, 1, 2, 3, 4$. Since separation of these complexes would be difficult, there would be no

way of knowing if either ligand caused the complex to be more active than the other.

5. The use of optically active ligands in transition metal catalysts used for asymmetric synthesis has become very important (61,62). It was found that Ni((-)-7)₄ acted as catalyst for the asymmetric isomerization of prochiral olefins (Eq. 28).



By the use of chiral shift reagents, it was determined that a 52% enantiomeric excess for (Eq. 28) had been obtained. It was thought that by using an optically active ligand which contained a methyl group at the equatorial 4,6 positions, a higher degree of conversion and enantiomeric excess might be obtained. The use of Ni(36)₄ as an asymmetric isomerization catalyst in equation 28 will be detailed herein.

6. The use of NiL₄ complexes (where L = 2-alkoxy-1,3,2-dioxaphosphorinane) as efficient hydrocyanation catalysts are now well documented (38). However, the use of these complexes in hydrocyanating 1,3-butadiene to form adiponitrile had yet to be explored. Due to its industrial applications, it was of interest to see if our best hydrocyanation catalysts, Ni(8)₄ and Ni(9)₄ could assist in the production of adiponitrile from 1,3-butadiene.

Heterogenized homogeneous catalysts

The use of catalysts in chemical reactions has become one of the most important areas of chemical research (63). When discussing this

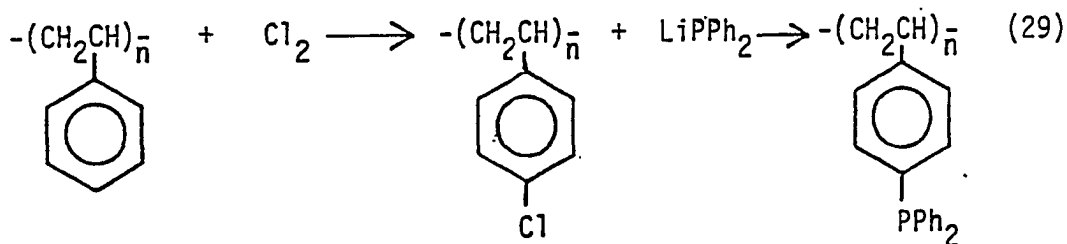
area, one must differentiate between two main classes; namely, heterogeneous and homogeneous catalysis. Heterogeneous catalysis implies that the catalytic reaction takes place at the interface of two or more phases. For example, in the catalytic hydrogenation of an olefin by a metal, studies have shown that the actual reaction takes place at the interface of the gas and solid phases (63). Homogeneous catalysis usually implies that the reaction occurs in the same phase, as is the case when the catalyst and reactants are dissolved in a solvent. As can be seen in Table 5, the advantages and disadvantages of both types of catalysis are numerous. In recent years, many reviews have been published which detail previous attempts to prepare heterogenized homogeneous catalysts in which a transition metal complex, which is known

Table 5. Relative advantages and disadvantages of different types of catalysts

Type of catalysis	Advantages	Disadvantages
Heterogeneous	<ol style="list-style-type: none"> 1. ease of separation 2. high mechanical strength 3. high activity 4. use in packed and fluidized bed reactors 	<ol style="list-style-type: none"> 1. lack of knowledge of actual active sites 2. limited access to catalyst's active site 3. High temperatures and pressures needed
Homogeneous	<ol style="list-style-type: none"> 1. well documented mechanistic information available 2. mild operating conditions 3. electronic and steric properties of ligands can be changed to improve catalysis 	<ol style="list-style-type: none"> 1. difficult to separate catalyst from reaction mixture 2. catalysts tend to be more sensitive to O₂, H₂O and temperature

to act as a homogeneous catalyst, is bound to a solid support (64,65,66). These hybrid catalysts have been shown to possess properties which incorporate the best features of each class of catalyst, while at the same time reducing some of the disadvantages of both. In particular, it has been found that these hybrid catalysts allow for easy separation of the catalyst from a reaction mixture, in some cases resulting in a reduction in the loss of valuable precious metal catalyst. At the same time, these catalysts are often more durable than their homogeneous analogues, allowing for in some cases several recycles of the supported catalysts (66).

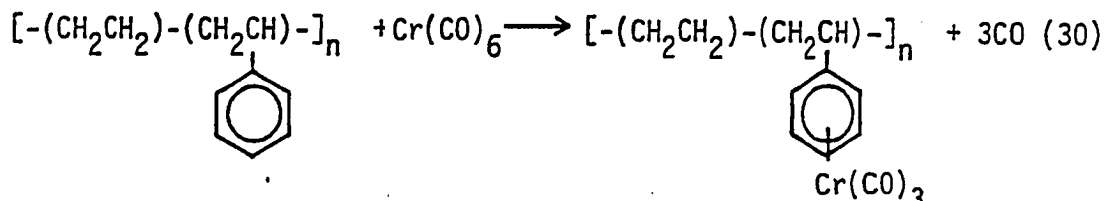
Two basic types of solid supports have been used to anchor homogeneous catalysts. The first type includes organic polymer supports, usually consisting of a polystyrene divinyl benzene resin which is functionalized with phosphine, cyclopentadiene, bipyridyl, or benzene ligands. Equation 29 illustrates a common technique used to prepare these types of functionalized supports.



The metal complex is then anchored on the support by exchanging one of its ligands with a -PPh_2 group. Grubbs and co-workers have used this technique to heterogenize $\text{Rh(PPh}_3)_3\text{Cl}$ (67). This type of support has

also been used to anchor $\text{H}_4\text{Rh}_4(\text{CO})_{12}$ (68), $\text{Ni}(\text{CO})_2(\text{PPh}_3)_2$ (69) and $\text{W}(\text{CO})_6$ (70), to cite just a few of many examples.

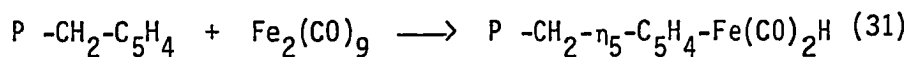
Polystyrene-divinylbenzene co-polymers have also been used to directly bind metal carbonyls such as $\text{Cr}(\text{CO})_6$ (Eq. 30).



Complexation has been accomplished by subjecting a mixture of polystyrene resin, metal carbonyl, and solvent, to conditions such as heat (71), high pressure (72), and ultra violet radiation (73).

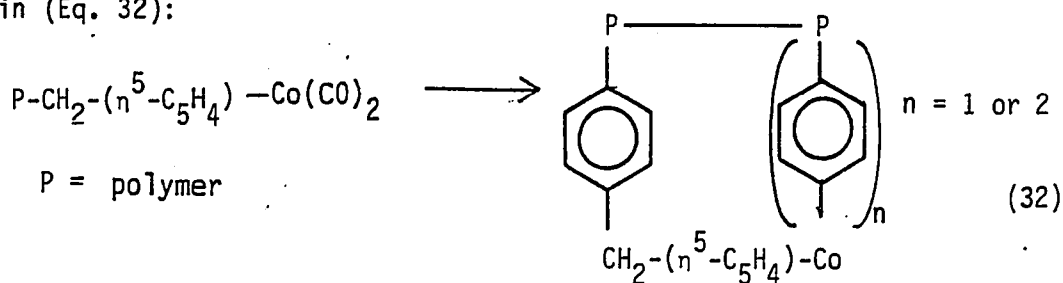
Pittman (73) and Masuda and Stille (74) have been successful in forming heterogeneous catalysts by polymerizing soluble metal complexes which contain ligands having functionalities such as olefins. Stille has also been successful in producing polymers which contain optically active ligating groups that can bond to certain metal complexes. These polymers have been used successfully as catalysts for asymmetric synthesis (75).

One of the advantages of these catalysts is their ability to stabilize complexes which are not stable in solution. Gubtosa and Brintzinger (76) have shown that a $\text{Fe}(\text{CO})_2\text{H}$ unit can be stabilized on cyclopentadienyl functionalized polystyrene (Eq. 31). The resulting



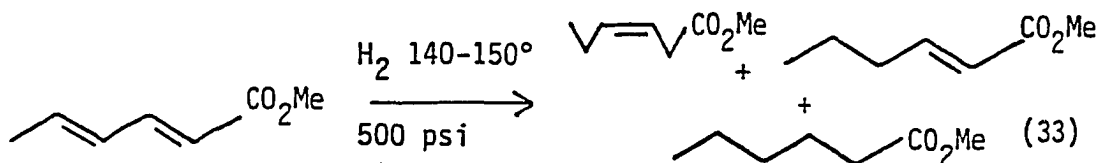
P = polymer backbone

anchored complex has been found to be indefinitely stable, whereas in solution, $(\eta^5\text{-C}_5\text{H}_5)\text{Fe}(\text{CO})_2\text{H}$ quickly dimerizes with subsequent loss of hydrogen to form $[(\eta^5\text{-C}_5\text{H}_5)\text{Fe}(\text{CO})_2]_2$ (76). They have also shown that a $\text{Co}(\text{CO})_2$ unit can be supported similarly, by reaction of the cyclopentadienyl-derivatized resin and $\text{Co}_2(\text{CO})_8$. Subsequent irradiation of the polymer causes a loss of CO to form a bis-arene complexed cobalt resin (Eq. 32):



Whereas, complexes of the type $\eta^5\text{-(C}_5\text{H}_5)_2\text{Co}_2(\text{CO})_2$, $\eta^5\text{-(C}_5\text{H}_5)_2\text{Co}_2(\text{CO})_3$, and $\eta^5\text{-(C}_5\text{H}_5)\text{Co}_3(\text{CO})_3$ were observed to form upon irradiation of solutions containing the homogeneous analogue $\eta^5\text{-(C}_5\text{H}_5)\text{Co}(\text{CO})_2$ (77). Thus, these types of polymers can be used to stabilize metal moieties that would be otherwise unstable in solution. This provides the possibility of producing new types of catalysts that could not be obtained by any other means.

One of the main disadvantages in the use of these catalysts is that the rates of catalysis are often lower than those observed for the analogous homogeneous catalysts. Pittman and co-workers (78) have shown that $\text{Cr}(\text{CO})_6$ can be supported on polystyrene and that methyl sorbate can be hydrogenated with such a catalyst (Eq. 33). At 160° , the selectivity



for (Z)-methyl-3-hexenoate is 96-98% for 100% conversion in 24 hrs, while at 140° the selectivity is 99%. Cais and co-workers (79), however, have reported 95% conversion for the hydrogenation of methyl sorbate using $\text{Cr}(\text{CO})_6$ under the same conditions in only 7 hrs. Pittman and co-workers (80) have also reported a retardation in the rate of hydroformylation of 1-pentene using $\text{Rh}(\text{PPh}_3)_3\text{H}(\text{CO})$ bound to polystyrene. It was found that at 40° and 250 psig, the polymer-bound $\text{Rh}(\text{PPh}_3)_3\text{H}(\text{CO})$ was 0.22 times as active as the homogeneous catalyst. While at 60° and 800 psig the ratio of activity increased to 1.08. It has also been found (80) that the rate at which anchored $\text{Ni}(\text{PPh}_3)_2(\text{CO})_2$ cyclooligomerizes butene at 112°C is equal to the rate at which the analogous homogeneous catalyst operates at 90°.

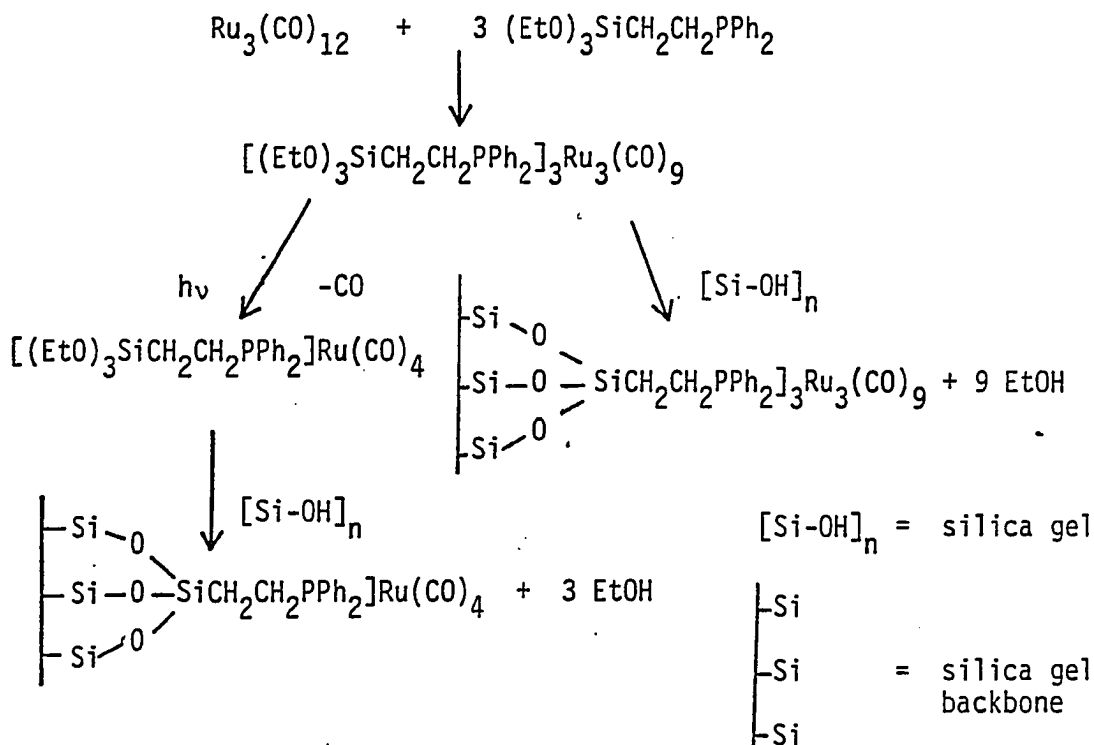
These reductions in catalysis rates have been ascribed to diffusional limitations created by the resin for migration of the substrate into the active site. The rate of diffusion is dependent upon the pore size within the resin which in turn is dependent upon the amount by which the resin swells upon being placed in a solvent. However, the rate of diffusion of the substrate into the resin is also dependent upon

polarity gradients which develop between the bulk solvent and active sites within the resin. Therefore, by carefully choosing the degree of crosslinking in the resin (the more crosslinking the smaller the pore size), and the type of solvent system used, one is able to control the selectivity of the catalyst toward a particular reaction or substrate (66).

In order to circumvent the problems of swelling of organic polymers as supports for transition metal catalysts, many workers have tried anchoring these complexes to inorganic supports such as silica, alumina, zeolites or derivatized silica and alumina due to their increased rigidity (66). Metal carbonyls such as $\text{Cr}(\text{CO})_6$ (81) and $\text{Ru}_3(\text{CO})_{12}$ (82) have been supported on Al_2O_3 and SiO_2 , respectively, and shown to function as hydrogenation catalysts. In these types of catalysts, the adherence of the complex to the support is maintained by strong carbonyl-surface interactions (81,82).

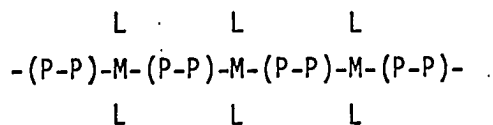
Attachments of metal complexes can also be accomplished by placing ligands on the metal which contain functional groups which further react and bind to OH groups on the surface on the support. Recently, Wrighton and Liu (83) have shown that $\text{Ru}_3(\text{CO})_{12}$ can be supported on silica in two ways (Scheme 4).

Wrighton has shown that these supported compounds can act as isomerization or hydrosilylation catalysts under the proper conditions. Capka and Hetflejs (84) have also succeeded in attaching groups as $-\text{PPh}_2$, $-\text{SiCH}_2\text{CH}_2\text{PPh}_2$ and $-\text{Si}(\text{CH}_3)_2(\text{CH}_2)_3\text{CN}$ to inorganic materials such as γ -alumina, zeolites, and glass in order to prepare similar types of catalysts.



Scheme 4. Attachment of metal carbonyl compounds to derivatized silica gel (83)

Based upon our knowledge of the NiL_4/H^+ catalyst system we began a study to find ways to heterogenize these homogeneous catalysts. We were successful in designing a new type of polymeric complex, which also functions as an isomerization catalyst. The polymer produced was of the type:



where M is a metal atom which is connected to other atoms by P-P, a diphosphorus nonchelating ligand. This ligand was designed to mimic as closely as possible the electronic and steric properties of the ligands contained within the homogeneous catalyst. The synthesis and properties of these types of catalysts will be described in this thesis.

We have also been able to heterogenize these NiL_4 catalysts by supporting them on cation exchange resins. In our case, macroreticular resins were used to ensure diffusion of the NiL_4 complex into the bead. The preparation, activities, and formulations of these catalysts will be discussed.

EXPERIMENTAL PROCEDURES

All solvents were reagent grade or better. The following solvents were further purified by distillation from drying agents: diethyl ether (K metal); tetrahydrofuran, toluene and benzene (Na), methanol and pyridine (CaH₂); acetonitrile (P₄O₁₀); acetone (molecular sieves).

These chemicals were obtained from the following suppliers and were used as received: pentaerythritol, 2,2-dimethyl propanediol, 1,3-butanediol, 1,1,1-trishydroxymethylethane, triphenyl phosphine, 1,3,5-trihydroxy benzene, 1,2,4-butanetriol, diethylaluminum chloride (1 M solution in hexane), and triethylaluminum were obtained from Aldrich Chemical Co. Nickel carbonyl, nickel tetrafluoroboratehexahydrate, and the macroreticular resins were obtained from Alfa-Ventron, Inc. 1,4-Dibromo-benzene and 4,4-dibromobiphenyl were obtained from Eastman Kodak. 3-Methyl-1-pentene-3-ol was obtained from Fluka A.G. Rhodium trichloride trihydrate was obtained from Engelhard Minerals.

Proton NMR spectra were obtained on either a Varian EM-360 or a Perkin-Elmer/Hitachi RB-20 NMR spectrometer. Me₄Si was used as an internal standard in all cases. ³¹P NMR spectra were obtained on samples contained in 10 mm tubes on either a Bruker HX-90 spectrometer operating at 36.4 MHz or a Bruker WM-300 spectrometer operating at 121.5 MHz. In both cases, the spectrometers operated in the FT mode with an internal ²H lock provided by ²H atoms contained in the solvent. The external standard was 85% H₃PO₄ sealed in a 1 mm capillary tube held coaxially in the sample tube by a Teflon vortex plug. All downfield shifts of H₃PO₄

were considered positive. ^{13}C NMR spectra were obtained on a JEOL FX 90Q spectrometer operating at 22.5 MHz in the FT mode. An internal ^2H lock was provided by the ^2H atoms contained in the solvent. The carbon atoms of the solvent (CDCl_3) acted as a reference. ^{27}Al NMR spectra were obtained on a Bruker WM-300 spectrometer operating in the FT mode at a frequency of 78.21 MHz. A sealed 1 mm diameter capillary tube containing a 1 M solution of AlCl_3 dissolved in D_2O acted as both an external reference and an external ^2H lock. ^{11}B NMR spectra were also obtained on a Bruker WM-300 NMR spectrometer operating at 96.3 MHz in the FT mode. An internal ^2H lock was maintained by the ^2H atoms contained in the solvent. All spectra were referenced to $\text{Et}_2\text{O}:\text{BF}_3$.

Mass spectra were obtained on a Finnegan 4000 or an AE1 MS902 mass spectrometer. UV-visible spectra were obtained on a Perkin-Elmer 320 UV-visible spectrometer. Quartz cells (1 cm x 1 cm x 10 cm) were used to obtain spectra of compounds contained in organic solvents. Fisher brand polystyrene (10 mm x 10 mm x 45 mm) cuvetts were used to obtain spectra of compounds contained in aqueous solutions. Infrared spectra were obtained using a Perkin-Elmer 281 double beam infrared spectrometer. In all cases, the spectra were obtained on liquid solutions contained in matched NaCl solution in cells.

Analysis of catalytic isomerization was performed on a Varian series 1700 gas chromatograph equipped with a thermal conductivity detector. Separations were carried out on a 8' x 0.25" copper column packed with 10% diisodecylphthalate on chromosorb P. The column and support were prepared by a previously described method (85,86). Analyses of mixtures

obtained in the catalytic hydrocyanation of 1,3-butadiene were carried out using a Varian model 3700 gas chromatograph equipped with a flame ionization detector, automatic peak integrator, and a glass capillary column containing SE-30 as a stationary phase.

All preparations of NiL_4 complexes were carried out under a nitrogen atmosphere. All manipulations involving these complexes were done using the appropriate Schlenk vessels or nitrogen-filled glove bags.

Experiments on the catalytic isomerization of 3-butenitrile were carried out using the following procedure. The NiL_4 complex (0.10 mmole) was placed in a 25 ml nitrogen-flushed roundbottom flask, equipped with a stirring bar and rubber septum. The flask was then placed in a water bath maintained at $25^\circ C \pm 0.2^\circ C$. Benzene (5.0 ml) was added via a syringe through the septum into the flask. The flask and its contents were equilibrated for 30 min. in the cooling bath and timing began after addition of 0.88 g (12 mmole) of 3-butenitrile and 1 ml of a 1.0 M solution of F_3CCO_2H in benzene. Periodically, 0.5 ml samples were removed from the solution for GC analysis. Calculations of yields of isomerized products were carried out by cutting out and weighing the peaks in the chromatogram. The yields were calculated based upon response factors which were determined independently for 3-butenitrile, cis-2-butenitrile, and trans-2-butenitrile. The presence of cis and trans 2-butenitrile in the mixture was initially confirmed by preparative gas chromatography and subsequent proton NMR analysis.

Catalytic hydrocyanations of olefins were carried out by the following procedure. HCN was prepared before each run by adding

approximately 10 mls of 18 M sulfuric acid to approximately 20 g of NaCN contained in a nitrogen-flushed 100 ml flask. The gaseous hydrogen cyanide produced was transferred via a cannula into a N₂ filled centrifuge tube which was stoppered with a rubber septum. The tube was chilled to -78°C in order to facilitate the collection of the HCN.

Attempts to hydrocyanate norbornene were then carried out using the method of Gultneh (38). Attempts to hydrocyanate 1,3-butadiene were carried out by the procedure of Drinkard and Lindsey (51). The NiL₄ complex (0.07 mmole) was placed in a nitrogen-flushed 3-necked 25 ml flask which had been fitted with a rubber septum. Xylene (4.0 mls) was then added to the flask via a syringe. In some experiments, the flask would also be charged with ZnCl₂ and excess ligand. The flask was then heated to 120° ± 0.5°C and allowed to equilibrate for 15 minutes. The 1,3-butadiene was bubbled slowly (10 ml/1 min.) into the centrifuge tube containing the liquid HCN held at 0°. The HCN/1,3-butadiene gas mixture was transferred from the tube into the flask via a cannula which was held below the level of the NiL₄/xylene solution. Upon addition of the equivalent of 1 liquid ml of HCN over the course of 2 hrs., the experiment was ended and samples were removed for capillary gas chromatographic analysis. The yields of adiponitrile and other products from the reaction were obtained by integration of the peaks contained in the chromatogram. The existence of adiponitrile in the mixture was confirmed by comparison of the chromatogram to a chromatogram of pure adiponitrile recorded under the same conditions.

The purity of a particular ligand or phosphorochloridite was determined by its boiling point and ^{31}P NMR spectrum. The purity of a NiL_4 compound was determined by its ^{31}P NMR spectrum exclusively. It was observed (38) that the different classes of compounds showed single peaks within a narrow range of chemical shifts (Table 5). In all cases, these compounds appeared as sharp singlets in the ^{31}P NMR spectrum. A particular compound was judged to be pure if it exhibited no other peaks in the ^{31}P NMR spectrum or if the area of the peak comprised 95% or greater of the total area of all peaks contained in the spectrum.

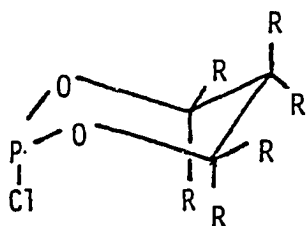
Preparations

KSeCN This compound was prepared via the procedure of Waitkins and Shutt (87).

$\text{Ni}(\text{CH}_2=\text{CHCN})_2$ This compound was first prepared by Schrauzer (88). However, the compound was prepared here by the following simplified procedure. $\text{Ni}(\text{CO})_4$ (6.60 g, 38.6 mmole) and 60.0 ml of acrylonitrile was added to a nitrogen-flushed 250 ml 2-necked flask equipped with a condenser and nitrogen inlet. The mixture was refluxed under nitrogen for 2 hrs and then cooled to room temperature. The orange precipitate which formed was allowed to settle and the supernatant was removed via a cannula. The product was washed three times with 25 ml portions of dry, degassed ether and the resulting solid was dried under a stream of nitrogen gas. The material was used immediately without further purification.

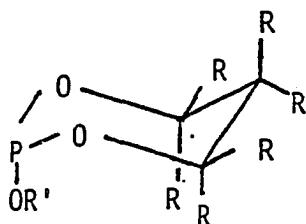
Table 6. Ranges of chemical shift (rel. to H_3PO_4) for compounds discussed in this thesis.

Class of compound	^{31}P NMR chemical shift range (ppm)
-------------------	---



160-180

R = Me or H in various combinations



120-135

R = Me or H in various combinations

R' = Me, Et, *i*-Pr, *sec*-Bu, *t*-Bu, or Ph

NiL_4

140-170

L = Phosphite

2-Chloro-1,3,2-dioxaphosphorinane (1) This compound was prepared via the method of Verkade and co-workers (89) with the following adjustment. Triethyl amine was not employed; instead, the HCl produced by the reaction of the diol and PCl_3 was removed by passing a slow stream of nitrogen through the flask during the course of the reaction. The compound was obtained in 62% yield after distillation ($b_4 = 47-50^\circ$, lit. $b_5 = 36-38^\circ$ (89); ^{31}P NMR (C_6D_6) 150.8, lit. 153.5 (89)).

2-Chloro-5,5-dimethyl-1,3,2-dioxaphosphorinane (2) This compound was prepared in 59% yield from the reaction of 2,2-dimethyl-1,3,-propanediol and PCl_3 via the same procedure used to prepare 1 ($b_{12} = 70^\circ$, lit. $b_{12} = 70^\circ$ (89); ^{31}P NMR (C_6D_6) 146.1, lit. 146.0 (89)).

2- β -Chloro-4- α -methyl-1,3,2-dioxaphosphorinane (3) This compound was prepared in 59% yield by the reaction of 1,3-butanediol and PCl_3 by the procedure used for 1. ($b_3 = 59^\circ$, lit. $b_{0.5} = 30^\circ$ (89); ^{31}P NMR (C_6D_6) 150.8).

2- β -Chloro-4,6- α,α -dimethyl-1,3,2-dioxaphosphorinane (4) This compound was prepared in 55% yield by the reaction of meso-2,4-pentanediol and PCl_3 using the procedure of 1. ($b_{13} = 72^\circ$, lit. $B_{12} = 71-73^\circ$; ^{31}P NMR (C_6D_6) 148.0).

2-Methoxy-5,5-dimethyl-1,3,2-dioxaphosphorinane (5) This compound was prepared via the method of Gultneh (38).

2-sec-Butyl-5,5-dimethyl-1,3,2-dioxaphosphorinane (6) This compound was prepared via the method of Gultneh (38).

2- β -Methoxy-4- α -methyl-1,3,2-dioxaphosphorinane (7) This

compound was prepared via the method of Gultneh (38).

2- β -Methoxy-4,6- α,α -dimethyl-1,3,2-dioxaphosphorinane (8) This

compound was prepared via the method of Gultneh (38).

2- β -Phenoxy-4,6- α,α -dimethyl-1,3,2-dioxaphosphorinane (10) To a

solution of 10.0 g (0.0595 mol) of 4 in 50 ml of dry ether at 0°C was added a solution of 5.61 g (.0597 mole) of phenol and 6.00 g (0.0594 mole) triethyl amine in 25 ml of ether. The addition was carried out dropwise over a period of 0.5 hour. The mixture was stirred for an additional hour and then filtered. The ether was removed on a rotary evaporator. The product was distilled in 76% yield. ($b_5 = 115-120^\circ$; ^{31}P NMR (C_6D_6) 119.2; ^1H NMR (CDCl_3) 7.15m 5H C_6H_5 , 4.65m 2H CH, 1.6m 2H CH_2 , 1.2d ($J_{\text{H-H}} = 6 \text{ Hz}$) 6H CH_3).

4-Methyl-2,6,7-trioxa-1-phospha-bicyclo[2.2.2]octane (11) This

compound was prepared via the method of Verkade and co-workers (90).

2,7,8-Trioxa-1-phospha-bicyclo[3.2.1]octane (12) This compound

was prepared via a literature method (91).

2,8,9-Trioxa-1-phosphaadamantane (13) This compound was prepared

via the method of Hutteman (92).

2-Chloro-1,3,2-dioxaphospholane (14) This compound was prepared

via a literature method (93).

2-Isopropoxy-1,3,2-dioxaphospholane (15) This compound was

prepared via a literature method (93).

2-R-1,3,2-dioxaphosphorinane (R = diethylamino (16), R = piperdino

(17)) These compounds were prepared by reacting 0.10 moles of 1 and 0.20 moles of the corresponding amine in 100 ml of ether via a method similar to one described by Denney and Chang (94). Compounds 16 and 17 were obtained in 65 and 81% yield, respectively, upon distillation (16: $b_{15} = 78-84^\circ$; ^{31}P NMR (C_6D_6) 146.6; (17): $b_{10} = 90-95$, ^{31}P NMR (C_6D_6) 141.3).

2- α -R-4- α -methyl-1,3,2-phosphorinane (R = Diethylamino (18), R =

piperdino (19)) These compounds were prepared via the method of Denney and Chang (94).

2-R-5,5-dimethyl-1,3,2-dioxaphosphorinane (R = dimethylamino (20)

R = piperdino (21)) These compounds were prepared by reacting 0.1 mole of 2 and 0.2 mole of the corresponding amine in 150 ml of ether at 0°C . The amine hydrochloride was filtered and washed with ether. The ether was removed on a rotary evaporator and the resulting solid was sublimed. Compound 20 was sublimed at $27^\circ/0.05$ Torr resulting in a yield of 88%. Compound 21 was sublimed at $60^\circ/0.25$ Torr resulting in a yield of 71% ((20): $m = 28-29^\circ$, ^{31}P NMR (C_6D_6) 144.0; (21): $m = 65^\circ-67^\circ$, ^{31}P NMR (C_6D_6) 142.3).

$\text{Ni}(\text{P}(\text{OMe})_3)_4$

This compound was prepared by a literature procedure (95).

$\text{Ni}(\text{P}(\text{OEt})_4)_4$

This compound was prepared via the method of Vinal and Reynolds (96).

Ni(P(OPh)₃)₄ This compound was prepared by a literature procedure (97).

NiL₄(L = 5, 6, 7, 8, 9, 10, 12, 15) These compounds were prepared via the procedure of Gultneh (38).

Ni(13)₄ To a suspension of 0.25 g (0.0015 mole) of Ni(CH₂=CHCN)₂ in 10 ml of toluene was added 0.98 g (0.0061 mole) of 13 dissolved in 5 ml of toluene. A white solid precipitated after 30 min of stirring. The solid was recrystallized from ethanol in 48% yield (m = decomp > 265°, ³¹P NMR (C₆D₆) 153.0, lit. 153.0 (98)).

Ni(18)₄ To a suspension of 0.49 g (0.0029 mole) of Ni(CH₂=CHCN)₂ was added 2.1 g (0.012 mole) of 18 dissolved in 5 ml of toluene. The mixture was stirred for 1 hr. and the toluene was removed under vacuum to yield a yellowish-white solid. The solid was chromatographed on an alumina column to yield a white powdery solid in 42% yield (³¹P NMR (C₆D₆) 163.6).

2-β-Phenoxy-4,6-α,α-dimethyl-2-α-seleno-1,3,2-dioxaphosphorinane

(22) Neat 10 (2.00 g (0.00881 mole)) was added to a solution of 1.26 g (0.00881 mole) of KSeCN dissolved in 25.0 ml of dry acetonitrile and the mixture was stirred for 2 hrs. The solution was filtered and the acetonitrile was removed on a rotary evaporator. A white solid was obtained in 94% yield (³¹P NMR (CD₃CN) 57.4d J_{31P-77Se} = 1024 Hz).

3,9-Dimethyl-2,4,8,10-tetraoxa-3,9-diphosphaspiro[5.5]undecane

(23) This compound was prepared by White (99). However, attempts to repeat this preparation were unsuccessful. Therefore, the following procedure was used. In a 50 ml flask equipped with a distillation apparatus was placed 6.8 g (0.051 mole) of $C(CH_2OH)_4$ and 11.8 g (0.0952 mole) of $P(OMe)_3$. The flask was heated to $100^\circ C$ and methanol slowly began to distill off. Heating was maintained for approximately five hours. At this point, not quite all the $C(CH_2OH)_4$ had dissolved in the $P(OMe)_3$. The mixture was placed under vacuum in order to remove any residual trimethyl phosphite and methanol. Sublimation of the crude material at $95^\circ/2$ mm yielded the product in 30% yield ($m = 122-125^\circ$, lit. $124-7^\circ$ (99); ^{31}P NMR (C_6D_6) 126.1).

$[Ni(23)(L')_2]_n$ $L' = P(OMe)_3$, 5, 7 In 20 ml of dry acetonitrile contained in a nitrogen-flushed 50 ml flask was dissolved 0.0010 moles of the NiL'_4 complex and 0.25 g (0.0010 mole) of 23 dissolved in 5 ml of acetonitrile was added to the flask via syringe. After 2 minutes of stirring, a thick gelatinous precipitate formed in the flask. The mixture was stirred for an additional 30 min., then filtered and repeatedly washed with fresh acetonitrile to remove any unreacted NiL'_4 , 23, or L' . The white solid obtained was dried for several hours under vacuum. Attempts to dissolve this solid in various organic solvents proved to be unsuccessful.

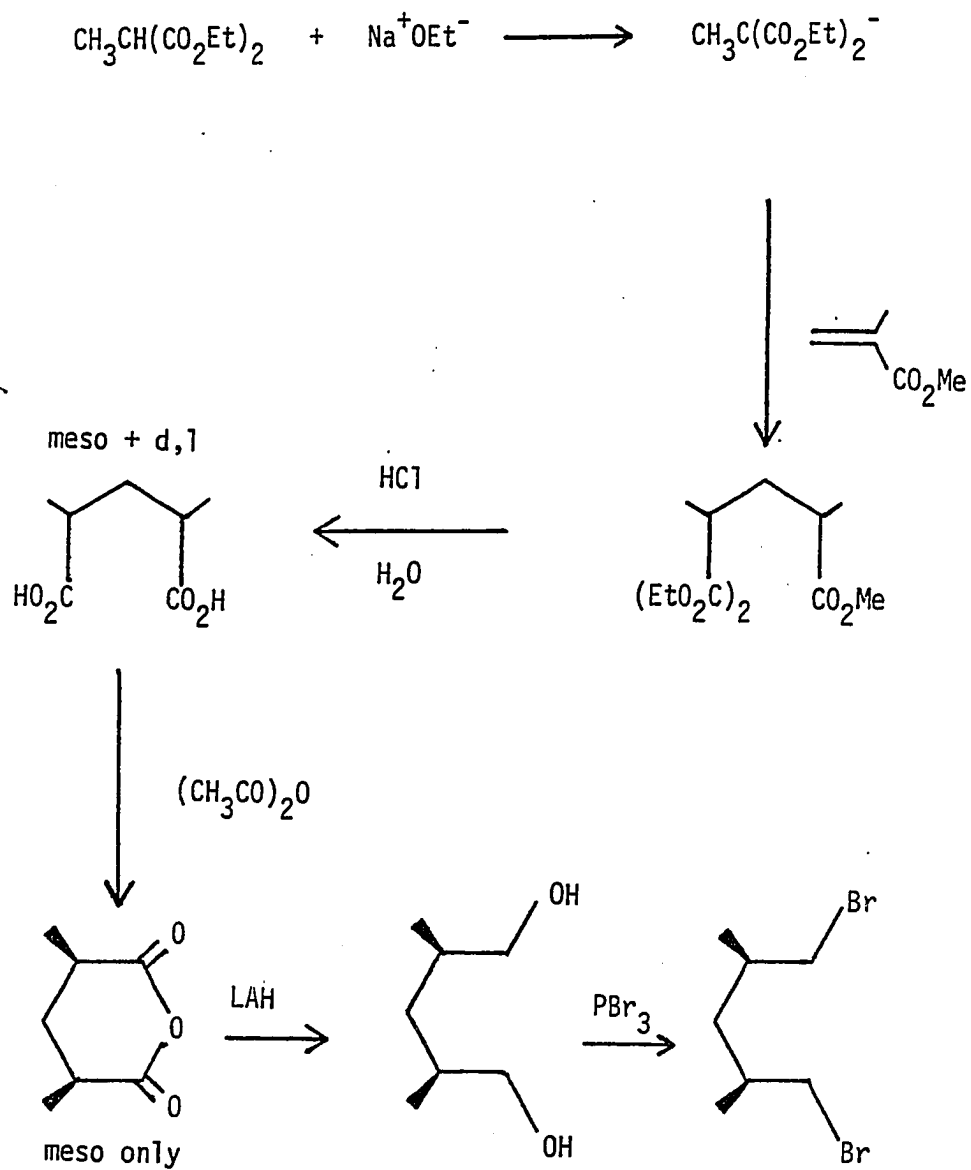
Reaction of $[Ni(23)(P(OMe)_3)_2]_n$ and O_3 A sample of $[Ni(23)(P(OMe)_3)_2]_n$ (0.090 g, 0.00016 mole) was placed in a 100 ml flask

fitted with a medium fritted filter stick. Fifty ml of CH_2Cl_2 was added to the flask, which was then cooled to -78°C . Ozone produced from an ozone generator designed and built in the Chemistry Department at Iowa State University was bubbled through the flask for 2 hr resulting in the solution turning dark blue. The flask was warmed to room temperature and the blue color faded. The CH_2Cl_2 was removed by distillation at atmospheric pressure. ^{31}P NMR analysis of the remaining oil showed only two peaks at 2.2 and -0.63 ppm in the ratio of 0.9 to 1. ^{31}P NMR spectra of authentic samples of $(\text{MeO})_3\text{P}=\text{O}$ and $(\text{MeO})_2(\text{O})\text{P}(\text{OCH}_2)_2\text{C}(\text{CH}_2\text{O})_2\text{P}(\text{O})\text{OMe}$ exhibited single peaks at 2.2 and -6.3 ppm, respectively.

Nickel analysis of $[\text{Ni}(\underline{23})(\text{P}(\text{OMe})_3)_2]_n$ and $[\text{Ni}(\underline{23})(7)_2]_n$

A sample of the polymer weighing 0.1800 g was placed in a 25 ml Erlenmeyer flask. A mixture consisting of 2 ml 70% HNO_3 and 2 ml 72% HClO_4 was added to the flask. The mixture was then slowly heated in a silicon oil bath to 200°C . The solution was allowed to boil vigorously for 30 seconds and the flask was then removed from the oil bath and allowed to cool to approximately 130°C . To ensure that all of the polymer had been properly digested, the flask was again heated to 200°C for an additional 2.5 minutes. The resulting green solution was cooled to room temperature and a gravimetric nickel analysis was carried out as previously described by Skoog and West (100). Results of these analyses can be found in the results and discussion section of this chapter.

meso-2,4-Dimethyl-1,5-dibromopentane This compound was prepared via the method of Noller and Pannell (101) (Scheme 5), which was amended



Scheme 5. The synthesis of meso-2,4-dimethyl-1,5-dibromopentane

as follows. The reaction conditions for the preparation of meso- α,α -dimethyl glutaric acid were not changed. However, the work up procedure used was the following. The resulting aqueous solution containing the glutaric acid was vacuum distilled to remove the water. The residual water was then removed by azeotropic distillation with benzene (30 ml benzene/10 g solid). When all the water had been removed, approximately 50% of the benzene was removed and a volume of heptane equal to half the volume of the remaining benzene was added. The resulting mixture was heated to redissolve any solid which had precipitated from solution. The product was obtained by cooling the solution at 5°C for 24-48 hr. The compound was obtained in 69.5% yield as opposed to the literature yield of 74% (101) ($m = 98^\circ$ - 104° lit. 101- 109° (101), $^1\text{H NMR}$ (CDCl_3) 11.5s 2H COOH, 2.6-2.2m 2H CH, 1.9-1.6m 2H CH, 1.2d ($J_{\text{H-H}} = 10$ Hz) 6H CH_3). For the meso-2,4-dimethyl-1,5-pentanediol the reaction conditions were not changed. However, the product was obtained in 83% yield (lit. 88.5%) (101) using the workup procedure of Fieser and Fieser (102) ($B_2 = 95$ - 99° , lit. 97- 99° ; $^1\text{H NMR}$ (CDCl_3) 4.45d $J_{\text{H-H}} = 11$ Hz 4H CH_2O , 3.3s 2H OH, 1.9-1.5m 4H CH_2 and CH, 1.95d $J_{\text{H-H}} = 12$ Hz 6H CH_3).

Dichloroisopropylphosphinite (24) This compound was prepared by the method of Gultneh (38).

Bis-(2-methyl-*n*-propyl)isopropylphosphinite (25) In a 3-neck 1000 ml flask equipped with a dropping funnel and mechanical stirrer was added 125 ml dry Et_2O and 3.2 g (0.13 mole) of Mg turnings. To the

solution was added 0.5 ml $\text{BrCH}_2\text{CH}_2\text{Br}$ and the mixture was stirred for 15 minutes. 2-Methyl-1-bromopropane (11.9 g, 0.0875 mole) in 50 ml of ether was added over a period of one hour. After the completion of the addition, the resulting solution was stirred for an additional 30 min. The reaction mixture was then cooled to -78°C . A solution of 24 (7.0 g, 0.043 mole) and pyridine (14.0 g, 0.167 mole) in 25 ml of dry ether was added drop-wise over 30 minutes. After stirring for an additional 30 minutes, the mixture was warmed to room temperature and stirred for 1.5 hours. After filtering in a nitrogen-filled glove bag, the ether was removed from the filtrate via distillation at 30 Torr. The product was obtained in 63% yield (^{31}P NMR (C_6D_6) 122.0; ^1H NMR (CDCl_3) 4.2-3.4m 1H CH, 2.1-0.7m 24H CH_3 , CH, and CH_2).

2-Isopropyl-2-phosphorinane (26) This compound was prepared in the same manner as 25, using 20.0 g (0.0871 mole) of 1,5-dibromopentane, 10.0 g (0.411 moles) Mg turnings, 14.1 g (0.090 moles) 24, and 27.5 g (0.348 moles) of pyridine. A clear oil weighing 1.9 g was obtained. The ^{31}P NMR spectrum of the oil showed only two peaks at 108.7 and 126.0 ppm in the ratio of 20 to 1. Attempts to distill the product at reduced pressure (1 Torr) resulted in its decomposition. This was evidenced by the disappearance of the peaks at 108.7 and 126.0 ppm and the appearance of new peaks from +70 to 40 ppm.

2- β -Isopropoxy-4,6- α,α -dimethyl-2-phosphorinane (27), 2- α -isopropyl-4,6- α,α -dimethyl-2-phosphorinane (28) Attempts were made to prepare this compound from meso-2,4-dimethyl-1,5-dibromopentane and 24

via the method of Gultneh (38) and the method used to prepare 26. All attempts to prepare a pure sample of this compound were unsuccessful as evidenced by the existence of many peaks in the ^{31}P NMR spectrum of the brown oil obtained. Three sets of peaks in the regions of 220-205 ppm, 111 to 106 ppm and 60 to 40 ppm showed that many different compounds formed in the reaction. Attempts to distill this material according to the conditions (56-58°/2 Torr) of Gultneh were unsuccessful. In fact, heating this mixture during the distillation resulted in the disappearance of the peaks located at 220 to 205 and 111 to 106 ppm with the subsequent appearance of new peaks in the region of 70 to 40 ppm.

2-Triphenylmethyl-2-oxophosphorinane (29) The oil (1.7 g)

obtained in the synthesis of 26, 3.0 g (0.011 mol) of triphenylmethyl chloride and 30 ml of dry degassed acetonitrile were refluxed for 5 hr. The acetonitrile was removed on a rotary evaporator and the resulting oily yellow solid was chromatographed on silica gel using a 3 to 1 mixture of hexane and acetone. The yellowish oil which was obtained (0.46 g) showed only one spot on TLC (using hexane and acetone as solvents) (^{31}P NMR ($\text{CD}_3\text{C}(\text{O})\text{CD}_3$) 52.0; ^1H (CDCl_3) 7.65-7.20m 15H C_6H_5 , 2.15-1.40m 10H CH_2 ; $\nu(\text{P}=\text{O})$ (CHCl_3) 1147 cm^{-1} ; $\text{P}^+ \frac{m}{e} = 360.1$ meas., 360.1 calc).

2- α -Triphenylmethyl-2- β -oxo-4,6- α , α -2-phosphorinane (30),

2- β -Triphenylmethyl-2- α -oxo-4,6- α , α -2-phosphorinane (31) In 30 ml of dry acetonitrile which contained 3.0 g (0.011 mole) of triphenylmethyl chloride was dissolved 1.2 g of the brown oil containing 27 and 28. The

mixture was refluxed under N_2 for 2 hours. A yellow solid was obtained upon removal under vacuum of the acetonitrile. The ^{31}P NMR spectrum of this material showed several peaks from +80 to +34 ppm, including 2 peaks at 56.0 ppm and 53.6 ppm in an approximately 4 to 1 ratio.

Chromatography of this solid on a column of silica gel using a 9 to 1 mixture of hexane and acetone yielded only a brownish oil. Large colorless crystals were observed in the oil after one week. The crystals which were extracted from the oil with cold acetone showed a single peak in the ^{31}P NMR at 53.2 ppm. The remaining oil showed a single resonance at 55.7 ppm ((30) ^{31}P NMR ($CD_3C(O)CD_3$) 53.2 ppm; $P^+ \frac{m}{e} = 388.1$ meas., 388.7 calc; (31) ^{31}P NMR ($CD_3C(O)CD_3$) 55.7 ppm; $P^+ \frac{m}{e} = 388.1$, meas. 388.7 calc).

X-ray experimental details for 30 A clear colorless crystal 0.2 x 0.3 x 0.3 mm was sealed in a 0.3 mm Lindemann capillary tube and mounted on a Syntex P_2 diffractometer equipped with a monochromator and Cu X-ray tube. Analysis of the crystal showed it to be orthorhombic with $a = 16.554(7) \text{ \AA}$, $b = 17.628(3) \text{ \AA}$, and $c = 14.910(3) \text{ \AA}$; $v = 4351(8) \text{ \AA}^3$, $\rho = 1.18 \frac{g}{cm^3}$ (calcd), $N = 8$. Data were collected using an ω scan technique out to a 2θ limit of 100.0° . A variable scan rate was used to collect data at a minimum rate of $4^\circ/\text{min}$ and a maximum rate of $29^\circ/\text{min}$. A total of 3717 reflections were measured. Repeated measurement of a single strong reflection after every 75 reflections showed no evidence of crystal decay. Analysis of the data showed the systematic absences $h00$, $h = 2n$; $0k1$, $l = 2n$; $0k0$, $k = 2n$; $h0l$, $h = 2n$; $00l$, $l = 2n$; $hk0$, $k = 2n$

indicative of the orthorhombic space group P_{cab} . Data averaging yield 1473 reflections ($F_0 > 3\sigma$). The positions of all nonhydrogen atoms were found using MULTAN (103). The refinement proceeded without difficulty to yield a final R of 0.083. Hydrogen atom positions were then calculated and their positions were refined with no apparent improvement in the final agreement factor. A final difference map showed no unexplained electron density.

X-ray experimental details for Ni(6)₄ Ni(6)₄ (0.3 g) was

dissolved in a minimum (~1 ml) of boiling heptane contained in a 15 dram vial. The vial was placed in a small Dewar. The top of the Dewar was packed with a paper towel and then placed in a freezer which was maintained at -15°C . After cooling for 24 hours, the vial was removed from the dewar and large (3 x 3 x 3 mm average) crystals were observed on the bottom. The heptane supernatant was decanted off and the crystals were then allowed to air dry. The compound appeared to have no air sensitivity.

Analysis of the crystals under a microscope showed that many of them were twinned. However, a small (0.3 x 0.3 x 0.3 mm) nontwinned fragment was cut off of a larger crystal and then mounted in a 0.3 mm Lindemann capillary. A data set was collected at room temperature using a four-circle X-ray diffractometer designed and built in the Ames Laboratory. Data were obtained using graphite monochromated molybdenum radiation. The quality of the data set obtained at room temperature appeared poor owing to the fact that many of the reflections proved to be unobserved.

However, the data set was reduced and averaged. All nonhydrogen atom positions were found successfully using this data set. Refinement of the structure proceeded until it was noticed that the isotropic temperature factors for the exocyclic secbutyl carbons were found to be equal to about 29.0. This indicated that there was excess thermal motion in the molecule.

The refinement was suspended and a new data set was collected at $-95^{\circ}\text{C} \pm 2^{\circ}\text{C}$. The crystal was found to be monoclinic with $a = 13.873(1) \text{ \AA}$, $b = 17.195(1) \text{ \AA}$, $c = 20.351(3) \text{ \AA}$, $\beta = 101.97(1)^{\circ}$, $z = 4$, $v = 4748.8(7) \text{ \AA}^3$ and $\rho = 1.23 \text{ g/cm}^3$ (calcd). The only systematic absence, $h0l$, $l = 2n$, indicated the space group $P2_1/c$ which was later confirmed by solution of the structure. Data collection yielded 3879 reflections measured over 3 octants with a 2θ limit of 50° . There was no observed decomposition of the crystal based upon repeated observation of three standard reflections. Averaging of equivalent data yielded 1987 independent reflections ($F_o > 3\sigma$). Block matrix least squares isotropic refinement of the nonhydrogen positions yielded a conventional R of 0.135 and a weighted R of 0.149. A full matrix anisotropic refinement of the nonhydrogen atoms led to a final conventional R of 0.086 and a weighted R of 0.108. An electron difference map of the unit cell failed to show any unexplained electron density.

1,4-Bis(diphenylphosphino)benzene (32) This compound was prepared by the procedure of Baldwin and Chang (104).

1,4-Bis(diphenylphosphinito)benzene (33) Hydroquinone (4.0 g, 0.036 mole) and 11.0 g (0.109 mole) triethyl amine were dissolved in 100 ml of dry ether. The solution was cooled to 0°C and 16.0 g (0.072 mole) diphenylchlorophosphine in 100 ml of dry ether was added dropwise over 30 min. The solution was stirred with the aid of a mechanical stirrer for a period of 1 hr. The mixture was filtered and the ether was removed on a rotary evaporator. The yellow oil obtained was dissolved in boiling n-propanol and long slender crystals formed upon cooling. The product was obtained in 11.1% yield (m = 130-131°; ^{31}P NMR (C_6D_6) 112.4; ^1H NMR (CDCl_3) 7.4m 20H C_6H_5 , 6.95m 4H C_6H_4).

4,4'-(Diphenylphosphino)biphenyl (34) A solution of 8.6 g (0.028 mole) of 4,4'-dibromobiphenyl in 35 ml of dry THF was placed in a 3-neck 250 ml flask equipped with a nitrogen inlet, dropping funnel and mechanical stirrer. The solution was chilled to -78°C and 30 ml (0.066 mole) of 2.2 M solution of n-butyl lithium in hexane was added dropwise over one hour. Upon completion of the addition, 12.3 g (0.056 mole) of diphenylchlorophosphine was added to the reaction mixture over 10 min. The solution was stirred for an additional thirty minutes and then filtered. The solid which was obtained was washed with water and then refluxed overnight in methanol to remove any remaining unreacted 4,4'-dibromobiphenyl. The remaining solid was filtered and dried under vacuum for several hours. The product was obtained in 15.3% yield (m = 189-190°, lit. = 192-194° (105); ^{31}P NMR (C_6D_6) -6.0; ^1H (CDCl_3) 7.50m C_6H_5 , C_6H_4).

Rh(P(C₆H₅)₃)₃Cl (35) This compound was prepared using the procedure of Osborn and Wilkinson (106).

Reaction of 32 and 35 In order to obtain polymers similar to those obtained with NiL₄ complexes, 0.23 g (0.00025 mole) of 35 and 0.12 g (0.00026 mole) of 32 were mixed in 20 ml of methylene chloride. The mixture was stirred overnight with no evidence of any polymer formation. Further refluxing of this material for 24 hrs. also failed to produce any polymeric material.

Reaction of 34 and 35 In 20 ml of methylene chloride was mixed 35 (0.16 g, 0.00017 mole) and 34 (0.088 g, 0.00017 mole). After 32 hrs. of stirring at room temperature and 16 hrs. of refluxing, no polymeric material was observed to have formed.

Reaction of 33 and 35 In 20 ml of chloroform was mixed 35 (0.31 g, 0.00033 mol) and 33 (0.17 g, 0.00033 mole). The mixture was refluxed for 30 min. After stirring overnight, a dark red precipitate was observed to have formed. The solid (0.1 g) was filtered and dried in vacuum. Attempts to dissolve this material in any organic solvents were unsuccessful. Attempts were made to use this material as a catalyst for the hydrogenation of 1-hexene according to the procedure of Gultneh (38); however, the compound proved to be catalytically inactive.

1-chloro-3-methyl-2-pentene Attempts to prepare this material by the procedure of Gultneh (38) failed. The following amended procedure was used. To a mixture of 32.5 g (0.276 mole) of 3-methyl-pentene-3-ol

and 28.8 g (0.343 mole) of pyridine in 125 ml of ether was added dropwise, 43.6 g (0.366 mole) of freshly distilled thionyl chloride, over the course of 30 min. at room temperature. The mixture was stirred for an additional 2 hours and then filtered. The ether was removed and the residual yellow liquid was vacuum distilled to give the product in 36.7% yield ($b_{160} = 85^\circ$; ^1H (CDCl_3) 6.2-4.8m 1H CH, 3.9d $J_{\text{H-H}} = 12$ 1H CH_2Cl , 2.3-1.8m 2H CH_2 , 1.65s 3H CH_3 , 0.85t $J_{\text{H-H}} = 10$ Hz 3H CH_3).

3-methyl-3-hexenenitrile A solution of 6.0 g (0.051 mole) of 1-chloro-3-methyl-2-pentene, 4.0 g (0.083 mole) of NaCN, and 0.3 g (0.003 mole) of KI in 125 ml of acetone was refluxed for 16 hrs. The mixture was cooled to room temperature and filtered. The acetone was removed and the remaining liquid was vacuum distilled to give the product in 27.0% yield ($B_{12} = 35-38^\circ$; $\nu(\text{C}=\text{N}) = 2255 \text{ cm}^{-1}$; ^1H NMR (CDCl_3) 5.5-5.0m 1H CH, 3.1d $J_{\text{H-H}} = 12$ Hz 2H CH_2CN , 2.3-1.9m 2H CH_2 , 1.7s 3H CH_3 , 1.1dt 6H CH_3).

Supported NiL_4 complexes on macroreticular resins The resin (0.53 g, 0.0016 mole of H^+), 3.5 g (0.0048 mole) of $\text{Ni}(\text{P}(\text{OEt})_3)_4$ and 10 ml of dry, degassed toluene were placed in a nitrogen-flushed 50 ml round bottom flask equipped with a stirring bar. The mixture was stirred for 12 hr. under nitrogen at room temperature. The toluene was then removed and the resin was washed with four 15 ml aliquots of fresh toluene. The beads were then immediately used as catalysts. Resins containing different NiL_4 complexes were prepared in an analogous manner using the same ratios of reagents.

Analysis of NiL₄-supported macroreticular resins The resins were

digested with HNO₃/HClO₄ mixtures using the same procedure used in the nickel analysis of the [Ni(²³)₂L']_n complexes. The resulting acid solutions were analyzed quantitatively for nickel using the previously described procedure of Snell (107).

Results and discussion

The catalytic properties of a NiL₄ complex are due in large measure to the ability of the complex to dissociate. Dissociation of a ligand provides an open site which is available for coordination of small molecules such as olefins. Ordinarily, only NiL₄ complexes which contain bulky ligands, as defined by their ligand cone angles, are extensively dissociated in solution. Examples of these types of ligands are P(O-i-Pr)₃ and P(O-o-tolyl)₃. In fact, nickel(0) complexes of these ligands have been shown to dissociate extensively in solution to NiL₃ complexes (108). However, for complexes with smaller ligands, dissociation does not occur until the complex is protonated in solution. As stated previously in the introduction, dissociation of a ligand upon protonation is probably facilitated by reduced π-back donation of electron density from the nickel atom to the phosphorus atom. The reduction in π-back donation is caused by the electrophilicity of the proton upon coordination. The decrease in back donation reduces the strength of the Ni-P bond which promotes dissociation. Though Tolman contends that dissociation in complexes containing ligands with small ligand cone angles is aided by protonation of the complex, he maintains that the

steric properties of the ligand determine the extent to which these complexes dissociate.

Gultneh has used steric arguments to explain why adding methyl groups to the equatorial 4,6 positions of the phosphorinane ring causes the NiL_4 complexes of these ligands to be more efficient catalysts. Gultneh has also observed that large groups in the exocyclic positions on phosphorus also brought about an increase in the catalytic activity of the complex. This effect is maximized by having an isopropyl group in this position. Groups larger than isopropyl tend to cause a decrease in the catalytic activity of the complex. Gultneh erroneously contends that the main cause for the decrease in activity of NiL_4 complexes containing ligands which have these larger groups is the increased basicity of the phosphorus atom. This increase in phosphorus basicity was thought to be due to either increased amounts of electron donation to phosphorus by the alkyl groups, or, by the steric interactions within the complex which cause the larger exocyclic groups to adopt the more basic equatorial position. However, on the basis of J_{p-H} data given in his thesis, the change in relative phosphorus basicity of the ligands would appear to be slight (Table 7). Moreover, an X-ray structural analysis of $Ni(\underline{6})_4$ (given later in this thesis) indicates that large exocyclic groups are not forced to adopt an equatorial position at least in the solid state. The reduction in activity is probably due to the larger steric bulk of these groups which impedes the ability of an olefin to coordinate to the nickel atom.

Table 7: ^{31}P NMR chemical shift and $J_{\text{P-H}}$ values of some selected monocyclic phosphite ligands upon protonation with FSO_3H at -50°C (38).

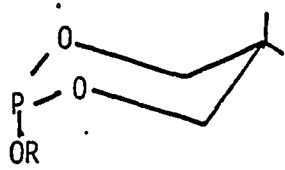
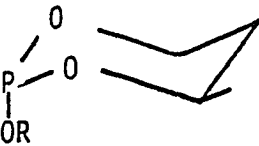
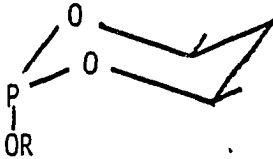
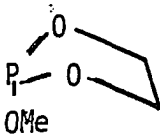
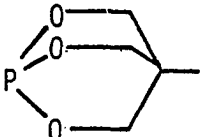
L	$\delta \text{ } ^{31}\text{P}(\text{HL}^+) \text{ ppm}$	$J_{\text{P-H}} (\pm 4 \text{ Hz})$
		
R = Me	18.0	861
<u>i</u> -Pr	16.5	852
<u>l</u> -methyl	16.9	853
<u>l</u> -bornyl	16.2	856
		
R = Me	17.5	871
<u>i</u> -Pr	16.8	855
<u>l</u> -menthyl	16.9	865
<u>l</u> -bornyl	17.2	854

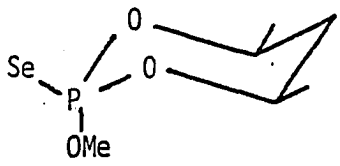
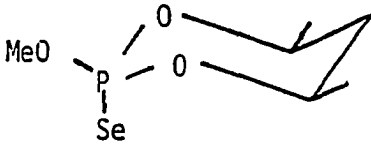
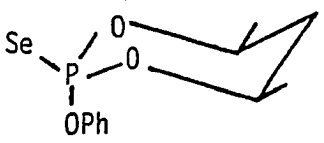
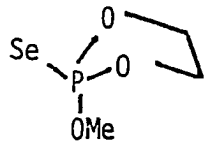
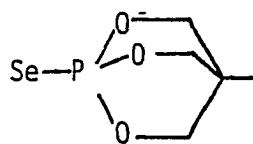
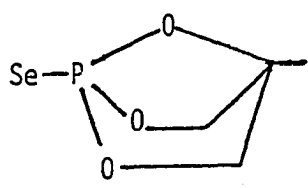
Table 7. (continued)

L	δ $^{31}\text{P}(\text{HL}^+)$ ppm	$J_{\text{P-H}}$ (± 4 Hz)
		
R = Me	16.5	861
= <u>i</u> -Pr	16.8	853
= <u>l</u> -menthyl	16.9	853
= bornyl	16.6	854
	43.7	913 ^a
	21.4	899 ^b

^aReference (109).^bReference (110).

Tolman (19) has suggested that the steric properties of a ligand are the major factors in determining the extent to which it dissociates from the complex. However, in order to see if the electronic properties of the ligand had any role in shaping the catalytic properties of a complex, several new ligands and their NiL_4 complexes were prepared and tested as isomerization catalysts. $\text{Ni}(\underline{10})_4$ was shown to be completely inactive as a catalyst. Gas chromatographic analysis showed that the complex failed to isomerize 3-butenitrile to cis and trans-2-butenitrile. This seemed unreasonable in view of the high activity of $\text{Ni}(\underline{9})_4$. Models of $\text{Ni}(\underline{10})_4$ seem to show that the phenoxy groups have almost the same steric properties as an isopropyl group. This is also illustrated by the similarity in the ligand cone angles of $\text{P}(\text{O}-i\text{-Pr})_3$ and $\text{P}(\text{OPh})_3$ of 130° and 128° , respectively. In order to determine the relative basicity of this ligand, its corresponding selenide was prepared and its $J_{31\text{P}-77\text{Se}}$ value was measured (19). This value was found to be 1024 Hz. As can be seen in Table 8 this coupling constant is much higher relative to the coupling constant of the selenide of 8 (compound 8 was shown by $J_{\text{P-H}}$ data to be electronically similar to 9). In fact, ligand 10 would seem to have electronic properties much closer to the constrained phosphites, $\text{P}(\text{OCH}_2)_3\text{C}(\text{Me})$, $\text{OCH}_2\text{CH}_2\text{OP}(\text{OMe})$ and $\text{P}(\text{OCH}_2)_2\text{CO}(\text{Me})$. The reduced basicity of 10, which seems similar to that of the 5 member ring phosphite 37, probably is due to resonance delocalization of electron density from the oxygen to the phenyl ring as shown in fig. 4. The build up of positive charge on oxygen brings about a build up of positive charge on

Table 8. ^{31}P - ^{77}Se spin-spin couplings and ^{31}P NMR chemical shifts (rel. to H_3PO_4) of some selected selenophosphoryl compounds(13)

Compound	$\delta^{31}\text{P}$ (± 0.1 ppm)	$J^{31}\text{P}-^{77}\text{Se}$ (± 1 Hz)
$\text{SeP}(\text{OMe})_3$	78.0	954
	66.8	996
	68.8	949
	57.4	1024
	88.0	1011
	60.1	1053
	61.4	1099

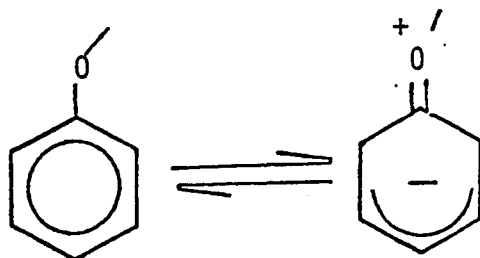


Fig. 4. Resonance structures for a phenoxy group.

phosphorus thus reducing its basicity and decreasing the extent to which the NiL_4 complex is protonated. This is evidenced by the failure of a solution of $\text{Ni}(\underline{10})_4$ to turn yellow upon addition of acid. Such a failure of the solution to turn yellow has been shown in the past (38) to stem from the lack of protonation of the NiL_4 complex.

This reduced basicity argument has been used to explain why NiL_4 complexes containing 5-member ring phosphite ligands such as 37 also fail to act as catalysts for olefin isomerization (38). Structural studies of these types of ligands have shown their P-O-C angles to be constrained, thus causing a decrease in their phosphorus basicity as discussed previously (111). This reduction in basicity and hence the basicity of the nickel is observed by the low degree (5% by ^{31}P NMR) to which $\text{Ni}(\underline{37})_4$ protonates in acidic solution. This decrease in the extent of protonation is also demonstrated by the failure of solutions of $\text{Ni}(\underline{37})_4$ to turn yellow in color upon addition of acid. The effect of decreased phosphorus basicity by molecular constraint on 5-member ring phosphites

is so great that it can not be overcome by large electron donating groups in the phosphorus exocyclic position. This was exemplified by the preparation of Ni(15)₄, which contains an isopropyl group in the exocyclic position, and its observed inactivity as an isomerization catalyst. ³¹P NMR analysis showed that the complex failed to protonate in solution.

In order to investigate the effect of increased phosphorus ligand basicity on the catalytic activity of complexes, several ligands were prepared which contained amine functions in the exocyclic position. The increase in phosphorus basicity by replacing the alkoxy group with an amino group is best illustrated by the decrease in $J_{31\text{P}-71\text{Se}}$ of Se=P(OMe)₃ compared to Se=P(NMe₂)₃ from 954 to 784 Hz (19). In order to test this effect, the series of aminophosphite ligands, 16, 17, 18, 19, 21 and 22 were prepared along with their corresponding series of NiL₄ complexes. In every case, all of these complexes were shown to be totally inactive as isomerization catalysts. Attempts were made to measure the $J_{\text{P-H}}$ values of the protonated forms of these ligands using ³¹P NMR in order to estimate their relative basicity. However, in all cases, upon adding FSO₂H to the NMR tube containing the ligand according to the procedure of Weiss and co-workers (111), a darkening of the solution was observed. Subsequent ³¹P NMR analysis indicated that the ligand had undergone extensive decomposition upon mixing with the acid.

In an attempt to determine how this decomposition of the ligand might have been responsible for the inactivity of the complexes, a low-temperature ³¹P NMR analysis of the protonation of one of these complexes

was carried out. Fig. 5 is an example of what is observed in the ^{31}P NMR when a nickel complex of a phosphite, 6, is protonated in a 5 to 1 H^+ to Ni ratio. As can be seen upon addition of acid, the singlet at 154.6 ppm corresponding to the NiL_4 complex shrinks with subsequent formation of a doublet at 136.8 ppm ($J_{\text{P-H}} = 33$ Hz), indicative of protonation. In the case of $\text{Ni}(\underline{20})_4$ ($\delta^{31}\text{P} = 163.8$ ppm), addition of even one equivalent of acid brings about apparent decomposition of the NiL_4 complex as evidenced by formation of new peaks in the ^{31}P NMR spectrum at 172, 169, 165, 145, 140, 133 and 116 ppm (Fig. 6). Upon addition of another equivalent of acid (Fig. 7), even more decomposition is observed. At a ratio of 10 acid to 1 Ni (the ratio which was shown to give an optimum rate of catalysis for phosphite complexes (38)), the ^{31}P NMR spectrum seems to suggest that all of the NiL_4 complex has decomposed (Fig. 8). However, there appears to be a small doublet centered at 127.5 ppm which shows a coupling constant of 32 Hz, suggestive of a protonated NiL_4 complex. Integration of this doublet shows that it comprises only about 4% of the total area of all the peaks in the spectra, however.

On the basis of these experiments, the inactivity of these complexes as catalyst can be explained by their decomposition in acid solution. It is possible that instead of the nickel being protonated, as occurs with phosphite complexes, the nitrogen of the ligand is preferentially protonated. The protonation of the nitrogen facilitates weakening of the P-N bond thus leading to decomposition of the ligand and subsequently the NiL_4 complex.

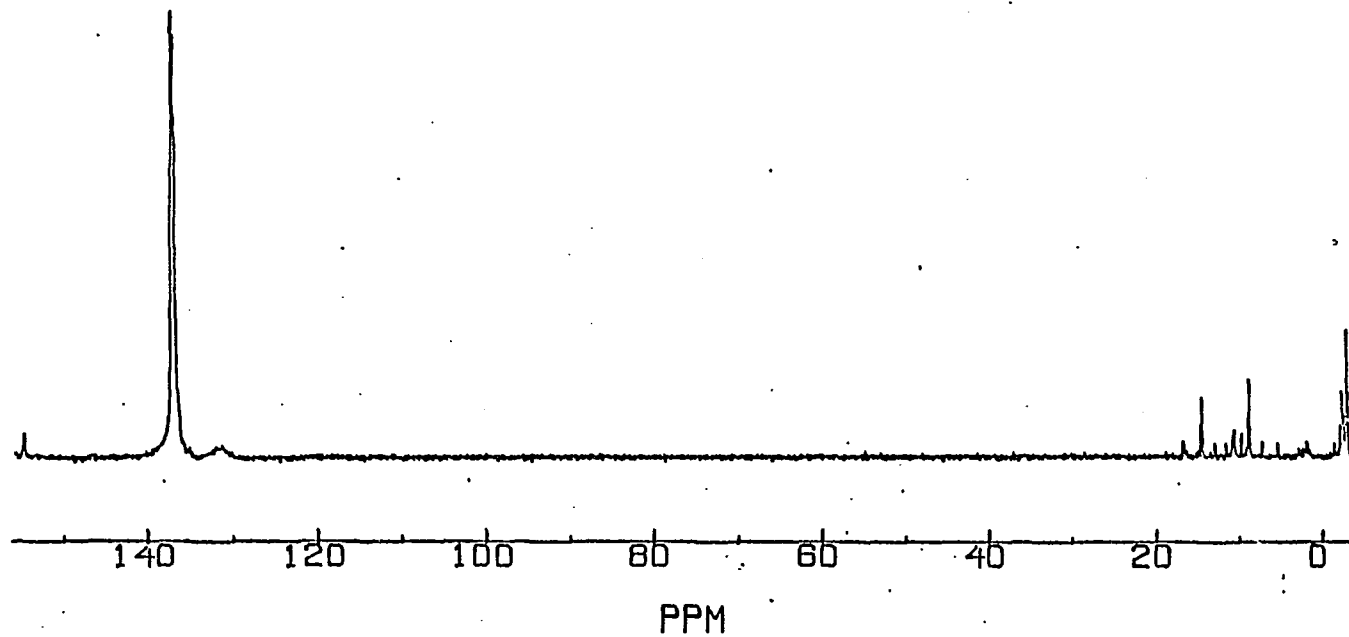


Figure 5. ^{31}P NMR spectrum of a C_6D_6 solution of $\text{Ni}(\underline{6})_4$ acidified with 5 equivalents of F_3CCOOH at room temperature

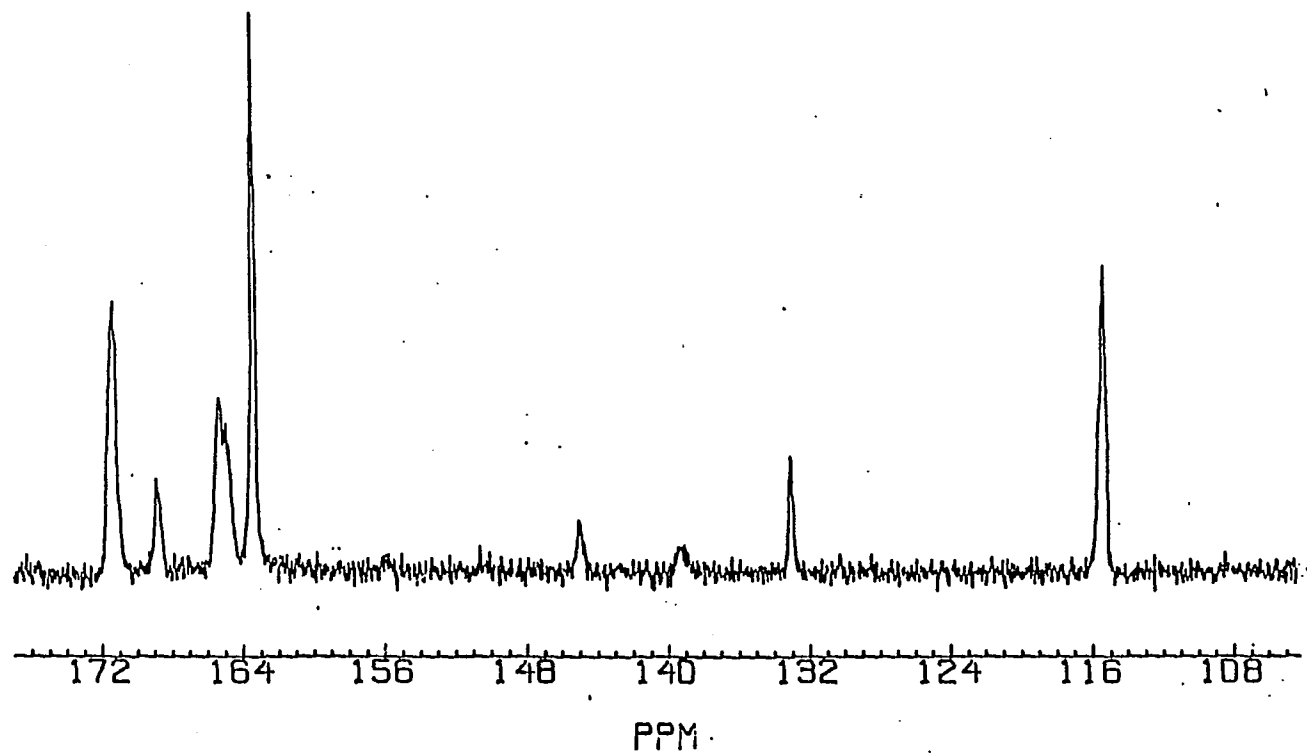


Figure 6. ^{31}P NMR spectrum of a C_6D_6 solution of $\text{Ni}(\underline{20})_4$ acidified with 1 equivalent of F_3CCOOH at 200 K

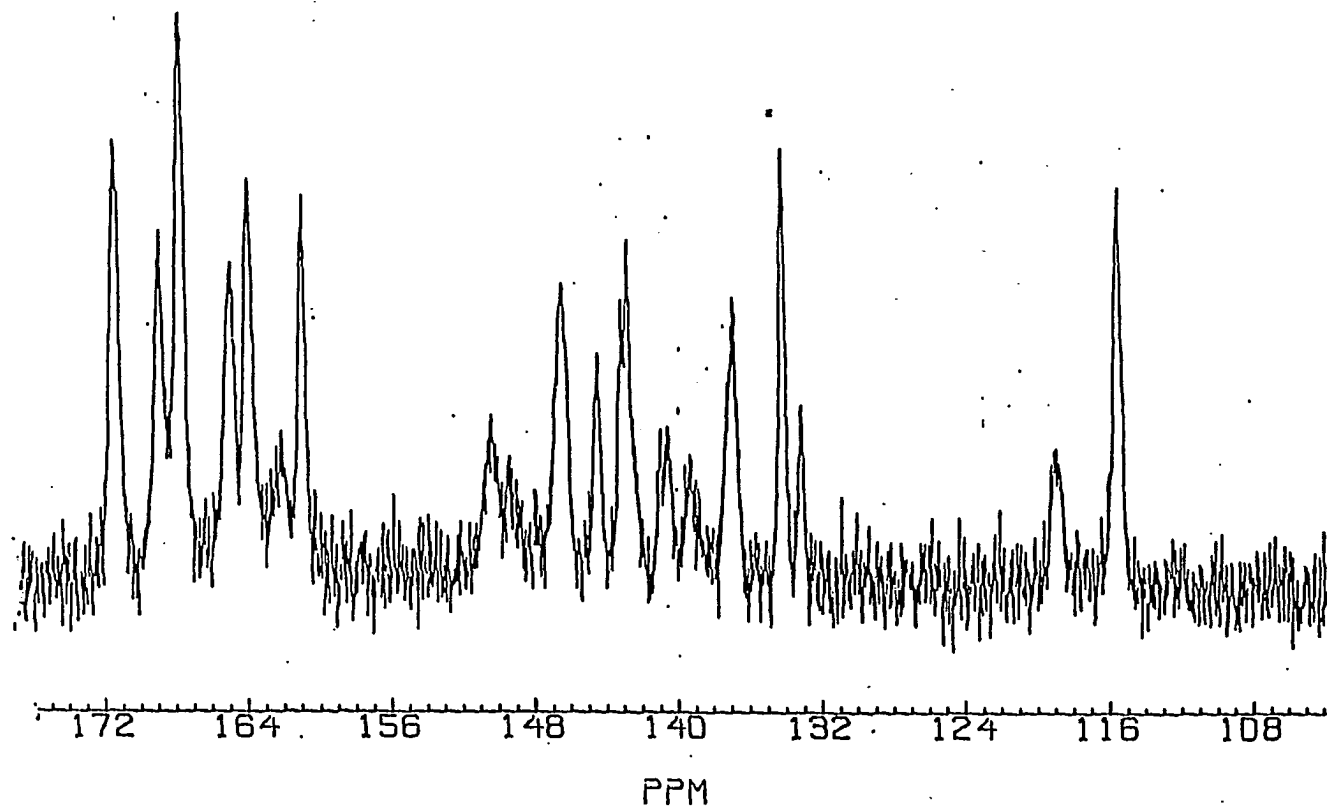


Figure 7. ^{31}P NMR spectrum of a C_6D_6 solution of $\text{Ni}(\underline{20})_4$ acidified with 2 equivalents of F_3CCOOH at 200 K

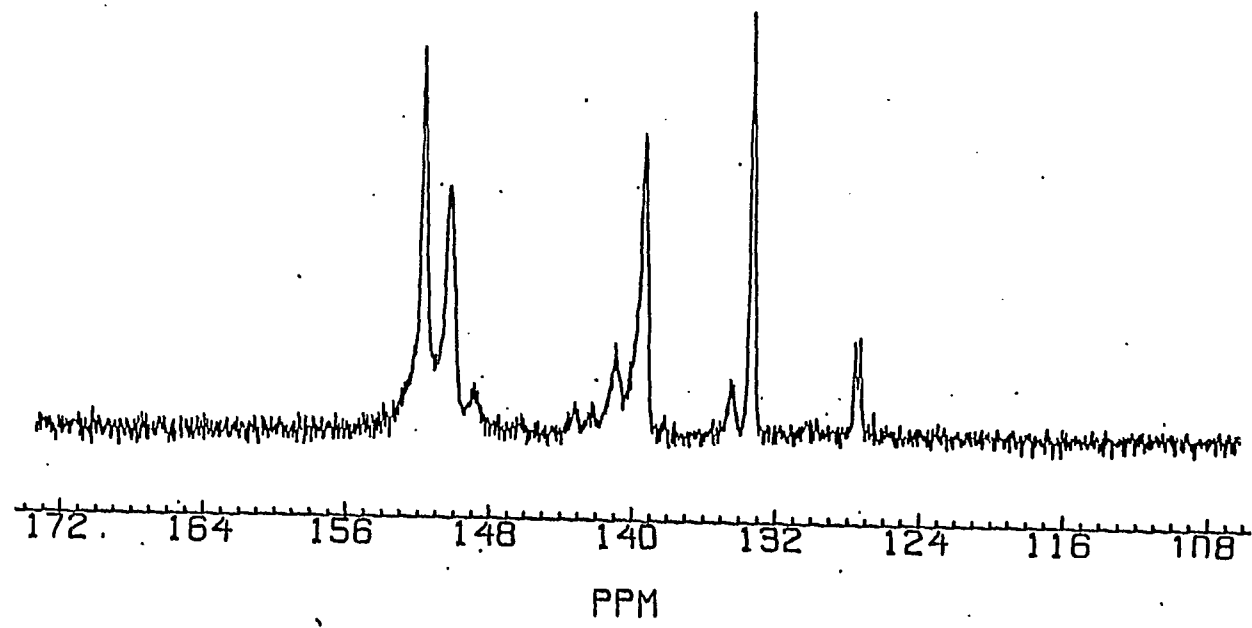


Figure 8. ^{31}P NMR spectrum of a C_6D_6 solution of $\text{Ni}(\underline{20})_4$ acidified with 10 equivalents of F_3CCOOH at 200 K

On the basis of these results, it would appear that the electronic properties of the ligand are very important in determining the extent to which an NiL_4 complex is protonated in solution. However, it also seems that as long as the nickel atom is able to undergo protonation, the steric properties of the ligand influence the catalytic activity of the complex in two ways: firstly, by promoting dissociation of a ligand, and secondly, as will be seen in the work with asymmetric catalysis, by influencing the extent of olefin coordination to the metal atom.

Use of Lewis acid cocatalysts in the isomerization of 3-butenitrile

Gultneh observed that Lewis acids such as AlCl_3 , TiCl_3 , and ZnCl_2 acted as efficient cocatalysts in the isomerization of olefins. It was observed that in most cases the rates of catalysis using these compounds were similar to that observed with protic acids (Table 9).

It was found that benzene solutions containing catalytically active mixtures of NiL_4 complexes and Lewis acids were yellow in color, as was observed in protic acid solutions. In fact, the visible spectra of these solutions exhibited absorption maxima in the region of 355 nm as was also observed with H^+/NiL_4 systems (38). Moreover, addition of $\text{P}(\text{OMe})_3$ to solutions containing a NiL_4 complex, (L = 2-alkoxy-1,3,2-dioxaphosphorinane) and a Lewis acid such as AlCl_3 brought about redistribution of the ligands to form complexes of the type $\text{NiL}_x(\text{P}(\text{OMe})_3)_{4-x}$ (38). This was confirmed by ^{31}P NMR analysis (38).

Based upon the similarities between the Lewis and protic acid systems, Gultneh contended that the role of Lewis acid in the catalysis

Table 9. Comparison of activity of Lewis acids to H⁺ as cocatalyst in the isomerization of 3-butenitrile ^{a,b,c},

Ligand	Lewis acid		
	cycles in 30 min (± 2)		
	AlCl ₃	ZnCl ₂	H ⁺
<u>5</u>	54	15	25
<u>7</u>	88	20	60
<u>8</u>	124 (4.0 min)	30	124 (4.0 min)

^a[Lewis acid]/[NiL₄]/3-butenitrile = 1/1/124.

^bTime (± 0.2 min) taken to complete 124 cycles.

^cRef. (38).

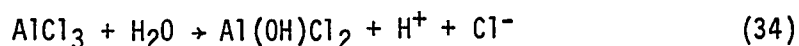
was similar to H⁺. His proposal of a NiL₄:AlCl₃ adduct was based upon the visible absorbance which was previously mentioned. However, at the time, the exact bonding interaction between the nickel and aluminum was not understood. Based upon the presence of a molar conductivity of 15.4 ohm⁻¹ cm² mole⁻² in CH₃CN for a 1 to 1 mixture of Ni(9)₄ and AlCl₃, the following mechanism was proposed for the interaction of a NiL₄ complex



Scheme 6. Proposed mechanism of Gultneh for the interaction of a NiL₄ complex and AlCl₃

with AlCl_3 . It was also reported that addition of excess ligand to these catalyst mixtures decreased the rate of catalysis.

The conductivity reported was extremely low for what would have been expected for a 1 to 1 electrolyte in CH_3CN ($120\text{-}160 \text{ ohm}^{-1} \text{ cm}^2 \text{ mole}^{-2}$) (112). A recheck of the conductivity of $\text{Ni}(\underline{9})_4/\text{AlCl}_3$ under nitrogen using freshly sublimed AlCl_3 and CH_3CN freshly dried from P_4O_{10} , showed that the system had no detectable conductivity. It is possible that the previously described value was caused from the partial hydrolysis of AlCl_3 by water contained within the system (Eq. 34).



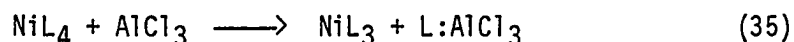
Since attempts by Gultneh (38) to isolate these adducts had failed, we sought to find a new way of proving or disproving their existence. A UV-visible spectroscopic study was carried out in order to achieve this goal and the following observations were made:

1. Addition of $\text{Ni}(\underline{9})_4$ in benzene showed no absorption in the visible spectrum. Likewise, $\underline{9}$ showed no visible adsorption.
2. Addition of $\text{Ni}(\underline{9})_4$ to CH_2Cl_2 caused the solution to turn slightly yellow in color. A slight absorption ($\epsilon = 2.7 \times 10^1$) at 340 nm was seen in the visible spectrum.
3. A 1 to 1 molar mixture of $\text{Ni}(\underline{9})_4$ and AlCl_3 in CH_2Cl_2 shows absorptions at 420 nm ($\epsilon = 9.6 \times 10^{-1}$) and 340 nm ($\epsilon = 2.3 \times 10^1$).

4. Addition of excess ligand to the mixture described in 3 causes an increase in the size of the peak at 420 ($\epsilon = 1.1 \times 10^1$) and a decrease in the size of the peak at 340 ($\epsilon = 9.0$).
5. The visible spectrum of AlCl_3 and free ligand 9 in CH_2Cl_2 showed an absorption at 420 nm ($\epsilon = 6.0$).

The data would seem to suggest that the peak at 340 nm is from a NiL_3 species while the peak at 420 nm is from an adduct which forms between the AlCl_3 and the free ligand.

Tolman and Gosser (108) have previously shown that NiL_3 species such as $\text{Ni}(\text{P}(\text{O}-\underline{\text{o}}\text{-tolyl})_3)_3$ exhibits an absorption maximum at 420 nms, while a solution of $\text{Ni}(\text{P}(\text{O}-\underline{\text{i}}\text{-Pr})_3)_4$ exhibits an absorption maximum at 430 nm upon heating, indicative of the formation of $\text{Ni}(\text{P}(\text{O}-\underline{\text{i}}\text{-Pr})_3)_3$. The reasons for the lower wavelength absorption at 340 nm of $\text{Ni}(\underline{\text{9}})_4$ (in CH_2Cl_2) as compared to the 410 nm absorption of $\text{Ni}(\text{P}(\text{O}-\underline{\text{i}}\text{-Pr})_3)_3$ are not known as yet. It is perhaps caused by a difference in the value of $10 Dq$, resulting from the difference in the ligand basicity and steric arrangement in the resulting $\text{Ni}(\underline{\text{9}})_3$ complex. The above results suggest that the role of AlCl_3 in this system is that of a dissociation promoter (Eq. 35).



The AlCl_3 in this case assists in shifting the equilibrium toward the coordinatively unsaturated NiL_3 species which can then isomerize 3-butenitrile through a π -allylic mechanism. In order to further substantiate these ideas, an ^{27}Al NMR study was carried out in order to

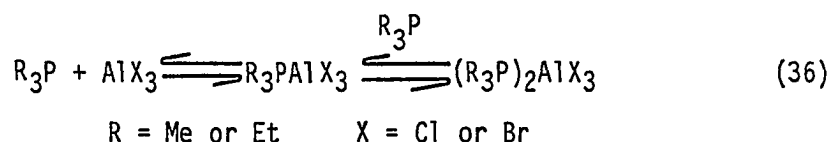
determine what changes, if any, take place around the aluminum atom when the AlCl_3 is added to the NiL_4 complex.

Aluminum has been found to be a very good NMR nucleus (113). Reasons for this are: the aluminum-27 isotope is 100% abundant and the relative receptivity of the nucleus to the NMR experiment is 20% that of hydrogen (phosphorus having a receptivity of only 6.6% relative to that of hydrogen). Although the aluminum-27 nucleus possesses a quadrupole moment with a spin of 5/2, it is still possible to obtain spectra which contain very narrow lines. However, this is observed only when there is a high degree of symmetry around the aluminum atom. Thus, the highly symmetric $\text{Al}(\text{H}_2\text{O})_6^{+3}$ ion has been shown to have a line width of only 3 Hz (114).

Aluminum-27 NMR chemical shifts (relative to $\text{Al}(\text{H}_2\text{O})_6^{+3}$) have been shown to be dependent upon the type of coordination around the aluminum atom (113). Complexes which possess octahedral symmetry are usually found to exhibit chemical shifts in the region of +20 ppm to -50 ppm. While tetrahedrally coordinated compounds are found to have chemical shifts from -28 to +221 ppm. Therefore, upon obtaining both line width and chemical shift data, it is found that aluminum-27 NMR provides an extremely useful tool in determining the chemical environment around an aluminum atom.

The existence of stable adducts between phosphorus bases and aluminum containing Lewis acids has been known for some time. Vriezen and Jellinek (115) have shown that AlX_3 , ($X = \text{Cl}$ or Br) can form stable adducts with trialkylphosphines. They found that the following

equilibrium (Eq. 36) is maintained in solutions containing these compounds.



It was observed that the relative concentrations of the mono and diphosphorus adducts could be controlled by adjustment of the ratio of PR_3 to AlX_3 in solution. Titration of the $AlCl_3$ with PEt_3 in toluene showed that the ^{27}Al resonance varied from +109.9 ppm (rel. to $Al(H_2O)_6^{+3}$) for a 1 to 1 adduct, to a limiting value of 55.9 ppm for $(R_3P)_2AlCl_3$. The rather large difference in chemical shift (54 ppm) was attributed to the change from sp^3 hybridization in Et_3PAICl_3 to dsp^2 hybridization in $(Et_3P)_2AlCl_3$ (115).

As can be seen in Table 10, the ^{27}Al chemical shifts for the aluminum species produced from a 1 to 1 mixture of $AlCl_3$ and free ligand ($P(OEt)_3$ or 9), is about 103.7 ppm. The peak falls in the same region as is observed for a 1 to 1 $AlCl_3/PET_3$ adduct. It should also be noticed that the same chemical shift is observed for a 1 to 1 mixture of $AlCl_3$ and the corresponding NiL_4 complex. It would be highly coincidental if the chemical shift of an adduct formed between the $AlCl_3$ and the nickel atom, as proposed by Gultneh, came at the same place as the shift of an $AlCl_3$ /phosphite adduct. Therefore, on the basis of this evidence we are fairly confident that the role of a Lewis acid, in particular $AlCl_3$, is to promote ligand dissociation, as shown in equation 33. As further

Table 10. ^{27}Al NMR data for various AlCl_3 , ligand, and NiL_4 complex mixtures^{a,b}

components in mixture	ratio of components	δ ^{27}Al (ppm)	Line width (Hz)
AlCl_3	---	91.0	300
$\text{AlCl}_3/\text{P}(\text{OEt})_3$	1/1	103.5	50
$\text{AlCl}_3/\text{Ni}(\text{P}(\text{OEt})_3)_4$	1/1	103.9	50
$\text{AlCl}_3/(\underline{9})$	1/1	103.6	132 ^c
$\text{AlCl}_3/\text{Ni}(\underline{9})_4$	1/1	103.9	10 ^c

^aRel. to $\text{Al}(\text{D}_2\text{O})_6^{+3}$.

^bIn toluene solution.

^cThe reason for the large difference in the line width between the spectra of the NiL_4 complex and the ligand is not known as yet.

evidence for this mechanism, the same type of study was done with the $\text{AlCl}_3/\text{Ni}(\underline{11})_4$ system. A 1 to 1 mixture of AlCl_3 and 11 exhibits a ^{27}Al NMR shift of 104.0 ppm. However, a 1 to 1 mixture of AlCl_3 and $\text{Ni}(\underline{11})_4$ shows only a peak at +91.0 ppm indicative of AlCl_3 dissolved in solution. It would appear that in this case an adduct fails to form between (11) and AlCl_3 . This can be explained by the lack of dissociation of a ligand from the $\text{Ni}(\underline{11})_4$ complex due to the high strength of the Ni-P bond.

Attempts to observe the chemical shift of an adduct formed between AlCl_3 and 12 were also unsuccessful. It appears that 12 is not sufficiently basic enough to form an adduct with aluminum. In fact, the $J_{\text{P-H}}$ value of $\text{H}(\underline{12})^+$ (929 Hz) indicates that it is even less basic than 11 ($\text{H}(\underline{11})^+$, $J_{\text{P-H}} = 899$ Hz (109)).

For the AlCl_3 /phosphite adduct, there exists the possibility of two different modes of coordination of the phosphite to AlCl_3 . Coordination can take place through either the lone pair on phosphorus or through one of the lone pairs on oxygen. Cohen and Smith (116) have shown that coordination occurs exclusively through the lone pair on phosphorus, however. This was illustrated by a ^1H NMR study of the adduct formed between $\text{P}(\text{OMe})_3$ and AlMe_3 . The ^1H NMR resonance for the methoxy protons appeared as a single doublet. This suggests that either all the methoxy groups were equivalent due to phosphorus coordination to aluminum or the aluminum was rapidly exchanging coordination with all the oxygens of the phosphite. However, IR studies showed very little change in the P-O-C stretching frequencies upon coordination of the aluminum. Therefore, Cohen and Smith suggested that coordination takes place exclusively through the phosphorus atom.

This mode of coordination was also found to be consistent with ^{13}C NMR data taken on a 1 to 1 mixture of $\text{P}(\text{OEt})_3$ and AlCl_3 . The ^{13}C NMR spectrum of $\text{P}(\text{OEt})_3$ in C_6D_6 shows two doublets at 57.67 ($J_{\text{C-P}} = 13.5$ Hz) and 16.85 ($J_{\text{C-P}} = 6$ Hz) ppm. Upon addition of one equivalent of AlCl_3 , there appears to be no change in any of chemical shifts, nor in the values of $J_{\text{C-P}}$.

It was observed that a major limitation in working with AlCl_3 was its low solubility in aromatic solvents, namely, 0.7% by weight in toluene (117). In order to investigate the effect of higher concentrations of Lewis acid on the rate of catalysis, AlEt_3 was tried as a cocatalyst due to its much higher solubility in solvents such as

benzene. Catalytic isomerization of 3-butenitrile involving $\text{Ni}(\text{P}(\text{OEt})_3)_4/\text{AlEt}_3$, in a 1 to 1 ratio, showed the system to be completely inactive. Higher Al to Ni ratios were also shown to be inactive as catalyst systems. In ratios higher than 3 to 1, it appeared that the AlEt_3 led to decomposition of the $\text{Ni}(\text{P}(\text{OEt})_3)_4$ complex as evidenced by ^{31}P NMR spectroscopy.

Attempts to use $\text{Ni}(\underline{9})_4/\text{AlEt}_3$ in a 1 to 1 ratio as cocatalysts were also unsuccessful as shown by the lack of any isomerized product produced in 24 hrs. However, using a 10 to 1 ratio of AlEt_3 to $\text{Ni}(\underline{9})_4$, 116 cycles were observed in 24 hrs for the isomerization of 3-butenitrile (cis/trans = 1.2). This decrease in activity as compared to AlCl_3 is probably due to reduced electrophilicity of aluminum by the electron donating ethyl groups. This effect is thought to interfere with the extent to which adducts form between the AlEt_3 and the dissociated ligand.

In order to achieve a compromise between increased solubility and electrophilicity, AlEtCl_2 was tried as a cocatalyst. ^{27}Al NMR data for the $\text{Ni}(\underline{9})_4/\text{AlEtCl}_2$ system is shown in Table 11. The large downfield shift of 130.7 ppm for AlEtCl_2 as compared to 91.0 ppm for AlCl_3 and 87.1 for neat $\text{Al}(\underline{i}\text{-Bu})\text{Cl}_2$ (118) is presently unexplained. This large downfield shift may be attributed to concentration or solvent effects. However, addition of 1 equivalent of free ligand (9) to AlEtCl_2 causes the resonance to shift upfield to 103.8 ppm. A 1 to 1 molar ratio of

Table 11. ^{27}Al NMR data for various AlCl_2Et , ligand, and NiL_4 complex mixtures^a

Mixture	Ratio of components	δ ^{27}Al (ppm)
AlCl_2Et	---	130.7 ppm
$\text{AlCl}_2\text{Et}/\underline{9}$	1/1	103.8 ppm
$\text{AlCl}_2\text{Et}/\text{Ni}(\underline{9})_4$	1/1	104.0 ppm

^aRelative of $\text{Al}(\text{D}_2\text{O})_6^{+3}$.

$\text{Ni}(\underline{9})_4$ and AlEtCl_2 also shows a single resonance in about the same position (104.0 ppm). Attempts to use AlEtCl_2 as a cocatalyst were successful only when the $\text{Ni}(\underline{9})_4$ and AlEtCl_2 were present in a 1 to 1 molar ratio. This ratio of AlEtCl_2 proved to be a much better cocatalyst than AlEt_3 as illustrated by the 115 cycles achieved in 1.75 hrs. for the isomerization of 3-butenitrile. Attempts were made to carry out the isomerization at higher ratios of Al to Ni such as 5 to 1 and 10 to 1. However, these attempts proved to be unsuccessful and ^{31}P NMR studies revealed the decomposition of the NiL_4 complex at these higher concentrations of AlEtCl_2 . The reason for this decomposition may be due in part to rearrangement of the ligands. Cohen and co-workers (119) have found that the $(\text{MeO})_3\text{PAlEtCl}_2$ adduct rearranges to form the phosphonate complex, $(\text{MeO})_2\text{MePOAlEtCl}_2$. Adducts formed from either $(i\text{-PrO})_3\text{P}$ or $(t\text{-BuO})_3\text{P}$ with AlEtCl_2 were not obtained, as they spontaneously decomposed to give olefins, ethane, and alkyl chlorides.

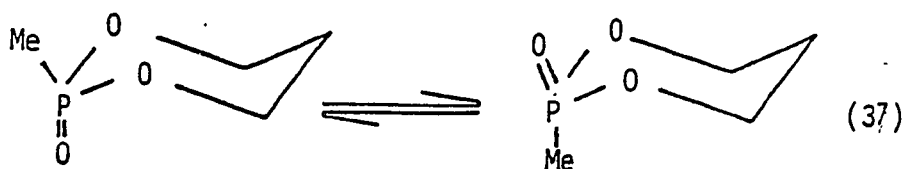
Phosphites are also known to form adducts with boron compounds, such as BH_3 and BF_3 . Gultneh (38) found that BF_3 fails to act as a cocatalyst in the isomerization of 3-butenitrile. An attempt was made to use BH_3 as a cocatalyst. It was observed that these systems were catalytically inactive. The NiL_4 complex appeared to completely decompose upon addition of BH_3 (as $\text{BH}_3:\text{THF}$ complex). ^{11}B NMR was employed to investigate the mode of decomposition of this system. A 1 to 1 mixture of 9 and BH_3 in C_6D_6 showed a doublet in the ^{11}B NMR spectrum at -42.7 ppm, ($J_{\text{B-p}} = 102$ Hz). This chemical shift and coupling constant is consistent with what is observed for other BH_3 adducts of various phosphites (120). However, addition of 1 equivalent of $\text{THF}:\text{BH}_3$ to an equivalent of $\text{Ni}(\underline{9})_4$ in C_6D_6 failed to show any peaks in the region of -42 ppm. The only peaks observed were at $+17.5$ and -0.06 ppm. The peak at -0.06 was later shown to be from unreacted THF/BH_3 complex (120). The peak at $+17.5$ ppm was found to be consistent with the resonance observed for other alkyl borates (120). In particular, $\text{B}(\text{O-}i\text{-Pr})_3$ exhibits a resonance at $+17.5$ ppm (120).

It would appear that instead of promoting dissociation of NiL_4 complexes, as was the case with AlCl_3 , BH_3 coordinates to one of the oxygens in the phosphite and facilitates the breaking of the P-O bond and subsequent formation of a B-OR linkage. Decomposition of the ligand probably occurs while it is coordinated to the nickel atom, since it is known that stable adducts form when the ligand is uncoordinated. It is conceivable that this decomposition occurs with the breaking of either or both the exocyclic and cyclic P-O-C linkages. ^{11}B NMR analysis

of a 1 to 1 mixture of Ni(11)₄ and THF:BH₃ showed the presence of a single peak in the borate region of the spectrum at +18.3 ppm. Due to the bicyclic structure of 11 this would seem to indicate that BH₃ can cleave a cyclic P-O-C linkage. It is thus reasonable to believe that BH₃ can also open up the P-O-C linkage in the phosphorinane ring. The resulting B-O-R linkage produced is structurally similar to a B-O-i-Pr group, thus giving an identical chemical shift.

Crystal and molecular structure of Ni(6)₄

As was previously stated, work with 2-alkoxy-1,3,2-dioxaphosphorinanes showed that these ligands can adopt conformations wherein the alkoxy group is equatorial or axial with respect to the ring. When methyl groups are placed in the equatorial 4,6 positions of the ring it is possible to isolate products isomeric at phosphorus (58). The rings are locked into their conformations since 1,3-diaxial interactions between methyl groups would occur if the ring changed its conformation. However, when these methyl groups are not present the ring can easily exchange conformation via a ring flip. Support for this statement comes from the small ΔH value of 1.34 kcal/mole for equilibrium in Equation 37 (58).



As previously stated, this isomerization at phosphorus leads to differences in the phosphorus basicity of the ligands. In discussing the differences in the catalytic activity of various NiL_4 complexes, Gultneh (38) suggested that the lack of activity of complexes with ligands which do not contain 4,6 methyl groups arises from changes in conformation of the ligand upon coordination. This would account for changes in the electronic properties of the ligand and hence the complex. In complexes containing 2-alkoxy-5,5-dimethyl-1,3,2-dioxaphosphorinane ligands, it is conceivable that 1,3-syndiaxial steric interactions could force the exocyclic groups to adopt an equatorial conformation via a flipping of the ring. In the 4-methyl or 4,6-dimethyl systems, such a ring flip would be energetically unfavorable, but it still would be possible for the ring to adopt a twist boat conformation which could lead to differences in the steric properties of the ligand.

In order to see if the ligand could change conformation upon coordination to a zero valent nickel atom, an X-ray structural analysis was carried out. First, an X-ray crystallographic analysis of $Ni(54)_4$ was attempted. However, attempts to solve the structure proved unsuccessful due to the apparent high symmetry of the ligand and the complex it formed. In order to eliminate the problem of high symmetry, $Ni(6)_4$ was prepared. In this complex, the isopropyl group was replaced with a less symmetric sec-butyl group. Upon making this change, subsequent solution of the structure was carried out successfully. Final positions, bond distances and angles, and anisotropic thermal parameters for $Ni(6)_4$ can be found in Tables 12, 13, 14, and 15, respectively.

Table 12. The final positional parameters for atoms contained in Ni(6)₄ with their estimated standard deviations (in parentheses) ^a

atom	x	y	z
Ni	0.0	0.2735(1)	0.2500
PA	0.4381(2)	0.8418(2)	0.3164(2)
O1A	0.3269(5)	0.8715(5)	0.2894(4)
O2A	0.4283(5)	0.7973(5)	0.3852(4)
O3A	0.4863(6)	0.9254(5)	0.3441(4)
C1A	0.2727(12)	0.9056(9)	0.3365(8)
C2A	0.3729(11)	0.8322(10)	0.4294(7)
C3A	0.2656(11)	0.8486(11)	0.3947(8)
C4A	0.2132(10)	0.7736(10)	0.3686(8)
C5A	0.2150(12)	0.8931(13)	0.4459(8)
C6A	0.5929(10)	0.9318(8)	0.3624(9)
C7A	0.6279(12)	0.9222(12)	0.4393(8)
C8A	0.6160(13)	1.0100(12)	0.3330(13)
C9A	0.7255(30)	1.0181(14)	0.3523(17)
PB	0.6178(2)	0.7077(2)	0.3040(2)
O1B	0.7022(5)	0.6815(5)	0.2644(4)
O2B	0.6821(5)	0.7535(5)	0.3683(4)
O3B	0.6012(7)	0.6229(5)	0.3358(6)
C1B	0.7953(11)	0.6532(10)	0.3033(9)
C2B	0.7760(10)	0.7181(10)	0.4028(8)
C3B	0.8468(9)	0.7109(10)	0.3557(8)
C4B	0.9419(10)	0.6690(11)	0.3967(9)
C5B	0.8716(9)	0.7864(8)	0.3247(8)
C6B	0.5163(11)	0.6096(11)	0.3653(10)
C7B	0.4779(13)	0.5242(11)	0.3422(11)
C8B	0.5558(16)	0.6186(15)	0.4401(12)
C9B	0.4766(20)	0.6086(18)	0.4758(15)

^aPositional parameters are listed in fractional unit cell coordinates.

Table 13. Bond distances (Å) and their estimated standard deviations (in parentheses) for Ni(6)₄^a

Ni-PA	2.103(3)	Ni-PB	2.101(3)
PA-01A	1.609(7)	PB-01B	1.618(9)
PA-02A	1.627(9)	PB-02B	1.626(8)
PA-03A	1.636(8)	PB-03B	1.629(9)
O1A-C1A	1.457(20)	O1B-C1B	1.451(16)
O2A-C2A	1.430(19)	O2B-C2B	1.477(16)
O3A-C6A	1.453(16)	O3B-C6B	1.447(22)
C1A-C3A	1.555(23)	C1B-C3B	1.520(22)
C3A-C2A	1.536(20)	C3B-C2B	1.514(23)
C3A-C4A	1.520(24)	C3B-C4B	1.580(20)
C3A-C5A	1.571(26)	C3B-C5B	1.514(23)
C6A-C7A	1.548(23)	C6B-C7B	1.599(26)
C6A-C8A	1.533(27)	C6B-C8B	1.515(30)
C8A-C9A	1.495(43)	C8B-C9B	1.448(40)

^aFor symmetry nonrelated ligands.

Table 14. Bond angles ($^{\circ}$) and their estimated standard deviations (in parentheses) for Ni(6)₄^a

PA-Ni-PB	109.97(13)		
Ni-PA-01B	116.68(34)	Ni-PB-01B	116.97(33)
Ni-PA-02A	114.11(35)	Ni-PB-02B	113.41(33)
Ni-PA-03A	121.35(39)	Ni-PB-03B	122.08(35)
O1A-PA-02A	101.38(46)	O1B-PB-02B	101.69(42)
O2A-PA-03A	102.55(47)	O2B-PB-03B	102.37(48)
O1A-PA-03A	97.63(44)	O1B-PB-03B	97.15(49)
PA-O1A-C1A	119.48(75)	PB-O1B-C1B	118.38(93)
PA-O2A-C2A	119.70(87)	PB-O2B-C2B	117.74(84)
PA-O3A-C6A	118.46(77)	PB-O3B-C6B	119.94(96)
O1A-C1A-C3A	111.76(1.27)	O1B-C1B-C3B	113.63(1.26)
C1A-C3A-C2A	104.88(1.30)	C1B-C3B-C2B	103.04(1.22)
C1A-C3A-C4A	111.71(1.25)	C1B-C3B-C4B	107.05(1.33)
C1A-C3A-C5A	107.79(1.46)	C1B-C3B-C5B	112.43(1.31)
C3A-C2A-O2A	112.55(1.15)	C3B-C2B-O2B	110.84(1.19)
O3A-C6A-C7A	109.90(1.36)	O3B-C6B-C7B	105.82(1.50)
O3A-C6A-C8A	104.52(1.11)	O3B-C6B-C8B	104.16(1.37)
C6A-C8A-C9A	105.24(1.67)	C6B-C8B-C9B	109.74(1.85)
C7A-C6A-C8A	116.15(1.49)	C7B-C6B-C8B	114.70(1.77)
C2A-C3A-C4A	110.64(1.41)	C2B-C3B-C4B	106.44(1.28)
C2A-C3A-C5A	107.93(1.20)	C2B-C3B-C5B	115.27(1.37)

^aFor symmetry nonrelated ligands.

Table 15. Thermal parameters and their estimated standard deviations (in parentheses) for Ni(6)₄^a

atom	B ₁₁	B ₂₂	B ₃₃	B ₁₂	B ₁₃	B ₂₃
Ni	3.8(1)	4.8(1)	5.5(1)	0.0(0)	0.2(1)	0.0(0)
P1	4.3(2)	5.3(2)	5.5(2)	0.5(1)	0.1(1)	-0.1(1)
P2	4.6(2)	4.8(2)	6.4(2)	0.3(1)	0.2(1)	0.3(1)
O1A	4.4(3)	6.7(4)	5.9(4)	0.9(3)	0.4(3)	0.2(4)
O2A	5.9(4)	7.7(5)	5.2(4)	1.3(4)	0.9(4)	0.7(4)
O3A	5.9(4)	5.5(4)	8.3(5)	-0.4(3)	0.5(4)	-1.6(4)
O1B	4.7(4)	5.9(4)	8.2(5)	1.1(3)	1.5(4)	-0.9(4)
O2B	4.6(4)	6.5(4)	6.3(4)	0.8(3)	-0.7(3)	0.2(4)
O3B	6.0(4)	5.4(4)	11.8(7)	0.6(4)	0.8(5)	2.3(4)
C1A	6.7(6)	8.4(9)	7.4(9)	2.6(8)	0.1(7)	-1.0(8)
C2A	6.6(9)	11.0(12)	6.7(8)	0.5(8)	1.9(7)	1.4(9)
C3A	7.1(8)	12.1(12)	6.3(8)	4.2(9)	1.5(6)	1.0(9)
C4A	6.1(7)	10.7(11)	9.7(10)	-1.9(8)	0.4(6)	0.9(9)
C5A	10.2(10)	17.8(16)	7.5(8)	5.9(10)	3.8(8)	-1.1(10)
C6A	6.0(8)	4.4(7)	11.6(11)	-0.7(6)	0.7(7)	-1.1(7)
C7A	8.9(9)	17.2(15)	6.6(9)	-1.1(10)	-1.4(8)	-0.9(10)
C8A	4.3(8)	8.6(11)	18.9(20)	0.5(7)	-0.3(10)	-0.3(12)
C9A	17.5(21)	11.1(15)	24.3(25)	-0.2(15)	4.3(19)	2.1(16)
C1B	6.2(9)	7.8(9)	12.4(15)	2.9(8)	1.4(8)	-0.2(10)

^aThe form of the anisotropic thermal parameter is $\exp[-(B_{11}a^2h^2 + B_{22}b^2k^2 + B_{33}c^2l^2 + (B_{12} a*b* hk + B_{13} a*c*hl + B_{23}b*c*kl)/2)]$.

Table 15. (continued)

atom	B ₁₁	B ₂₂	B ₃₃	B ₁₂	B ₁₃	B ₂₃
C2B	5.8(7)	9.9(10)	5.9(8)	1.5(7)	-1.4(7)	1.4(7)
C3B	4.3(6)	9.6(10)	7.7(8)	2.2(7)	-0.2(6)	-1.4(8)
C4B	6.2(7)	13.8(13)	11.1(11)	4.4(8)	-1.0(7)	2.6(10)
C5B	5.9(7)	6.6(7)	10.0(9)	-1.0(6)	0.2(6)	0.9(7)
C6B	6.3(7)	11.3(12)	9.3(11)	0.8(8)	1.8(8)	3.3(9)
C7B	9.3(10)	9.3(10)	17.6(17)	-3.8(9)	4.4(11)	1.3(11)
C8B	11.9(13)	14.5(15)	11.7(15)	-0.1(14)	5.7(12)	1.4(14)
C9B	16.3(18)	19.7(23)	20.1(23)	5.4(18)	7.4(17)	5.1(20)

Structure factors for the complex can be found in Appendix 1. An ORTEP diagram of the fragment containing the nickel atom and two of its four symmetry nonrelated ligands is shown in Fig. 9. For clarity, the symmetry-related ligands are not shown.

Solution of the structure revealed that a slightly distorted tetrahedral coordination was maintained around the nickel atom (\angle P-Ni-P = 110.0°). This coordination has been found in other zero-valent nickel complexes such as Ni(PPh₃)₂(CO)₂ (121), Ni(CH₂=CHCN)₂(P(OPh)₃)₂ (5) and Ni(CO)₃(P(t-Bu)₃) (122). This geometry is consistent with sp³ hybridization on nickel due to its filled d¹⁰ configuration.

The ligand used in the preparation of Ni(6)₄ is believed to contain the sec-butyl group primarily in the axial conformation (38) in its uncoordinated state. It thus appears that this remains the case upon coordination.

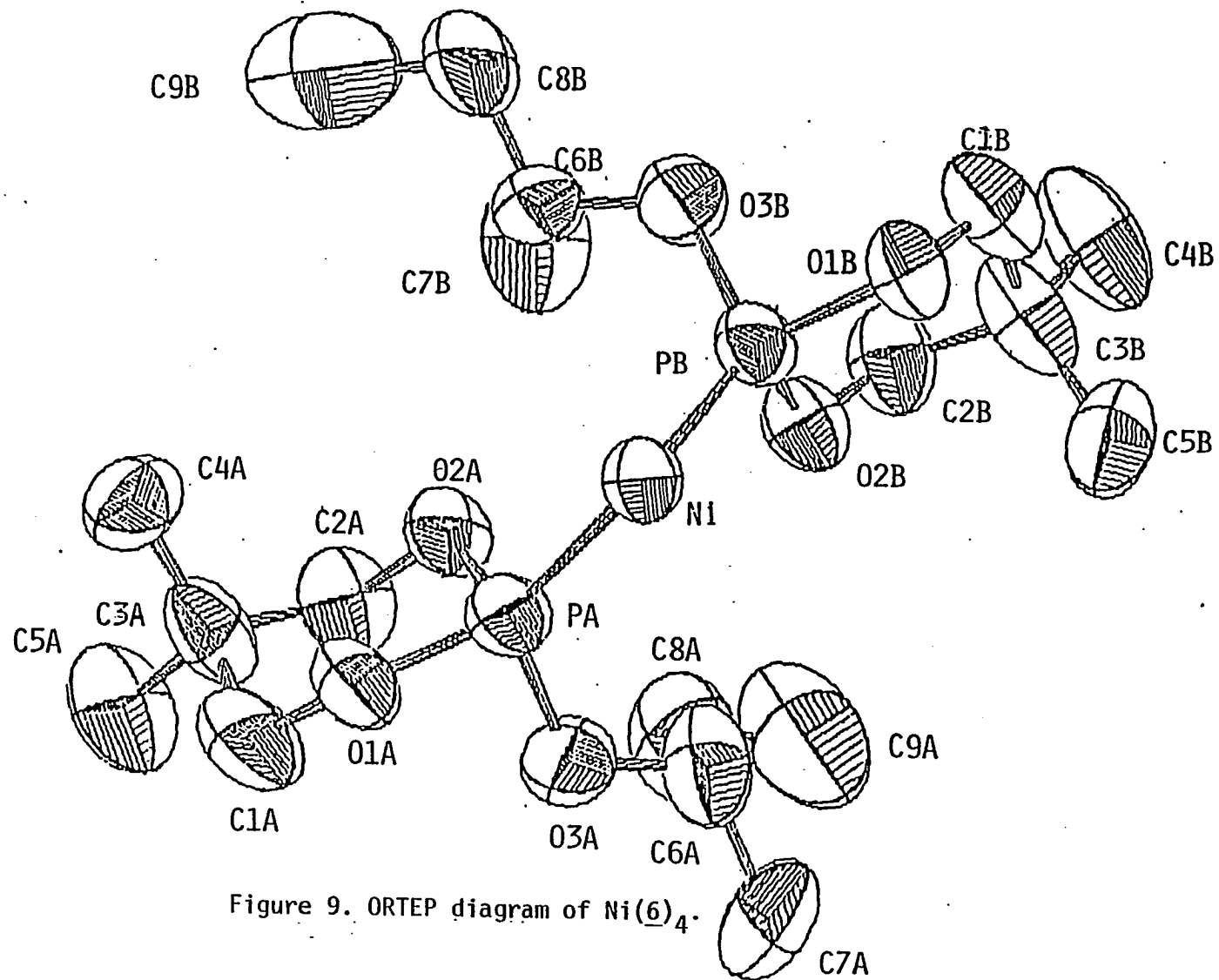


Figure 9. ORTEP diagram of $\text{Ni}(\underline{6})_4$.

One of the most interesting features of the structure is the extremely short nickel phosphorus bond distance of 2.109(3)Å. In fact, this distance is as short as the 2.116(10)Å which has been observed in Ni(PF₃)₄ (123,124). This shorter distance is surprising considering the high degree of π-back donation from nickel to phosphorus which is believed to strengthen the Ni-P bond. The possible effect of increased π-back bonding may also be illustrated by shortening of the Ni-P bond in Ni(P(OMe)₃)₄ Br⁺ versus Ni(PMe₃)₄Br⁺; however, steric effect may be dominant. The averages for the axial and equatorial Ni-P distances in Ni(P(OMe)₃)₄Br⁺ are 2.18 Å and 2.22 Å, respectively (125), while in Ni(PMe₃)₄Br⁺ the distances are 2.25 Å and 2.25 Å, respectively (126). However, the reason for the short Ni-P distance in Ni(6)₄ is not known at this time. Further analysis revealed that all the phosphorinane bond distances and angles in Ni(6)₄ are consistent with those found in the similar phosphorinane complex, cis-Mo(CO)₄ (38)₂ (127). These bond distances and angles were also similar to those found in uncomplexed phosphorinane compounds (128). As previously stated, the ligands adopt a chair conformation with an axially oriented sec-butoxy group. Each of the symmetry nonrelated ligands failed to show any twist in their chair conformation as the torsional angles described by atoms O1B, O2A, C2A, C1A and O1B, O2B, C1B, C2B were equal to 0.0° and 1.39°, respectively. Molecular models of the complex indicate that there could be favorable hydrogen bonding interactions between an exocyclic oxygen and the hydrogen on the CH group of its symmetry related (C₂) sec-butoxy group.

The calculated H-O distance of 3.3 Å is at the outer limit of this type of bonding interaction (129).

One of the goals of this structural analysis was to understand the possible interactions between ligands which could account for the increased activity of a complex containing ligands with equatorial 4,6-dimethyl groups. Unfortunately, we were unable to crystallize a complex which contained these types of ligands. However, using data from the structural analysis of Ni(6)₄, we were able to calculate the imaginary positions of equatorial 4,6 methyl groups using a C4 to methyl distance of 1.54 Å and C(methyl)-C4-H(ax) angle of 109.5°. From these calculations, the distance between methyl groups on adjacent ligands is 6.0 Å, which is larger than the sum of the van der Waals radii (4 Å) of two methyl groups. Inspection of a model of the structure revealed that significant steric interactions exist only between methyls in the 4 and 6 positions of the ring and the exocyclic groups of other ligands. Calculations of the distance between the imaginary C4 and C6 methyl groups of the ring to the C8 methylene and C7 methyl groups contained on other ligands varied from 3.6 to 4.6 Å. These distances seem to suggest that there is the possibility of steric interactions among these groups. The structure also seems to suggest that as the exocyclic group grows larger from methyl to isopropyl, an interaction begins to develop between these groups and the methyl groups located in the equatorial 4,6 positions of the adjacent phosphorinane rings. However, when the exocyclic groups become exceedingly large, (e.g., t-butyl or bornyl), the exocyclic groups swing away from each other in order to reduce steric

interactions. This results in an increase in the distance between the exocyclic groups and 4,6 equatorial methyl groups on adjacent ligands, thus decreasing the steric interactions between the ligands.

These types of steric interactions may serve to increase the extent of ligand dissociation in these HNiL_4^+ complexes, thus resulting in the higher rates of catalysis for the isomerization of 3-butenitrile. The reason why $\text{Ni}(\underline{9})_4$ gives the highest rate of catalysis may be due to optimization of this steric effect when an isopropyl group is in the exocyclic position.

A decrease in the rate of catalysis was observed upon placing groups larger than isopropyl in the exocyclic position of the ring. A possible explanation of this result is that these groups sterically interfere with coordination of the olefin to the metal atom. However, this argument loses some of its attractiveness when one considers that if the phosphorinane ring fails to contain any methyl groups in the equatorial 4,6 positions, catalysis is observed only when a methoxy group is bound in the exocyclic position. Since no catalysis is observed with compound $\text{Ni}(\underline{39})_4$, while catalysis is observed with $\text{Ni}(\underline{9})_4$, it would seem unreasonable that the exocyclic group interferes with olefin coordination to the nickel. Therefore, it is more likely that the presence of 4,6 equatorial methyl/exocyclic group interactions account for the large changes in the observed rates of catalysis.

Effect of substitution of oxygens in the phosphorinane ring by carbon

As was mentioned earlier, a striking result of Gultneh's work was the tremendous increase in catalytic activity of $\text{Ni}(\underline{9})_4$ compared to its acyclic analogue, $\text{Ni}(\text{P}(\text{O}-\underline{i}\text{-Pr})_3)_4$. Gultneh contended that the source of this difference in activity was due to subtle changes in the electronic properties of the ligand. Verkade (12) has shown that some cyclic phosphites have a smaller P-O-C angle than what is observed in their acyclic analogues. This decrease in the P-O-C angle has been shown to bring about a decrease in the basicity of the phosphite. This decrease in basicity can be shown by measurement of the $J_{\text{P-H}}$ value upon protonation of the ligand.

As previously described, the more basic the phosphite, the smaller the value of $J_{\text{P-H}}$. The $J_{\text{P-H}}$ value for $\text{HP}(\text{O}-\underline{i}\text{-Pr})_3^+$ was found to be 795 Hz (109), while Gultneh (38) found the $J_{\text{P-H}}$ for $\text{H}(\underline{9})^+$ to be 853 Hz. Clearly, the acyclic ligand is the one which is more basic. This increased basicity should impart more basicity to the nickel atom, thus facilitating protonation. This increase in the extent of protonation should cause an increase in ligand dissociation, and hence increase the catalytic activity of the complex. However, this turns out to be directly opposite to what is observed experimentally.

Solutions which contain $\text{Ni}(\text{P}(\text{O}-\underline{i}\text{-Pr})_3)_4$ are yellow in color. Addition of acid to these solutions brings about an increase in the intensity of the yellow color. However, solutions of $\text{Ni}(\underline{9})_4$ appear colorless. The development of the yellow color occurs only when acid is added. It has been shown fairly conclusively (108) that this yellow

color indicates the presence of NiL_3 species in solution. Based upon either of the previously described isomerization mechanisms, HNiL_3^+ or NiL_3 are known to be the catalytically active intermediates. The question then posed is the following: If $\text{Ni}(\text{P}(\text{O}-\underline{i}\text{-Pr})_3)_4$ is more dissociated in solution than $\text{Ni}(\underline{9})_4$, then why is it a poorer catalyst than $\text{Ni}(\underline{9})_4$? In order to explain this difference in activity, Gultneh contends that $\text{Ni}(\text{P}(\text{O}-\underline{i}\text{-Pr})_3)_4$ decomposes more quickly in the strongly acid media than $\text{Ni}(\underline{9})_4$. However, results of the present work have shown that there is very little difference in the rate of decomposition of both complexes in acid solution. This decomposition is evidenced by the solution turning from yellow to green, indicative of the formation of Ni(II) species. Gultneh also contends that electronic factors cause a difference in the extent to which both compounds dissociate in solution. He also states, based upon previous work, that the steric difference between $\text{P}(\text{O}-\underline{i}\text{-Pr})_3$ and $\underline{9}$ is minor. These conclusions do not appear credible since: a) Tolman (19) has shown that steric factors are more important than electronic factors in the extent to which a NiL_4 complex will dissociate; b) Based upon the increase in the extent of dissociation which is observed from $\text{Ni}(\text{P}(\text{O}-\underline{i}\text{-Pr})_3)_4$ over $\text{Ni}(\underline{9})_4$ it would appear that $\text{P}(\text{O}-\underline{i}\text{-Pr})_3$ has greater steric bulk than $\underline{9}$. This increased extent of dissociation is evidenced by solutions of $\text{Ni}(\text{P}(\text{O}-\underline{i}\text{-Pr})_3)_4$ being yellow in color as opposed to solutions of $\text{Ni}(\underline{9})_4$ which are colorless. Tolman and Gosser have previously stated (108) that the yellow color stems from the presence of dissociated $\text{Ni}(\text{P}(\text{O}-\underline{i}\text{-Pr})_3)_3$ species. Unfortunately, measurement of the cone angle of the free ligand may not

provide any useful information about the steric demands of the ligand upon coordination to a metal, since there is no way of determining the exact orientation of the substituents on phosphorus in either a NiL_4 or NiL_3 complex. However, it can be argued that the number of degrees of freedom of the OR group on phosphorus are less in 9 than in $P(O-i-Pr)_3$ due to the cyclization of the ring. In fact, the isopropyl groups in $P(O-i-Pr)_3$ should be free to adopt any geometry which minimizes their interactions. It is believed that the isopropyl group in the resulting $Ni(P(O-i-Pr)_3)_3$ complex could partially block coordination of the olefin to the nickel atom, thus reducing the activity of the system. This argument can be extended to the $HNi(P(O-i-Pr)_3)_3^+$ species which forms in protic media.

Tolman and Gosser have suggested (108) that the geometry of a NiL_3 species is trigonal planar. His assertion is supported by a recent x-ray structural analysis of the isoelectronic compound $Pt(PPh_3)_3$ which was observed to be trigonal planar (130). Molecular models of $Ni(P(O-i-Pr)_3)_3$ would suggest that due to the higher degrees of freedom for the isopropyl arms of the ligand it is reasonable to expect that some of these isopropyl groups will spend part of their time situated above and below the nickel atom. This geometry is also stabilized by weak hydrogen bonding interactions which could develop between the CH of one isopropyl group and oxygens contained on adjacent ligands. One would expect that this geometry would hinder olefin coordination to the metal and thus slow the rate of catalysis.

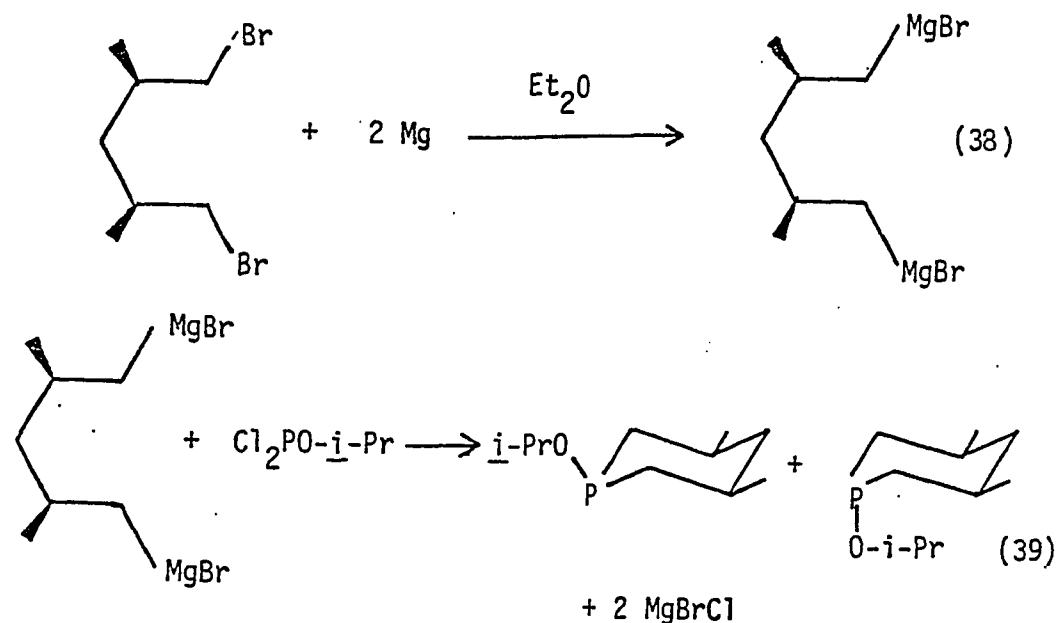
However, with Ni(9)₄ it would appear that steric interactions between the ligands are not large enough to cause ligand dissociation to take place in the unprotonated complex. Dissociation is thus only made facile upon protonation of the nickel. Once protonation does occur, the Ni-P bond is weakened sufficiently so that the steric interactions which occur in the complex can promote dissociation. Since there is less freedom of movement for the OR groups in the cyclic ligands, it should be more difficult for these groups to situate themselves directly above and below the nickel atom; thus, the olefin can easily coordinate to the metal atom and undergo isomerization.

In order to see if constraint of the P-O-C angles in 9 as compared to P(O-i-Pr)₃ could account for the large difference in activity of the complexes, Gultneh prepared the corresponding phosphinite ligands 25 and 28. In these ligands, molecular constraint of oxygen can not be present since the oxygens are replaced by CH₂ groups. It was reported that Ni(28)₄ is a more effective catalyst than its acyclic analogue, Ni(25)₄. However, the 12% difference in the number of catalytic cycles/30 min. that each produced was small compared to the 2000% difference that was observed with the analogous phosphites during same time period. It was suggested (38) that the large difference in rates between the phosphite and the phosphinite complexes was due to the presence of the oxygens contained in the phosphite ligands.

In the discussion of the phosphinite complexes, no mention was made of the presence of the conformational isomers 27 and 28. It was known that the conformation of the exocyclic group on phosphorus influences the

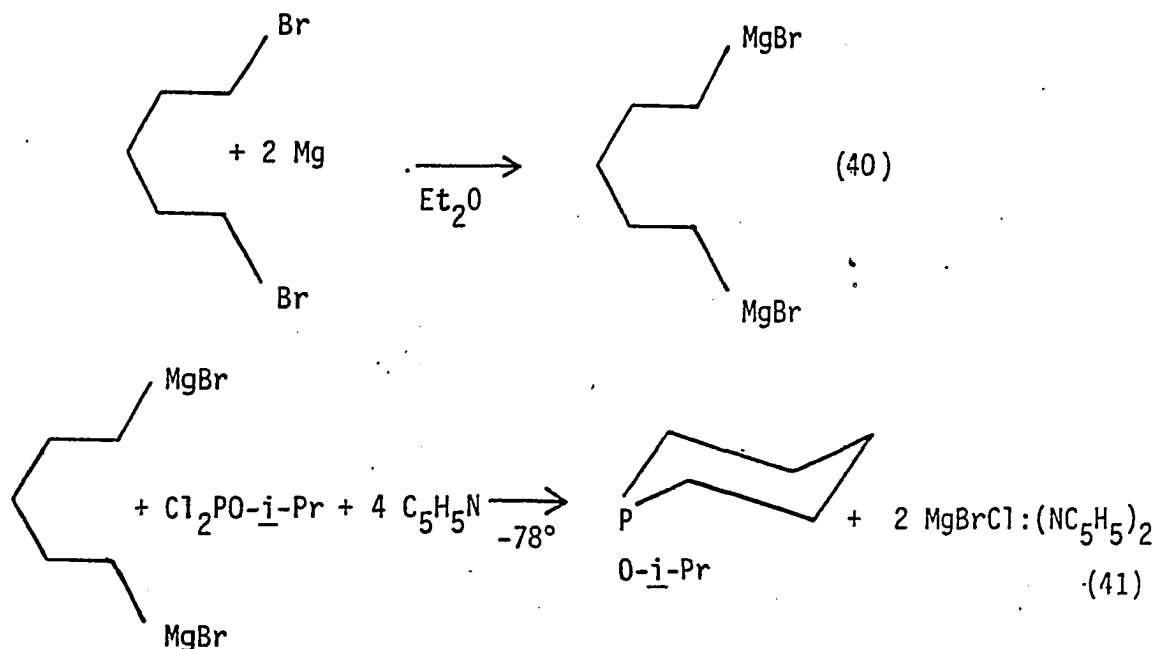
phosphorus basicity (19). Since it had been shown that both conformers 8 and 38 could be prepared and isolated, it seemed reasonable that conformers 27 and 28 could be prepared and isolated. It was thought that perhaps one of the conformers would produce a more active complex than the other due to basicity and/or steric differences. Perhaps the activity which was observed with the phosphinites was due to the weighted averages of the amount of each isomer coordinated to the nickel atom.

Attempts to prepare a sample of the free ligand according to the procedure of Gultneh (38) met with repeated failure (Eqs. 38, 39).



This problem was further complicated by the fact that the meso-2,4-dimethyl-1,5-dibromopentane was obtained in only 7.2% overall yield as described in scheme (5). In order to determine the optimum conditions

for producing 27 and 28, attempts were made to prepare the unsubstituted ring compound 26 via Equations 40 and 41 using the commercially available 1,5-dibromopentane.



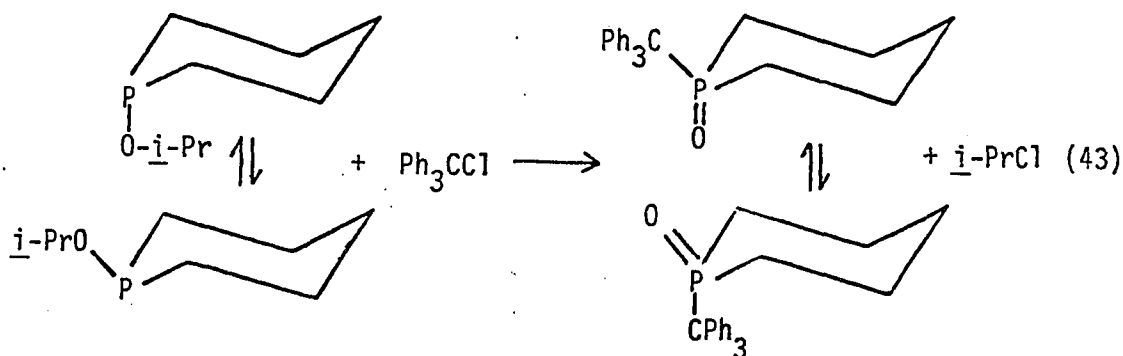
It was found that by adding pyridine to the reaction of the Grignard reagent and $\text{Cl}_2\text{P}(\text{O}i\text{Pr})$ (Eq. 41), the yield of cyclic phosphinite (26) could be enhanced. Kabachnik and Tsvetkov (131) were the first to show that the yield of a phosphinite ($\text{R}_2\text{P}(\text{OR})$) in these types of Grignard reactions could be greatly improved by the presence of pyridine. It appeared that the pyridine assisted in the displacement of the phosphinite from their complexes with the magnesium halide, which was produced in the above reaction.

As previously stated in the experimental section, the oil which was obtained from reaction (40) was shown to contain two phosphorus species

in a ratio of 20 to 1 by ^{31}P NMR spectroscopy. Integration of the ^1H NMR spectrum of the oil which was obtained was found to be consistent with the proposed structure of 26. Attempts to purify the material by distillation were unsuccessful due to decomposition that took place during heating. Kosolopoff and Maier have shown (132) that similar phosphinites are unstable towards rearrangement to tertiary phosphine oxides upon heating (Eq. 42).



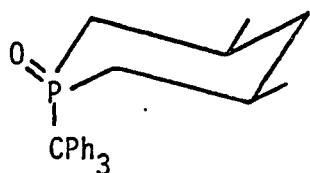
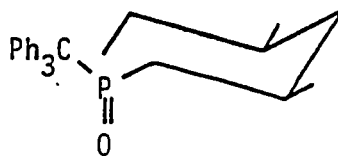
To further confirm the identity of the product of reaction (41), the oil which was obtained was derivatized by an Arbusov reaction (Eq. 43) using triphenylmethyl chloride. The ^1H NMR, ^{31}P NMR and mass spectral



data which were obtained on the product 29 was consistent with its proposed structure.

Upon developing the proper reaction conditions for the synthesis of these types of cyclic phosphinites, reactions 38 and 39 were reattempted. In order to determine the conformational distribution of 27 and 28 contained in the product, the mixture was immediately reacted with

triphenylmethyl chloride in order to obtain more stable derivatives. White (99) has shown that the Arbusov rearrangement of 8 and 38 with triphenylmethyl chloride proceeds with retention of configuration. Therefore, the relative amounts of compounds 29 and 30 should indicate the amounts of 27 and 28 in the original reaction mixture.

2930

^{31}P NMR analysis of the crude solid obtained from the reaction of 27 and 28 with triphenylmethyl chloride showed the presence of many peaks. However, two peaks at 56.0 ppm and 53.6 ppm were observed in a 3 to 1 ratio. Chromatographic separation of the mixture yielded an oil which exhibited only these peaks in the same ratio. Upon standing, crystals formed in the oil which exhibited a ^{31}P NMR chemical shift of 53.6 ppm. The remaining oil showed the other chemical shift at 55.7 ppm. Mass spectral analysis of both the oil and the crystals showed that they contained compounds which were similar in structure due to the similarity of their fragmentation patterns (Figs. 10 and 11) and the fact that they both yielded parent ions with m^+/e values of 388.1. An X-ray crystallographic analysis was carried out in order to determine whether conformer 29 or 30 was contained in the crystals. The analysis revealed the identity of the crystals to be 30. The final atomic positions, bond

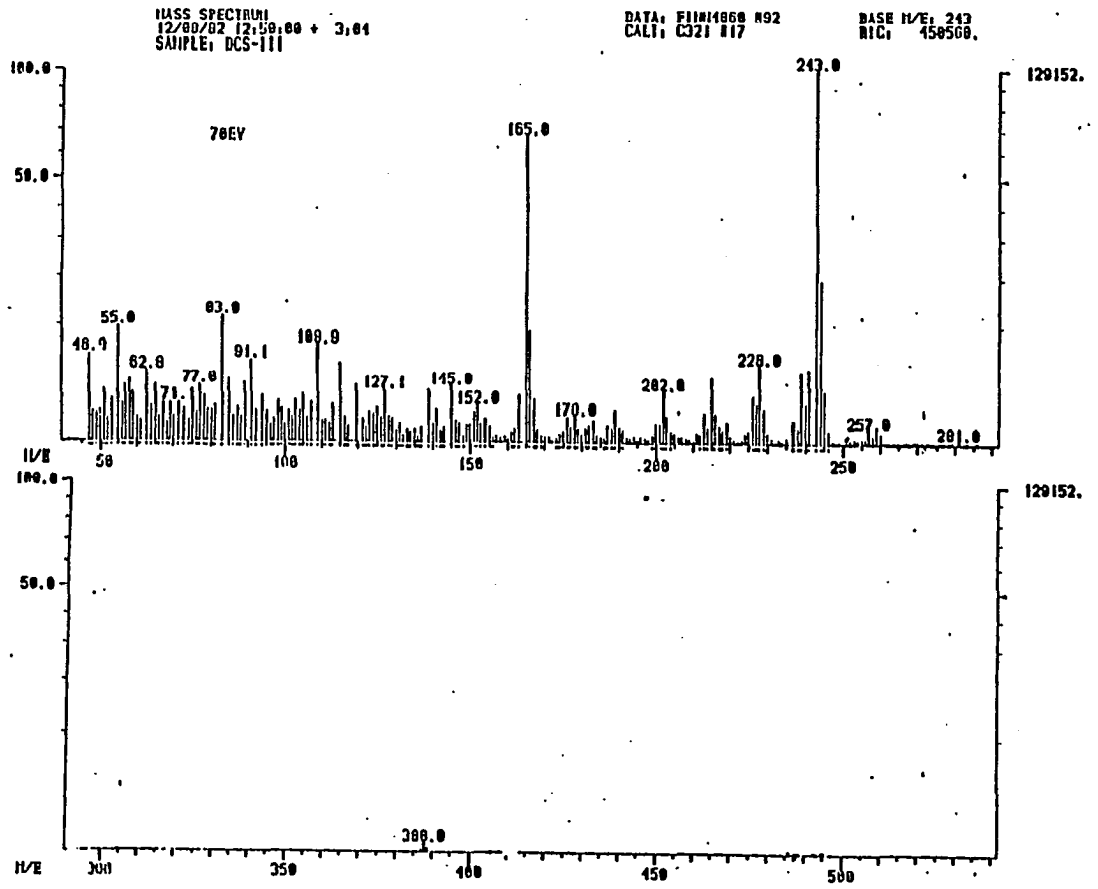


Figure 10. Mass spectrum of 29

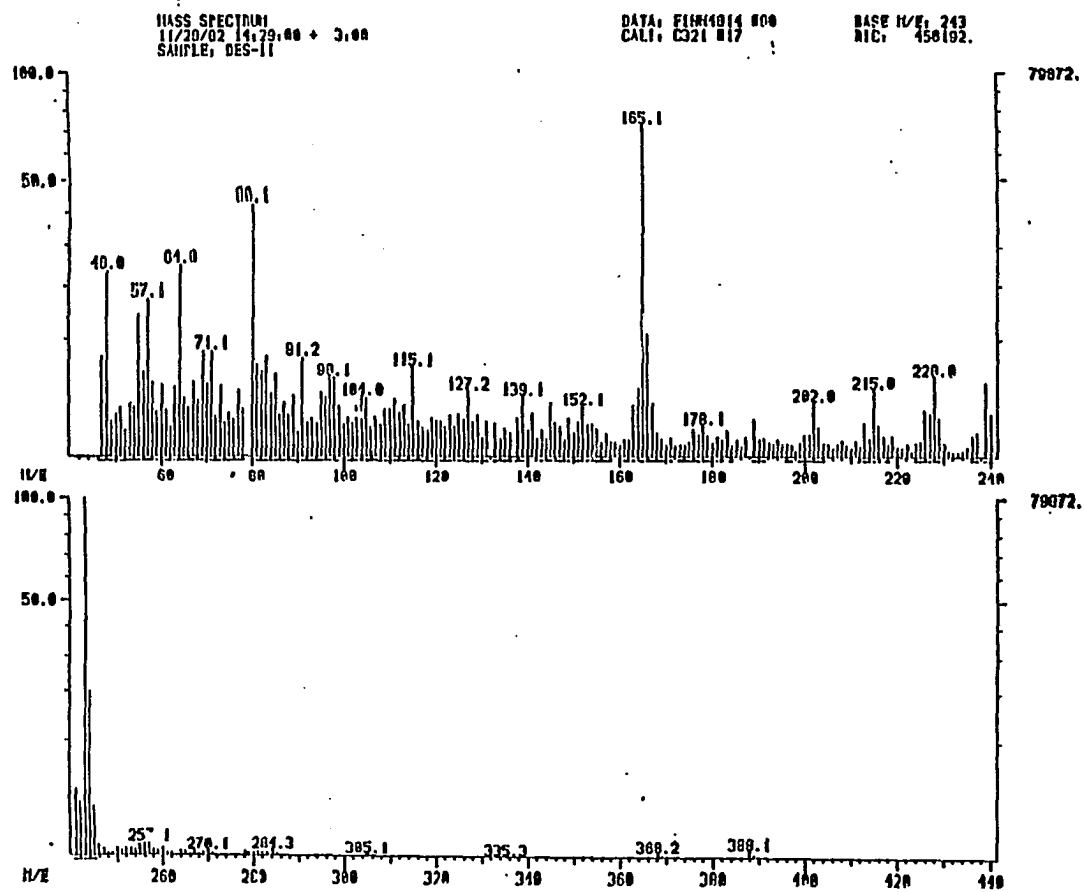


Figure 11. Mass spectrum of 30

lengths and angles, and anisotropic thermal parameters appear in Tables 16, 17, 18 and 19, respectively. Structure factors for the compound are found in Appendix 2. An ORTEP diagram of the structure can be found in Fig. 12. A view of the unit cell is shown in Fig. 13.

Table 16. Final positional parameters and their estimated standard deviations (in parentheses) for meso-
(C₆H₅)₃C(O)P[CH₂C(CH₃)H]₂CH₂ (30)^a

atom	x	y	z
P	0.0637(1)	0.0752(1)	0.2462(1)
O	0.1319(3)	0.0268(3)	0.2306(3)
C	0.0971(4)	0.1413(4)	0.3559(4)
C1A	0.0246(4)	0.1665(4)	0.4119(5)
C2A	0.0142(5)	0.1472(4)	0.5012(5)
C3A	-0.0545(5)	0.1675(5)	0.5493(5)
C4A	-0.1154(5)	0.2068(5)	0.5089(6)
C5A	-0.1089(5)	0.2274(4)	0.4198(6)
C6A	-0.0384(5)	0.2082(5)	0.3718(5)
C1B	0.1407(4)	0.2080(4)	0.3103(4)
C2B	0.2040(4)	0.1922(4)	0.2535(5)
C3B	0.2472(5)	0.2499(5)	0.2114(5)
C4B	0.2282(5)	0.3257(5)	0.2291(6)
C5B	0.1663(6)	0.3417(4)	0.2877(5)

^aPosition parameters are listed in fractional unit cell coordinates.

Table 16. (continued)

atom	x	y	z
C6B	0.1231(4)	0.2834(4)	0.3287(5)
C1C	0.1570(4)	0.1015(4)	0.4171(5)
C2C	0.1552(5)	0.0226(5)	0.4335(6)
C3C	0.2069(5)	-0.0105(5)	0.4963(6)
C4C	0.2623(5)	0.0300(5)	0.5435(5)
C5C	0.2655(5)	0.1086(5)	0.5264(5)
C6C	0.2138(5)	0.1424(5)	0.4640(5)
C1	0.0201(5)	0.1292(4)	0.1725(5)
C2	-0.0143(6)	0.0742(6)	0.1017(5)
C3	-0.0530(7)	0.1235(6)	0.0243(6)
C4	-0.0786(5)	0.0244(5)	0.1433(5)
C5	-0.1227(6)	-0.0802(6)	0.2496(7)
C6	-0.0524(6)	-0.0283(5)	0.2192(5)
C7	-0.0227(4)	0.0189(4)	0.3009(5)

Table 17. Bond distances (Å) and their estimated standard deviations (in parentheses) for *meso*-(C₆H₅)₃C(O)P[CH₂C(CH₃)H]₂CH₂ (30)

P-O	1.501(5)	C1C-C2C	1.413(11)
P-C	1.879(7)	C2C-C3C	1.397(12)
P-C1	1.816(8)	C3C-C4C	1.359(12)
P-C7	1.824(8)	C4C-C5C	1.411(12)
C1-C2	1.542(12)	C5C-C6C	1.398(11)
C2-C3	1.580(13)	C6C-C1C	1.374(11)
C2-C4	1.513(13)		
C4-C6	1.528(12)		
C6-C5	1.548(14)		
C6-C7	1.556(11)		
C-C1A	1.528(10)		
C-C1B	1.539(10)		
C-C1C	1.519(10)		
C1A-C2A	1.385(11)		
C2A-C3A	1.392(11)		
C3A-C4A	1.364(12)		
C4A-C5A	1.381(12)		
C5A-C6A	1.41(11)		
C6A-C1A	1.409(11)		
C1B-C2B	1.376(10)		
C2B-C3B	1.393(11)		
C3B-C4B	1.398(11)		
C4B-C5B	1.375(12)		
C5B-C6B	1.393(11)		
C6B-C1B	1.387(10)		
C1C-C2C	1.413(11)		
C2C-C3C	1.397(12)		
C3C-C4C	1.359(12)		
C4C-C5C	1.411(12)		
C5C-C6C	1.398(11)		
C6C-C1C	1.374(11)		

Table 18. Bond angles ($^{\circ}$) and their estimated standard deviations (in parentheses) for meso-(C_6H_5) $_3C(O)P[CH_2C(CH_3)H]_2CH_2$ (30)

O-P-C	111.96(31)	C2B-C1B-C6B	118.44(67)
O-P-C1	110.19(33)	C1B-C2B-C3B	121.26(69)
O-P-C7	112.38(34)	C2B-C3B-C4B	119.92(73)
C-P-C1	109.88(34)	C3B-C4B-C5B	118.84(76)
C-P-C7	110.46(33)	C4B-C5B-C6B	120.69(75)
C1-P-C7	101.50(36)	C1B-C6B-C5B	120.78(73)
P-C-C1A	110.25(48)	C-C1C-C2C	122.93(66)
P-C-C1B	106.88(43)	C-C1C-C6C	120.68(66)
P-C-C1C	110.06(49)	C2C-C1C-C6C	116.29(69)
C1A-C-C1B	112.77(59)	C1C-C2C-C3C	120.95(75)
C1A-C-C1C	108.63(54)	C2C-C3C-C4C	122.81(79)
C1B-C-C1C	108.21(57)	C3C-C4C-C5C	116.59(74)
C-C1A-C2A	123.38(65)	C4C-C5C-C6C	121.01(73)
C-C1A-C6A	120.16(64)	C1C-C6C-C5C	122.34(74)
C2A-C1A-C6A	116.36(67)	P-C1-C2	109.44(56)
C1A-C2A-C3A	122.23(71)	C1-C2-C3	107.69(74)
C2A-C3A-C4A	120.52(74)	C1-C2-C4	110.11(66)
C3A-C4A-C5A	119.99(78)	C3-C2-C4	109.47(79)
C4A-C5A-C6A	119.35(75)	C2-C4-C6	117.17(76)
C1A-C6A-C5A	121.52(70)	C4-C6-C5	111.27(79)
C-C1B-C2B	118.24(62)	C4-C6-C7	110.07(73)
C-C1B-C6B	123.15(64)	C5-C6-C7	108.99(69)
		P-C7-C6	107.71(53)

Table 19. Thermal parameters and their estimated standard deviations^a
(in parentheses) for *meso*-(C₆H₅)₃C(O)P[CH₂C(CH₃)H]₂CH₂ (30)

atom	B ₁₁	B ₁₂	B ₃₃	B ₁₂	B ₁₃	B ₃₃
P	6.0(1)	6.1(1)	4.8(1)	-0.5(1)	-0.1(1)	0.0(1)
O	6.6(3)	7.3(3)	6.8(3)	0.6(3)	1.0(2)	-1.0(3)
C	5.5(5)	6.1(4)	3.9(4)	0.5(4)	-0.4(3)	-0.4(4)
C1A	6.0(5)	5.6(5)	5.9(4)	-0.3(5)	-0.1(4)	-0.2(4)
C2A	6.2(6)	7.0(6)	5.4(4)	0.0(5)	1.0(4)	1.0(4)
C3A	9.2(6)	8.3(6)	5.7(6)	-0.7(6)	1.3(5)	0.4(5)
C4A	8.1(7)	8.1(6)	7.3(6)	0.1(6)	2.1(5)	0.10(5)
C5A	7.0(6)	8.1(6)	7.0(6)	0.9(5)	-0.1(5)	-0.6(5)
C6A	7.6(8)	7.9(6)	5.2(5)	0.4(5)	0.8(5)	-0.5(5)
C1B	5.8(5)	5.3(5)	4.9(4)	-0.0(4)	-0.6(4)	-0.4(4)
C2B	6.1(5)	6.1(5)	6.2(5)	-0.7(4)	0.1(5)	0.4(4)
C3B	6.8(6)	8.1(6)	6.5(5)	-0.8(6)	-0.1(4)	-0.2(5)
C4B	7.8(6)	8.0(7)	7.3(6)	-2.2(6)	-0.6(5)	1.2(6)
C5B	9.5(7)	5.9(6)	7.9(6)	0.5(6)	-0.5(5)	0.1(5)
C6B	7.6(6)	5.9(5)	6.2(5)	-0.27(5)	0.1(4)	-0.1(4)
C1C	5.2(5)	6.6(5)	5.0(4)	-0.7(4)	-0.3(4)	-0.4(4)
C2C	7.5(6)	6.7(6)	7.8(6)	-0.5(5)	-2.6(5)	0.2(5)
C3C	9.5(6)	7.0(5)	8.4(6)	-0.3(5)	-3.1(6)	0.6(5)

^aThe form of the anisotropic thermal parameter is $\exp[-(B_{11}a^2h^2 + B_{22}b^2k^2 + B_{33}c^2l^2)/r + (B_{12}a^*b^*hk + B_{13}a^*c^*hl + B_{23}b^*c^*kl)/2]$.

Table 19. (continued)

atom	B ₁₁	B ₂₂	B ₃₃	B ₁₂	B ₁₃	B ₂₃
C4C	7.0(6)	7.9(6)	6.4(5)	0.7(6)	-1.11(5)	1.1(5)
C5C	6.6(6)	9.2(7)	6.0(5)	-1.0(5)	-1.3(5)	0.1(5)
C6C	6.9(5)	7.1(5)	5.9(5)	0.2(5)	-0.7(4)	1.4(5)
C1	8.1(5)	6.3(5)	4.2(4)	0.5(4)	-0.5(4)	0.8(4)
C2	11.7(7)	9.5(6)	6.1(5)	-3.8(6)	-1.9(5)	0.6(5)
C3	15.2(8)	9.9(7)	6.9(6)	-1.7(6)	-4.9(6)	2.9(5)
C4	8.0(6)	9.9(7)	5.8(5)	-1.2(5)	-1.3(5)	-0.9(5)
C5	11.8(8)	12.2(8)	10.3(7)	-7.3(7)	0.5(7)	-0.1(7)
C6	11.5(7)	9.7(6)	5.5(5)	-3.7(6)	-2.7(5)	0.9(5)
C7	5.6(4)	7.5(5)	5.9(4)	-1.9(4)	1.3(4)	0.8(4)

As can be seen in Fig. 12, the triphenylmethyl group adopts the equatorial position with respect to the phosphorinane ring. The ring adopts the chair conformation which appears to be free of any twist as the torsional angles described by atoms P, C1, C2, C4 and P, C7, C6, and C4 are equal to 59.7° and -60.8, respectively. The acute angle formed by the planes C1-P-C7 and C7-C6-C2-C1 is 53.6°, which is fairly close to the 60° angle found in the perfect chair conformation of cyclohexane. The rear of the phosphorinane ring comprised of the C2, C4, and C6 atoms does appear to be somewhat flattened since the acute angle between the least square planes encompassing the C2, C4, C6 and C1, C2, C6, C7 atoms is

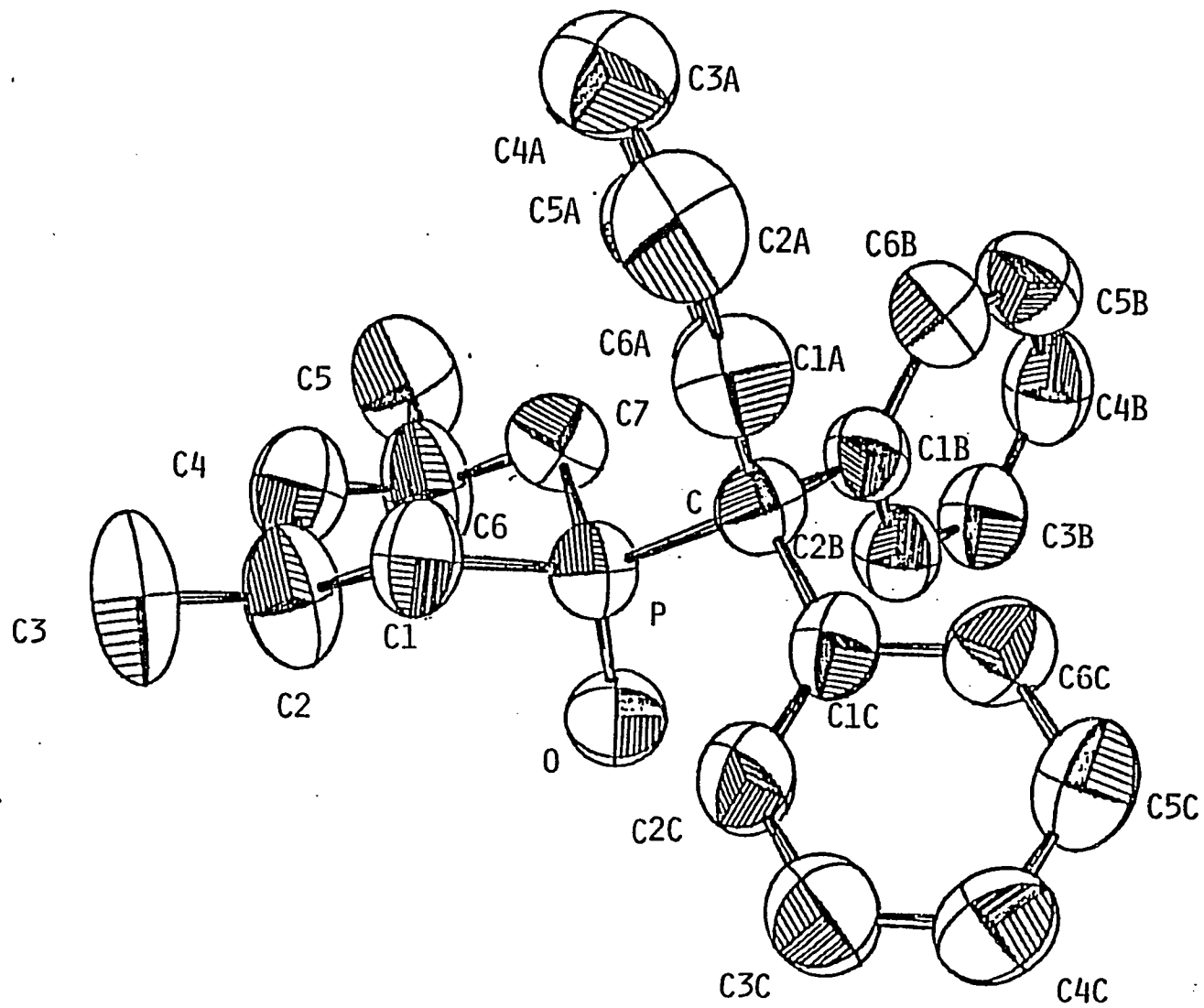


Figure 12. ORTEP diagram of 30.

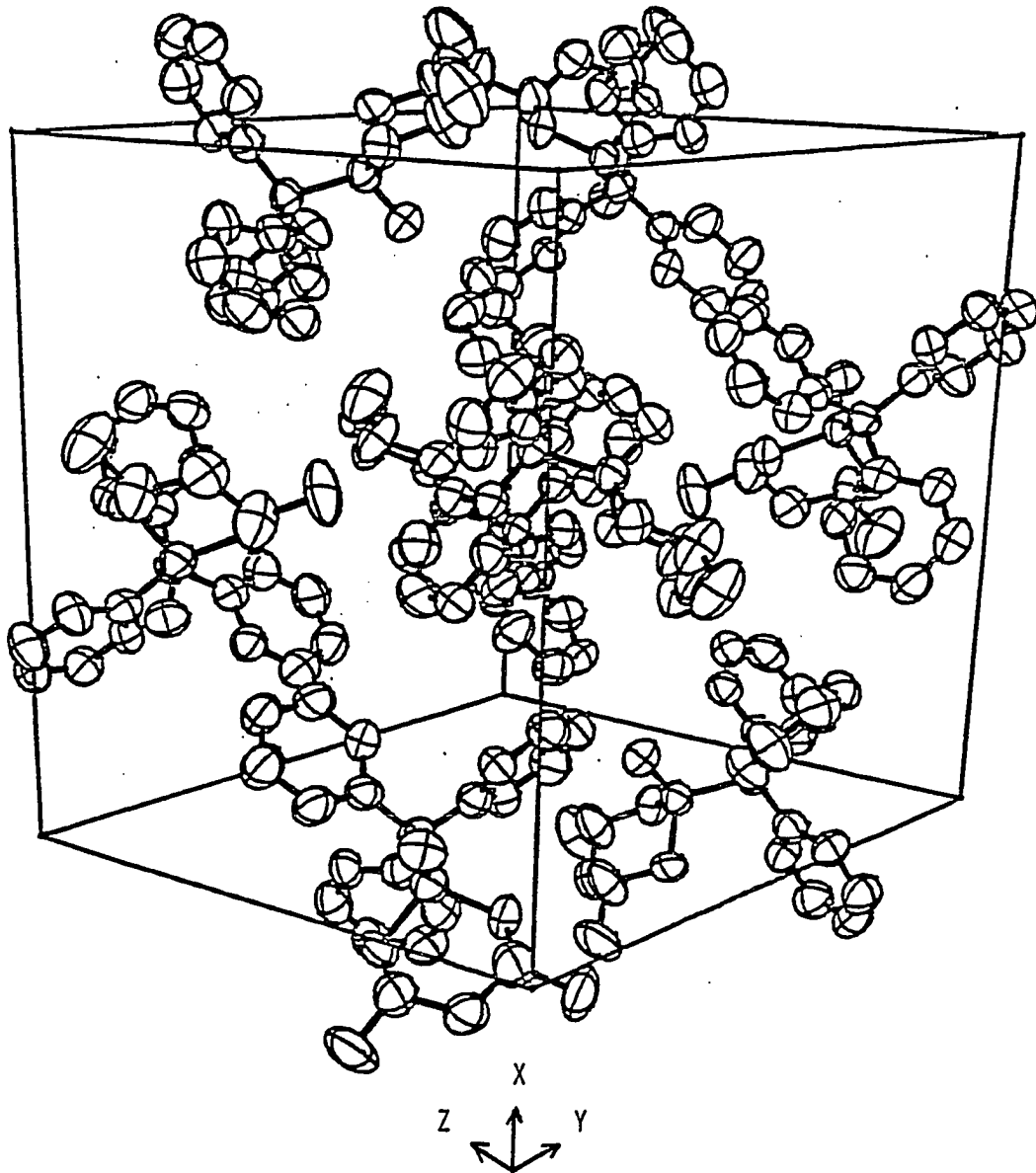


Figure 13. Unit cell diagram of 30.

equal to 39.2° . This deviation from 60° can only be ascribed to packing forces within the crystal, since there appears to be no steric interactions with any other parts of the molecule which could account for this flattening. All other bond distances and angles are consistent with those found in other 2-alkoxy-2-oxo-1,3,2-dioxaphosphorinanes (99).

Reactions of cyclic phosphites and triphenylmethyl chloride are known to yield Arbusov products in which the original conformation about phosphorus is retained (133). Since the reaction of the phosphinite and triphenylmethyl chloride presumably takes place by the same mechanism as with a phosphite, the percentage of each configuration in the resulting tertiary phosphine oxide mixture should be the same as in the starting phosphinite mixture. Based upon information supplied by the X-ray crystallographic analysis, we are able to assign the peak at 53.6 ppm of the phosphine oxide mixture to configuration 30 while the peak at 56.0 ppm is assigned to 29. Since the ratio of the peak areas in the ^{31}P NMR spectrum is 3 to 1, this should correspond to a ratio of 3 to 1 in the original phosphinite mixture.

As stated previously, in 2-alkoxy-1,3,2-dioxaphosphinanes the conformation with the axial alkoxy group and an equatorial lone pair is preferred. This conformation is preferred in order to minimize electronic interactions between the lone pairs on phosphorus and the lone pairs on oxygen. However, phosphorinanes which do not contain oxygen in the ring prefer to adopt the conformation which has the alkoxy group in an equatorial position and a lone pair in the axial position. This

conformation reduces the steric interaction between the exocyclic group and the rest of the ring (19).

The 3 to 1 ratio of configurations was also verified by a ^{31}P NMR analysis of the product mixture obtained in reactions (37 and 38). Previous work had shown that compound 26 exhibited a sharp singlet at 108.8 ppm. Close scrutiny of the NMR spectrum of the mixture showed three peaks at 111.1, 109.4, and 107.4 ppm in a ratio of 1 to 3 to 1. The peaks at 109.4 and 107.4 ppm were assigned to compounds 27 and 28, respectively. While the peak at 111.1 was ascribed to possibly oligomeric products formed in the reaction. The peaks were assigned as shown since work with the derivatized material indicated a 3 to 1 mixture of starting phosphinites. Also, it appeared that these peaks were observed to have ^{31}P NMR chemical shifts which were on either side of the corresponding unsubstituent phosphinite. As can be seen in Table 20, the decreasing ^{31}P NMR chemical shifts fall in the order: 55, 56, and 57. Though the magnitudes of the differences in chemical shifts between compounds may be different in phosphites and phosphinites, the trends in chemical shifts may be expected to be the same due to the similarity of the compounds.

Attempts to prepare and separate 27 and 28 had proved unsuccessful. ^{31}P NMR peak integration has shown that the compounds were prepared in less than 10% yield. Due to the low yield of the compounds and the fact that there was no known way of converting back the derivatized products to their starting phosphinites, it seemed that

Table 20. ^{31}P NMR Chemical shifts for selected phosphorinane compounds

Compound	Chemical shift (ppm)	Compound	Chemical Shift (ppm)
<u>55</u>	132.9	<u>27</u>	109.4
<u>56</u>	130.0	<u>26</u>	108
<u>57</u>	127.1	<u>28</u>	107.4

^aReference (38).

^bReference (133).

separation of the isomers would not be feasible. However, it was known (38) that NiL_4 complexes of 28 and 27 could be made by reaction of the ligand obtained in reaction (38) with $\text{Ni}(\text{CH}_2=\text{CHCN})_2$. The amount of $\text{Ni}(\text{CH}_2=\text{CHCN})_2$ to be used was determined by the ^{31}P NMR spectrum of the oil which indicated the relative amount of 27 and 28 contained in a specific amount of the mixture. Unfortunately, repeated attempts to synthesize $\text{Ni}(\text{27,28})_4$ were met with failure. In every case, unrecognizable products were obtained. ^{31}P NMR analysis of this material indicated the lack of any of the NiL_4 complex as Gultneh (38) had described. However, attempts to prepare $\text{Ni}(\text{25})_4$ were successful. The final product obtained by chromatography under N_2 was a greyish white solid which exhibited only one ^{31}P NMR chemical shift at +144.9 ppm, 22.9 ppm downfield of the free ligand. In all the previously discussed

complexes, a downfield shift of approximately 20 ppm was observed for the ligand upon coordination.

Attempts to use this compound in the catalytic isomerization of 3-butenitrile were unsuccessful. It was observed that upon addition of the acid to a benzene solution of the complex the solution took on a yellow-orange color. However, after about fifteen minutes the color had changed to green, indicative of nickel oxidation. This observation agrees with work of Carriatta and co-workers (134) who showed that only zero-valent platinum phosphine complexes could be protonated by acid. Attempts to protonate the analogous tetrakis phosphine palladium and nickel complexes yielded only nickel and pallium salts of the corresponding acid.

This instability of NiL_4 complexes of phosphines and phosphinites toward acids can be explained by the electronic properties of the ligands. Since these ligands are known to be more basic than phosphites, they should impart more electron density to the nickel atom thus making it easier for its oxidation by acids. On the other hand, the phosphite is able to decrease the electron density on the nickel atom due to its increased π -acceptor and poorer σ donation properties. It is this reduced electron density on nickel which prevents immediate oxidation by the acid. However, this reduction in electron density is still not enough to entirely prevent oxidation of the Ni(0) species. It only serves to slow down oxidation as evidenced by oxidation of a $Ni(P(OR)_3)_4$ complex in acid approximately 6 hrs. (under anaerobic conditions). Fortunately, during this period, the $HNiL_3^+$ species, which is generated

from the NiL_4 complex in protic acids, and the NiL_3 species generated with nonprotic acids can act as catalysts for olefin isomerization. However, it should also be realized that removal of electron density from the nickel by strong π -acceptor ligands can become so great, as in the case of 11 and 12, that the corresponding NiL_4 fails to protonate; or in the case of nonprotic acid media, fails to dissociate sufficiently. Thus, it would appear that the unique electronic properties of phosphite ligands facilitate their use in NiL_4 /acid catalyst systems.

Asymmetric isomerization of $(\text{CH}_3\text{CH}_2)(\text{CH}_3)\text{C}=\text{CHCH}_2\text{CN}$

Gultneh (38) found that $\text{Ni}((-)\text{-7})_4$ catalyzed the asymmetric isomerization of $\text{Et}(\text{Me})\text{C}=\text{CHCH}_2\text{CN}$ to $\text{Et}(\text{Me})\text{CHCH}=\text{CHCN}$. He observed that approximately 70% of the starting prochiral olefin could be isomerized, and a 52% enantiomeric excess could be achieved in a period of 2 hrs.

Results obtained in the isomerization of 3-butenenitrile had shown that the most active catalysts were those which contained methyl groups in the equatorial 4 and 6 positions on the ring. It was thought that by synthesizing a chiral ligand with methyl groups in these positions and incorporating it in a NiL_4 complex, isomerization of the above compound could be carried out more quickly with possibly a higher degree of enantiomeric excess. Compound 36 was prepared by the reaction of 4 and d-sec butanol in the presence of triethyl amine. The NiL_4 complex was prepared using the aforementioned method. Subsequent ^{31}P NMR analysis showed that the complex was completely protonated by a 10 to 1 acid to nickel ratio. This was evidenced by the disappearance of a singlet at

151.3 ppm for the NiL_4 species and the appearance of a doublet at 131.8 ppm ($J_{H-M-p} = 30$ Hz) upon addition of acid.

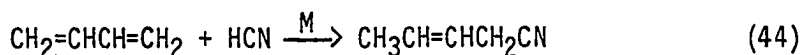
The complex was tried as a catalyst for the isomerization of $Et(Me)C = CHCH_2CN$. However, repeated attempts showed that the complex was completely inactive as a catalyst. However, other experiments showed that the compound could efficiently isomerize 3-butenitrile to cis and trans 2-butenitrile (90 cycles/30 min). On the basis of these results, it was felt that $Ni(\underline{36})_4$ failed to isomerize the prochiral olefin due to the latter's larger size compared to 3-butenitrile. It would appear that $Ni(\underline{7})_4$ was able to isomerize the prochiral olefin since the ligand was smaller than 36 and thus the prochiral olefin could more easily coordinate to the metal center and undergo isomerization.

These results would seem to suggest, as was previously suggested by Parshall (1), that when designing a metal complex to be used as a catalyst, one must not only take into account the steric requirements of the ligands about the metal, but also the steric requirements of the substrate.

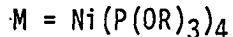
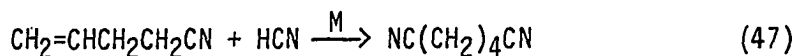
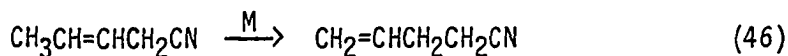
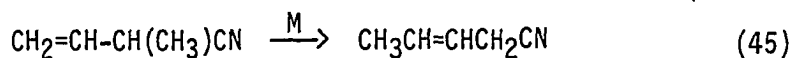
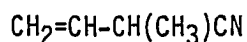
Hydrocyanation of 1,3-butadiene to adiponitrile

The catalytic hydrocyanation of olefins has been of interest to industrial chemists for many years. The hydrocyanation of butadiene to adiponitrile ($NC(CH_2)_4CN$) is of considerable interest, because of the use of adiponitrile as a chemical intermediate in the production of synthetic polymers, such as nylon. Chemists at Dupont have patented the use of cuprous halides and nickel(0) complexes containing phosphite ligands, in

particular $P(OPh)_3$ (51) as catalysts for the production of adiponitrile from butadiene. The reaction of butadiene and HCN in the presence of these catalysts is thought to proceed via the following series of Equations 44-47.



+



It is claimed that complexes such as $Ni(O\text{-}o\text{-tolyl})_3$ can affect the conversion of 1,3-butadiene to adiponitrile in high yield and with high selectivity (1).

It should also be noted that Monsanto Corporation has patented a process for the production of adiponitrile by electrodimmerizing acrylonitrile (135). Acrylonitrile can be easily prepared by addition of HCN to acetylene via the use of catalysts such as $Co_2(CO)_8$ and $Ni(P(OEt)_3)_4$ (47). The advantage of this process is that the adiponitrile can be produced without production of unwanted isomers as is the case with 1,3-butadiene.

Gultneh (38) found that the NiL_4 complexes he used for olefin isomerization were also effective hydrocyanation catalysts. It was observed that the most efficient isomerization catalysts were also the most efficient for hydrocyanation. However, two major differences were observed. Though hydrocyanation of olefins such as norbornene was maximized with NiL_4 complexes containing ligands with methyl groups in the equatorial 4,6 positions of the phosphorinane ring, changing the size of the exocyclic group had only a small effect in controlling the activity of the complex. It was observed that placement of an isopropyl group in the exocyclic position did seem to maximize the amount of catalysis observed in 4,6-dimethyl phosphorinane system. However, increasing the exocyclic group size to a t-butyl group only reduced the number of turnovers per hour by 15%, whereas in isomerization the rate decreased by 60%. Secondly, addition of excess ligand to the hydrocyanation system brought about an increase in the amount of hydrocyanated product formed. This is opposite to what was observed in the isomerization of 3-butenitrile, where addition of excess ligand brought about a decrease in the extent of catalysis. The probable explanation of this observation is that excess ligand limits the extent to which hydrogen cyanide complexes to the nickel atom, hence slowing down the rate of oxidation of the catalyst to catalytically inactive $Ni(CN)_2$ species.

Since Gultneh had found that these complexes were active catalysts for the hydrocyanation of olefins such as norbornene, allylbenzene, and 1,5-octadiene, it seemed worthwhile to attempt to hydrocyanate 1,3-

butadiene using the catalysts he found to be the most active, namely, $\text{Ni}(\underline{8})_4$ and $\text{Ni}(\underline{9})_4$. The reactions were carried out under the same conditions as used by Drinkard and Lindsey for the production of adiponitrile (46). The mixtures were analyzed for adiponitrile using capillary gas chromatography. As can be seen in Table 21, the yields of adiponitrile were quite low. The values which were obtained are even considerably lower than what was obtained in the hydrocyanation of the previously mentioned olefins. Analysis of the results suggest that $\text{Ni}(\underline{8})_4$ in the presence of ZnCl_2 and excess ligand produced the most active catalyst mixture. It also appeared that having a methyl group instead of an isopropyl group in the exocyclic position produced a more active catalyst. This result is opposite to what was observed by Gultneh for the olefins which he used. The precise reasons for the increased activity of the methyl complex is not yet known. However, it is possible that subtle differences in the steric properties of the ligands cause $\text{Ni}(\underline{8})_4$ to be a more efficient catalyst for the hydrocyanation of 1,3-butadiene. As seen in Table 21, the highest number of turnovers for the $\text{Ni}(\underline{8})_4$ is observed when excess ligand is present. As previously stated, this is probably due to excess ligand preventing complexation of excess HCN to the Ni atom. We are currently unable to give a justification for the lower amount of turnovers observed for the $1/1/8 \text{Ni}(\underline{9})_4/\text{ZnCl}_2/9$ system as compared to the $1/1 \text{Ni}(\underline{9})_4/\text{ZnCl}_2$ system. Previous work (38) would have led to the expectation of a larger number of catalytic cycles for the former system.

Table 21. The preparation of adiponitrile from butadiene and HCN using various catalyst systems at 120°C in xylene

Catalyst mixture	mole of adiponitrile produced mole of Ni/2 hr (± 1)
Ni(<u>8</u>) ₄	4.0
Ni(<u>8</u>) ₄ /ZnCl ₂ / <u>8</u> : 1/1/17	13.6
Ni(<u>9</u>) ₄	0.0
Ni(<u>9</u>) ₄ /ZnCl ₂ : 1/1	6.7
Ni(<u>9</u>) ₄ /ZnCl ₂ / <u>9</u> : 1/1/8	3.0
Ni(<u>9</u>) ₄ /ZnCl ₂ / <u>9</u> : 1/1/15	5.4

It would appear that these catalysts, though good for the hydrocyanation of some olefins, are poor at converting 1,3-butadiene to adiponitrile. Attempts were made to carry out the reaction at 25°C in order to increase the residence time of the butadiene (bp = -4.4°C) and HCN (bp = 26°C) in the flask. However, experiments with Ni(9)₄, ZnCl₂ and 9 in a ratio of 1/1/15 at 25° failed to produce any adiponitrile. It is possible that the reaction fails to proceed at this temperature and the residence time of the reagents may not even be a factor in the lack of activity.

GC-MS analysis of the reaction mixture showed that besides adiponitrile being produced in these reactions, pentenenitrile and compounds of higher molecular weight than adiponitrile were also produced. The yields of these compounds were found to be approximately equal to that of adiponitrile. The identities of these higher molecular weight compounds are not known at this time. However, they are probably oligomers of either 1,3-butadiene or pentenenitrile since Tolman has shown previously that Ni(P(OR)₃)₄ complexes are efficient catalysts for the codimerization of olefins (136). No further work was done with this system due to the apparent lack of activity or selectivity for the production of adiponitrile.

Heterogenized NiL₄ catalysts

As stated in the introduction of this chapter, the advantages in the use of heterogeneous catalysts are numerous. Based upon our knowledge of the NiL₄ catalyst system, we sought to find ways to heterogenize these

catalysts. We were well aware of previous attempts to heterogenize homogeneous catalysts (66). Generally, these techniques involved substitution of a ligand in a homogeneous complex with a ligand bound to a polymer support. However, we decided to attempt a markedly different approach, that of directly incorporating the active metal center in a polymer framework. By doing this, it was hoped that it would be possible to prepare a catalyst which would function heterogeneously while at the same time providing easy access of the substrate to the catalytically active metal site.

First, attempts were made to prepare metal complex polymers of the following type (Fig. 14):

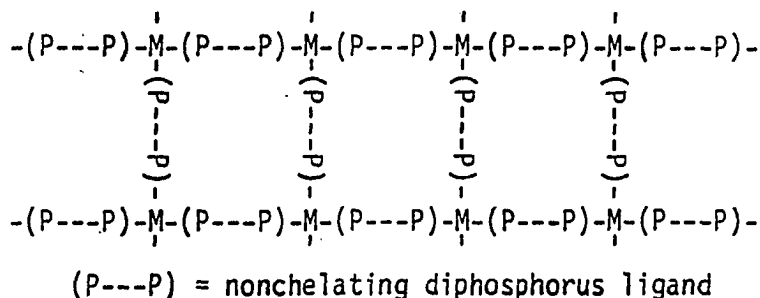
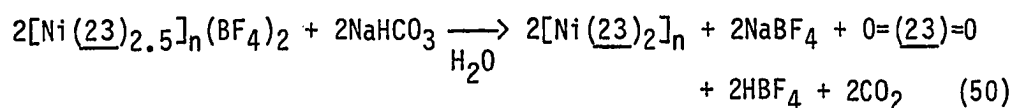
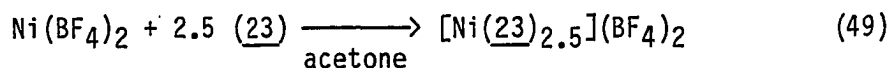
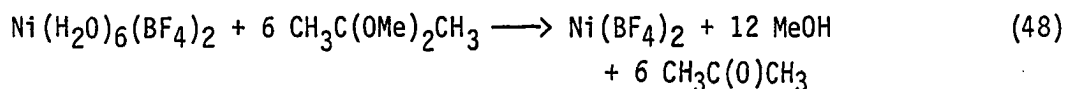


Figure 14. Proposed structure of metal complex polymer. In selecting a ligand which would link metal centers it was deemed necessary that the ligand: 1) not chelate the metal atom, and 2) mimic as closely as possible the structural and electronic properties of the ligand it replaced in the homogeneous NiL_4 complex. Compound 23 was selected to be used as the linking ligand. A recent x-ray structural analysis had shown (41) that the phosphorus lone pairs were unable to chelate a metal atom due to the structural features of the molecule; at the same time its six member ring structure was similar to that shown to

be effective in our homogeneous reaction studies. Attempts to prepare a polymer of the type $[\text{Ni}(\underline{23})_2]_n$ were carried out via the following reactions.



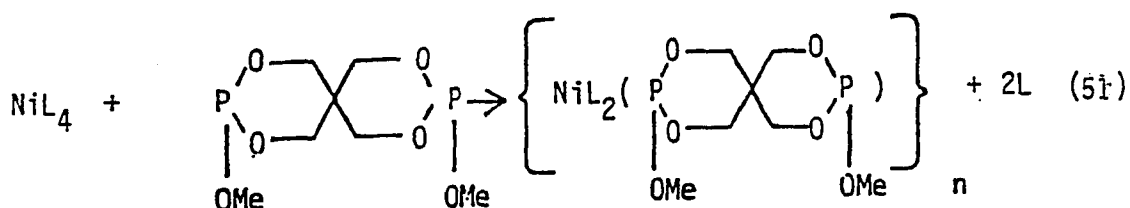
Previously, work with nickel(II) phosphite complexes had shown them to be pentacoordinate (137). Since each molecule of 23 contains two phosphorus atoms it was deemed necessary that a 2.5 to 1 ratio of 23 to nickel ratio should be used. The product from reaction (47) was a bright yellow orange solid which was observed to be insoluble in all solvents including water. The powder was ground very finely and then added to an aqueous bicarbonate solution. Gas evolution was observed as had been observed in similar reactions of $\text{Ni}(\text{P}(\text{OR})_3)_5^{+2}$ and KHCO_3 (138). Upon stirring for 2 hr under N_2 the orange solid had turned white, indicative of a Ni(0) species.

Attempts to reduce $[\text{Ni}(\underline{23})_{2.5}]_n(\text{BF}_4)_2$ with LiAlH_4 and NaBH_4 at room temperature proved to be unsuccessful as evidenced by the brownish-green

intractable solids produced in the reactions. However, reduction with NaBH_4 at -78°C did prove to be successful in producing a white solid.

The white solids which were obtained in these reactions were tried as catalysts in the isomerization of 3-butenitrile. The solid was suspended in a benzene solution which contained the 3-butenitrile. Upon addition of acid to the suspension, the solid turned yellow in color, indicative of protonation of the nickel. Subsequent analysis of the solution showed that the polymer was incapable of isomerizing the olefin.

The inactivity of this catalyst was probably due to its inability to undergo ligand dissociation. As previously stated, the important step in the isomerization mechanism is the dissociation of a ligand from the HNiL_4^+ complex to form a coordinatively unsaturated HNiL_3^+ species. In this type of polymer, ligand dissociation is limited since most of the ligands are part of the polymer framework. In order to overcome this problem, a new type of polymer was designed (139). It was thought that by exchanging ligands between a NiL_4 complex and 23, a new type of polymer could be formed (Eq. 49).



The advantages of this type of catalyst over the previous polymer was that it contained monodentate phosphite ligands(L) which could now undergo dissociation upon protonation of the metal. The strand-like nature of this polymer might also allow for an increase in the availability of the metal atom to coordination of an olefin. Total utilization of all the nickel atoms in the other polymer would not be possible since most of the nickel atoms were buried deep within the polymer framework.

Reaction (51) was found to proceed when L = 5, 7, and P(OMe)₃. Surprisingly, the reaction failed when L = 8. One of the main problems in characterizing these materials was the complete insolubility in all organic solvents, which is indicative of their polymeric nature. This ruled out their analysis using most standard spectroscopic techniques. In order to determine the ratio of 23 to L in these types of polymers, a sample of [Ni(23)(P(OMe)₃)₂]_n was subjected to ozonolysis for 2 hours. ³¹P NMR showed that the only products obtained in this reaction were (MeO)(O)P(OCH₂)₂C(CH₂O)₂P(O)(OMe) and (MeO)₃PO in a ratio of 1.1 to 1 (based on phosphorus), which is slightly greater than the 1 to 1 ratio which would have been expected. A gravimetric nickel analysis was done to determine the percent of nickel in the polymer. [Ni(23)(P(OMe)₃)₂]_n was found to contain 9.4% nickel whereas 10.4% would be expected for a compound of that formulation. [Ni(23)(7)₂]_n analyzed slightly better with a value of 9.1% Ni as compared to an expected value of 9.5%. The polymers were all tried as catalysts in the isomerization of 3-butenitrile, and all were shown to function as catalysts. However,

there was a sharp decline in the activity of these compounds as opposed to their homogeneous analogues (Table 22).

In order to prove that these catalysts operated heterogeneously, the following experiment was carried out. A freshly prepared sample of $[\text{Ni}(\underline{23})(\text{P}(\text{OMe})_3)_2]_n$ was divided in half. One half was used to make sure that the sample could isomerize 3-butenitrile to cis/trans 2-butenitrile. Once the activity of the sample had been established, the other half was used in an identical catalysis experiment. As soon as the complex started to isomerize the olefin (as shown by gas chromatography), the reaction mixture was filtered under a nitrogen atmosphere. The

Table 22. The number of turnovers per unit time produced by various $[\text{Ni}(\underline{23})_2(\text{L})_2]_n$ polymers versus their homogeneous NiL_4 complexes for the isomerization of 3-butenitrile^a

L	$[\text{Ni}(\underline{23})(\text{L})_2]_n$	
	Turnovers/time (± 10)	Turnovers/time (± 10)
$\text{P}(\text{OMe})_3$	120/18 hrs	74/30 min
<u>5</u>	0	60/30 min
<u>7</u>	72/24 hrs	92/30 min

^a3-Butene nitrile/acid/Ni = 124/10/1.

^bRef. (38).

yellow solid could be easily filtered out by glass wool placed at the end of pipette to yield a clear, colorless solution. Subsequent analysis of the solution revealed that the catalysis had stopped upon filtration of the catalysts. The reduced activity of these complexes as compared to their homogeneous counterparts is probably due in part to the following two factors:

1. The different steric environment around the nickel atom in these polymers as compared to the homogeneous NiL_4 complexes could have inhibited olefin coordination and isomerization.

2. These polymers contain only two ligands that are completely free to dissociate (23 is used to maintain the polymer framework) whereas there are four ligands which are free to dissociate in the corresponding NiL_4 complex. Therefore, the polymer's ability to dissociate a ligand and provide an open site for the coordination of olefin is reduced.

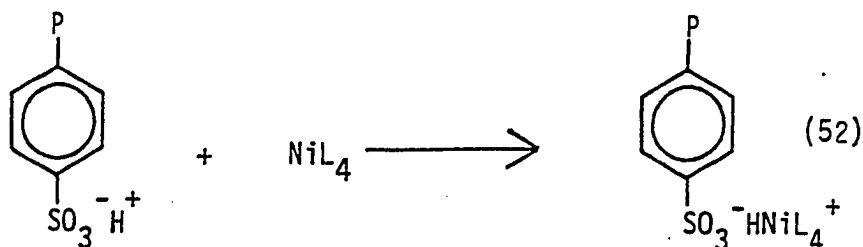
Attempts were also made to polymerize Wilkinson's catalyst. Again, linking ligands were selected on their ability not to chelate the metal atom, and their similarity to the monodentate ligands they were to replace. Initial attempts to polymerize $\text{Rh}(\text{PPh}_3)_3\text{Cl}$ via reaction (51) proved unsuccessful, as no polymeric materials were obtained. Attempts were then made to use 34 as a linking ligand. This ligand was used in an attempt to provide more distance between the (RhClPPh_3) units in the event that their size and proximity inhibited formation of a polymer. The reaction of a 1 to 1 mixture of 33 and $\text{Rh}(\text{PPh}_3)_3\text{Cl}$ was carried out. The reaction yielded a small amount of solid which was close in appearance to $\text{Rh}(\text{PPh}_3)_3\text{Cl}$ but yet did not exhibit any of the solubility

characteristics of the complex. An attempt was made to hydrogenate 1-hexene using this material via the procedure of Osborn and co-workers (21). However, analysis of the catalysis mixture by gas chromatography showed that none of the hexene had been hydrogenated.

Since it was known that PPh_3 was able to dissociate from $\text{Rh}(\text{PPh}_3)_3\text{Cl}$ (22), whereas dissociation of $\text{P}(\text{OMe})_3$ from $\text{Ni}(\text{P}(\text{OMe})_3)_4$ was limited (19), it was felt that perhaps the linking ligand dissociated too quickly from the rhodium atom, thus inhibiting polymer formation. Therefore, (33) was prepared in the hope that it would bind more tightly to the rhodium atom and help ensure polymerization. However, attempts to prepare a polymer from this ligand and $\text{Rh}(\text{PPh}_3)_3\text{Cl}$ were also unsuccessful.

As stated in the introduction, many workers had been successful in finding ways of supporting transition metal complexes on functionalized resins in order to heterogenize homogeneous catalysts. Most of these preparations involved some sort of ligand exchange reaction between the complex and the support. Generally, this technique employed the use of complexes which were observed to undergo facile ligand exchange (i.e. $\text{Rh}(\text{PPh}_3)_3\text{Cl}$). However, in order to anchor appreciable amounts of a complex on the support it was necessary to stir a mixture of the complex and the resin in a solvent for up to three weeks (64). It was known that the NiL_4 ($\text{L}=\text{P}(\text{OR})_3$) complex did not undergo appreciable rates of ligand exchange unless acid was added (38). The use of an acid catalyst to speed up the rate of ligand exchange between a NiL_4 complex and a functionalized support was ruled out, since it was felt that the acid would oxidize most of the complex before it would have a chance to be

anchored to the support. It did seem reasonable to suppose, however, that a NiL_4 complex could be supported on a cation exchange resin via reaction (Eq. 52). In this case the resin would actually act as the acid



which would protonate the complex. At the same time the complex would be anchored on the resin and therefore would act as a heterogeneous catalyst.

In order to maximize diffusion of the NiL_4 complex into the resin, it was decided that macroreticular resins, which are known to have large porosities would be used. Amberlyst IR-15 and XN-1010 were two such resins which have porosities of 32% and 47%, respectively (140). However, the XN-1010 resins had a larger surface area of 540 sq.m/gm. as compared to the 45 sq.m/gm of IR-15 (140). It was thought that the high porosity and surface areas would help diffusion of the NiL_4 complex and substrate into the resin.

The catalyst was prepared by stirring the beads in a toluene solution containing a two fold excess of NiL_4 complex based upon the amount of H^+ in the resin, for approximately 12 hrs. Analysis of the resin indicated that additional hours of stirring failed to significantly

increase the amount of nickel in the bead.

At first, the IR-15 resin was used to investigate the activity of these types of catalysts. The catalyst was prepared as described, and after stirring, the excess NiL_4 complex was removed. This was accomplished by washing the resin under nitrogen with 4 to 5 portions of toluene with each portion being equal in volume to the original amount of toluene used. Proof of heterogeneity of the catalyst was provided by the same experiment that had been used with the polymer catalyst. When a sample was proved active, the catalyst was removed and the catalytic isomerization was observed to have stopped.

In order to determine the amount of nickel present in the resin, the resins were digested in a $HNO_3/HClO_4$ solution. Due to the low concentration of nickel contained in the resin (at most 3.3 mmole/gram resin), the exact amount of nickel present was determined spectrophotometrically. The nickel was complexed using 4-(2-pyridylazo) resorcinol and its concentration was established by measurement of the visible adsorption at 494 nm (107). Each time a new portion of catalyst was prepared, it was analyzed for its nickel content. Table 23 shows the numbers of H^+ cations per nickel atom found. As can be seen for the acyclic phosphites, the larger the ligands, the smaller the amount of complex which was observed to be contained in the resin. The three cyclic compounds were observed in ratios that fell in a small range, with $Ni(8)_4$ appearing to have the highest concentration of nickel in the resin.

Table 23. Amount of H⁺/nickel found in NiL₄/XN-1010 resin catalysts^a

Ligand L	Moles H ⁺ /Moles Ni (±0.5)
P(OMe) ₃	5.5
P(OEt) ₃	6.6
P(OiPr) ₃	8.7
(7)	6.0
(8)	4.6
(58)	7.1

^a3.3 Meq. H⁺/gm of resin.

These resins were used as catalysts in the isomerization of 3-butenitrile under the same conditions as was used in the homogeneous catalyses with the exception that no acid was added. As can be seen in Table 24, in all cases the heterogeneous catalysts were much less efficient than their homogeneous analogues. The reasons for this reduction in rate could lie in any of the following reasons.

Gultneh had found that the highest rates of catalysis were obtained at a 10 to 1 acid to nickel ratio. This allowed for the complete protonation of the NiL₄ as shown in Equation 53. Within the resin, this



Table 24. Number of turnovers/unit time of supported NiL_4 complexes versus their homogeneous analogue for the isomerization of 3-butenitrile

L	Turnovers per unit time for isomerization of 3-butenitrile (± 5)	
	Supported catalysts	Homogeneous catalyst
P(OMe)_3	0	74/30 min
P(OEt)_3	130/24 hrs	52/30 min
P(OiPr)_3	0	35/30 min
(7)	128/12 hr	92/30 min
(8)	132/12 hr	640/30 min
(58)	0	124 cycles/23 min

high ratio could not be achieved since addition of excess acid would have led to the formation of HNiL_4^+ species in solution which could then diffuse out of the resin resulting in homogeneous catalysts.

Secondly, the environment around the NiL_4 complex may not have been conducive to olefin coordination. Since sulfonic acid groups are attached to styrene groups, it is possible that the phenyl rings of the styrene group impede coordination of the olefin to the metal upon ligand dissociation.

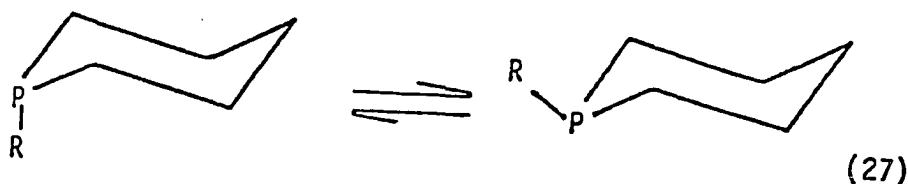
Thirdly, the diffusion of a polar olefin such as 3-butenitrile into the bead may have been limited due to the lack of polar gradients which develop between the resin (which is largely aromatic due to its styrene makeup) and the aromatic solvent (toluene) used (66).

Hence, due to the reduced activity of these catalysts as compared to their homogeneous counterparts, no further work was deemed warranted.

PART II:
STEREOELECTRONIC EFFECTS OF CYCLIZATION IN
AMINOPHOSPHINE SYSTEMS: A STRUCTURAL,
PES, AND NMR STUDY OF $\text{Me}_2\text{NP}(\text{OCH}_2)_2\text{CMe}_2$
AND $\text{CH}_2(\text{CH}_2\text{CH}_2)_2\text{NP}(\text{OCH}_2)_2\text{CMe}_2$

INTRODUCTION

The chemistry of phosphorinanes has been an area of great interest over the past several years (141,142). Much work has been done to elucidate their structures in both the solid and solution phases. The results of previous work have shown that in all cases phosphorinanes adopt a chair conformation. However, this conformation has been found to be slightly modified from that found in cyclohexane (142). In most compounds, the phosphorinane ring has been observed to be slightly flattened at the phosphorus end. This flattening has been attributed to steric interactions which develop between the exocyclic groups on phosphorus and the rest of the phosphorinane ring. Studies have also shown that the exocyclic groups on phosphorus can adopt either the axial or equatorial positions with respect to the ring. Quin and co-workers have prepared many 2-alkyl-(aryl) phosphorinanes (143) and have studied their conformational equilibria (Eq. 27) using NMR techniques (60).



They have found that at lower temperatures (130-150 K) the conformer with an equatorial exocyclic group is slightly favored ($K_{e/a} = 2.03$ (CH₃), 2.10 (C₂H₅), 2.33 (C₆H₅)). The axial conformation is thought to be destabilized by interactions between the exocyclic group and the axial

4,6 protons. It was also observed that the entropy change was significant for Equation 52 ($\Delta S = -3.4$ eu (CH_3), -3.2 eu (C_2H_5), -2.5 eu (C_6H_5)), while the ΔH was low (-0.68 kcal/mol for $R = \text{CH}_3$) (60). As a consequence, upon heating solutions of these compounds to 300 K the equilibrium was found to shift toward the axial conformer ($K_{e/a} = 0.56$ (CH_3), 0.65 (C_2H_5), 0.72 (C_6H_5)) (60).

Over the past ten years our group has focused particular attention upon the 2-alkoxy-1,3,2-dioxaphosphinanes system (24). Unlike the previously mentioned phosphine analogues, we have found that these compounds overwhelmingly adopt the conformation with an axial R group (24). This would seem to suggest that steric factors are less important than electronic factors in determining the conformation of the ring. Hudson and Verkade (144) have shown that when the lone pair on phosphorus is in the axial position with respect to the ring, there arises an interaction between it and a lone-pair contained in a p orbital on a ring oxygen. As a result, the conformation with an axial OR group and an equatorial lone-pair is preferred. Mosbo (58) found that when the -OR group was replaced with an NR_2 group, the conformation with an axial lone-pair and an equatorial NR_2 group was preferred. The factor which stabilizes this conformation is the steric interaction which develops between a nitrogen methyl group and the axial 4,6 hydrogens of the ring which are present within conformation a and not in b (Fig. 15). The dimethylamino group is forced to adopt the orientation as shown with respect to the ring due to the repulsion of the lone-pair on phosphorus and the N-P π MO (145).

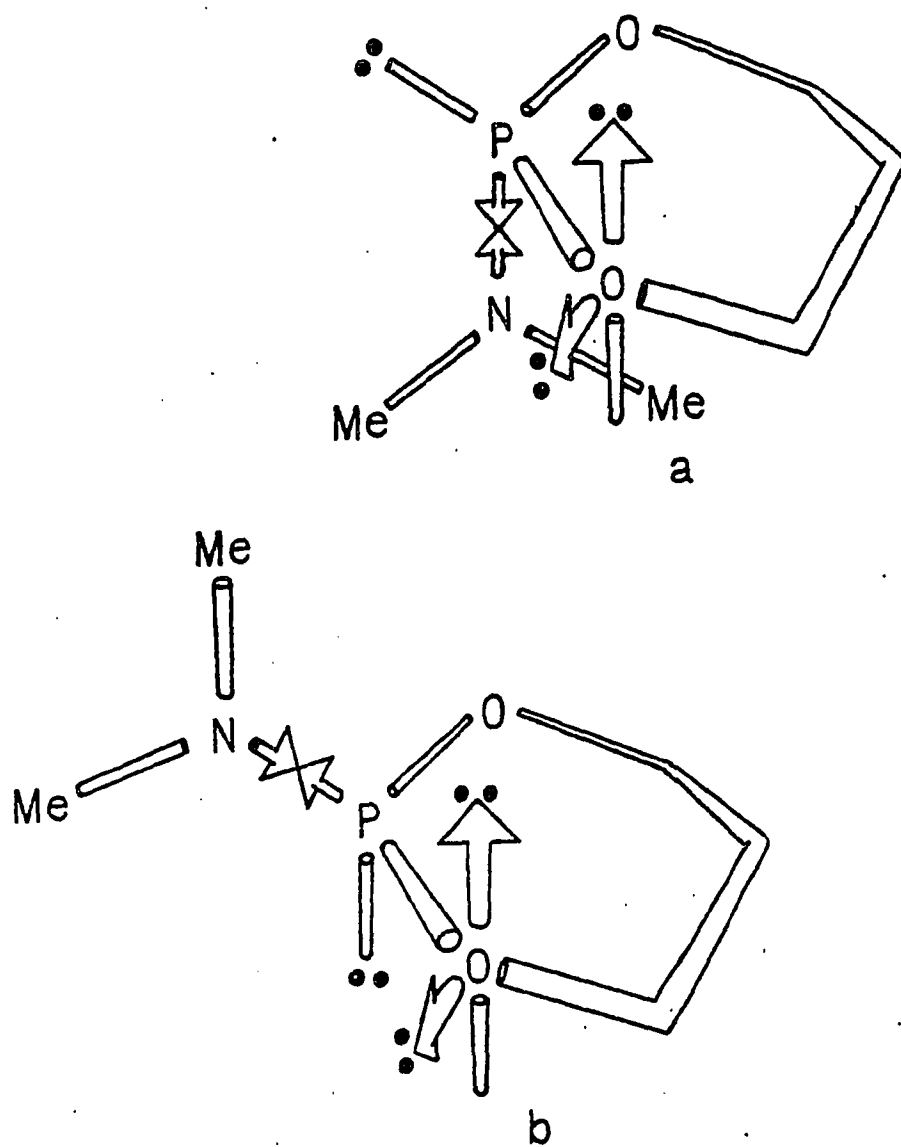


Figure 15. Orientation of electron lone pairs in each of the two possible conformations of 2-dimethylamino-1,3,2-dioxaphosphorinane

In the past, there has been much interest in the structural and electronic properties of aminophosphorus compounds, in particular $P(NMe_2)_3$ (27). However, much of the solid state structural information which is known about 2-amino-1,3,2-dioxaphosphorinanes is inferred from analogous compounds in which the phosphorus is pentavalent. In fact, proof of the preference of the Me_2N group to be equatorial originally came from dipole moment studies of the corresponding 2-amino-1-oxo-1,3,2-dioxaphosphorinanes (58). Since 20 and 21 were trivalent and solids at ambient temperatures, an opportunity was provided to compare their structural and conformational preferences to their pentavalent analogues via the use of X-ray diffraction. We also sought to investigate the electronic properties of these cyclic compounds and compare them to their acyclic analogues using photoelectron spectroscopy and the J_{p-Se} coupling data of their corresponding selenides. It was hoped that their electronic properties could be rationalized using information obtained in the X-ray structural analysis.

In this chapter, we will report that compounds 20 and 21 prefer the same conformation in the solid, solution and gaseous states, that the nitrogens are nearly planar in the solid state, and that 20 and 21 are less basic than their acyclic analogue $(Me_2N)P(OMe)_2$ in the gas and solution states.

Experimental procedures

All solvents and other materials were of reagent grade or better. Diethyl ether was dried by refluxing over NaK alloy. Acetonitrile was

dried over P_4O_{10} , benzene was dried by refluxing over Na metal.

Trimethyl phosphite and dimethylamine were obtained from Eastman Kodak Company. Piperdine was obtained from Fisher Chemical Company, while 2,2-dimethyl-1,3-propanediol was obtained from the Alrich Chemical Company. All the above reagents were used as received with no further purification.

All 1H NMR spectra were obtained on deuterated chloroform solutions contained in 5 mm tubes. Chemical shifts were obtained relative to the internal standard tetramethylsilane. All 1H NMR spectra were obtained using a Varian EM-360 NMR spectrometer. All ^{31}P NMR spectra were obtained on either C_6D_6 or $CD_3C(O)CD_3$ solutions contained in 10 mm tubes. The spectra were obtained on a Bruker WM-300 NMR spectrometer operating in the FT mode at 121.5 MHz. The external standard was a sealed capillary tube containing 85% H_3PO_4 . The capillary was held coaxially in the tube by means of a Teflon vortex plug. The spectrometer operated using a 2H lock provided by the deuterium atoms contained in the solvent.

All ^{13}C NMR spectra were obtained using a Jeol FX-90Q spectrometer operating at 22.5 MHz in the FT mode, while locked on the deuterium atoms contained in the solvent $CD_3C(O)CD_3/CF_2Cl_2$. The spectra were obtained using the carbon atoms of the solvent as a reference. All mass spectral data were obtained using a Finnegan 4000 mass spectrometer. All melting point data were collected on a Thomas-Hoover Unimelt apparatus. Melting points were obtained uncorrected. PES data were recorded as described earlier (27).

Preparations

2- β -Chloro-4,6- α,α -dimethyl-1,3,2-dioxaphosphorinane (4) The preparation of this compound can be found in chapter one of this thesis.

Dimethylphosphochlorodite (40) This compound was prepared via the procedure of Ramirez and co-workers (146).

Dimethyldimethylphosphoramidite (41) Attempts to prepare this compound via the reaction of 1 equivalent of tris(dimethyl amino)phosphine and two equivalents of methanol in the presence of a catalytic amount of dimethylamine hydrochloride via the method of Bentrude and co-workers (147) were unsuccessful. The compound was successfully prepared via the reaction of 40 and dimethylamine in a manner similar to a procedure described previously (128). The compound was obtained in 73% yield via distillation ($b_{42} = 42-45^\circ$, lit. $b_{45} = 50-51^\circ$ (147); $^1\text{H NMR}$ (CDCl_3) 3.4d $J_{\text{P-H}} = 12$ Hz 6H OCH_3 , 2.6d $J_{\text{P-H}} = 9$ Hz 6H $-\text{N}(\text{CH}_3)_2$, lit. (147) 3.3d $J_{\text{P-H}} = 12$ Hz 6H OCH_3 , 2.6d $J_{\text{P-H}} = 9$ Hz 6H $\text{N}(\text{CH}_3)_2$).

2-Dimethylamino-5,5-dimethyl-1,3,2-dioxaphosphorinane (20) This compound's preparation is described in Chapter One of this thesis.

2-Piperdino-5,5-dimethyl-1,3,2-dioxaphosphorinane (21) This compound's preparation is described in Chapter One of this thesis.

2- β -Dimethyl amino-4,6- α,α -dimethyl-1,3,2-dioxaphosphorinane (42),

2- α -dimethylamino-4,6- α,α -dimethyl-1,3,2-dioxaphosphorinane (43)

Mixtures of these compounds were first prepared via two procedures described by Mosbo (58). The first procedure entailed the reaction of 4 and dimethylamine, while the second used the reaction of meso-2,4-pentanediol and tris (dimethylamino) phosphine. In both procedures, Mosbo reports a conformational ratio of 9 to 1 for 43 and 42, respectively. However, upon repeating this work it was found that the first procedure produced a 2 to 1 mixture of 43 and 42, while the second procedure yielded a 4 to 1 mixture of 43 and 42. Heating a neat mixture of 43 and 42 for 3 hr. under N_2 at $130^\circ C$ failed to affect any change in the conformational distribution obtained in either reaction. A 4 to 1 mixture of 43 to 42 could be obtained from a 2 to 1 starting mixture by heating 0.5 g of the neat 2 to 1 mixture with 5 mg of para-toluenesulfonic acid at $90^\circ C$ for 3 hr. Determination of the isomeric distribution was made by integration of each set of dimethylamino resonances in the 1H NMR spectrum. The compounds were obtained as a mixture of isomers in 81% yield by distillation. No attempts were made to separate the isomers ($b_3 = 46^\circ$, lit. $b_2 = 44-46^\circ$ (58); (43) ^{31}P NMR (C_6D_6) 141.4, lit. 141.0 (58), 1H NMR ($CDCl_3$) 4.3-3.7m 2H CH, 2.5d $J_{P-H} = 9$ Hz, 6H $N(CH_3)_2$, 1.1d $J_{H-H} = 6$ Hz, 6H CH_3 , 1.0m 2H CH_2 ; (42) ^{31}P NMR (C_6D_6) 137.6, lit. 137 (58); 1H NMR ($CDCl_3$) 4.3-3.7m 2H CH, 2.3d $J_{P-H} = 8$ Hz 6H $N(CH_3)_2$, 1.1d $J_{H-H} = 6$ Hz 6H CH_3 , 1.0m 2H CH_2).

KSeCN This compound was prepared via the procedure of Waitkins and Shutt (87).

Dimethyldimethylselenophosphoramidate (44) This compound was

prepared by reacting 0.55 g (0.0039 mole) KSeCN and 0.53 of 41 in 25 ml of acetonitrile. The mixture was stirred for 3 hr. at room temperature and filtered. The compound was obtained in 94% yield upon removal of the acetonitrile using a rotary evaporator. No further purification was necessary as evidenced by ^{31}P NMR (^{31}P NMR ($\text{CD}_3\text{C}(\text{O})\text{CD}_3$) 87.1d $J_{\text{P-Se}} = 903$ Hz).

2-Dimethylamino-2-seleno-5,5-dimethyl-1,3,2-dioxaphosphorinane (45)

This compound was prepared by the reaction of 0.81 g (0.0056 mole) of KSeCN and 0.83 g (0.0055 mole) of 20 in 20 ml of acetonitrile. The solution was stirred for 4 hrs, then filtered, and the acetonitrile was removed under vacuum to yield a white solid. The product was obtained in 86% yield via sublimation at $85^\circ/1.5$ Torr (^{31}P NMR ($\text{CD}_3\text{C}(\text{O})\text{CD}_3$) 79.2d $J_{\text{P-Se}} = 914$ Hz).

2-Piperdino-2-seleno-5,5-dimethyl-1,3,2-dioxaphosphorinane (46)

This compound was kindly provided by Dr. Steven Socol.

2- α -Dimethylamino-2- β -seleno-4,6- α,α -dimethyl-1,3,2-dioxaphorinane

(47), 2- β -Dimethyl amino-2- α -seleno-4,6- α,α -dimethyl-1,3,2-dimethyl-

1,3,2-dioxaphosphorinane (48) This compound was prepared via the reactions of a 4 to 1 mixture of 43 and 42 and KSeCN via the procedure described for 44. The resulting liquid which was obtained in 81% yield was used without further purification ((47) ^{31}P NMR ($\text{CD}_3\text{C}(\text{O})\text{CH}_3$) 75.1d $J_{\text{P-Se}} = 895$ Hz; (48) ^{31}P NMR ($\text{CD}_3\text{C}(\text{O})\text{CD}_3$) 77.6d $J_{\text{P-Se}} = 924$ Hz).

Experimental details for X-ray data collection for compounds 20 and 21

Crystals of both 20 and 21 suitable for x-ray diffraction were grown by separately sealing approximately 0.5 g of the purified compound in an evacuated (~0.1 Torr) 10 cm long 1/4" ID glass tube. The bottom of the tube was placed in a sand bath and slowly heated. Compounds 20 and 21 sublimed at 27° and 60°, respectively. Due to the low melting point of compound 20 (28°C), it was necessary to select and mount crystals in a cold room which was maintained at 14°C. A colorless crystal of 20 in the shape of a parallelepiped (0.3 x 0.4 x 0.2 mm) was mounted in a 0.5 mm I.D. Lindemann capillary. The capillary was sealed to prevent hydrolysis by atmospheric moisture. The crystal was found to be triclinic with $a = 6.542(1)\text{Å}$, $b = 11.731(3)\text{Å}$, $c = 6.440(2)\text{Å}$, $\alpha = 101.53(4)$, $\beta = 83.52(3)$ and $\gamma = 90.96(3)\text{Å}$. A density of 1.22 g/cm^3 was computed on a volume of $481.1(2)\text{Å}^3$. A Howells, Phillip, and Rodgers' plot (148) indicated a centrosymmetric lattice which led unambiguously to the space group $P\bar{1}$ which was later confirmed by subsequent solution and refinement of the structure. The data were collected at $-130 \pm 3^\circ$ on a Syntex diffractometer with graphite monochromated MoK_α radiation ($\lambda = 0.70954\text{ Å}$) employing a previously described procedure (149). Low-temperature data were collected in order to minimize thermal motions. Four octants were collected within the sphere of $2\theta < 50^\circ$ yielding 2645 measured intensities. There was no significant crystal decomposition as judged by repeated measurements of three standard reflections. Averaging of equivalent data yielded 1270 observed reflections ($F_0 > 3\sigma(F_0)$).

Lattice constants were obtained by a least squares refinement of the $\pm 2\theta$ ($|2\theta| > 20^\circ$) measurements of 24 standard reflections.

The structure was solved by standard heavy atom procedures following location of the phosphorus atom from interpretation of the Patterson maps. Refinement of the structure was carried out using block matrix least-squares methods. Fourier-difference maps and least squares refinements led to location of the positions of all nonhydrogen atoms. Isotropic refinements of these positions gave a conventional R factor of 0.19 and a weighted R factor of 0.265. Anisotropic refinement of these positions gave a conventional R factor of 0.114 and a weighted R factor of 0.172. Ring hydrogen positions were calculated and a final full matrix least-squares refinement of all atoms led to a final conventional R of 0.074 and weighted R of 0.121.

The structure of compound 21 was determined using the same methods as used on compound 20. Initial attempts at solving the structure of compounds at -130°C were unsuccessful due to computational problems which arose from apparent pseudosymmetry in both the nitrogen and phosphorus rings. Re-collection of the data at $21^\circ\text{C} \pm 3^\circ$ seemed to allow for more thermal movement in both rings which eliminated the pseudosymmetry.

The pyramidal shaped crystal ($0.4 \times 0.2 \times 0.2$ mm) was found to be orthorhombic with $a = 8.464(1)\text{\AA}$, $b = 9.868(2)\text{\AA}$, $c = 27.832(2)\text{\AA}$, $Z = 8$, volume = $2323.9(6)\text{\AA}^3$ and $\rho = 1.24 \text{ g/cm}^{-3}$ (calculated). Systematic absences $0k0$ $k = 2n$; $h0l$ for $h + l = 2n$; $0kl$, $k = 2n$; $hk0$ for $h=2$, and $00l$ for $l = 2n$ indicated the space group P_{bna} which was later confirmed by solution of the structure.

Data were collected on a four circle diffractometer designed and built in the Ames Laboratory, equipped with a scintillation counter and interfaced to a PDP-15 computer. The data were collected with graphite monochromated MoK_α radiation with 1465 reflections in 2 octants being observed within a sphere of $2\theta < 50^\circ$.

There was no observed decomposition of the crystal based upon repeated observation of three standard reflections. Averaging of equivalent data yielded 560 independent reflections ($F_o > 3\sigma(F_o)$). Block matrix least square isotropic refinement of the nonhydrogen positions yielded a conventional R of 0.103 and a weighted R of 0.141. Hydrogen positions were calculated and a final full matrix anisotropic refinement of the nonhydrogen positions led to a final conventional R of 0.084 and a weighted R of 0.117.

Results and discussion

Tables 25 and 26 list the bond angles and bond distances for compounds 20 and 21, respectively. Tables 27 and 28 list their respective fractional coordinates, while Tables 29 and 30 give their respective anisotropic thermal parameters. The structure factors for 20 and 21 can be found in Appendices 3 and 4 of this thesis.

ORTEP drawings of 20 and 21 may be found in Figs. 16 and 17. Unit cell drawings of these compounds are shown in Figs. 18 and 19. As can be seen, each of the compounds adopts the chair conformation with the amino group in the equatorial position with respect to the ring. Previous structural investigations of other 2-amino-2-oxo-1,3,2-dioxaphosphorinane

Table 25. Bond distances (Å), angles (°), and their standard deviations for $\text{Me}_2\text{NP}(\text{OCH}_2)_2\text{CMe}_2$ (20)

Bond distance		Bond angle	
P-01	1.640(4)	N-P-01	99.23(22)
P-02	1.652(4)	N-P-02	101.50(22)
P-N	1.642(5)	O1-P-02	97.73(20)
O1-C3	1.452(7)	C1-N-C2	115.12(49)
O2-C4	1.453(7)	C1-N-P	125.30(45)
N-C1	1.447(7)	C2-N-P	119.58(37)
N-C2	1.469(9)	P-01-C3	114.75(24)
C3-C5	1.525(7)	P-02-C4	112.32(29)
C4-C5	1.532(8)	O1-C3-C5	111.80(38)
C5-C6	1.549(9)	O2-C4-C5	109.92(34)
C5-C7	1.547(7)	C3-C5-C4	108.80(30)
		C3-C5-C6	108.08(40)
		C3-C5-C7	111.83(36)
		C4-C5-C6	108.11(37)
		C4-C5-C7	109.99(35)
		C6-C5-C7	110.63(35)

Table 26. Bond distances (Å), angles (°) and their standard deviations for $\text{CH}_2(\text{CH}_2\text{CH}_2)_2\text{NP}(\text{OCH}_2)_2\text{CMe}_2$ (21)

Bond distance		Bond angles	
P-01	1.675(16)	O1-P-02	97.39(79)
P-02	1.623(18)	N-P-01	100.61(93)
P-N	1.637(12)	N-P-02	100.18(90)
O1-C3	1.461(32)	C1-N-P	120.88(95)
O2-C4	1.426(33)	C2-N-P	124.33(106)
N-C1	1.505(22)	C1-N-C2	114.25(118)
N-C2	1.502(21)	P-01-C3	115.87(140)
C3-C5	1.515(44)	P-02-C4	114.77(137)
C4-C5	1.556(43)	O1-C3-C5	112.18(188)
C5-C6	1.53(21)	O2-C4-C5	112.76(186)
C5-C7	1.556(20)	C3-C5-C6	110.61(222)
C1-C3N	1.582(28)	C3-C5-C7	109.65(228)
C2-C4N	1.521(30)	C4-C5-C6	110.00(238)
C3N-C5N	1.501(26)	C4-C5-C7	111.82(74)
C4N-C5N	1.632(27)	C6-C5-C7	107.53(119)
		N-C7-C3N	108.04(161)
		C1-C3N-C5N	112.22(151)
		C3N-C5N-C4N	106.27(143)
		C5N-C4N-C2	110.13(153)
		C4N-C2-N	109.55(173)

Table 27. Final positional parameters and their standard deviations for $\text{Me}_2\text{NP}(\text{OCH}_2)_2\text{CMe}_2$ (20)^a

	x	y	z
P	0.0848(2)	0.2816(1)	-0.0080(2)
O1	0.1347(5)	0.2862(3)	0.7382(6)
O2	0.8443(5)	0.2385(3)	0.9884(6)
N	0.2044(7)	0.1593(4)	0.9917(8)
C1	0.2081(10)	0.0559(5)	0.8250(11)
C2	0.3179(9)	0.1496(6)	0.1718(11)
C3	0.0011(8)	0.3625(4)	0.6617(8)
C4	0.7134(8)	0.3200(5)	0.9214(9)
C5	0.7770(7)	0.3247(4)	0.6869(8)
C6	0.6428(9)	0.4184(5)	0.6277(10)
C7	0.7458(9)	0.2044(5)	0.5442(9)
H1A	-0.0889	0.4281	0.7654
H1B	-0.0681	0.3363	0.5204
H2A	0.7278	0.4031	1.0200
H2B	0.5597	0.2929	0.9398

^aFractional coordinates of unit cell.

Table 28. Final positional parameters and their standard deviations for $\text{CH}_2(\text{CH}_2\text{CH}_2)_2\text{NP}(\text{OCH}_2)_2\text{CMe}_2$ (21)^a

	x	y	y
P	0.7472(10)	0.1762(3)	0.0892(1)
O1	0.5972(15)	0.2863(15)	0.0932(4)
O2	0.8897(10)	0.2834(15)	0.0997(3)
N	0.7355(27)	0.1019(13)	0.1417(4)
C1	0.7189(31)	0.9509(17)	0.1458(5)
C2	0.7156(28)	0.1738(18)	0.1884(6)
C3	0.6058(29)	0.4026(27)	0.0615(7)
C4	0.8967(27)	0.3957(27)	0.0670(8)
C5	0.7503(40)	0.4895(14)	0.0710(5)
C6	0.7641(39)	0.6043(16)	0.0338(5)
C7	0.7385(29)	0.5567(15)	0.1214(5)
C3N	0.8435(21)	0.8985(21)	0.1838(6)
C4N	0.8394(24)	0.1263(20)	0.2240(6)
C5N	0.8203(20)	0.9624(18)	0.2322(6)
H3A	0.4962	0.4596	0.0656
H3B	0.5996	0.3654	0.0244
H4A	0.9970	0.4601	0.0761
H4B	0.9108	0.3650	0.0371
H1A	0.6171	1.000	0.1581
H1B	0.7611	1.000	0.1148
H2A	0.7281	0.2795	0.1839
H2B	0.5995	0.1561	0.2028
H3NA	0.9593	0.9221	0.1710
H3NB	0.8330	0.7946	0.1875
H4NA	0.8006	0.0688	0.2557
H4NB	0.9410	0.0744	0.2155
H5NA	0.7123	1.019	0.2397
H5NB	0.9126	1.200	0.2489

^aFractional coordinates of unit cell.

Table 29. Final thermal parameters and their standard deviations (in parentheses)^a for Me₂NP(OCH₂)₂CMe₂ (20)

	B ₁₁	B ₂₂	B ₃₃	B ₁₂	B ₁₃	B ₂₃
P	2.4(1)	2.5(1)	2.9(1)	0.3(4)	-0.8(4)	0.3(1)
O1	2.4(1)	3.1(2)	3.6(2)	0.3(1)	-0.1(1)	1.0(1)
O2	2.4(2)	4.3(2)	3.4(2)	0.2(2)	-0.4(1)	1.9(1)
N	3.1(2)	3.3(2)	4.0(2)	0.5(2)	-1.2(2)	0.7(2)
C1	4.3(3)	2.6(2)	5.0(3)	0.5(2)	-0.7(2)	-0.1(2)
C2	3.6(3)	5.3(3)	5.0(3)	0.7(2)	-1.8(2)	2.3(2)
C3	3.0(2)	2.8(2)	3.3(2)	0.1(2)	-0.6(2)	1.1(2)
C4	2.1(2)	4.4(3)	3.4(3)	0.8(2)	0.0(2)	1.6(2)
C5	2.2(2)	2.9(2)	2.9(2)	-0.1(2)	-0.7(2)	1.1(2)
C6	3.4(3)	4.2(3)	5.3(3)	0.3(2)	1.1(2)	2.3(3)
C7	4.8(3)	3.6(3)	4.0(3)	-1.2(2)	-2.0(2)	0.6(2)

^aThe form of the anisotropic thermal parameter is $\exp[(-B_{11}a^2h^2 + B_{22}b^2k^2 + B_{33}c^2l^2)/4 + (B_{12}a*b*hk + B_{13}a*c*hl + B_{23}b*c*kl)/2]$.

Table 30. Final thermal parameters and their standard deviations (in parentheses)^a for CH₂(CH₂CH₂)₂NP(OCH₂)₂CMe₂ (21)

	B ₁₁	B ₂₂	B ₃₃	B ₁₂	B ₁₃	B ₂₃
P	4.2(2)	2.6(1)	2.5(1)	-0.3(4)	0.5(6)	-0.1(1)
O1	1.6(7)	2.8(8)	3.9(6)	0.4(6)	-0.1(6)	0.4(7)
O2	3.2(8)	3.8(9)	3.0(7)	0.3(7)	-0.2(6)	-0.3(6)
N	5.7(9)	3.1(6)	3.1(5)	0.6(13)	-0.3(10)	-0.3(4)
C3	7.5(16)	1.7(15)	2.0(8)	-1.2(18)	1.0(11)	-0.2(10)
C4	1.7(15)	6.5(15)	3.6(10)	-1.6(18)	-0.3(11)	1.0(12)
C5	2.5(9)	2.4(6)	3.8(6)	-1.4(22)	-1.9(14)	-0.2(5)
C6	3.7(10)	3.4(7)	4.3(7)	2.1(16)	1.6(13)	1.4(6)
C7	3.0(9)	3.0(7)	3.9(7)	-0.2(15)	1.0(13)	-0.1(6)
C1	5.8(16)	3.9(8)	2.2(6)	0.9(11)	-0.1(8)	0.5(6)
C2	9.7(18)	3.2(7)	4.0(7)	2.0(12)	1.6(11)	0.2(8)
C3N	4.5(11)	3.2(8)	5.0(10)	1.0(10)	-1.0(8)	-0.2(8)
C4N	7.7(15)	3.5(9)	2.6(7)	0.1(10)	0.4(8)	0.3(7)
C5N	3.3(11)	3.2(9)	4.9(9)	-0.0(7)	1.3(7)	-1.3(7)

^aThe form of the anisotropic thermal parameter is $\exp[(-B_{11}a^2h^2 + B_{22}b^2k^2 + B_{33}c^2l^2)/4 + (B_{12}a*b*hk + B_{13}a*c*hl + B_{23}b*c*kl)/2]$.

investigation indicates for the first time that this preference persists when phosphorus is trivalent. Each of the compounds contains nitrogens which are planar. This is illustrated by the sum of the angles around nitrogen being equal to 360.0° and 359.5° for 20 and 21, respectively.

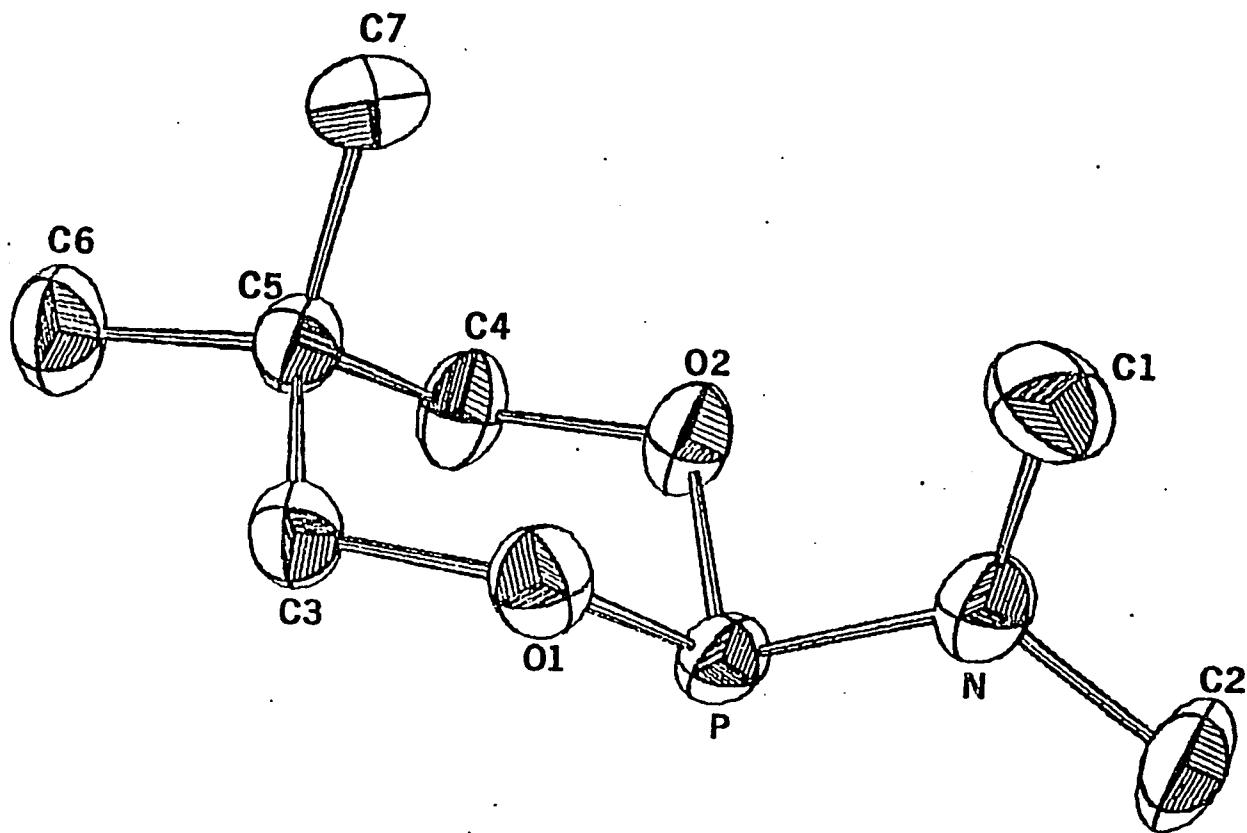


Figure 16. ORTEP diagram of 20

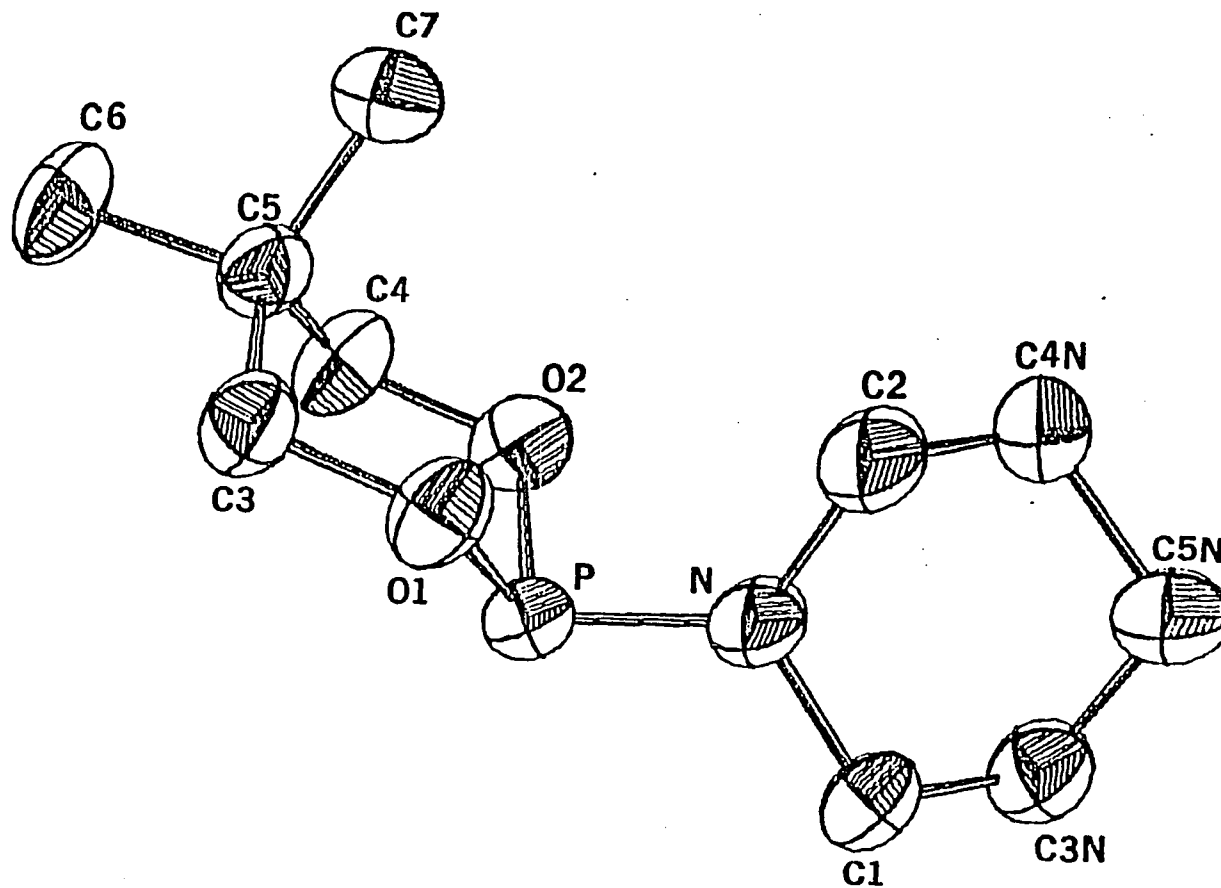


Figure 17. ORTEP diagram of 21

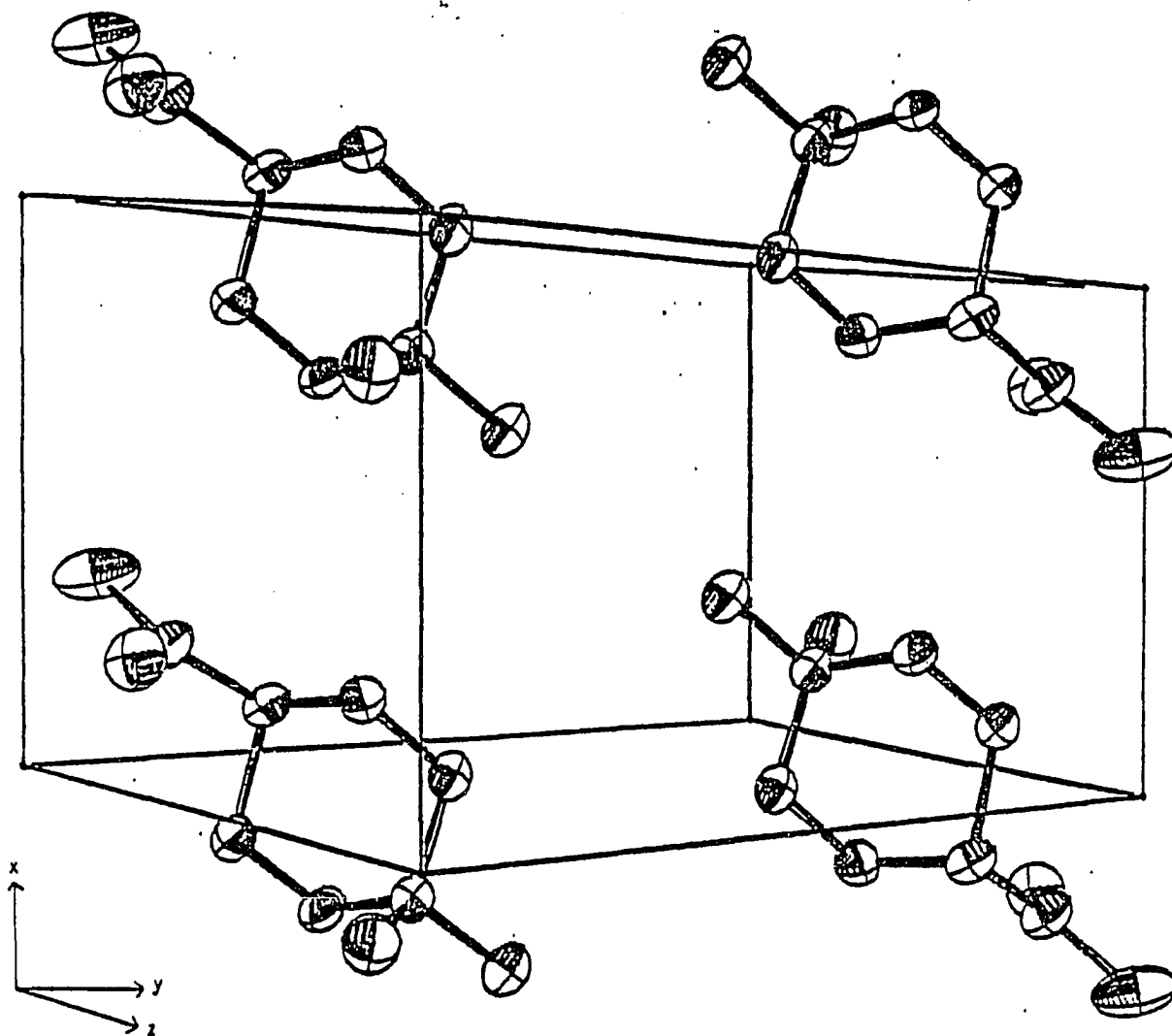


Figure 18. Unit cell diagram of 20

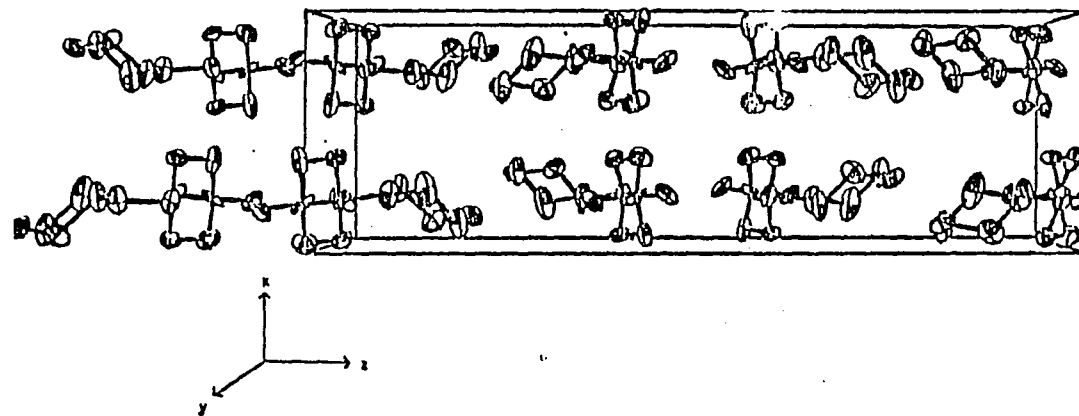


Figure 19. Unit cell diagram for 21

The nitrogen is rehybridized from sp^3 to sp^2 as illustrated by its planarity and the short N-P bond distance of 1.642(5) Å and 1.637(12) Å in 20 and 21, respectively. These distances clearly indicated the presence of some multiple bonding between nitrogen and phosphorus. Previous workers have accepted a nitrogen-phosphorus single bond to be 1.769 Å long (as is found in $\text{Na}[\text{H}_3\text{NPO}_3]$ (151)), while a nitrogen-phosphorus double bond is accepted to be 1.52 Å long (as is found in $[\text{NPCl}_2]_5$ (152)). The source of this multiple bonding between nitrogen and phosphorus stems from the presence of electronegative substituents on phosphorus such as oxygen in 20, 21, and 49 (153) or halogens in R_2NPX_2 (154). These electronegative groups cause a buildup in positive charge on phosphorus which in turn causes an increased interaction to develop between the lone-pair on nitrogen and an empty d-orbital on phosphorus, resulting in multiple bonding between the atoms. Recent X-ray structural studies of $\text{SeP}[\text{N}(\text{CH}_2\text{CH}_2)\text{CH}_2]_3$ (155) and $\text{P}[\text{N}(\text{CH}_2\text{CH}_2)\text{CH}_2]_3$ (156) shows that each compound contains only 2 planar nitrogens while the other is tetrahedral. It is probable that in these cases all three nitrogens render the phosphorus insufficiently electronegative to maintain the planarity of all three nitrogens. This has also been observed by Socol and Verkade (157) in the solid state structure of $\text{Ag}(\text{P}(\text{NMe})_3)_2^+ \text{BPh}_4^-$. It was found that only two of the nitrogens on each phosphorus were planar while the third was tetrahedral. Since 20 and 21 each contain two oxygen atoms, phosphorus is rendered sufficiently electronegative to preserve the planarity of the nitrogen. It appears that the tendency toward planarity of the nitrogen is strong enough to overcome the

puckering tendency of the piperidine ring in compound 21. This is also true in $P(N(CH_2CH_2)_2CH_2)_3$ (156) and $SeP[N(CH_2CH_2)_2CH_2]_3$ (155). This has also been observed in the corresponding morpholino compounds $SeP[N(CH_2CH_2)_2O]_3$ and $P[N(CH_2CH_2)_2O]_3$ (155). The piperidine ring in 21 is able to accommodate the planar nitrogen by increasing the C_1-N-C_2 bond angle to 114° and by flattening the C_1-N-C_2 plane with respect to the $C1-C3N-C4N-C2$ plane. The acute angle between both planes is 53° as opposed to the 60° angle found in the cyclohexane chair conformation. The reasons for the long $C4N-C5N$ distance (1.632 Å) in the piperidine ring are not known at this time, since the anisotropic thermal parameters for these atoms are not unusual nor are there any close intermolecular contacts within the unit cell.

Typical of R_2NPX_2 (154,158,159) and $R_2NP(O)X_2$ ($X_2 = OCCC O$ or $OCCCN R$) ring systems (153) is the tendency of the C_2NP plane to be nearly perpendicular to that of the bisector of the PX_2 angle. This conformational property is also seen in 20 and 21, wherein the C_2N planes are rotated from perpendicularity to the PO_2 plane by 2.2° and 1.9° , respectively. This observation is consistent with the notion that the nitrogen and phosphorus lone-pairs avoid repulsion and the nitrogen lone-pair enhances its opportunity to pi bond with phosphorus by adopting the observed conformation. Rotation of the P-N bonds in these compounds is apparently facile since the ^{13}C NMR of 20 shows no perceptible change down to -84° in $(CD_3)_2CO/CF_2Cl_2$.

The P-N bonds in 20 and 21 (1.642(5) and 1.637(1)Å, respectively) are typical of those observed for several P(III)-N compounds (160), a

result which is consistent with the presence of pi bonding in the P-N bond. Further evidence for enhanced P-N pi bonding in 20 and 21 can be construed to emanate from their P-O-C angles which average 113.5 and 115.3°, respectively. These angles are distinctly smaller than the POC angles in the rings of 23 which average 119.9° (41). This is consistent with the idea that the hybridization around the oxygens in 20 and 21 is closer to sp³ whereas in 23 it is nearer to sp². The exocyclic POC angle in 23 (117.80°) is also larger than the POC angles in 20 and 21 (41). These results are consistent with the idea that the R₂N substituent is more capable of N-P pi bonding than a methoxy group. This postulate is also supported by the slightly longer average P-O bond distances in 20 and 21 (1.646(4) and 1.649(4), respectively) compared with 23 (1.617(5)Å). A consequence of the larger POC angle in 23 is that the esteratic portion of each chair is more flattened than in 20 and 21. Thus, the acute angle between the planes made by the O1-P-O2 and O1-O2-C3-C4 portions of the ring in 1 and 2 is 74.1° and 76.5°, respectively. This compares with the corresponding angle of 36.9° in 23. The sum of the angles around phosphorus in P(III) compounds generally falls in the range 295-300° (155). The corresponding sums in 1 and 2 are not unusual in this respect (298.5° and 298.8°, respectively).

In order to determine the electronic properties of 20 and 21, a UV photoelectron study of these compounds was carried out in collaboration with Cowley and co-workers. The He(I) UV-PE spectra of these compounds can be found in figures 20 and 21. Table 30 shows the possible band assignments for 20 and 21 and several related compounds including 16.

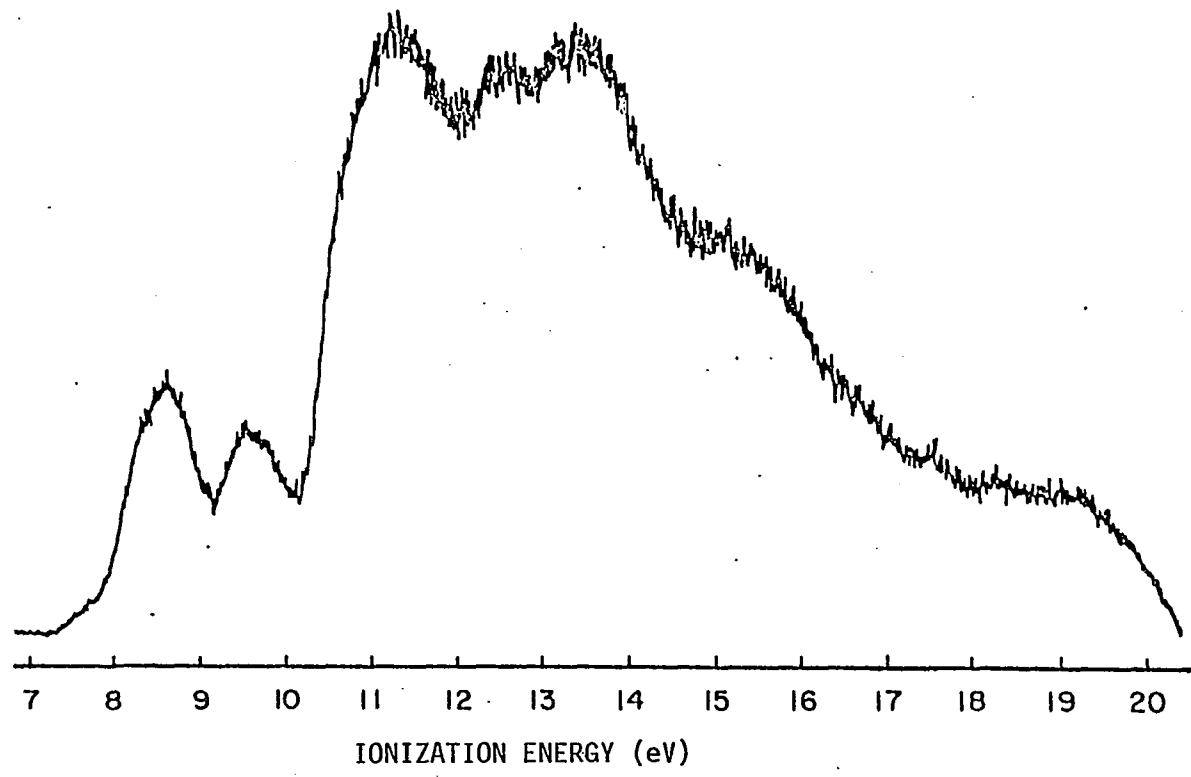


Figure 20. UV photoelectron spectrum of 20

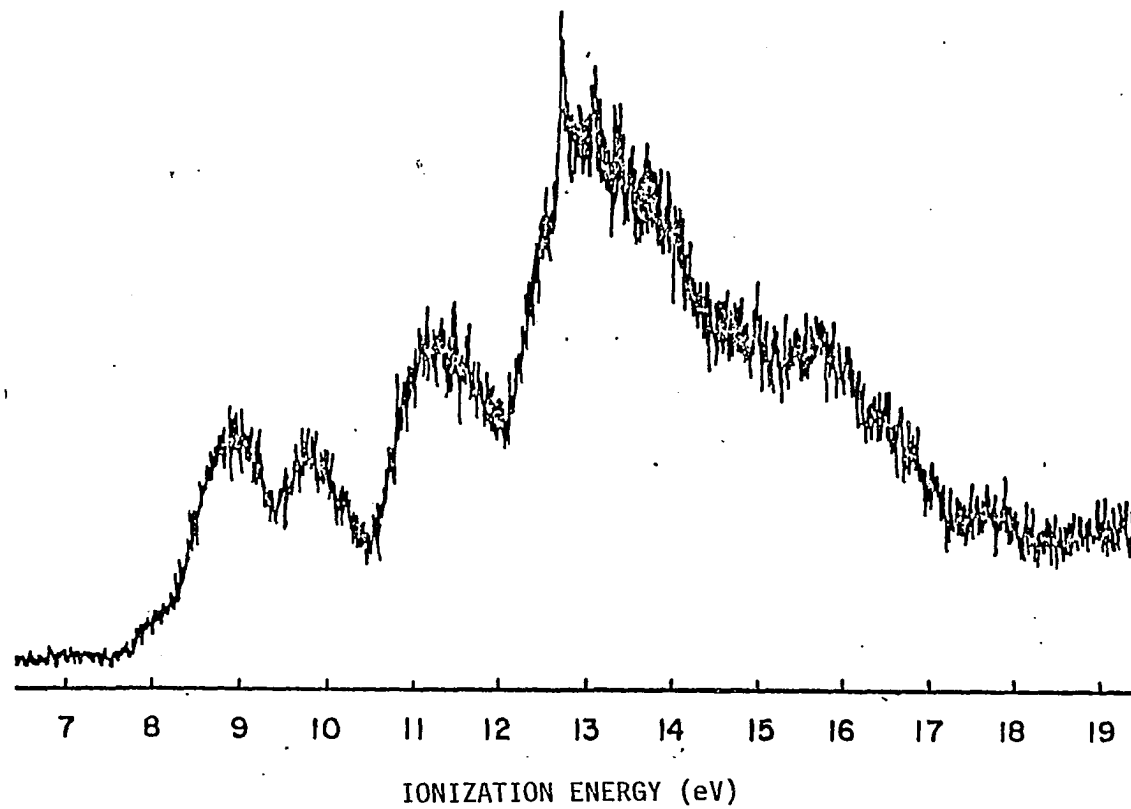


Figure 21. UV photoelectron spectrum of 21

Table 31. Ionization energies^a

	IE _N	IE _p	IE ₀
P(OMe) ₃ ^b		9.22	10.54, 11.11, 11.3
Me ₂ NP(OMe) ₂ ^c	8.63	8.93	10.56(a', a''), 11.01(nσ)
<u>20</u> ^d	a) 8.95	8.95	9.80(a', a''), 11.30(nσ)
	b) 8.95	9.80	11.30(a', a''), 12.53(nσ)
<u>21</u> ^d	a) 8.56	8.56	9.60(a', a''), 11.30(nσ)
	b) 8.56	9.60	11.30(a', a''), 12.53(nσ)
<u>16</u> ^e	8.70	8.70	10.0, 11.26
(Me ₂ N) ₂ POMe ^c	7.80(a''), 9.15(a')	8.59	10.63
P(NMe ₂) ₃ ^f	7.89(a''), 8.77(a')	7.58	
	9.90(a')		

^aIn eV. "Lone pair" energies unless stated otherwise.

^bRef. 161.

^cRef. 162.

^dThis work.

^eRef. 163.

^fRef. 27.

The values of IE_N for 20 and 21 bracket closely the value for Me₂NP(OMe)₂. All three of these values are larger than the average of the IE_N for (Me₂N)₂POMe (8.48 eV), as might be expected from the presence of a second electron donating Me₂N group and one less electron

withdrawing alkoxy group on phosphorus. Although the averages of the first two values of IE_N for $P(NMe_2)_3$ are lower than the IE_N energies for 20, 21 or $Me_2NP(OMe)_2$, the third value for $P(NMe_2)_3$ is unexpectedly higher. The difference in IE_N values of the nitrogens in $P(NMe_2)_3$ has been attributed to an interaction between one of the nitrogen lone-pairs and the lone-pair on phosphorus (27). This interaction is evidenced by the differences in the experimentally observed IE_P value for $P(NMe_2)_3$ versus what one would normally expect. The stepwise decrease in IE_P from $P(OMe)_3$ to $Me_2NP(OMe)_2$ to $(Me_2N)_2POMe$ is approximately 0.3 ev. If one assumes that the decrease in IE_P from the last compound to $P(NMe_2)_3$ should be the same, then the IE_P for $P(NMe_2)_3$ should be 8.3 ev. However, the experimentally found value is 7.6 ev. If the difference in these two values (0.7 ev) is applied to the 9.90 ev value of IE_N , this then results in an average IE_N for $P(NMe_2)_3$ of 8.6 ev. This is still 0.3 ev higher than the average of the other two IE_N values. This 0.3 ev difference can be rationalized by the fact that X-ray structural analysis of compounds such as $SeP(NMe_2)_3$ have shown (155,156) one of the nitrogens to be tetrahedral as opposed to planar, thus leading to an increase in the ionization energy of its lone-pair. This interaction between the nitrogen and phosphorus lone-pairs is illustrated by the MO diagram illustrated in fig. 22.

As can be seen in Table 31, there are two possible assignments for the ionization energies of the lone-pairs on phosphorus and oxygen in compounds 20 and 21. Originally, assignment b) was favored on the basis of the greater sp^3 character of the oxygens in 20 and 21 as opposed to 23.

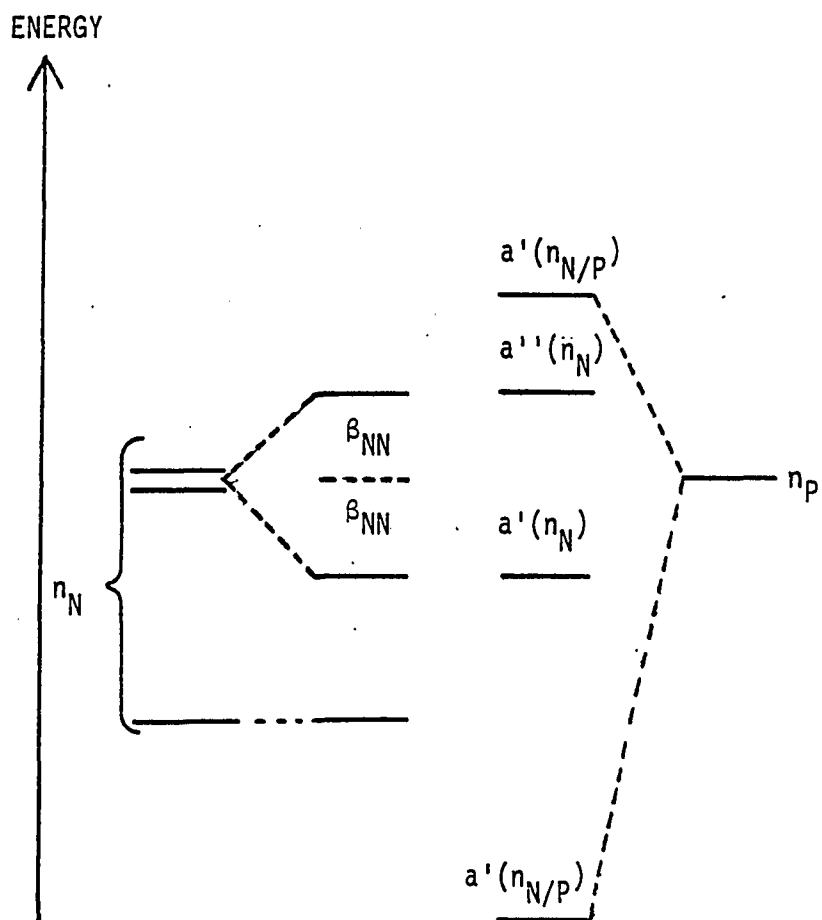


Figure 22. MO diagram for nitrogen and phosphorus lone pairs in $P(NMe_2)_3$.

and $\text{P}(\text{OMe})_3$. The greater sp^3 hybridization was evidenced by the smaller P-O-C angles of 113.5° and 115.3° in compounds 20 and 21 as compared to 120° angle found in 23 and $\text{P}(\text{OMe})_3$. It was felt that this increase in sp^3 hybridization should lead to a decrease in π -bonding from O to P in 20 and 21 which would lead to a higher positive charge on phosphorus and a higher IE_P . The higher IE_O values for assignment b) in compounds 20 and 21 as compared to $\text{P}(\text{OMe})_3$ could be attributed to an increase in s orbital involvement between oxygen and phosphorus upon rehybridization. However, it was also observed that assignment b) failed to agree with the $J_{31\text{P}-77\text{Se}}$ data obtained on the selenides of 20, 21 and other similar compounds.

One bond $^{31}\text{P}-^{77}\text{Se}$ coupling constants have been observed over a wide range of frequencies (500 Hz) (13). The use of these coupling constants have been shown to be an effective method of measuring the inductive effects on phosphorus stemming from variations in substituent electronegativities and from molecular constraint (13). Table 32 shows the $\delta^{31}\text{P}$ and $J_{31\text{P}-77\text{Se}}$ values for the corresponding selenides of 20 and 21 along with the values of some related compounds. Previous work has shown that as the positive charge on phosphorus increases, either by molecular constraint or increased substituent electronegativity, the value of $J_{31\text{P}-77\text{Se}}$ increases. Therefore, as can be seen, the value of $J_{31\text{P}-77\text{Se}}$ increases upon replacement of Me_2N groups by MeO groups. Although the values of $J_{31\text{P}-77\text{Se}}$ for 45 and 46 are larger than that for $\text{Me}_2\text{N}(\text{Se})\text{P}(\text{OMe})_2$, as would be expected on the grounds of increased molecular constraint, it is very surprising that the couplings are

Table 32. ^{31}P NMR chemical shifts (ppm) and $J_{^{31}\text{P}-^{77}\text{Se}}$ coupling constants (Hz)

	$\delta^{31}\text{P}$ (± 0.5)	$^1J_{^{31}\text{P}-^{77}\text{Se}}$ (± 1 Hz)
$\text{SeP}(\text{OMe})_3^{\text{a}}$	78.0	954
<u>51</u> ^a	68.6	985
<u>52</u> ^a	66.8	996
<u>53</u> ^a	68.8	949
$\text{Me}_2\text{N}(\text{Se})\text{P}(\text{OMe})_2^{\text{b}}$	87.1	903
<u>45</u> ^b	79.2	914
<u>46</u> ^b	76.9	909
<u>47</u> ^b	75.1	895
<u>48</u> ^b	77.6	924
$\text{SeP}(\text{NMe}_2)_3^{\text{a}}$	82.5	784

^aSee ref. 13.

^bThis work.

substantially lower than for $\text{SeP}(\text{OMe})_3$. This would not be expected due to the lower IE_P values for $\text{P}(\text{OMe})_3$ as compared to those given in assignment b for 20 and 21. Secondly, it is odd that a small change in $J_{^{31}\text{P}-^{77}\text{Se}}$ from $\text{Me}_2\text{NP}(\text{Se})(\text{OMe})_2$ to 45 (11 Hz) would correspond to a 0.9 eV difference in IE_P values of the parent phosphites, whereas the small change in $J_{^{31}\text{P}-^{77}\text{Se}}$ values of 5 Hz in going from $\text{SeP}(\text{OMe})_3$ to 53 corresponds to a much smaller difference in IE_P (0.16 eV) of their parent phosphites (26). Thirdly, it is not yet clear why the approximately sp^3

hybridizational character of oxygen in 20 and 21 (used to support assignment b) in Table 31 is not at least similar in $\text{Me}_2\text{NP}(\text{OMe})_2$, thus leading to a higher IE_p value than the 8.93 eV assigned to this acyclic analogue by others (162). Fourthly, given the structural similarity of 21 and 16, it seems questionable that there should be such a large increase in IE_p (0.8 eV). Fifthly, the conformation of $\text{Me}_2\text{NP}(\text{OMe})_2$ as calculated by semi-empirical MNDO methods should be that of C_s symmetry Fig. 23 (162). The arrangement of lone-pairs in this conformation should cause a higher IE_p than for the conformation of 20 and 21 (as illustrated by the conformations of lone-pairs in similar compounds (Fig. 24) (163)). This is due to lack of interaction between the lone-pairs on oxygen and phosphorus in the acyclic compounds, which would normally tend to raise the energy of the phosphorus lone-pair. However, the approximate equivalence of the IE_p values under assignment a) with that of $\text{Me}_2\text{NP}(\text{OMe})_2$ may be due to greater sp^3 character in the ring oxygens of 20 and 21 which would tend to reduce lone-pair interactions between phosphorus and oxygen.

The photoelectron assignments given in a) would seem best since they remove all five objections to assignment b). At the same time the values in assignment a) for 20 and 21 are in agreement with those found for $\text{Me}_2\text{NP}(\text{OMe})_2$ (162) and 16 (163). However, it would appear that the IE_0 for the a', a'' interactions of the p AOs on the oxygens in 20 and 21 are quite low compared to those for $\text{Me}_2\text{NP}(\text{OMe})_2$. This would not be expected especially if the oxygens in 20 and 21 possess more sp^3 character.

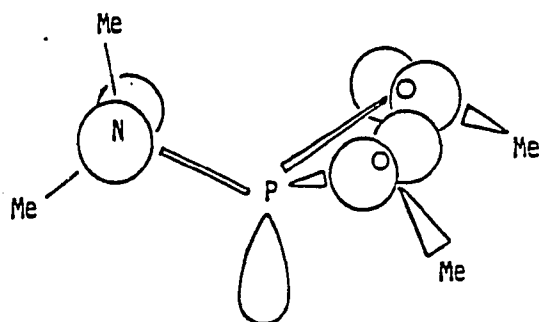


Figure 23. Conformation of $\text{Me}_2\text{NP}(\text{OMe})_2$ as calculated by semiempirical MNDO methods (162)

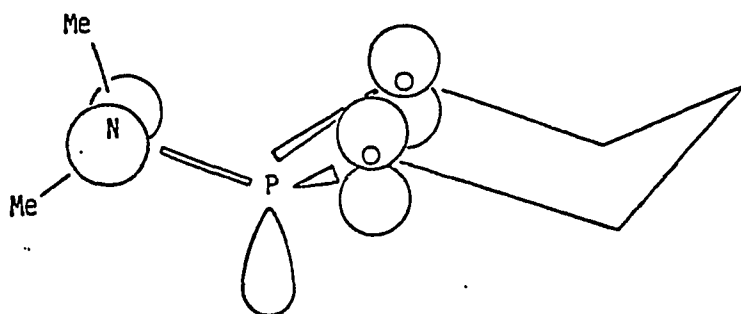


Figure 24. Proposed conformation of 16 (163)

We now know that compounds such as 20 and 21 adopt the equatorial amino group conformation in the solid phase. Previous work by Mosbo and this work confirm that this conformation is preferred in the solution phase. It is logical to question if this conformational preference holds in the gas phase wherein their PE spectra are measured. Upon analysis of the PE data, we believe this to be the case due to the following observations. The PE spectrum of 58 (which is known to be 100% in the axial MeO conformation in solution as judged by the exclusive presence of this conformation upon equilibration of 8 and 38) is similar to the PE spectra of 8 but is quite different from the PE spectrum of 38 (26). Therefore, since the methoxy derivative shows the same conformation in the gas phase as that observed in the solution phase it seems reasonable that the equatorial Me₂N group is favored in the gas phase as it is in the solution phase. This conclusion seems reasonable since it is steric factors and not electronic factors which dominate in the solid and solution phases and there is no reason to assume that electronic factors would become dominant in the gas phase and cause the axial Me₂N conformer to become favored.

PART III:
THE USE OF PHOSPHORUS CONTAINING DERIVATIZING
REAGENTS FOR THE ANALYSIS OF ALCOHOLS

INTRODUCTION

NMR spectroscopy has become an extremely important analytical tool over the past twenty five years. This is particularly true of ^1H NMR, as it has become the main method of structural analysis of organic compounds. During the same period, ^{31}P NMR has also proved to be an important technique in the study of phosphorus-containing compounds.

One of the advantages of ^{31}P NMR is that the range of chemical shifts is large (ca. 500 ppm) as compared to 40 ppm for ^1H NMR. Since different classes of phosphorus compounds (phosphines, phosphites, phosphates, etc.) have markedly different chemical shifts, a ^{31}P NMR analysis of a mixture of phosphorus compounds can afford information on the types of compounds contained within the mixture.

NMR can also be used as a quantitative method of analysis. As is the case with ^1H NMR, under optimum conditions, the peak areas contained in continuous wave ^{31}P NMR spectra are proportional to the relative amounts of each of the phosphorus compounds contained in the sample. However, over the past ten years Fourier Transform (FT) techniques have been applied to ^{31}P NMR and essentially replaced the use of continuous wave techniques. The use of FT techniques has allowed ^{31}P NMR to be used as a rapid method of qualitative analysis for phosphorus compounds in concentrations of 10^{-2} M or higher.

The area under a peak contained in an NMR spectrum depends upon several factors (Eq. 52);

$$\text{Peak area} \propto \frac{NB_1\mu^2}{KT(1 + \gamma B_1^2 T_1 T_2)^{1/2}} \quad (52)$$

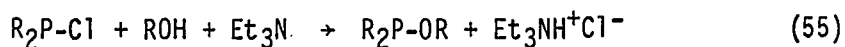
where N = number of nuclei giving the signal, B_1 = applied magnetic field, μ = magnetic moment, T_1 = spin-lattice relaxation time and T_2 = spin-spin relaxation time (164). As seen in Equation (52), the T_1 value can have a great effect on the peak area observed for a particular compound. Under continuous wave conditions relaxation time has little effect on the observed peak area. However, in order to obtain accurate peak areas under FT conditions, it is important to maintain the pulsing frequency sufficiently slow to allow the observed nuclei enough time to relax before being pulsed again. This point is especially important when compounds contained in the sample have very different T_1 values.

The spin-lattice relaxation times (T_1) for various phosphorus compounds vary over a wide range, from 1 to 25 seconds (165,166). It has been suggested (165) that in order to obtain valid analytical data using FT-NMR techniques one must allow three times the longest T_1 between successive pulses in order to obtain an accuracy of $\pm 5\%$. With compounds such as $P(O-i-Pr)_3$, which has a T_1 of 18 sec (165), this represents a delay of approximately 1 minute between each pulse. Under conditions of low concentration, where a large number of scans is required to achieve an reasonable signal to noise ratio, such a procedure would be unacceptable.

The most common method of reducing large T_1 values is to add a small amount of paramagnetic material to the NMR sample. Gurley and Ritchey (167) have reported the use of Fe(III) complexes as relaxation agents in the analysis of inorganic phosphates. Kasler and Tierney (168) have also used $\text{Cr}(\text{acac})_3$ in the quantitative analysis of phosphorus contained in various organic compounds. However, most trivalent phosphorus compounds can function as ligands. Due to differences in their ligating properties, it is possible that their relaxation properties may be different upon coordination to an iron or chromium atom. It is also possible that ligand exchange processes between the phosphorus compounds and these metals could lead to excessive line broadening which would render any quantitative NMR analysis of these compounds inaccurate (165).

In order to solve this problem, Stanislawski and Van Wazer (165) have investigated the use of the 4-hydroxy and 4-amino derivatives of 2,2,6,6-tetramethyl piperidinoxy free radical as shiftless relaxants. It was observed that these free radicals, to which phosphorus can not directly bond, could lower the T_1 values of compounds such as PPh_3 and $(\text{C}_2\text{H}_5\text{O})_3\text{PO}$ from 12.5 and 16.8 seconds to 0.58 and 0.63 seconds, respectively (molar concentration of P = 0.6 and molar concentration of free radical = 0.07).

It occurred to us that quantitative ^{31}P NMR could be applied to the analysis of alcohol mixtures via the use of the following reaction (Eq. 55).



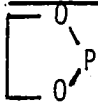
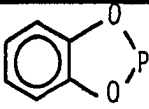

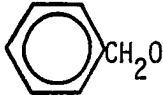
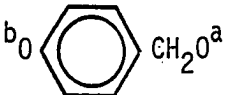
The use of this reaction to derivatize alcohols seemed attractive since equation (55) was known to proceed quantitatively (24). However, it was important that the proper derivatizing reagent be selected so as to be able to discern the types of alcohols in a mixture on the basis of resolution of the chemical shifts of the products esters.

Though gas chromatographic methods of analysis for mixtures of alcohols were already known (169), this method seemed promising for such uses as the analysis of alcohols contained in more heterogeneous mixtures, such as coal. In the past, investigators have used $(CF_3CO)_2O$ (170) and $(CH_3)_3SiCl$ (171) to characterize -OH, -NH, and -SH groups contained in coal. The use of the aforementioned chlorophosphorus compounds as derivatizing reagents seemed promising since reaction (55) was known to proceed in high yield and ^{31}P NMR analysis of the derivatized coal could give information on the types of -OR groups bound to phosphorus. Analysis of the observed chemical shifts, followed by comparison to those of known model compounds (derivatives of both aliphatic and aromatic alcohols) could provide information on the types of alcohols contained within the coal.

Preliminary work by Squires and co-workers (172) indicated that derivatizing reagents containing five membered rings, such as 14, gave the greatest difference in chemical shifts between compounds with different exocyclic groups. As can be seen in Table 33 (172) the 1,3,2-dioxaphospholanyl compounds exhibited the largest chemical shift difference (6 ppm) between aliphatic and aromatic alcohol derivatives.

Table 33. Phosphorus chemical shifts of model compound derivatives^a

$$R_2PCl + R'OH \rightarrow R_2P-OR' + HCl$$

R'O	R ₂ P		
			Ph ₂ P
	128.1	127.0	---
	134.7	127.1	113.9
CH ₃ CH ₂ CH ₂ CH ₂ O	134.6	127.2	111.0
	^a 135.1 ^b 128.4	^a 127.0 ^b 126.7	---

^appm downfield from external 85% H₃PO₄.

In this chapter is discussed further use of 14 as a derivatizing reagent for the analysis of various types of alcohols, the use of 2,2,6,6-tetramethyl piperidinoxy free radical as a shiftless relaxagent, the NMR parameters used in the development of this analysis technique and extension of this procedure to the analysis of alcohols contained in some selected coal-pyridine extracts and coal tars.

EXPERIMENTAL PROCEDURES

All solvents were reagent grade or better. All chemicals were used as received with the exception of phenol which was sublimed before use. The synthesis of the derivatizing reagent, 14, is described in chapter one of this thesis. The 4-amino-2,6-dimethylpiperidinoxy free radical was obtained from Aldrich Chemicals. ^{31}P NMR spectra were obtained on samples contained in 10 mm tubes on a Bruker WM-300 NMR spectrometer operating at 121.5 MHz. The spectrometer operated in the FT mode with an internal ^2H lock provided by ^2H atoms contained in the solvent. The external standard was 85% H_3PO_4 sealed in a 1 mm capillary tube held coaxially in the sample tube by a Teflon vortex plug. All downfield shifts of H_3PO_4 were considered positive. Various pulse sequences used during the collection of NMR data were generated by an Aspect 2000 computer system which was interfaced to the spectrometer.

A typical analysis of a particular alcohol or alcohol mixture was carried out in the following manner: In a 25 ml vial was placed 2.00 mmole of the alcohol or alcohols, 0.512 g (2.00 mmole) of triphenyl phosphine (acting as internal standard), 0.7 ml (0.005 mole) of triethylamine, 5.0 ml of CHCl_3 , and 0.7 (0.006 mole) of 14. The mixture was shaken for approximately 1 minute. Approximately 1.5 ml of this mixture were added to a 10 mm NMR tube which already contained 1.5 ml of CDCl_3 and 0.3 mmole of 2,2,6,6-tetramethylpiperidinoxy free radical.

Analysis of coal tar mixtures was carried out in the same manner, with the exception that 0.15 g of coal tar was used instead of the

alcohols. Preparation of the coal tars is described elsewhere (173). Analysis of the pyridine coal extract was carried out in the following manner. The coal extract (0.524 g) was mixed with 20 ml of fresh pyridine and sonocated for 10 min. The solution was filtered through a 0.05 μ m millipore filter. To a 10 mm NMR tube was added 1.5 ml of this solution, 0.0700 g (0.267 mmole) of PPh_3 , 0.3 mmole of the above-mentioned free radical, and 1.5 ml of CDCl_3 . The ^{31}P NMR spectrum of this mixture was then collected. Preparation of the pyridine coal extract was described previously (174).

A spectrum of the mixture was collected with either continuous or gated decoupling techniques. Continuous decoupling involves leaving the proton decoupler on at all times during the entire spectrum acquisition. Gated decoupling entails having the decoupler on only during data acquisition. The decoupler is then turned off during the delay time between pulses. A delay time between pulses of eight seconds was used. It was felt that eight seconds was sufficient to ensure the complete relaxation of the phosphorus nuclei in the presence of the piperidinoxy free radical since Stanislawski and Van Wazer had shown that similar compounds had T_1 values of 0.5 sec in the presence of a similar free radical (165).

Upon completion of collection of the spectrum, the peaks representing the PPh_3 (the internal standard) and the derivatized alcohol or alcohols ($\text{OCH}_2\text{CH}_2\text{OPOR}$) were expanded (0.25 ppm/1 inch of paper) and integrated with the aid of a planimeter in order to yield the relative

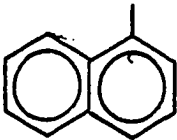
amounts of the alcohols compared to the standard contained in the mixture.

Results and discussion

The use of NMR techniques to identify and quantify materials is widespread. The technique described herein represents the first time that alcohols have been identified and quantified using phosphorus-containing derivatizing reagents. As seen in Table 34, the 1,3,2-dioxaphospholanyl derivatives possess a ca. 6 ppm difference in chemical shift between the aliphatic and aromatic oxygen derivatives. It would appear that due to the closeness of the chemical shifts within a particular class, the method would be inappropriate for distinguishing between, for example, t-butanol and sec-butanol in an unknown mixture. However, it certainly appears possible to identify and quantify the presence of both aliphatic and aromatic alcohols in a mixture.

Table 35 shows the ratio of integrated areas of 1,3,2-dioxaphospholanyl oxygen derivatives to PPh_3 compared to what was known to be present in the mixture. Accumulation of NMR data was obtained under continuous broad band proton decoupling. Table 36 shows the same information; however, accumulation of the spectrum was done with gated proton decoupling. As can be seen, the agreement between the determined and actual ratios is much closer under conditions of gated decoupling. The explanation of this result lies in the fact that under gated decoupling conditions the NOE enhancement of the ^{31}P NMR signal by the

Table 34. Phosphorus chemical shifts of 1,3,2-dioxaphospholanyl derivatives of various alcohols ($\text{OCH}_2\text{CH}_2\text{OP-OR}$)^{a,b}

R	Chemical shift (ppm) (± 0.3 ppm)
<u>n</u> -Bu	135.6
<u>sec</u> -Bu	136.5
<u>t</u> -Bu	135.2
PhCH ₂	135.7
Ph	129.7
	129.1
$\text{PhCH}_2\overset{\text{O}}{\parallel}{\text{C}}$	128.5
$\text{Ph}\overset{\text{O}}{\parallel}{\text{C}}$	129.0
<u>trans</u> -PhCH=CHC(O)	128.4

^aRelative to 85% H₃PO₄.

^bChemical shift of $\text{OCH}_2\text{CH}_2\text{OPCl}$ is 169.2 ppm.

Table 35. Comparison of ratios of peak areas of 1,3,2-dioxaphospholanyl derivatives ($\text{OCH}_2\text{CH}_2\text{OPOR}$) to PPh_3 under conditions of broad band decoupling

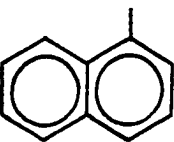
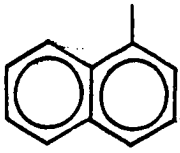
R	actual ratios of moles PPh_3 to moles of ROH in mixture (± 0.007)	Ratio of peak areas for moles of PPh_3 to moles of $\text{OCH}_2\text{CH}_2\text{OP(OR)}$ found by NMR (± 0.07)
<u>n</u> -Bu	1.062	1.03
<u>sec</u> -Bu	0.756	0.68
<u>t</u> -Bu	0.770	0.55
PhCH ₂	0.974	1.06
Ph	0.943	0.76
	0.889	0.70
Ph-C(=O)-	0.813	0.72

Table 36. Comparison of ratios of peak areas of 1,3,2-dioxaphospholanyl derivatives ($\overline{\text{OCH}_2\text{CH}_2\text{OP}}(\text{OR})$) to PPh_3 under conditions of gated decoupling

R	Actual ratio of moles PPh_3 /moles ROH in mixture (± 0.007)	Ratio of peak area for moles of PPh_3 to moles of $\overline{\text{OCH}_2\text{CH}_2\text{OP}}(\text{OR})$ found by NMR (± 0.07)
<u>n</u> -Bu	0.960	1.01
<u>sec</u> -Bu	0.631	0.61
<u>t</u> -Bu	0.676	0.67
PhCH_2	0.914	0.92
Ph	0.876	0.88
	1.422	1.29
$\text{Ph}-\overset{\text{O}}{\parallel}{\text{C}}-$	0.700	0.65

broad band decoupling of the protons is eliminated. Under conditions of continuous broad band decoupling, NOE enhancement of phospholanyl derivatives may differ from that of the PPh_3 , thus causing the lineshape of their NMR peaks to vary independently. This of course would render inaccurate any comparative integration of the peaks contained in the spectrum.

The procedure was also applied to mixtures of alcohols. Several different mixtures were prepared and analyzed. Table 37 gives a comparison of the actual percentages of a particular alcohol in the mixture to the percentages found in the analyses using broad band decoupling techniques. Table 38 gives the same comparison, using gated decoupling techniques. As was observed in the single alcohol analyses, gated decoupling gave the more accurate results. Again, this result must

Table 37. Results of ^{31}P NMR analysis of alcohol mixtures using 14 as derivatizing reagent, PPh_3 as an internal standard, and broad band decoupling

Mixture	R	Actual percentage of ROH in mixture (± 0.2)	Found percentage in mixture (± 0.2)
1	<u>n</u> -Bu	32.3	27.2
	<u>sec</u> -Bu	38.9	39.0
	Ph	28.8	33.8
2	<u>sec</u> -Bu	43.3	47.1
	PhCH=CHC(O)	13.7	12.0
	2-naphthyl	42.9	40.9
3	<u>sec</u> -Bu	36.2	35.8
	Ph	23.0	29.9
	PhC(O)	11.3	17.8
	PhCH ₂	29.6	16.5

Table 38. Results of ^{31}P NMR analysis of alcohol mixtures using 14 as derivatizing reagent, PPh_3 as an internal standard, and gated decoupling techniques

Mixture	R	Actual percentage of ROH in mixture (± 0.2)	Found percentage of ROH in mixture (± 0.2)
1	<u>n</u> -Bu	28.5	27.2
	<u>sec</u> -Bu	39.0	39.0
	Ph	32.4	33.7
2	<u>sec</u> -Bu	41.4	41.1
	PhC(O)	33.3	33.7
	2-naphthyl	25.2	25.3
3	<u>sec</u> -Bu	37.5	35.7
	Ph	27.6	29.9
	PhC(O)	18.0	17.8
	PhCH ₂	16.8	16.6

be due to removal of nonuniform NOE enhancement of the 1,3,2-dioxaphospholanyl derivatives contained within the mixture.

Attempts were made to qualify and quantify the types of -OH groups in coal tars and pyridine coal extracts using the above techniques. Due to the similarity of the chemical shifts of similar aliphatic and aromatic alcohol derivatives it does not appear feasible to differentiate sec-butyl alcohols from t-butyl alcohols or phenols from naphthols contained within the coal by-products. However, aliphatic alcohols can be differentiated from aromatic alcohols.

Subsequent analysis of coal tars and pyridine extracts of Kentucky #8 coal revealed that the amount of -OH functional groups in these materials was rather small. Previous analyses of these materials had shown them to contain only 8% oxygen by weight (175). In all cases, small humps were observed in the baseline of the gated decoupled ^{31}P NMR spectra of the derivatized coal products. These humps were centered at 134 and 128 ppm. This would seem to be indicative of the presence of both aliphatic and aromatic alcohols contained in the coal products. Due to their small size, accurate integration of these humps against a PPh_3 internal standard was not possible. However, it appeared as though the peak at 134 was approximately twice as large as the peak at 128 ppm. This would seem to imply that there was twice as much aliphatic alcohol as aromatic alcohol contained within the coal products. This result does not seem reasonable considering the highly aromatic nature of coal (175). Analysis of blanks (no extract or tar present) did show the presence of a small peak (< 4%) of area of peak for 14 at 134 ppm. Since the reported chemical shift of $\overline{\text{OCH}_2\text{CH}_2\text{O}}\text{POCH}_2\text{CH}_2\text{O}\overline{\text{POCH}_2\text{CH}_2\text{O}}$ is 133 ppm (176), it is possible that part of the peak at 134 ppm stems from traces of oligomeric impurities contained within the derivatizing reagent. These impurities could give the false impression that there is more aliphatic than aromatic alcohol in the coal extracts and tars. Though this procedure appears to be inappropriate for the analysis of -OH in coal, this procedure is useful for the analysis of alcohols when they are present in higher concentrations.

CONCLUSIONS

As shown in this dissertation the catalytic properties of a NiL_4 complex depend in large measure upon the steric properties of the ligands contained within the complex. An X-ray structural analysis of $Ni(\underline{6})_4$ showed the nickel atom to be tetrahedrally coordinated and there appeared to be no change in the ligand's conformation upon coordination. The results of this structural investigation suggests that the large differences in the catalytic properties of the complexes investigated stem from steric interactions between ligands contained within the complex.

This work suggests that the role of a Lewis acid cocatalyst is that of a ligand dissociation promoter. A Lewis acid, such as $AlCl_3$, was found to promote the formation of a coordinatively unsaturated NiL_3 species from the parent NiL_4 complex. The NiL_3 species is thought to bring about olefin isomerization via a π -allyl olefin isomerization mechanism as opposed to the σ -bonded alkyl isomerization mechanism which is invoked for the NiL_4/H^+ system. Attempts were made at heterogenizing these NiL_4 catalysts. However, in all cases these catalysts were found to be much less active than their homogeneous analogues. This reduction in activity was attributed to the structural characteristics of these hybrid catalysts.

An X-ray structural study of two aminophosphites, 20 and 21, showed each compound to have a planar stereochemistry about the nitrogen. Analysis of the structure also revealed substantial N-P multiple

bonding. Examination of PES data for 20 and 21 reveals that alternate assignments for the phosphorus lone-pair IEs had to be considered, one which suggests that these molecules are considerably less basic than their acyclic analogue, $\text{Me}_2\text{NP}(\text{OMe})_2$. The other assignment suggests that the basicity of all three molecules is the same. Solution ^{31}P - ^{77}Se NMR coupling data would seem to suggest that the basicity of all three compounds is the same.

Finally, a procedure was developed to quantify the amounts and types of alcohols contained within a mixture using a phosphorus-containing derivatizing reagent. The procedure uses quantitative ^{31}P NMR techniques to determine the actual amount of alcohol (or alcohols) contained within a mixture. Attempts to analyze alcohols contained in coal tars and coal pyridine extracts were unsuccessful due to the low concentration of OH groups in coal.

REFERENCES

1. Parshall, G. W., "Homogeneous Catalysis: the Application and Chemistry of Catalysis by Soluble Transition Metal Complexes", John Wiley and Sons, New York, 1980.
2. Shaw, B. L.; Tucker, N. I., "Organo-Transition Metal Compounds and Related Aspects of Homogeneous Catalysis", Pergamon Press: Oxford, 1973.
3. Dewar, M. J. S. Bull. Soc. Chim. Fr. **1957**, 18, C17.
4. Chatt, J.; Duncanson, L. A. J. Chem. Soc. **1953**, 2, 959.
5. Guggenberger, L. J. Inorg. Chem. **1973**, 12, 499.
6. Braterman, P. S. Struct. Bonding **1976**, 26, 1.
7. Tolman, C. A. Chem. Rev. **1977**, 77, 313.
8. Tolman, C. A. J. Am. Chem. Soc. **1970**, 92, 2953.
9. Angelici, R. J.; Malone, J. D. Inorg. Chem. **1967**, 6, 1731.
10. Bigorgne, M. J. Inorg. Nucl. Chem. **1964**, 26, 107.
11. McFarlane, W.; White, R. F. M. J. Chem. Soc., Chem. Commun. **1969**, 744. Sheldrick, G. M. Trans. Faraday Soc. **1967**, 63, 1077.
12. Verkade, J. G. Phosphorus and Sulfur **1976**, 2, 251.
13. Kroshefsky, R.; Weiss, R.; Verkade, J. G. Inorg. Chem. **1979**, 18, 469.
14. Watanabe, H.; Nagasawa, K. Inorg. Chem. **1967**, 6, 1068.
15. Keiter, R. L.; Verkade, J. G. Inorg. Chem. **1969**, 8, 2115.
16. McFarlane, W.; Rycroft, D. S. J. Chem. Soc., Chem. Commun. **1973**, 336.
17. Yarbrough, L. W.; Hall, M. B. Inorg. Chem. **1978**, 17, 2269.
18. Cowley, A. H.; Lattman, M.; Stricklen, P. M.; Verkade, J. G. Inorg. Chem. **1982**, 21, 543.
19. Tolman, C. A. J. Am. Chem. Soc. **1970**, 92, 2956.

20. Tolman, C. A.; Seidel, W. C.; Gosser, L. W. J. Am. Chem. Soc. **1974**, 96, 53.
21. Osborn, J. A.; Jardine, F. H.; Young, J. F.; Wilkinson, G. J. Chem. Soc. **1966**, 1711.
22. Jardine, F. H.; Osborn, J. A.; Wilkinson, G. J. Chem. Soc. **1967**, 1574.
23. Mosbo, J. A.; Verkade, J. G. J. Am. Chem. Soc. **1973**, 95, 204.
24. White, D. C.; Bertand, R. D.; McEwen, G. K.; Verkade, J. G. J. Am. Chem. Soc. **1970**, 92, 7125.
25. Hudson, R. F.; Verkade, J. G. Tetrahedron Lett., **1975**, 3231.
26. Hodges, R. V.; Houle, F. A.; Beauchamp, J. L.; Montag, R. A.; Verkade, J. G. J. Am. Chem. Soc. **1980**, 102, 932.
27. Cowley, A. H.; Lattman, M.; Montag, R. A.; Verkade, J. G. Inorg. Chim. Acta **1977**, 25, L151.
28. Taylor, P.; Orchin, M. J. Am. Chem. Soc. **1971**, 93, 6504.
29. Cramer, R. J. Am. Chem. Soc. **1966**, 88, 2272.
30. Tolman, C. A. J. Am. Chem. Soc. **1972**, 94, 2994.
31. Adams, R. W.; Batley, G. E.; Bailar, J. C. J. Am. Chem. Soc. **1968**, 90, 6051.
32. Emerson, G. F.; Petit, R. J. Am. Chem. Soc. **1962**, 84, 4591.
33. Hendrix, W. T.; Cowherd, F. G.; von Rosenberg, J. L. J. Chem. Soc., Chem. Commun. **1968**, 97.
34. Green, M.; Hughes, R. P.; J. Chem. Soc., Dalton Trans. **1976**, 1907.
35. Green, M.; Hughes, R. P. J. Chem. Soc., Chem. Comm. **1975**, 619.
36. Tolman, C. A. J. Am. Chem. Soc. **1970**, 92, 4217.
37. Rix, C. J.; Verkade, J. G. Coord. Chem. Rev. **1975**, 16, 129.
38. Gultneh, Y., Ph.D. Thesis, Iowa State University, Ames, Iowa, **1981**.

39. Walker, B. J. "Organophorus Chemistry", Penguin Book Ltd.: Middlesex, 1972.
40. Drinkard, W. C.; Eaton, D. R.; Jesson, J. P.; Lindsey Jr., R. V. Inorg. Chem. **1970**, 9, 392.
41. Carpenter II, L. E.; Jacobson, R. A.; Verkade, J. G. Phosphorus and Sulfur **1979**, 6, 475.
42. Milbrath, D. S.; Springer, J. P.; Clardy, J. C.; Verkade, J. G. J. Am. Chem. Soc. **1976**, 98, 5493.
43. Bogdanovic, A. B.; Wilke, G.; Benneman, P. Angew. Chem. Int. Ed. **1967**, 6, 804.
44. Shriver, D. R. J. Am. Chem. Soc. **1963**, 85, 3509.
45. Drinkard, W. C. U. S. Patent 3,496,218; Fr. Patent 1,544,658; Neth. Patent 67 06555; Brit. Patent 1,112,539; Belg. Patent 698,332.
46. Drinkard, W. C.; Lindsey, R. V.; Brit. Patent 1,104,140; Chem. Abstr., 68,77795 (1968); U. S. Patent 3,496,215; Belg. Pat. 698,333; Neth. Patent 67 05556; U. S. Patent 3,496,217.
47. Brown, E. S. Aspect. Homo. Catal. **1974**, 2, 57.
48. Drinkard, W. C.; Ger. Patent 1,807,088; Chem. Abstr., 71, 38383 (1969); Belg. Patent 723,381; Neth. Patent 68 15,746.
49. Arthur, P., England, D. C.; Pratt, B. C.; Whitman, G. M. J. Am. Chem. Soc., 70, 5364 (1954).
50. Drinkard, W. C.; Taylor, B. W.; Belg. Patent 723,383; Neth. Patent 68 15,812.
51. Drinkard, W. C.; Lindsey, R. V.; U. S. Patent 3,496,215.
52. Rick, E. A.; Brown, E. S. J. Chem. Soc. D **1969**, 112.
53. Drinkard, W. C.; Taylor, B. W. Ger. Patent 1,807,089; Chem. Abstr. 71,101350 (1969); Belg. Patent 723,380; Neth. Patent 68 15744 and 68 15746.
54. Kwiatek, J.; Seyler, J. K. J. Organomet. Chem. **1965**, 3, 433.
55. Johnson, M. D.; Tobe, M. L.; Wong, L. Y. J. Chem. Soc. A **1969**, 929.
56. Drinkard, W. C. Ger. Patent OLS 1,806,096; Chem. Abstr. 71,30093, (1969); Neth. Patent 68 15560; Belg. Patent 723,126.

57. King, C. M.; Seidel, W. C.; Tolman, C. A. U. S. Patent 3,925,445.
58. Mosbo, J. A., Ph.D. Thesis, Iowa State University, Ames, Iowa, 1970.
59. Mosbo, J. A.; Verkade, J. G. J. Am. Chem. Soc. 1973, 95, 4659.
60. Quin, L. D.; Featherman, S. L. J. Am. Chem. Soc. 1973, 95, 1699.
61. Merrill, R. D. Chemtech 1981, 11, 118.
62. Apsimon, J. W.; Seguin, R. P. Tetrahedron 1981, 35, 2797.
63. Haggin, J. Chem. Eng. News, Nov. 15, 1982, 11.
64. Bailar, J. C. Catal. Rev. Sci. Eng. 1977, 10, 17.
65. Grubbs, R. H. Chemtech 1977, 7, 512.
66. Bailey, D. C.; Langer, S. H. Chem. Rev. 1981, 81, 109.
67. Grubbs, R. H.; Kroll, L. C.; Sweet, E. M. J. Macromol. Sci. Chem. 1973, A7, 1047.
68. Otero-Schipper, Z.; Lieto, J.; Gates, B. C. J. Catal. 1980, 63, 175.
69. Evan, G. O.; Pittman, C. U.; McMillan, R.; Beach, R. T.; Jones, R. J. J. Organomet. Chem. 1974, 67, 295.
70. Wauvel, S.; Buschmeyer, P. Angew. Chem., Int. Ed. Engl. 1978, 17, 137.
71. Pittman, C. U.; Marlin, G. V.; Rounsefell, T. D. Macro. Mol. Sci. 1973, 6, 1.
72. Gray, H. B.; Rembaum, A.; Gupta, A. Ger. Patent 2,633,959; Chem. Abstr. 87, 173430q (1977).
73. Pittman, C. U. Organomet. React. Synth. 1977, 6, 1.
74. Masuda, T.; Stille, J. K. J. Am. Chem. Soc. 1978, 100, 268.
Takaishi, N.; Imai, H.; Bertelo, C. A.; Stille, J. K. J. Am. Chem. Soc. 1978, 100, 264.
75. Padmakumari Amma, J.; Stille, J. K. J. Org. Chem. 1982, 47, 468.
76. Gubtosa, G.; Brintzinger, H. H. J. Am. Chem. Soc. 1977, 99, 5174.

77. Lee, W. S.; Brintzinger, H. H. J. Organomet. Chem. **1977**, 87, 127.
78. Pittman, C. U.; Kim, B. T.; Douglas, W. M. J. Org. Chem. **1975**, 40, 540.
79. Cais, M.; Frankel, E. N.; Butterfield, R. O. Tetrahedron Lett. **1968**, 1919 (1968).
80. Pittman, C. U.; Smith, L. R.; Hanes, R. M. J. Am. Chem. Soc. **1975**, 97, 1742.
81. Brenner, A.; Hucul, D. A.; Hardwick; S. J. Inorg. Chem. **1979**, 18, 1478.
82. Robertson, J.; Webb, G. Proc. Royal Soc. London, Ser. A. **1974**, 341, 383.
83. Wrighton, M. S.; Liu, D. K. J. Am. Chem. Soc. **1982**, 104, 898.
84. Capka, M.; Hetflejs, J. J. Coll. Czech. Chem. Commun. **1974**, 39, 154.
85. Barltrop, J. A.; Carless, H. A. J. J. Am. Chem. Soc. **1972**, 94, 1951.
86. McGreer, D. E.; Page, D. P.; Kaushal, D. P. Can. J. Chem. **1973**, 51, 1239.
87. Waitkins, G. R.; Shutt, R. Inorg. Synth. **1946**, 2, 186.
88. Schrauzer, G. N. J. Am. Chem. Soc. **1959**, 81, 5310.
89. White, D. W.; Bertrand, R. D.; McKwen, G. K.; Verkade, J. G. J. Am. Chem. Soc. **1970**, 92, 7125.
90. Verkade, J. G.; Huttemann, T. J.; Fung, M.; King, R. W. Inorg. Chem. **1965**, 4, 83.
91. Kainosho, M.; Nakamura, A. Tetrahedron **1960**, 25, 4071.
92. Huttemann, T. J. Ph.D. Thesis, Iowa State University, Ames, Iowa, **1965**.
93. Lucas, H. J.; Mitchell, Jr., F. W.; Sculley, C. N. J. Am. Chem. Soc. **1950**, 72, 2491.
94. Denney, D. B.; Chang, L. L. J. Org. Chem. **1977**, 43, 782.

95. Bigorne, M. Bull. Soc. Chim. Fr. **1960**, 1986.
96. Vinal, R. S.; Reynolds, L. T. Inorg. Chem. **1964**, 3, 1062.
97. Levinson, J. J.; Robinson, S. D. Inorg. Synth. **1972**, 13, 105.
98. Coskran, K. J.; Bertrand, R. D.; Verkade, J. G. J. Am. Chem. Soc. **1967** 89, 4535.
99. White, D. W. Ph.D. Thesis, Iowa State University, Ames, Iowa, 1970.
100. Skoog, D. A.; West, D. M. "Analytical Chemistry, An Introduction"; Holt, Rinehart and Winston, New York, 1974.
101. Noller, C. C.; Pannell, C. E. J. Am. Chem. Soc. **1955**, 77, 1862.
102. Fieser, L. F.; Fieser, M. "Reagents for Organic Synthesis", John Wiley and Sons: New York, 1967.
103. Main, P. M.; Woolfson, M. M.; Germain, G. "MULTAN: A Computer Program for the Automatic Determination of Crystal Structures", Dept. of Physics, University of York, England, 1971.
104. Baldwin, R. A.; Chang, M. T. J. Org. Chem. **1967**, 32, 1572.
105. Baldwin, R. A.; Washburn, R. M. J. Org. Chem. **1965**, 30, 3860.
106. Osborn, J. A.; Wilkinson, G. Inorg. Synth. **1967**, 10, 67.
107. Snell, F. D. "Photometric and Fluorometric Methods of Analysis", John Wiley and Sons: New York, 1978.
108. Tolman, C. A.; Gosser, L. W. Inorg. Chem. **1970**, 9, 2350.
109. Vande Griend, L. F. Ph.D. Thesis, Iowa State University, Ames, Iowa, **1975**.
110. Vande Griend, L. F.; Verkade, J. G. Phosphorus **1973**, 3, 13.
111. Weiss, R.; Vande Griend, L. F.; Verkade, J. G. J. Org. Chem. **1979**, 44, 1860.
112. Angelici, R. "Synthesis and Technique in Inorganic Chemistry", 2nd Ed.; Saunders: Philadelphia, 1977; Appendix.
113. Harris, R. K.; Mann, B. E. "NMR and the Periodic Table", 1st ed.: Academic Press: New York, 1978, Chapter 9.
114. Epperlein, B. W.; Lutz, O. Z. Naturforsch. **1968**, A(23), 1413.

115. Vriezen, W. H. H.; Jellinek, F. Rev. Trav. Chim. **1970**, 89, 1306.
116. Cohen, B. M.; Smith, J. D. J. Chem. Soc. A **1969**, 2087.
117. Linke, W. F. "Solubilities of Inorganic and Metal-Organic Compounds", 4th ed., Van Nostrand, Princeton, 1958; p. 169.
118. O'Reilly, D. E. J. Chem. Phys. **1960**, 32, 1007.
119. Cohen, B. M.; Cullingworth, A. R.; Smith, J. D. J. Chem. Soc. A **1969**, 2193.
120. Henderson, W. G.; Mooney, E. F. Ann. Review NMR Spect. **1969**, 2, 219.
121. Kroger, C.; Tsay, Y. H. Cryst. Struct. Comm. **1974**, 3, 455.
122. Pickardt, J.; Rosch, L.; Schumann, Z. Anorg. Allg. Chem. **1976**, 66, 426.
123. Marriott, J. C.; Salthouse, J. A.; Ware, M. J.; Freeman, J. M. J. Chem. Soc. Chem. Comm. **1970**, 595.
124. Andreu, B.; Almengenmar, B. Acta Chem. Scand **1970**, 24, 1599.
125. Milbrath, D. S.; Springer, J. P.; Clardy, J. C.; Verkade, J. G. Inorg. Chem. **1975**, 14, 2665.
126. Dartiguenave, M.; Dartiguenave, Y.; Gleizes, A.; Saint-Joly, C.; Galy, J.; Meier, P.; Merbach, E. A. Inorg. Chem. **1978**, 17, 3508.
127. Jacobson, R. J.; Karcher, B. A.; Montag, R. A.; Socol, S. M.; Vande Griend, L. J.; Verkade, J. G. Phosphorus and Sulfur **1981**, 11, 27.
128. Schiff, D. E.; Richardson, J. W., Jr.; Jacobson, R. J.; Cowley, A. H.; Lasch, J.; Verkade, J. G. Unpublished paper, Department of Chemistry, Iowa State University, Ames, Iowa, 1983.
129. Cotton, F. A.; Wilkinson, G. "Basic Inorganic Chemistry", 1st Ed.: John Wiley and Sons, New York, 1976; Chapter 9.
130. Albanov, V.; Bellon, P. L., Scatturin, V. J. Chem. Soc. Chem. Commun. **1966**, 507.
131. Kabachnik, M. I.; Tsvetkov, E. N. Doklady Akademii SSSR **1960**, 135, 323.

132. Kosolopoff, K.; Maier, L. "Organic Phosphorus Compounds", 1st Ed., John Wiley and Sons, New York, 1967; Chapter 6.
133. Crutchfield, M. M.; Dungan, C. H.; Letcher, J. H.; Mark, V.; Van Wazer, J. R. Top. Phos. Chem. **1967**, 5, 267.
134. Carriatta, F.; Ugo, R.; Bonati, F. Inorg. Chem. **1966**, 5, 1128.
135. Baizer, M. "Organic Electrochemistry", 1st Ed.; Marcel Dekker, New York, 1977.
136. Tolman, C. A. J. Am. Chem. Soc. **1970**, 92, 6777.
137. Jenkins, J. M.; Huttemann, T. J.; Verkade, J. G. Adv. Chem. Ser. **1966**, 62, 604.
138. Coskran, K. J.; Huttemann, T. J.; Verkade, J. G. Adv. Chem. Ser. **1966**, 62, 590.
139. Verkade, J. G. U. S. Patent 4,267,195.
140. Published in catalogue of products, Alfa-Ventron Corporation, Beverly, Massachusetts, 1981.
141. Maryanoff, B. E.; Hutchins, R. O.; Maryanoff, C. A. "Topics in Stereochemistry", Allinger, N. L.; Eliel, E. L.; Eds., Vol. 11, John Wiley and Sons, Inc.: New York, 1979; p. 187.
142. Quin, L. D. "The Heterocyclic Chemistry of Phosphorus", John Wiley and Sons: New York; 1981.
143. Featherman, S. L.; Lee, S. O.; Quin, L. D. J. Org. Chem. **1974**, 39, 2899.
144. Hudson, R. F.; Verkade, J. G. Tetrahedron Lett. **1975**, 3231.
145. White, D. W.; Gibbs, D. E.; Verkade, J. G. J. Am. Chem. Soc. **1979**, 101, 1937.
146. Ramirez, F.; Chow, Y. F.; Maracek, J. F.; Ugi, T. J. Am. Chem. Soc. **1974**, 98, 2429.
147. Bentrude, W. G.; Johnson, W. D.; Khan, W. A. J. Org. Chem. **1972**, 37, 642.
148. Howells, E. R.; Phillip, D. C.; Rodgers, D. Acta Cryst. **1950**, 3, 210.
149. Tayosagawa, F.; Jacobson, R. A. Acta Cryst. **1978**, B34, 213.

150. Wadsworth, W. S.; Larsen, S.; Horten, H. L. J. Org. Chem. **1973**, 38, 256.
151. Hobbs, E.; Corbridge, D. E. C.; Rastrick, B. Acta Cryst. **1963**, 6, 621.
152. Schlueter, A. W.; Jacobson, R. A. J. Am. Chem. Soc. **1966**, 88, 2051.
153. Carpenter, L. E. II; Powell, D.; Jacobson, R. A.; Verkade, J. G. Phosphorus and Sulfur **1982**, 12, 287.
154. Morris, E. D.; Nordman, C. E. Inorg. Chem. **1969**, 8, 1673.
155. Romming, C.; Songstad, J. Acta Chem. Scand. **1979**, A33, 187.
156. Romming, C.; Songstad, J. Acta Chem. Scand., **1978**, A32, 688.
157. Socol, S. M.; Verkade, J. G. Submitted for publication to Inorg. Chem., 1983.
158. Fonti, P.; Damiana, D.; Favero, P. G. J. Am. Chem. Soc. **1973**, 95, 756.
159. Brittain, A. H.; Smith, J. E.; Lee, P. L.; Cohn, K.; Schwendeman, R. H. J. Am. Chem. Soc. **1971**, 93, 6772.
160. Clardy, J. C.; Kolpa, R. L.; Verkade, J. G. Phosphorus **1974**, 4, 133.
161. Worley, S. D.; Hargis, J.; Chang, L.; Mattson, G. A.; Jennings, W. B. Chem. Phys. Lett. **1981**, 79, 149.
162. Arshinova, R. P.; Zverev, V. V.; Villem, Y. Y.; Villem, N. V. J. Gen. Chem. USSR **1981**, 51, 1503.
163. Arshinova, R. P. J. Gen. Chem. USSR **1978**, 238, 47.
164. Leyden, D. E.; Cox, R. H. "Analytical Applications of NMR", John Wiley and Sons, New York, 1977.
165. Stanislawski, D. A.; Van Wazer, J. R. Anal. Chem. **1980**, 52, 96.
166. Dale, S. W.; Hobbs, M. E. J. Phys. Chem. **1971**, 75, 3537.
167. Gurley, T. W.; Ritchey, W. M. Anal. Chem. **1975**, 47, 1444.
168. Kasler, F.; Tierney, M. Microchim. Acta **1978**, 411.

169. McNair, H. M.; Bonelli, E. J. "Basic Gass Chromatography", Consolidated Printers: Berkeley, 1968.
170. Sleevi, P.; Glass, T. E.; Dorn, H. G. Anal. Chem. **1979**, 51, 1931.
171. Schweighardt, F. K.; Retcofsky, H. L.; Friedman, S.; Hough, M. Anal. Chem. **1978**, 50, 368.
172. Squires, T. G.; Venier, C. G.; Verkade, J. G.; progress report submitted to the U. S. Dept. of Energy, Ames Laboratory, Iowa State University, Ames, Iowa, July 1, 1980.
173. Squires, T. G.; Aida, T.; Chen, Y. Y.; Smith, B. F. Am. Chem. Soc. Div. Fuel Chem. Prepr. Pap. **1983**, 28, 228.
174. Squires, T. G.; Venier, C. G.; Hunt, J. D.; Shei, J. C.; Smith, B. F. Fuel, **1982**, 61, 1170.
175. Squires, T. G.; Private communication, U. S. Department of Energy, Ames Laboratory, Iowa State University, Ames, Iowa.
176. Burgada, R.; Germa, H. Compt. Rend. Ser. C **1968**, 267, 270.

ACKNOWLEDGEMENTS

I wish to thank Dr. J.G. Verkade for the leadership given to me as major professor over the past five years. I deeply appreciate his guidance and advice throughout this work. I also would like to thank Drs. Angelici, McCarley, Barton, and Ulrichson for taking the time to serve on my committee. I am also indebted to Dr. Ulrichson for helping me to set up my minor in chemical engineering. I would also like to acknowledge the help of Mr. James Richardson in the X-ray crystallographic studies of some of the compounds discussed in this thesis.

I also would like to thank the past and present group members for their friendship and insights into this chemistry. I particularly would like to thank Drs. Yilma Gultneh and Padmakumari Amma in this regard. The assistance of Ms. Joyce Gilbert for the use of her office and drafting equipment in the preparation of this manuscript is greatly appreciated. I'm also deeply appreciative of Ms. Elaine Wedeking for typing this thesis and putting up with my atrocious handwriting.

I wish to acknowledge the love and support of my fiancée, Jackie, who provided me with the strength and encouragement in carrying out this work. Most importantly, this thesis is dedicated to my parents and brother whose love and encouragement for the things I wished to accomplish in my life laid the foundation for this work.

APPENDIX 1: STRUCTURE FACTORS FOR Ni(6)₄

-5 6 725 711	-12 7 252 -298	0 4 319 -242	-5 8 482 404	-10 1 449 -417	-2 7 213 -155	-9 11 331 -288
-5 8 1080-1078	-12 8 246 270	0 8 1092 926	-5 9 338 250	-10 3 540 356	-2 8 1162-1088	-9 13 402 342
-5 10 575 572	-12 9 435 432	0 10 1567-1475	-5 10 289 -294	-10 4 340 353	-2 9 950 -903	-9 14 249 265
-5 11 280 -292	-12 11 274 -323	0 12 1234 1178	-5 12 240 -239	-10 5 786 -820	-2 11 587 373	-9 15 380 -358
-5 12 205 -229	-12 13 197 165	0 18 335 -329	-5 13 401 -408	-10 6 277 -252	-2 12 525 -523	-9 16 300 -323
-5 13 320 309	-10 1 910 -967	2-14 168 -144	-5 16 158 -104	-10 7 434 412	-2 13 746 -688	-9 17 167 137
-5 14 288 -252	-10 3 1007 1077	8-14 228 -200	-5 17 251 272	-10 14 232 166	-2 14 601 541	-7 1 724 -978
-5 15 184 -252	-10 5 686 -733	8 -8 190 240	-5 18 208 213	-10 15 183 168	-2 15 328 275	-7 2 1532-1550
-5 16 166 172	-10 6 200 134	10 -2 205 -27	-3 1 199 -99	-10 17 182 -180	-2 17 298 247	-7 3 947 862
-3 1 725 -734	-10 8 212 -176	16 -7 265 -243	-3 5 977 -911	-8 1 721 794	0 2 742 661	-7 4 575 503
-3 2 198 -84	-10 13 198 -127		-3 7 520 589	-8 2 226 -228	0 4 572 461	-7 5 1381-1356
-3 3 886 907	-10 15 266 239	H = -5	-3 8 292 -271	-8 3 798 -865	0 6 1890-1632	-7 7 646 606
-3 4 636 582	-8 1 893 879	K L FO FC	-3 9 310 -352	-8 4 279 326	0 8 1838 1989	-7 8 235 -239
-3 5 450 -332	-8 2 540 -507	-19 1 158 121	-3 11 580 556	-8 5 1003 985	0 10 775 -766	-7 9 154 108
-3 6 524 -599	-8 3 1090-1075	-17 9 205 -174	-3 12 462 502	-8 6 559 -561	0 12 977 921	-7 10 220 225
-3 8 484 492	-8 5 868 863	-15 3 152 210	-3 13 381 -419	-8 7 158 -124	0 14 638 -644	-7 11 177 254
-3 10 797 -736	-8 6 137 -182	-15 8 269 279	-3 15 633 587	-8 8 454 358	0 16 281 -340	-7 12 296 278
-3 11 491 492	-8 7 335 -369	-15 11 236 -294	-3 16 361 -354	-8 14 187 -165	0 18 342 325	-7 13 221 -188
-3 13 586 -548	-8 8 293 200	-13 1 287 257	-3 17 162 -235	-8 15 167 -176	2-17 203 -171	-7 14 318 -288
-3 14 323 316	-8 12 259 -270	-13 5 224 -228	-1 1 487 -478	-8 16 311 312	4 -7 128 102	-7 15 156 160
-3 15 245 237	-8 14 143 195	-13 8 417 -376	-1 3 338 310	-8 17 311 316	6 -6 150 -204	-7 16 210 277
-1 1 276 235	-8 15 210 -208	-13 10 390 380	-1 4 185 -176	-8 19 332 -274	8-15 184 -139	-7 17 251 -279
-1 2 637 -529	-8 17 221 232	-13 11 169 149	-1 6 218 -249	-8 21 178 147	12-11 193 -100	-7 18 221 -261
-1 3 305 238	-6 1 536 -301	-13 12 257 -298	-1 7 2026-1898	-6 1 728 -659	14 -8 168 113	-5 1 874 1013
-1 4 277 -237	-6 2 896 940	-11 1 220 -157	-1 9 1735 1643	-6 2 667 696	16 -5 168 141	-5 2 581 428
-1 6 492 469	-6 3 1066 1129	-11 2 718 -723	-1 10 246 137	-6 3 812 871		-5 3 1225-1301
-1 7 201 -114	-6 4 416 -394	-11 3 184 -168	-1 11 1016 -997	-6 4 709 -697	H = -3	-5 4 931-1039
-1 9 486 509	-6 5 771 -804	-11 4 635 581	-1 12 293 -279	-6 5 862 -853	K L FO FC	-5 5 1550 1511
-1 10 298 370	-6 7 472 474	-11 5 262 232	-1 13 908 849	-6 6 325 432	-17 4 223 -210	-5 6 429 418
-1 11 770 -705	-6 8 235 -199	-11 6 452 -417	-1 16 367 352	-6 7 150 131	-17 6 176 218	-5 7 992 -987
-1 13 269 256	-6 12 147 147	-11 8 209 183	1-17 209 184	-6 8 215 -256	-17 8 194 -215	-5 10 173 -157
-1 17 307 272	-4 1 487 453	-11 10 158 -197	3-20 256 186	-6 9 560 546	-15 1 254 311	-5 11 314 -305
-1 19 206 -232	-4 2 955 -961	-11 12 249 257	9-15 203 -131	-6 10 149 139	-15 2 222 -175	-5 12 290 -300
1 -9 397 67	-4 3 768 -790	-9 1 377 369	9 -3 134 123	-6 11 157 -159	-15 3 162 -90	-5 14 643 670
3-13 177 -197	-4 4 682 616	-9 2 1058 1084	11-14 208 -150	-6 13 132 -79	-15 4 228 252	-5 15 214 251
5 -7 167 -130	-4 5 695 627	-9 4 1030-1077	17 -9 141 -73	-6 14 150 133	-15 6 201 -243	-5 16 458 -363
5 -6 159 103	-4 6 234 176	-9 6 665 630	17 -8 202 -120	-6 15 252 214	-15 9 274 270	-5 18 148 137
7-16 161 218	-4 7 324 -468	-9 7 339 -364	17 -7 194 181	-6 16 273 -267	-13 1 160 -144	-5 19 233 -278
9-14 248 238	-4 10 592 -582	-9 11 274 246		-6 17 499 -434	-13 2 427 409	-5 21 193 191
9 -9 161 174	-4 12 337 351	-9 16 280 -192	H = -4	-6 18 296 229	-13 3 269 287	-3 1 659 698
11-12 151 124	-4 14 487 -482	-7 1 505 -571	K L FO FC	-6 19 285 303	-13 5 475 -457	-3 3 1152 989
11-11 148 122	-4 15 288 266	-7 2 867 -904	-18 1 220 -13	-4 1 189 -106	-13 7 409 388	-3 4 608 -567
11 -5 158 115	-4 16 388 304	-7 3 549 494	-18 5 173 -132	-4 2 291 344	-13 8 259 -251	-3 5 2050-2166
13-13 168 -18	-4 18 152 -162	-7 4 984 969	-16 7 225 -210	-4 3 402 592	-13 9 285 -197	-3 6 593 491
13 -8 172 -190	-2 2 789 844	-7 5 263 -222	-16 10 238 226	-4 4 329 421	-13 10 342 315	-3 7 1091 1036
15 -9 152 100	-2 3 223 236	-7 6 257 -244	-14 6 201 -189	-4 6 1548-1431	-13 11 142 117	-3 8 403 347
15 -8 303 201	-2 4 589 -601	-7 7 330 289	-14 8 255 215	-4 7 858 -640	-13 12 219 -191	-3 10 807 -844
	-2 5 609 -585	-7 8 274 -206	-14 9 325 -319	-4 8 368 501	-11 2 243 -245	-3 12 926 784
H = -6	-2 7 228 217	-7 9 171 -85	-14 10 200 -238	-4 9 245 292	-11 3 712 781	-3 13 208 -254
K L FO FC	-2 9 138 114	-7 11 276 -325	-14 11 233 253	-4 13 379 374	-11 7 679 -647	-3 14 828 -856
-18 8 214 94	-2 10 1152 972	-7 13 185 203	-14 13 216 -171	-4 14 189 -231	-11 8 267 252	-3 16 234 315
-18 9 241 28	-2 12 857 -899	-7 17 207 -237	-12 1 325 311	-4 15 319 -331	-11 10 353 -289	-1 1 1545 1206
-16 2 191 -61	-2 14 207 309	-7 18 219 -266	-12 4 479 -481	-4 16 260 235	-11 13 250 -238	-1 2 633 316
-16 11 195 -109	-2 15 407 -355	-5 1 441 407	-12 6 569 606	-4 17 209 208	-11 14 198 -204	-1 5 140 140
-14 7 369 340	-2 16 248 -236	-5 2 221 195	-12 7 245 -314	-2 1 279 145	-9 2 388 386	-1 9 518 540
-14 9 444 -405	-2 17 206 183	-5 3 408 -369	-12 8 292 -289	-2 2 977 -761	-9 4 555 -540	-1 10 417 391
-12 1 194 215	-2 18 242 247	-5 4 727 -704	-12 9 406 411	-2 3 154 -196	-9 6 693 593	-1 11 936 -914
-12 3 192 -176	0 0 156 180	-5 6 651 627	-12 11 279 -319	-2 4 766 -868	-9 7 327 294	-1 12 527 -544
-12 5 162 170	0 2 323 329	-5 7 315 250	-12 13 157 180	-2 6 2428 2235	-9 9 130 69	-1 13 705 660

APPENDIX 2: STRUCTURE FACTORS FOR 30

L ⁻¹⁵			L ⁻¹²			L ⁻¹¹			L ⁻¹⁰			L ⁻⁹			L ⁻⁸			L ⁻⁷					
H	K	FC	H	K	FC	H	K	FC	H	K	FC	H	K	FC	H	K	FC	H	K	FC	H	K	FC
1	3	96	7	1	107	8	3	107	9	4	171	3	5	141	4	0	145	4	0	145	160		
1	3	128	7	3	98	8	5	118	9	7	114	5	6	184	4	12	139	4	12	139	139		
2	4	86	9	1	115	8	6	130	10	1	128	6	2	634	4	11	169	4	11	169	161		
3	4	80	9	6	74	9	1	115	10	3	103	6	2	189	6	2	151	4	9	151	154		
4	1	78	10	6	84	10	5	85	10	5	85	6	3	232	4	8	144	4	8	144	127		
4	3	97	10	3	104	10	6	112	10	6	112	6	4	207	4	6	332	4	6	332	310		
4	2	76	10	4	104	11	3	78	11	3	78	6	5	131	4	5	94	4	5	94	73		
5	1	74	11	1	126	11	1	93	11	3	81	6	8	87	4	4	347	4	4	347	360		
												6	9	130	6	9	130	6	9	130	193		
												7	1	104	7	1	234	7	1	234	256		
												7	2	107	7	2	88	7	2	88	70		
												7	3	187	7	3	99	7	3	99	102		
												7	4	121	7	4	248	7	4	248	163		
												7	5	204	7	5	154	7	5	154	89		
												8	0	385	8	0	335	8	0	335	340		
												8	1	281	8	1	313	8	1	313	300		
												8	2	131	8	2	304	8	2	304	644		
												8	3	221	8	3	134	8	3	134	304		
												8	5	92	8	5	207	8	5	207	167		
												8	6	112	8	6	140	8	6	140	216		
												8	8	152	8	8	157	8	8	157	82		
												8	9	89	8	9	135	8	9	135	171		
												9	1	190	9	1	140	9	1	140	171		
												9	2	96	9	2	157	9	2	157	86		
												9	4	148	9	4	306	9	4	306	288		
												10	2	167	10	2	266	10	2	266	319		
												10	3	111	10	3	284	10	3	284	182		
												10	5	111	10	5	186	10	5	186	89		
												10	9	83	10	9	90	10	9	90	128		
												11	3	88	11	3	178	11	3	178	337		
												11	4	91	11	4	117	11	4	117	121		
												2	0	121	2	0	93	2	0	93	100		
												2	12	94	2	12	120	2	12	120	111		
												2	19	103	2	19	113	2	19	113	111		
												2	6	230	2	6	339	2	6	339	84		
												2	5	264	2	5	202	2	5	202	121		
												2	3	224	2	3	242	2	3	242	407		
												2	1	243	2	1	80	2	1	80	91		
												1	7	186	1	7	88	1	7	88	116		
												1	5	132	1	5	230	1	5	230	67		
												1	4	255	1	4	271	1	4	271	486		
												1	3	289	1	3	94	1	3	94	84		
												1	2	143	1	2	103	1	2	103	135		
												1	1	109	1	1	89	1	1	89	166		
												2	0	132	2	0	232	2	0	232	156		
												2	8	92	2	8	95	2	8	95	80		
												2	12	94	2	12	122	2	12	122	159		
												2	10	339	2	10	104	2	10	104	107		
												2	10	145	2	10	111	2	10	111	92		
												2	9	230	2	9	139	2	9	139	274		
												2	7	193	2	7	140	2	7	140	351		
												2	5	193	2	5	152	2	5	152	252		
												2	3	237	2	3	129	2	3	129	406		
												2	3	107	2	3	86	2	3	86	76		
												2	1	107	2	1	115	2	1	115	357		
												3	9	84	3	9	92	3	9	92	70		
												3	8	362	3	8	146	3	8	146	94		
												3	7	167	3	7	99	3	7	99	100		
												3	6	92	3	6	83	3	6	83	185		
												3	5	82	3	5	91	3	5	91	139		
												3	4	171	3	4	107	3	4	107	184		
												3	3	130	3	3	84	3	3	84	94		
												3	3	130	3	3	94	3	3	94	102		
												3	1	179	3	1	84	3	1	84	192		
												3	1	232	3	1	94	3	1	94	248		
												3	1	232	3	1	106	3	1	106			

L = -4

H	K	FO	FC
0	0	2401	2625
0	-18	93	-105
0	-15	163	-178
0	-14	85	83
0	-13	186	179
0	-12	269	268
0	-9	439	407
0	-8	276	-263
0	-7	360	-349
0	-6	88	77
0	-5	212	-203
0	-4	313	-298
0	-3	390	-369
0	-2	858	831
0	-1	319	-313
1	15	103	66
1	-16	98	88
1	-10	88	51
1	-8	168	-171
1	-7	364	-332
1	-6	480	457
1	-4	725	697
1	-3	218	201
1	-2	473	468
1	-1	229	-230
2	0	1214	-1340
2	-17	86	-81
2	-14	121	128
2	-13	93	-96
2	-12	102	89
2	-11	137	136
2	-10	103	-86
2	-8	88	-61
2	-6	450	-627
2	-5	481	-444
2	-4	375	-346
2	-3	117	-115
2	-2	585	589
2	-1	475	-482
3	-16	118	124
3	-15	111	122
3	-14	217	201
3	-13	174	171
3	-11	77	-60
3	-10	287	-273
3	-8	192	-186
3	-7	266	-261
3	-6	910	860
3	-5	246	-221
3	-4	1031	1069
3	-3	229	186
3	-2	219	230
3	-1	439	-457
4	0	316	356
4	-13	269	-244
4	-11	249	-230
4	-10	137	-123

4	-9	153	-163
4	-8	503	440
4	-7	230	-216
4	-6	235	239
4	-5	917	-822
4	-4	292	-262
4	-3	881	-837
4	-2	321	-315
4	-1	737	759
5	1	645	661
5	2	635	-627
5	3	676	663
5	4	429	-416
5	5	181	-167
5	6	123	-126
5	7	110	-101
5	8	407	389
5	10	183	189
5	12	94	94
5	16	115	-136
6	0	595	-583
6	2	179	-159
6	3	757	-749
6	4	140	149
6	5	159	135
6	6	662	629
6	8	258	231
6	10	173	-174
6	11	106	-116
6	12	188	-177
7	1	599	-557
7	2	78	-53
7	3	391	366
7	4	273	257
7	6	152	-142
7	7	236	-251
7	8	164	146
7	10	140	172
7	12	116	121
7	15	85	84
7	16	78	-105
8	0	169	-152
8	1	263	-261
8	2	144	-159
8	3	132	-146
8	4	275	261
8	6	300	294
8	8	254	261
8	11	154	187
8	12	148	-142
8	14	94	-153
9	1	363	-341
9	3	99	-109
9	7	115	-142
9	8	114	-87
9	10	160	-176
10	0	283	-290
10	1	205	-173
10	2	262	-273

L = -3

H	K	FO	FC
1	-18	79	84
1	-16	133	137
1	-11	135	120
1	-10	326	-295
1	-9	86	99
1	-8	121	-114
1	-7	342	-335
1	-6	251	247
1	-5	322	-344
1	-4	375	399
1	-3	231	266
1	-2	586	-483
1	-1	562	-625
2	0	547	-601
2	-15	146	154
2	-14	180	-169
2	-13	165	-141
2	-9	321	-330
2	-8	387	354
2	-7	123	118
2	-6	296	344
2	-5	136	138
2	-4	491	-503
2	-3	459	-450
2	-2	481	413
2	-1	1035	1169
3	-14	147	167
3	-12	103	-88
3	-11	81	84
3	-10	88	-78
3	-9	197	196
3	-7	119	-150
3	-6	307	-307
3	-5	634	596
3	-4	405	416
3	-3	543	593
3	-2	581	603
3	-1	431	460
4	0	465	-467
4	-14	230	-245

4	-12	95	-78
4	-11	273	-256
4	-10	140	-139
4	-9	121	-155
4	-7	80	83
4	-6	1201	1176
4	-4	119	139
4	-2	857	-945
4	-1	274	-288
5	1	210	-217
5	2	542	553
5	3	516	524
5	4	349	337
5	5	610	605
5	6	65	51
5	7	571	-556
5	8	192	206
5	9	217	211
5	10	251	-255
5	11	86	125
5	13	163	-169
5	14	99	76
5	15	96	-139
6	1	985	963
6	3	406	-420
6	4	550	555
6	5	333	-328
6	6	679	662
6	8	418	414
6	9	74	65
6	10	219	-220
6	11	193	175
6	12	134	-158
6	13	213	-293
6	14	137	-139
6	15	80	62
6	16	98	-110
7	1	191	-190
7	2	543	528
7	3	412	391
7	4	385	375
7	5	453	433
7	7	192	162
7	8	434	-426
7	9	98	90
7	10	517	-557
7	11	111	124
7	12	110	-122
8	0	326	308
8	1	319	268
8	3	323	304
8	4	178	153
8	5	142	154
8	6	132	120
8	8	104	-104
8	9	243	271
8	11	189	215
8	12	95	106
8	14	103	-124

9	2	428	393
9	3	136	146
9	4	126	144
9	7	228	218
9	8	228	-238
9	9	83	-86
9	10	292	-309
9	12	191	-248
10	0	192	187
10	1	120	74
10	2	251	245
10	3	247	222
10	4	239	-224
10	5	145	-124
10	6	137	-154
10	7	85	106
10	8	118	-131
10	9	171	202
10	12	115	128
11	4	98	103
11	7	119	122
12	0	237	225
12	1	90	76
12	2	93	100
12	3	108	125
12	4	103	-93
12	8	145	-163
13	7	91	-92
14	0	294	285
14	2	125	141
14	3	80	-74
15	1	93	-91
15	2	252	-264
15	6	96	-86

L = -2

H	K	FO	FC
0	0	1111	-1237
0	-18	114	125
0	-15	224	223
0	-14	130	-120
0	-13	137	-128
0	-12	253	-239
0	-11	136	136
0	-9	282	-255
0	-8	918	898
0	-6	725	696
0	-4	917	-888
0	-3	895	-941
0	-2	383	-305
0	-1	1177	1347
1	-16	159	-163
1	-11	138	-114
1	-10	96	92
1	-9	71	52
1	-8	501	466
1	-7	300	-258
1	-6	944	-938
1	-5	172	165

1	-4	286	-267
1	-3	155	144
1	-2	181	258
1	-1	588	-647
2	0	543	-650
2	-14	184	-187
2	-10	301	-273
2	-8	249	-230
2	-7	228	198
2	-6	526	474
2	-5	476	427
2	-4	508	-548
2	-3	736	-779
2	-2	2403	-2694
2	-1	290	318
3	-18	75	-54
3	-16	104	-127
3	-14	107	-87
3	-12	118	113
3	-11	114	-111
3	-10	178	156
3	-9	263	241
3	-8	158	128
3	-7	477	-459
3	-6	140	-157
3	-5	292	285
3	-4	639	-628
3	-3	320	-376
3	-2	2125	-2176
3	-1	939	-1019
4	0	926	923
4	-16	100	-127
4	-14	111	125
4	-13	99	96
4	-12	75	-36
4	-10	111	-111
4	-7	501	457
4	-6	227	207
4	-5	152	-161
4	-4	613	-578
4	-3	89	-118
4	-2	979	991
4	-1	1121	-1200
5	2	332	330
5	3	245	242
5	4	520	539
5	6	371	-357
5	7	181	-179
5	8	255	-238
5	9	385	376
5	10	423	-407
5	12	162	-173
5	13	161	-190
5	14	90	76
5	16	83	69
6	0	328	319
6	1	308	-286
6	2	171	166
6	4	95	-88

6	5	118	-106
6	6	463	-470
6	7	248	-244
6	8	179	-190
6	9	112	-104
6	11	172	-183
6	12	278	301
6	13	196	-255
6	14	91	92
7	1	95	-86
7	2	104	92
7	3	105	-71
7	4	276	255
7	5	68	56
7	7	258	256
7	8	129	-123
7	10	78	-89
7	11	101	-98
8	0	207	197
8	1	117	-113
8	2	201	206
8	3	373	371
8	4	325	-284
8	5	186	186
8	6	311	-305
8	8	372	-382
8	14	110	125
9	1	223	203
9	2		

14 0 182 -162
 14 6 109 87
 14 8 126 170
 15 1 88 -75
 15 2 151 -143
 16 0 181 -179
 16 2 94 -94

L = -1
 H K FO FC
 1-18 74 -112
 1-16 236 -245
 1-13 176 -167
 1-12 84 75
 1 -9 86 70
 1 -7 112 -113
 1 -6 506 -485
 1 -5 1042-1005
 1 -4 658 -734
 1 -3 1152 1326
 1 -2 1676-1984
 1 -1 422 -649
 2 0 1793 2368
 2-14 214 199
 2-9 185 -156
 2-8 367 -317
 2-7 154 170
 2-6 329 354
 2-5 449 437
 2-4 474 -567
 2-3 1097-1129
 2-2 538 -519
 2-1 133 -80
 3 15 84 86
 3-14 99 -127
 3-12 320 309
 3-10 405 381
 3-9 488 454
 3-8 153 160
 3-7 221 -213
 3-6 375 327
 3-5 220 -225
 3-3 498 513
 3-2 793 -816
 3-1 720 694
 4 0 1044-1060
 4-16 111 123
 4-14 272 267
 4-12 297 279
 4-10 249 -226
 4 -9 75 -92
 4 -8 298 -277
 4 -7 135 123
 4 -6 947 -921
 4 -4 788 -858
 4 -3 554 -547
 4 -2 136 112
 4 -1 273 300
 5 1 333 -321

5 2 128 130
 5 3 184 -186
 5 4 341 -339
 5 5 382 -375
 5 6 75 -59
 5 7 516 -505
 5 8 290 -264
 5 9 76 74
 5 10 77 81
 5 11 78 -79
 5 12 137 177
 5 14 98 -91
 6 1 151 156
 6 2 265 -267
 6 3 140 -140
 6 4 1032-1019
 6 5 262 -257
 6 6 335 -345
 6 7 194 -172
 6 8 413 -405
 6 10 120 -110
 6 11 173 -186
 6 12 337 374
 6 16 107 154
 7 1 222 -206
 7 2 351 -334
 7 3 139 -119
 7 4 333 -347
 7 8 341 339
 7 9 147 -166
 7 10 394 421
 7 12 221 261
 7 13 107 130
 7 15 84 94
 7 16 82 -108
 8 0 106 -114
 8 1 238 246
 8 2 79 75
 8 3 258 260
 8 4 102 -105
 8 5 195 171
 8 6 79 -81
 8 8 142 160
 8 9 77 -78
 8 13 111 183
 9 1 119 103
 9 2 165 -158
 9 3 253 251
 9 4 360 -353
 9 5 205 -210
 9 6 137 -130
 9 7 205 -192
 9 8 457 433
 9 10 264 278
 9 11 104 123
 10 2 239 -238
 10 3 104 -118
 10 4 193 178
 10 5 280 -286

10 6 425 410
 10 8 176 199
 10 11 143 -210
 10 12 121 -179
 11 4 94 -85
 11 5 129 128
 11 6 105 -99
 11 8 101 82
 12 0 515 -503
 12 2 186 -180
 12 3 108 88
 12 5 151 -169
 12 6 245 241
 12 7 85 82
 12 8 168 185
 13 2 103 80
 13 4 240 250
 13 5 105 102
 14 1 117 100
 14 2 126 -118
 14 4 139 -143
 14 6 93 71
 14 8 90 74
 15 2 125 111
 16 1 113 133

L = 0
 H K FO FC
 0-18 111 -136
 0-16 181 -169
 0-14 319 315
 0-12 113 106
 0-10 94 84
 0 -8 181 159
 0 -6 993 974
 0 -2 594 471
 1-16 137 159
 1-12 211 197
 1-10 218 186
 1 -8 107 105
 1 -6 185 -179
 1 -4 1530 1489
 1 -2 1336 1470
 2 0 1318 1295
 2-14 333 313
 2-12 132 89
 2-10 169 -164
 2 -8 409 -419
 2 -6 146 -120
 2 -4 873 -839
 2 -2 708 736
 3-18 98 104
 3-16 147 159
 3-14 160 129
 3-12 157 -140
 3-10 681 -642
 3 -8 263 250
 3 -6 405 -406
 3 -4 1307 1343

4 0 495 524
 4-16 164 170
 4-14 136 -151
 4-12 270 244
 4-10 359 -323
 4 -8 241 246
 4 -6 515 514
 4 -4 956 -979
 5 2 292 -316
 5 4 209 -230
 5 6 478 454
 5 8 134 157
 5 10 324 352
 5 12 396 423
 6 0 554 -519
 6 2 98 38
 6 4 153 -144
 6 6 513 497
 6 12 113 -94
 7 4 317 301
 7 6 246 -236
 7 8 259 255
 7 10 88 101
 8 0 453 402
 8 2 475 -412
 8 4 487 495
 8 6 74 75
 8 8 319 324
 8 12 228 -252
 9 2 98 -72
 9 4 214 -215
 9 8 338 -352
 9 10 217 -250
 9 12 112 -129
 10 0 507 -479
 10 2 259 -238
 10 6 339 326
 10 8 139 165
 11 4 570 555
 11 6 388 409
 11 8 341 -407
 12 0 209 -187
 12 2 163 157
 12 4 141 -130
 12 6 117 -116
 12 8 98 144
 12 10 94 -115
 13 2 91 86
 13 4 267 257
 13 6 262 298
 13 8 123 -139
 14 0 159 165
 14 2 245 242
 14 8 92 -134
 15 2 141 -152
 15 4 218 229

L = 1
 H K FO FC
 7 6 74 -42
 11 3 81 -51
 15 4 99 -93

L = 2
 H K FO FC
 0 17 96 -83
 4 8 64 -26
 7 14 78 -105
 7 15 83 -136
 8 12 93 88

L = 3
 H K FO FC
 9 1 67 -61

L = 4
 H K FO FC
 2-15 78 46
 8 5 67 -32
 9 4 92 -58

L = 5
 H K FO FC
 1 -2 59 -16
 12 3 82 -67
 14 4 86 -80
 15 3 76 78

L = 6
 H K FO FC
 6 12 87 68
 14 0 97 -91
 14 2 85 -85

L = 7
 H K FO FC
 2 -8 79 -78

L = 8
 H K FO FC
 1 -6 88 -77
 7 2 76 54
 8 2 85 -87

L = 9
 H K FO FC
 3 2 75 43
 4-14 90 -95

L = 10
 H K FO FC
 4-13 86 105
 8 3 85 -57
 9 10 78 85
 10 0 98 59

L = 11
 H K FO FC
 1 1 78 72
 3 2 84 -52
 3 3 78 54
 4 -1 92 70
 7 2 79 -32
 9 3 74 -62

L = 12
 H K FO FC
 0 -1 105 139
 2 -5 91 60
 9 7 69 -68
 10 2 76 -88

L = 13
 H K FO FC
 4 -9 90 69

L = 14
 H K FO FC
 3 -8 80 100
 4 0 89 -90
 4 2 87 -64
 4 -7 81 -92
 5 3 74 72

APPENDIX 3: STRUCTURE FACTORS FOR 20

-5	0	129	-129	2	7	46	-52	6	7	32	-35	1	7	49	53	4	4	202	-179	1	-4	131	140	4	-8	99	98	
-4	-1	137	166	2	6	105	-106	7	-1	34	-36	1	9	171	-172	4	6	192	190	1	-3	215	199	4	-7	126	-139	
-4	-1	120	-132	2	9	29	24	7	3	38	-34	1	9	142	-146	4	7	85	-80	1	-2	76	19	4	-6	91	-88	
-4	0	178	-191	2	10	174	178	7	5	55	53	1	10	142	148	4	8	59	-55	1	-1	156	132	4	-5	224	217	
-4	1	82	80	2	12	83	-79					1	11	75	67	4	9	51	47	1	0	158	179	4	-4	70	-67	
-3	0	04	-64	3	-11	35	38	L =	0	0	0	1	12	83	-81	4	11	44	-46	1	1	1	68	60	4	-3	190	-107
-2	10	27	23	3	-10	34	-36	H	K	F	O	2	13	37	41	5	-10	74	-67	1	2	301	-311	4	-2	88	76	
0	-1	545	-825	3	-8	34	28	-7	-3	41	-44	2	-13	91	-90	5	-9	61	55	1	4	481	436	4	2	173	177	
0	0	414	451	3	-6	68	-78	-7	-2	32	-38	2	-11	149	140	5	-7	172	-166	1	5	68	-119	4	3	149	154	
0	0	45	47	3	-5	39	33	-7	1	37	-38	2	-10	81	-70	5	-6	43	41	1	6	169	-143	4	4	115	-90	
0	4	46	-47	3	-4	31	37	-7	2	29	30	2	-9	133	-128	5	-5	178	182	1	7	76	72	4	5	156	-147	
0	5	322	-593	3	-3	41	-40	-6	-3	63	-55	2	-8	273	280	5	-4	132	-123	1	8	93	-84	4	6	164	155	
0	6	27	-91	3	-2	71	-67	-5	-2	106	102	2	-7	67	60	5	-3	54	-59	1	9	95	-92	4	7	81	85	
0	7	129	126	3	-1	27	37	-5	-1	109	115	2	-6	266	-265	5	-2	122	110	1	10	43	36	4	8	117	-108	
0	9	83	-81	3	0	261	-237	-5	0	26	20	2	-5	45	58	5	3	82	-37	1	11	55	50	4	9	54	58	
0	10	23	-26	3	1	50	41	-5	1	61	-54	2	-4	208	221	5	4	55	-67	1	12	63	-65	4	10	44	39	
0	11	20	22	3	2	393	408	-5	0	42	43	2	-3	141	-96	5	6	40	24	2	-13	72	-73	4	11	64	-66	
0	13	37	36	3	3	29	12	-4	-2	123	129	2	-2	97	107	5	6	32	32	2	-12	46	-43	5	-10	83	-80	
1	-13	67	-70	3	4	127	-128	-4	-1	99	-64	2	-1	321	263	5	7	39	-43	2	-11	70	71	5	-8	33	33	
1	-10	56	34	3	5	44	-52	-4	0	58	-62	2	3	170	167	6	-7	35	-30	2	-9	166	-163	5	-7	110	-104	
1	-8	111	121	3	6	93	91	-4	1	140	136	2	4	170	-148	6	-6	47	40	2	-8	58	52	5	-6	52	-51	
1	-7	183	172	3	7	51	56	-3	-1	400	-356	2	5	138	-129	6	-5	75	68	2	-6	266	266	5	-4	52	-55	
1	-6	92	-85	3	8	65	-67	-3	0	100	-92	2	6	85	-86	6	-4	42	-38	2	-5	92	-47	5	-3	338	-341	
1	-5	69	-67	3	11	32	-32	-2	-1	421	-399	2	9	35	30	6	4	40	-35	2	-4	478	431	5	-2	173	156	
1	-4	71	95	3	12	66	-60	-2	0	362	-327	2	10	111	113	6	5	79	69	2	-3	91	-34	5	4	81	-79	
1	-3	40	-12	4	-10	42	-49	-1	0	445	463	2	11	39	34	6	6	42	38	2	-2	162	-180	5	5	51	51	
1	-2	133	-173	4	-8	36	-37	0	-2	633	-698	2	12	85	-84	6	6	42	38	2	-1	88	102	5	6	29	32	
1	-1	265	263	4	-5	68	65	0	-1	72	-76	3	-12	54	52	6	8	55	48	2	0	230	189	5	7	33	-36	
1	0	365	363	4	-4	55	-53	0	3	223	222	3	-11	82	82	6	8	55	48	2	1	196	-229	5	9	41	45	
1	0	336	-497	4	-3	124	-109	0	4	99	103	3	-10	33	-34	7	-5	32	-27	2	2	69	-65	6	-7	67	-57	
1	2	408	-348	4	-2	77	93	0	9	129	-152	3	-9	33	-38	7	-4	39	-38	2	3	159	157	6	-8	69	60	
1	4	69	32	4	0	40	-34	0	7	164	159	3	-8	66	65	7	5	60	60	2	4	117	-116	6	-4	35	-34	
1	5	77	68	4	1	86	-59	0	8	178	-61	3	-6	102	-101	7	5	60	60	2	5	107	-107	6	-3	122	-111	
1	6	46	30	4	2	199	174	0	8	138	-133	3	-5	117	113	8	6	47	45	2	6	47	45	6	3	93	-97	
1	7	42	82	4	4	138	-131	0	9	138	-133	3	-4	40	26	9	6	42	38	2	8	135	-141	6	4	29	-29	
1	8	133	-144	4	6	26	15	0	10	33	-3	3	-3	236	-248	10	5	143	-138	2	10	121	123	6	5	105	105	
1	10	126	125	4	7	58	61	0	11	29	22	3	-2	55	-55	11	6	31	-28	2	12	87	-97	6	6	34	28	
1	11	28	-32	4	8	28	-29	1	-13	45	-43	3	-2	372	320	12	7	29	-29	3	-11	54	53	6	7	124	-119	
1	13	55	52	4	9	41	-36	1	-13	81	-84	3	3	235	243	13	8	29	-29	3	-7	43	52	7	-4	55	-50	
2	-12	39	40	4	11	43	-47	1	-11	90	92	3	5	357	-345	14	9	33	-19	3	-6	103	-95	7	-3	94	87	
2	-11	69	73	5	-9	57	51	1	-10	141	-140	3	6	177	178	15	10	232	-242	3	-5	59	-46	7	5	56	56	
2	-10	60	-54	5	-7	59	-54	1	-9	141	-140	3	6	177	178	16	11	232	-242	3	-4	215	216	8	4	2	2	
2	-9	51	55	5	-6	55	53	1	-8	64	-47	3	7	40	-36	17	12	74	24	3	-4	215	216	9	3	189	-150	
2	-8	111	114	5	-5	67	68	1	-7	224	247	3	8	36	-38	18	13	397	377	3	-3	54	-57	10	2	40	40	
2	-7	34	-41	5	-3	92	-98	1	-6	194	-210	3	9	89	89	19	14	143	-138	3	-2	146	-150	11	1	34	33	
2	-6	155	-151	5	-2	69	56	1	-5	158	-170	3	10	45	53	20	15	31	-28	3	-1	119	104	12	0	29	30	
2	-5	53	-54	5	-1	156	155	1	-4	317	283	3	11	60	-60	21	16	230	204	3	1	197	-206	13	-2	28	12	
2	-4	162	167	5	0	62	-63	1	-3	309	284	3	12	41	-44	22	17	162	-161	3	3	261	255	14	-1	32	34	
2	-3	62	-49	5	1	51	-63	1	-2	32	-77	4	-10	67	-67	23	18	36	-36	3	4	232	-228	15	0	-2	418	-401
2	-2	29	-14	5	2	40	-41	1	-1	64	-44	4	-9	81	78	24	19	38	36	3	5	227	-226	16	0	-1	151	149
2	0	341	-293	6	-7	31	-30	1	1	36	-61	4	-7	181	-189	25	20	39	-39	3	6	289	291	17	0	3	189	-150
2	1	73	-72	6	-5	48	45	1	2	674	-650	4	-6	42	43	26	21	77	73	3	7	177	-169	18	0	4	233	246
2	2	36	39	6	-3	33	-33	1	3	184	168	4	-5	128	119	27	22	226	-233	3	8	177	-169	19	0	5	117	84
2	3	31	41	6	-1	52	52	1	4	108	-94	4	-4	108	-94	28	23	226	-233	3	9	51	52	20	0	6	62	-60
2	5	92	113	6	3	62	-54	1	4	34	63	4	-3	174	-159	29	24	184	184	3	10	110	111	21	0	7	100	90
2	6	89	91	6	3	62	-54	1	5	167	-154	4	-2	63	59	30	25	238	-248	3	11	33	-30	22	0	8	34	35
2	6	89	91	6	3	62	-54	1	6	108	107	4	-2	134	123	31	26	126	-153	3	12	53	-52	23	0	9	60	-48
2	6	89	91	6	3	62	-54	1	6	108	107	4	-2	134	123	32	27	126	-153	3	13	53	-52	24	0	11	40	-34

0	12	29	31	4	-3	243	-244	1-10	117	-126	4	-6	61	73	1-2	201	-205	4	3	36	28	2	-4	93	92
1	-10	46	-50	4	-2	46	-42	1-9	130	-139	4	-3	161	164	1-1	55	46	4	4	91	-84	2	-3	111	121
1	-9	40	-41	4	-1	97	95	1-8	177	191	4	-3	90	-85	1-0	182	173	4	5	62	-55	2	-2	141	-141
1	-7	110	107	4	0	99	-97	1-7	80	77	4	-2	25	-21	1-1	41	-35	4	6	53	49	2	-1	34	40
1	-6	182	-187	4	1	122	-119	1-6	87	-86	4	-1	57	57	1-2	162	-157	4	8	49	-59	2	0	146	-153
1	-5	188	-178	4	2	106	101	1-5	91	-104	4	0	82	-89	1-3	51	-49	5	-9	79	77	2	1	43	48
1	-4	237	218	4	3	77	69	1-4	32	26	4	0	45	-38	1-4	85	70	5	-8	47	45	2	2	75	-70
1	-2	219	-216	4	4	102	-99	1-3	81	-56	4	3	55	56	1-5	37	-35	5	-7	63	-62	2	3	132	127
1	-1	114	-73	4	5	36	-30	1-2	166	-166	4	3	55	56	1-6	53	-53	5	-5	133	134	2	4	49	43
1	0	231	234	4	7	76	49	1-1	50	42	4	4	167	-170	1-7	6	53	5	-3	168	-178	2	5	86	-81
1	1	150	80	4	10	82	80	1-0	110	113	4	5	89	-87	1-8	9	49	5	-2	90	93	2	6	30	32
1	2	37	15	5	-10	58	-60	1-0	53	-46	4	6	89	81	1-9	10	59	5	-1	89	97	2	7	40	43
1	4	43	49	5	-5	54	54	1-2	121	-118	5	-10	34	-36	2-11	64	61	5	0	73	-76	2	6	53	-49
1	5	153	131	5	-7	57	-51	1-3	118	125	5	-9	34	33	2-9	69	-68	5	3	45	-51	3	-11	67	66
1	6	28	-20	5	-5	83	85	1-4	49	33	5	-8	46	53	2-8	100	91	5	4	62	-66	3	-7	40	-34
1	8	30	-52	5	-4	49	44	1-5	75	-64	5	-6	37	31	2-7	174	169	5	5	44	41	3	-6	76	-67
1	9	85	-81	5	-3	244	-251	1-6	70	82	5	-5	102	103	2-6	262	-266	5	6	49	51	3	-5	63	67
1	10	58	53	5	-2	96	-101	1-7	52	62	5	-4	114	-111	2-5	198	-187	5	7	38	-36	3	-4	48	50
1	12	45	-44	5	-1	226	239	1-9	29	-36	5	-3	108	-113	2-4	214	213	6	-7	60	-61	3	-3	59	-55
2	-13	45	-48	5	0	61	-57	1-10	39	37	5	-1	86	97	2-2	61	-57	6	-5	41	45	3	-2	78	-84
2	-10	82	-86	5	1	79	-71	2-13	72	-70	5	1	104	-121	2-1	74	77	6	-3	29	-29	3	-1	38	33
2	-9	67	-61	5	2	119	134	2-11	70	69	5	2	29	22	2-1	173	-172	6	-2	40	44	3	0	26	27
2	-8	48	44	5	3	26	-23	2-10	49	-48	5	4	76	-75	2-3	178	182	6	0	89	-91	3	1	77	-80
2	-7	124	123	5	4	116	-124	2-9	90	-102	5	6	58	57	2-4	51	-55	6	2	39	38	3	2	48	49
2	-5	344	-310	5	5	48	48	2-8	138	148	6	-7	84	-84	2-5	55	-51	6	3	53	-53	3	3	100	95
2	-4	146	154	5	6	107	110	2-6	185	-177	6	-5	29	29	2-6	121	121	7	-2	59	82	3	5	73	-66
2	-3	255	218	6	-9	81	87	2-4	45	-53	6	-4	51	-50	2-7	40	41	7	-1	47	-43	3	6	38	43
2	-2	87	-66	6	-7	54	-54	2-3	35	7	6	-3	45	-42	2-8	94	-93	7	0	51	-56	3	7	67	58
2	-1	182	118	6	-6	29	-23	2-2	45	23	6	-2	55	53	3-12	41	43	8	-10	91	-88	4	-8	66	68
2	0	21	13	6	-4	51	-50	2-1	179	168	6	2	30	-32	3-11	64	62	9	-11	80	80	4	-7	85	-84
2	2	52	43	6	-3	32	-27	2-0	60	69	6	5	64	67	3-10	34	-33	10	-12	50	29	4	-6	95	-89
2	3	104	90	6	-2	35	39	2-1	177	-184	7	-5	38	42	3-9	53	-45	11	-13	34	-29	4	-5	86	84
2	4	44	-57	6	-1	111	111	2-2	41	49	7	-4	33	-34	3-8	34	31	12	-14	32	27	4	-4	68	84
2	5	124	-112	6	1	79	-85	2-3	96	93	7	-2	28	36	3-7	69	-73	13	-15	32	27	4	-3	174	-178
2	6	61	59	6	2	89	85	2-4	78	70	7	-1	32	-39	3-6	75	-72	14	-16	51	43	4	-2	59	-62
2	7	37	34	6	3	51	-46	2-6	94	-94	7	0	43	-44	3-5	50	45	15	-17	62	63	4	-1	159	157
2	8	83	-95	6	5	72	71	3-10	54	54	7	1	64	65	3-4	81	80	16	-18	122	-116	4	0	59	-62
2	9	58	-64	6	6	46	42	3-11	45	49	7	2	40	39	3-3	48	-46	17	-19	104	-103	4	1	56	-56
2	10	61	64	6	7	49	-51	3-10	40	-32	7	3	49	-49	3-2	105	104	18	-20	89	-108	4	2	112	116
2	12	48	-44	7	-6	41	39	3-8	28	12	8	4	89	-108	3-1	89	-108	19	-21	66	60	4	3	39	40
3	-11	40	37	7	-4	39	-41	3-7	98	-100	9	5	110	-109	3-2	110	-109	20	-22	66	60	4	4	103	-100
3	-3	160	180	7	-3	28	28	3-6	93	-93	10	6	123	-114	3-5	131	125	21	-23	93	-87	4	6	62	57
3	-1	69	86	7	3	33	-37	3-5	99	91	11	7	208	210	3-4	208	210	22	-24	60	61	5	-8	43	36
3	0	96	-76	7	4	33	-37	3-4	105	102	12	8	67	-67	3-3	67	-67	23	-25	70	-67	5	-7	58	-64
3	1	236	-243	8	-3	33	-37	3-3	26	15	13	9	123	-114	3-2	150	-147	24	-26	237	230	5	-5	67	72
3	2	68	58	8	-2	27	-20	3-2	94	92	14	10	64	-62	3-1	97	95	25	-27	43	-41	5	-4	37	40
3	3	130	125	9	-1	27	-20	3-1	93	-93	15	11	193	185	3-6	64	-62	26	-28	212	-225	5	-3	90	-94
3	5	163	-169	9	0	24	24	3-5	89	-87	16	12	138	-148	3-8	36	34	27	-29	129	123	5	-1	151	164
3	7	93	84	10	-2	305	-292	3-4	132	126	17	13	97	102	3-7	56	56	28	-30	74	82	5	0	71	-78
3	6	99	-96	11	0	121	-139	3-3	133	138	18	14	42	-38	4-10	60	-61	29	-31	91	-88	5	1	88	-94
3	10	96	94	12	0	121	-139	3-3	138	-148	19	15	112	76	4-7	64	-63	30	-32	64	-63	5	2	102	111
4	-12	51	52	13	0	5	106	-104	1-12	42	1-12	1-12	76	72	4-5	248	252	31	-33	104	-104	5	1	88	-94
4	-11	69	72	14	-1	25	12	1-11	174	-187	20	16	174	-187	4-4	35	-41	32	-34	64	-64	5	2	102	111
4	-9	29	27	15	0	97	112	3-6	69	59	21	17	147	151	4-3	203	-214	33	-35	45	49	6	-4	41	-45
4	-9	29	27	15	0	97	112	3-7	39	-45	22	18	229	241	4-2	70	76	34	-36	68	65	6	-3	48	-51
4	-6	30	-62	16	0	10	28	27	59	55	23	19	202	-211	4-1	130	134	35	-37	31	33	6	-2	30	29
4	-6	30	-62	16	0	10	28	27	59	55	23	19	202	-211	4-1	130	134	35	-37	31	33	6	-2	30	29
4	-5	178	195	17	-13	40	-39	4-10	45	-54	24	20	53	-61	4-0	1	55	36	-38	81	75	6	-1	34	36
4	-4	119	109	18	-11	147	148	4-7	99	-105	25	21	148	155	4-4	1	55	36	-38	81	75	6	-1	34	36
4	-4	119	109	18	-11	147	148	4-7	99	-105	25	21	148	155	4-4	1	55	36	-38	81	75	6	-1	34	36

L =

L =

L =

L =

L = 6				L = 7			
H	K	FO	FC	H	K	FO	FC
-3	2	30	-31	1	-7	80	83
-1	4	43	38	1	-6	99	-93
0	-2	57	-58	1	-5	46	-45
0	3	31	20	1	-4	61	65
1	-9	39	-48	1	0	42	39
1	-8	49	51	1	3	32	26
1	-5	69	-72	2	-7	63	59
1	-4	33	31	2	-6	32	-31
1	-3	81	84	2	-4	53	51
1	-2	66	-62	2	-1	40	42
1	0	109	102	2	1	37	-39
1	2	96	-88	3	-6	31	-36
1	4	29	25	3	-5	37	31
2	-8	51	42	3	-3	47	-44
2	-6	44	-42	3	-1	63	61
2	-3	88	81	3	1	57	-55
2	-2	29	-24				
2	-1	68	-65				
2	0	42	40				
2	1	37	-37				
2	2	34	-30				
2	3	47	44				
2	5	48	-46				
3	-9	37	-34				
3	-8	58	58				
3	-6	39	-35				
3	-3	48	-48				
3	0	39	-31				
3	1	51	-54				
3	2	29	24				
3	3	72	75				
3	4	42	-38				
3	5	53	-48				
4	-8	37	42				
4	-7	35	-35				
4	-6	42	-47				
4	-5	39	44				
4	-3	75	-71				
4	-2	41	-37				
4	-1	117	110				
4	1	110	-103				
4	2	55	50				
4	3	77	75				
4	4	46	-43				
5	-5	79	87				
5	-3	55	-60				
5	-2	32	-32				
5	-1	50	49				
5	0	43	43				
5	1	56	-55				
L = 7							
H	K	FO	FC				
-1	1	41	38				
0	-2	63	-65				
1	-8	38	32				

APPENDIX 4: STRUCTURE FACTORS FOR 21

H = -9				-2 24 57 -69	-2 1 49 61	0 14 528 -515	4 23 167 192	H = 1				3 2 894 -812	
K L	FO	FC		-1 15 60 -48	-2 1 38 -78	0 18 508 -511	4 26 68 56	K L	FO	FC		3 3 429 377	
-3 9	48	-2		-1 26 70 -61	-2 1 60 -45	0 22 627 597	4 27 92 124	0 3	223	-274		3 4 88 -163	
-1 7	59	-48			0 19 50 40	0 24 279 -278	4 31 141 -126	0 5	372	380		3 5 215 190	
H = -8				H = -4				0 26 98 -123	6 1	550	430		3 7 166 -103
K L	FO	FC		K L	FO	FC		0 28 85 -91	6 2	74 -58		3 8 660 650	
-6 0	68	80		-10 7	52	56		0 32 205 216	6 5	62 -31		3 9 509 -437	
-5 6	75	7		-9 0	62	-43		2 0	378	397		3 10 716 640	
-2 20	65	-83		-9 1	59	66		2 1	476	-507		3 11 609 -558	
-1 2	48	27		-9 5	59	-48		2 2	444	-519		3 12 257 -253	
H = -7				H = -2				2 3	171	310		3 13 469 404	
K L	FO	FC		K L	FO	FC		2 4	598	703		3 14 156 -168	
-5 11	59	52		-10 5	83	73		2 5	288	306		3 15 594 577	
-5 17	92	-71		-9 1	96	-69		2 6	754	647		3 16 391 -367	
-2 1	53	-41		-9 9	59	68		2 7	401	518		3 17 139 132	
-2 3	47	-40		-8 2	71	-43		2 8	338	317		3 19 99 139	
-1 18	77	61		-8 4	134	133		2 9	440	-380		3 20 312 345	
0 23	52	13		-8 6	184	174		2 10	1590	-1623		3 21 151 -139	
H = -6				H = -1				2 11	755	-654		3 22 188 187	
K L	FO	FC		K L	FO	FC		2 12	575	-595		3 23 140 -112	
-8 1	49	-65		-7 10	68	53		2 13	68	-125		3 24 196 -200	
-8 6	116	-122		-7 15	64	93		2 14	799	695		3 25 88 -100	
-8 12	79	90		-6 1	155	143		2 15	478	-482		3 26 155 -144	
-6 2	58	-43		-6 14	75	73		2 16	680	707		3 28 85 -80	
-6 3	50	59		-6 16	63	-65		2 17	73	61		3 29 86 88	
-6 19	67	-79		-6 21	76	-83		2 19	269	240		3 30 153 153	
-5 4	80	-80		-5 1	82	-82		2 19	462	462		3 32 80 86	
-5 9	60	-60		-5 2	71	-120		2 20	434	-430		4 1 74 -76	
-4 2	68	73		-5 6	54	-99		2 21	459	457		4 3 88 91	
-4 4	57	68		-5 12	54	-45		2 22	419	-438		4 5 77 -83	
-4 13	57	49		-5 13	84	-114		2 24	175	-140		4 6 43 24	
-4 21	58	-51		-5 18	62	89		2 25	198	-196		4 7 113 99	
-3 20	70	52		-5 20	57	-58		2 26	260	237		4 8 106 -84	
-2 26	78	-78		-4 12	55	-52		2 27	187	-184		4 10 51 -50	
-1 3	57	80		-4 26	82	51		2 28	204	207		4 11 70 -56	
-1 7	72	81		-3 3	44	54		2 31	149	151		4 13 89 -96	
-1 9	62	63		-3 10	53	45		2 32	114	-111		4 14 81 111	
0 24	62	-67		-3 12	55	60		4 0	685	-481		4 16 47 12	
H = -5				H = -3				4 1	782	547		4 17 57 39	
K L	FO	FC		K L	FO	FC		4 2	49	-21		4 19 62 60	
-10 2	50	29		-1 4	42	-17		4 3	86	47		4 22 69 -50	
-9 5	67	57		-1 10	49	31		4 4	363	-337		4 23 61 -63	
-8 1	44	40		-1 15	60	-56		4 5	532	398		5 1 531 -494	
-7 9	78	80		0 20	57	-90		4 6	516	-506		5 2 62 42	
-7 10	65	-56		H = 0				4 7	369	371		5 3 528 527	
-6 9	53	53		K L	FO	FC		4 8	355	373		5 4 456 459	
-5 15	62	41		-8 8	64	-76		4 9	744	-794		5 5 43 33	
-5 22	60	50		-8 11	74	39		4 10	382	349		5 6 436 383	
-4 4	52	30		-8 23	76	102		4 11	759	-696		5 8 118 -118	
-3 5	51	56		-6 14	51	-27		4 12	385	338		5 9 330 -310	
-3 9	62	-26		-4 25	68	-57		4 13	81	38		5 10 115 -112	
-3 11	73	55		0 2	491	279		4 14	58	-107		5 12 156 156	
-3 15	53	29		0 4	2011	-1852		4 15	262	295		5 13 144 -171	
-3 25	61	-48		0 6	2121	-2116		4 16	124	-99		5 14 147 148	
-2 10	65	58		0 8	625	-711		4 17	249	226		5 15 111 101	
				0 10	536	573		4 19	146	-120		5 17 130 138	
				0 12	771	773		4 20	115	94		5 18 59 -52	
				0 14	73	109		4 21	193	-226		5 19 125 174	
								4 22	101	-120		5 20 174 -130	

1	6	136	-130	4	25	200	193	1	22	118	129	7	2	73	-52	2	20	92	126	1	21	166	-178	2	6	132	137	
1	9	107	111	4	28	85	46	1	23	167	166	7	3	158	127	2	21	164	-150	1	23	69	-71	2	7	170	73	
1	11	59	-55	5	0	71	-42	1	24	145	101	7	5	200	-207	2	22	234	224	1	24	74	-74	2	8	56	-49	
1	14	88	-126	5	4	184	219	1	27	106	-102	7	7	358	-361	2	25	88	94	2	6	73	45	2	10	105	-177	
1	16	70	107	6	9	180	-177	1	29	74	-81	7	8	82	64	3	4	61	-79	2	7	92	-75	2	12	105	-100	
1	19	170	-179	6	0	525	510	2	2	96	84	7	11	212	221	4	5	187	-213	3	1	87	80	2	13	137	-125	
1	21	92	86	6	2	210	243	2	3	63	27	7	12	73	89	4	7	72	52	3	2	125	111	2	14	89	94	
1	24	55	-26	6	3	189	-160	2	4	68	-49	7	13	98	109	4	9	225	259	3	4	106	108	2	16	112	-102	
2	0	550	473	6	4	245	-242	2	5	104	74	7	15	150	-160	4	10	117	-116	3	5	101	-174	2	19	104	116	
2	1	727	-718	6	6	518	-545	2	7	127	-96	7	17	151	-139	4	10	117	-116	3	5	101	-174	2	19	104	116	
2	2	241	185	6	7	440	462	2	9	79	66	7	21	65	56	4	11	165	162	3	8	170	-164	3	0	60	-71	
2	3	1160	-1122	6	8	355	-395	2	12	65	56	7	21	65	56	4	11	165	162	3	8	170	-164	3	0	60	-71	
2	4	416	-394	6	9	312	326	2	15	100	-93	8	24	97	-77	4	15	182	-180	3	9	237	252	3	4	50	44	
2	5	296	-288	6	10	279	290	2	17	116	108	9	2	61	-67	4	17	70	-50	3	10	97	-104	4	1	49	37	
2	6	129	-131	6	11	256	-251	3	1	139	-143	9	3	97	96	5	19	111	117	3	11	152	160	4	3	140	130	
2	7	191	213	6	12	385	404	3	2	622	-529	9	4	109	-117	5	12	42	21	3	12	47	-31	4	6	91	90	
2	8	280	289	6	13	365	-368	3	3	154	-127	9	6	57	-69	5	12	42	21	3	13	81	-93	4	9	157	-162	
2	12	427	368	6	17	153	153	3	4	470	-450	9	8	120	125	5	18	47	-43	3	14	144	133	4	10	171	59	
2	13	305	-286	6	19	101	95	3	6	101	126	9	10	134	138	6	0	161	-144	3	15	194	-206	4	11	100	-100	
2	16	85	77	6	25	112	-129	3	12	112	-94	9	11	100	-106	6	4	135	125	3	17	160	-163	4	12	84	29	
2	19	275	259	6	0	291	-273	3	14	248	-259	9	11	100	-106	6	4	135	125	3	17	160	-163	4	12	84	29	
2	20	62	16	6	1	160	168	3	16	141	-155	0	0	914	-976	6	6	176	172	3	21	80	70	6	2	51	17	
2	22	146	-138	6	3	205	214	3	18	62	63	0	2	555	-571	6	10	201	-185	5	1	106	62	6	4	58	-76	
2	23	141	-128	6	7	92	73	3	20	186	183	0	4	618	598	6	16	90	97	5	4	66	-61	6	6	112	-106	
2	24	93	-96	6	11	88	-76	3	24	86	-88	0	4	618	598	6	16	90	97	5	4	66	-61	6	6	112	-106	
2	25	96	-102	6	16	83	96	4	2	56	-51	0	6	122	110	8	18	81	106	5	6	133	-131	7	5	190	-176	
2	29	100	107	10	1	60	-50	4	7	74	-51	0	10	259	-258	8	3	112	144	6	6	108	94	8	0	13	55	
3	0	122	147	10	3	103	132	4	10	101	111	0	12	320	-301	8	4	110	-118	6	2	61	51	9	0	55	-37	
3	1	79	-37	10	9	148	-164	4	11	52	31	0	14	94	-85	8	5	74	107	6	4	66	-77	1	1	66	56	
3	5	58	-60	4	14	58	-61	0	13	94	90	0	16	246	240	8	7	186	-182	6	5	45	-13	1	5	77	-70	
3	7	93	91	4	16	63	-94	0	14	58	-61	0	20	129	-94	8	9	149	-152	6	14	50	32	1	8	63	-46	
3	8	103	-88	4	19	56	-71	0	16	63	-94	0	22	64	-87	8	10	180	186	7	2	83	-125	1	10	49	-44	
3	9	80	73	4	20	75	69	1	0	109	-121	0	26	75	88	8	14	70	-63	7	4	70	-70	1	11	61	70	
3	13	73	-79	4	22	64	18	1	1	63	-42	1	0	109	-121	0	26	75	88	8	14	70	-70	1	11	61	70	
3	18	71	-81	5	1	290	-282	1	4	76	67	1	1	63	-42	1	0	109	-121	0	26	75	88	8	14	70	-70	
3	21	65	55	5	2	203	221	1	5	65	47	1	4	76	67	1	1	63	-42	1	0	109	-121	0	26	75	88	
4	1	338	301	5	3	113	114	1	10	68	-61	1	5	65	47	1	4	76	67	1	4	131	112	2	7	73	109	
4	3	579	582	5	4	84	108	1	14	74	72	1	6	63	-80	0	3	170	-170	7	9	122	-118	3	8	172	169	
4	4	234	240	5	5	308	309	1	19	94	86	1	14	74	72	1	6	63	-80	7	11	123	-138	5	2	49	63	
4	5	83	77	5	5	308	309	1	19	94	86	1	14	74	72	1	6	63	-80	7	11	123	-138	5	2	49	63	
4	7	552	-518	5	6	216	-228	2	0	231	240	2	0	9	73	60	0	7	62	34	7	12	114	-98	5	4	63	55
4	8	320	-341	5	9	129	-98	2	0	231	240	2	0	9	73	60	0	7	62	34	7	12	114	-98	5	4	63	55
4	9	605	-628	5	10	178	-83	2	3	131	114	2	3	131	114	1	3	131	114	1	3	131	114	1	3	131	114	
4	10	307	-263	5	11	176	-188	2	4	128	-132	2	4	128	-132	1	4	131	139	0	4	277	-277	3	10	102	101	
4	13	532	525	5	12	343	351	2	5	93	-94	2	5	93	-94	1	5	451	477	0	4	277	-277	3	10	102	101	
4	14	231	251	5	14	205	214	2	6	308	-297	2	6	308	-297	1	6	187	190	0	4	277	-277	3	10	102	101	
4	15	375	374	5	17	170	179	2	9	91	-46	2	9	91	-46	1	7	336	338	0	6	109	-95	2	14	84	86	
4	17	169	-178	5	18	141	-148	2	10	346	346	1	9	109	-111	1	9	109	-111	0	6	109	-95	2	14	84	86	
4	18	172	168	5	20	171	-178	2	11	97	97	1	9	109	-111	1	9	109	-111	0	6	109	-95	2	14	84	86	
4	19	407	-429	5	21	95	-92	2	12	232	238	1	11	373	-379	1	11	373	-379	0	10	162	147	2	15	164	166	
4	20	186	-183	5	23	82	-82	2	13	198	204	1	11	373	-379	1	11	373	-379	0	10	162	147	2	15	164	166	
4	21	105	-111	5	24	90	90	2	14	146	-150	2	14	146	-150	1	14	146	-150	1	14	146	-150	2	15	164	166	
4	22	180	-189	5	25	125	-125	2	15	101	83	1	15	101	83	1	15	101	83	1	15	101	83	1	15	101	83	
4	23	182	-189	5	26	66	-53	2	16	281	-283	1	17	171	180	2	1	171	180	2	1	171	180	2	1	171	180	
4	23	182	179	5	27	1	249	253	2	19	199	-204	2	19	199	-204	1	20	122	119	2	4	69	69	2	4	69	69

H = 10